Nasa CR 65499

ER-6917

TRW INC.

BIPROPELLANT PULSED ENERGY TURBOALTERNATOR POWER SYSTEM DEVELOPMENT

GPO PRICE $ _____

CFSTI PRICE(S) $ _____

Hard copy (HC) 3.25

Microfiche (MF) 1.75

ff 653 July 65

FINAL REPORT

AUGUST 1966

NASA Manned Spacecraft Center
General Research Procurement Branch
Houston, Texas

CONTRACT NAS 9-4820

TRW EQUIPMENT LABORATORIES
A DIVISION OF TRW INC. • CLEVELAND, OHIO 44117

ER-6917

BIPROPELLANT PULSED ENERGY TURBOALTERNATOR POWER SYSTEM DEVELOPMENT

FINAL REPORT

AUGUST 1966

NASA Manned Spacecraft Center
General Research Procurement Branch
Houston, Texas

CONTRACT NAS 9-4820

TRW EQUIPMENT LABORATORIES
A DIVISION OF TRW INC. • CLEVELAND, OHIO 44117

TABLE OF CONTENTS

LIST OF FIGURES

LIST OF TABLES

1.0 INTRODUCTION

This report describes the work conducted under Contract No. NAS 9-4820 for the NASA Manned Spacecraft Center. The objective of this program was to prove the feasibility of a pulsed energy turboalternator power generation system for space applications utilizing earth storeable hypergolic propellants. The work described in this report covers the design, fabrication and testing phases of the program which were accomplished from September 1, 1965 to July 14, 1966.

2.0 SUMMARY

A turboalternator, gas generator and associated controls were designed using the results of studies reported in ER-6630, "Optimization Studies, Preliminary Design and Program Definition, Turbine-Alternator Power Generation System."[1] Three turboalternator units, four gas generators and one controls unit were fabricated. Two turboalternators were assembled and the third set of parts was utilized as spares where necessary. All four gas generators and the controls unit were used in the feasibility program.

Preliminary tests were conducted on turboalternator Unit #1 for the purpose of system and facility integration and development. After these preliminary tests, endurance tests were conducted on Unit #1. System performance data such as power output, propellant consumption, coast times, and critical temperatures were obtained from the endurance tests. A total test time of 80.24 hours was realized with Unit #1. Unit #2 was acceptance tested for 2.66 hours.

The test results were analyzed to determine system performance at various power levels and at two oxidizer/fuel (0/F) ratios. Analysis indicated an SPC of 11.9 lb/KW-HR at an equivalent electrical load of 3 KW at the DC terminals and an SPC of 11.1 lb/KW-HR at 4.5 KW at the DC terminals. At times during the test program, severe operating conditions were imposed by test facility malfunction, and by other inadvertent conditions. In two instances while testing Unit No. 1, laboratory scavenge pump stoppages resulted in overloading the alternator and bearings with oil. Operation at 35 to 40 shaft H. P. for 4 to 5 secs. occurred before manual shut down could be initiated. Pulses occurred each second during this period with no damage to the unit. At other times operation with partial oil starvation for short periods resulted in no bearing or seal failures. In the early development tests, altitude chamber temperatures up to 500°F were encountered with resultant Moog valve seat damage but no other permanent damage.

Figure 2-1 shows two views of the turboalternator Unit No. 1 after the endurance tests.

[1] Subscripts refer to references at end of report

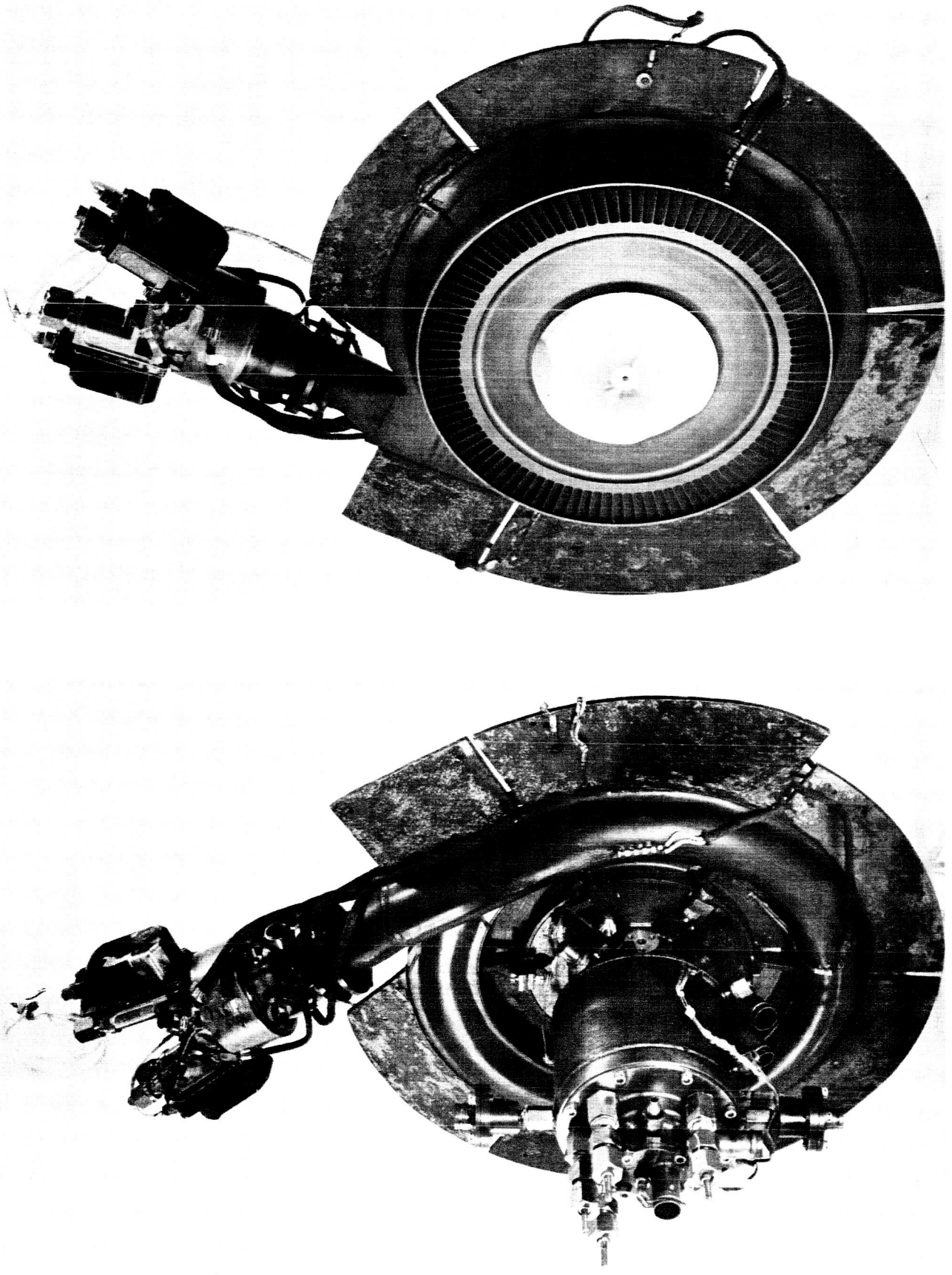

FIGURE 2-1 TURBOALTERNATOR UNIT #1

3.0 CONCLUSIONS AND RECOMMENDATIONS

The feasibility of the pulsed energy turboalternator power system was well proven by operating the first system for 80.24 hours under a variety of operating conditions including endurance as well as development testing. Under all operating conditions, including conditions of extreme overload, high ambient temperatures and brief periods of partial oil starvation, the turboalternator performed well. Successful completion of the Acceptance Test on Unit No. 2 further increases confidence in the soundness of the basic design.

Operation of the turbine at 10% below rated speed, with above normal tip clearance and with thick blade leading edges is reflected in an increased overall system specific propellant consumption, as was expected.

Future effort should be directed toward refinement of the existing design to improve specific propellant consumption and increase the continuous power rating to 6 KW. Analysis indicates that these goals can be accomplished by incorporating the following design changes:

a) Reduce turbine tip clearance to .030".

b) Improve the surface finish of the turbine nozzles and blades.

c) Slightly reduce turbine blade leading edge and trailing edge thickness.

d) Increase pulse width from .2 sec. to .4 sec.

e) Operate the turbine at 36,000 rpm (the design speed).

f) Improve heat dissipation by an improved turbine scroll-fin combination.

g) Redesign the injector head to provide heavy wall tubing.

h) Reduce heat flow from the alternator flange to the bearing cavity.

These refinements represent minor design revisions. Further effort is also required to incorporate safety circuitry, to improve the alternator terminal design, to integrate the electrical system, to achieve best efficiency and to package the system for flight.

4.0 TECHNICAL DISCUSSION

4.1 System Design

The power system consists of the turboalternator, closed loop lubrication system, and electrical system. The alternator is directly driven by a single stage turbine. The rotating assembly is supported on rolling element bearings lubricated with MIL-L-7808 oil. The open cycle turbine is driven by hot gas produced in the gas generator from the hypergolic reaction of nitrogen tetroxide with a 50-50 mixture of anhydrous hydrazine and unsymmetrical dimethyl hydrazine (UDMH).

The hot gas is sent in pulses to the turbine. The pulsing sequence is regulated by the speed control which regulates the pulsing rate, as required. When the speed control senses that alternator output frequency has decreased below a predetermined set point, it causes the bipropellant valve to open for a given period of time, presently set at 0.2 seconds. The turboalternator speed increases during the pulse period and decreases to the low speed set point during the coast period. The voltage regulator controls the voltage by regulating the field current. The alternator output is rectified to 29 VDC.

4.1.1 Turboalternator Mechanical Design

Figure 4-1 shows a cross section of the turboalternator. The turbine wheel and shaft are integral. The alternator rotor and bearings are assembled on the shaft and held with a locknut. The nozzle-scroll-gas generator assembly is attached to the alternator housing by three pins 120° apart. There is approximately a .0002 in. to .0004 in. loose fit between the pins and both parts to permit free radial movement of the scroll with respect to the alternator front flange. Thus, any thermal distortion occurring in the high temperature scroll will not be transmitted to the alternator housing. In addition, use of pins to support the scroll restricts the path for heat transfer to the alternator.

4.1.1.1 Turbine Disk and Blade Analysis

The turbine wheel and blades were analyzed on the basis of the design data in Table 4-1.

Table 4-1. Turbine Wheel and Blade Design Data

Pitch line velocity	1600 ft/sec.
Turbine tip diameter	11 in.
Turbine blade leading edge height	.938 in.
Turbine blade trailing edge height	1.000 in.
Number of blades	101
Radial temperature distribution in disk	See figure 4-2

FIGURE 4-1 TURBOALTERNATOR CROSS SECTION

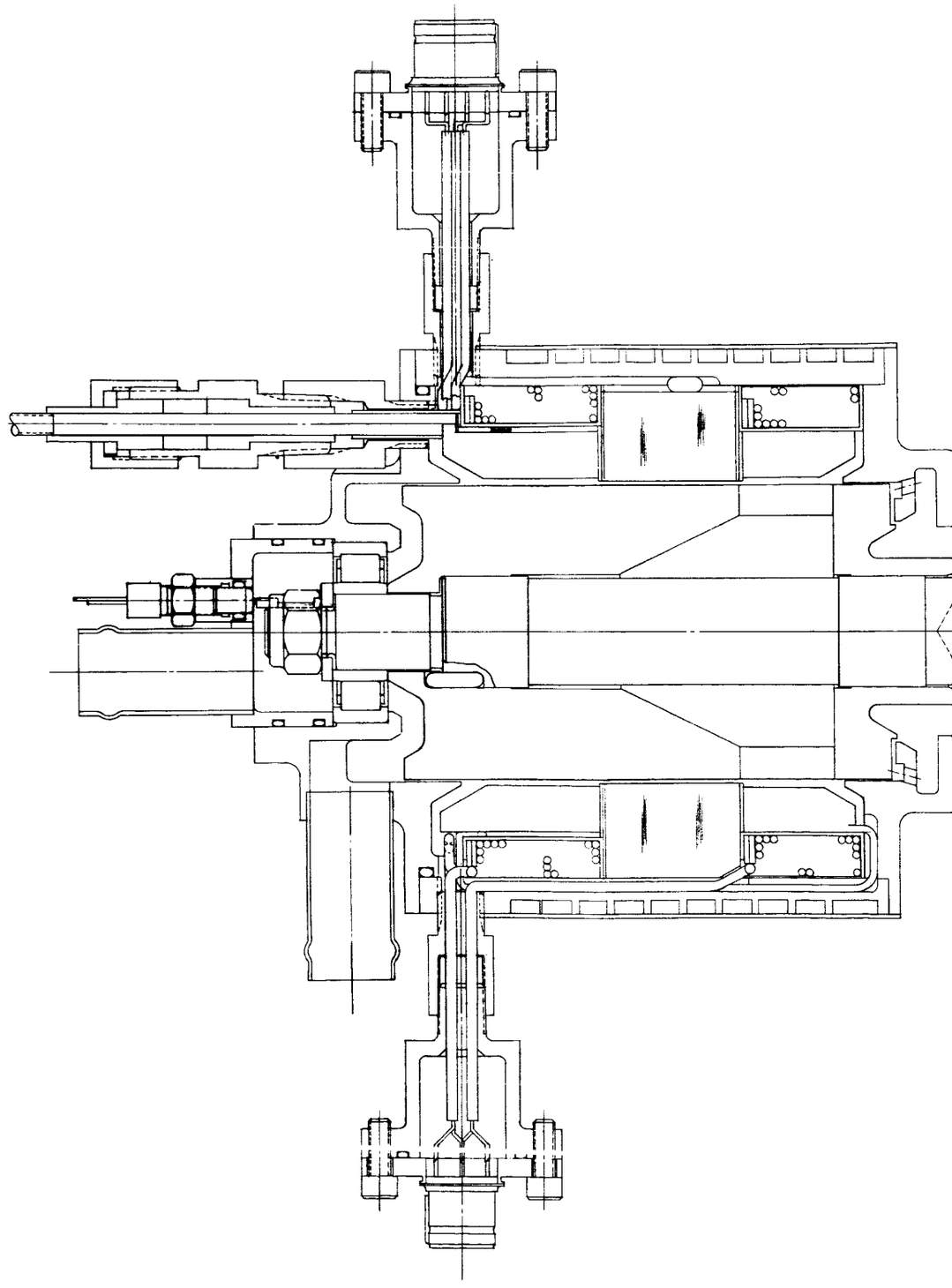

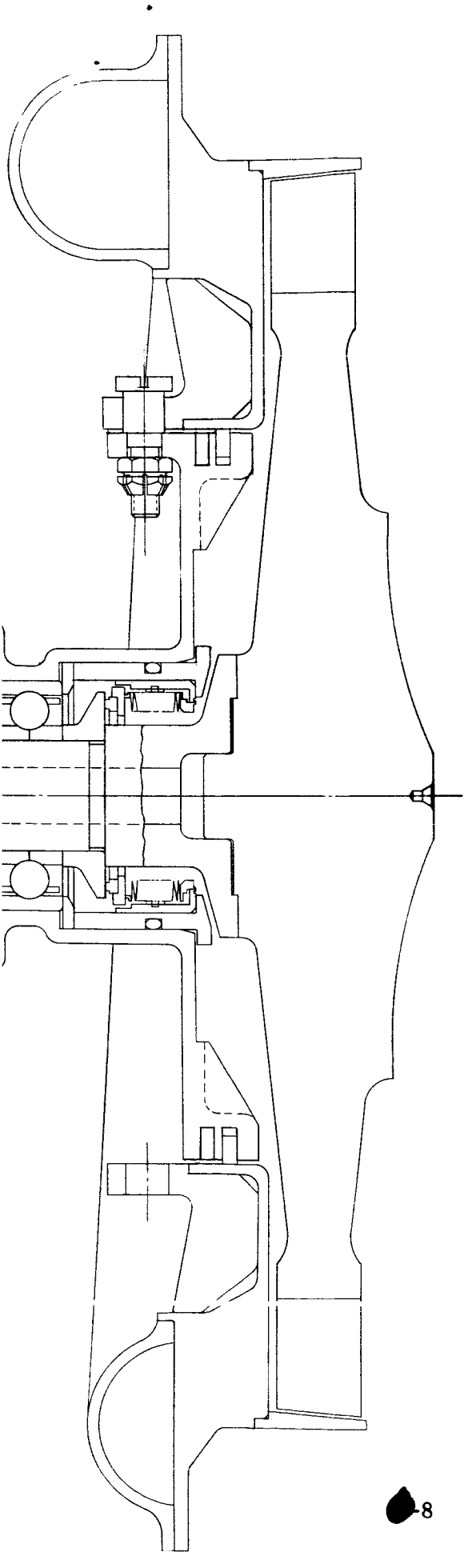

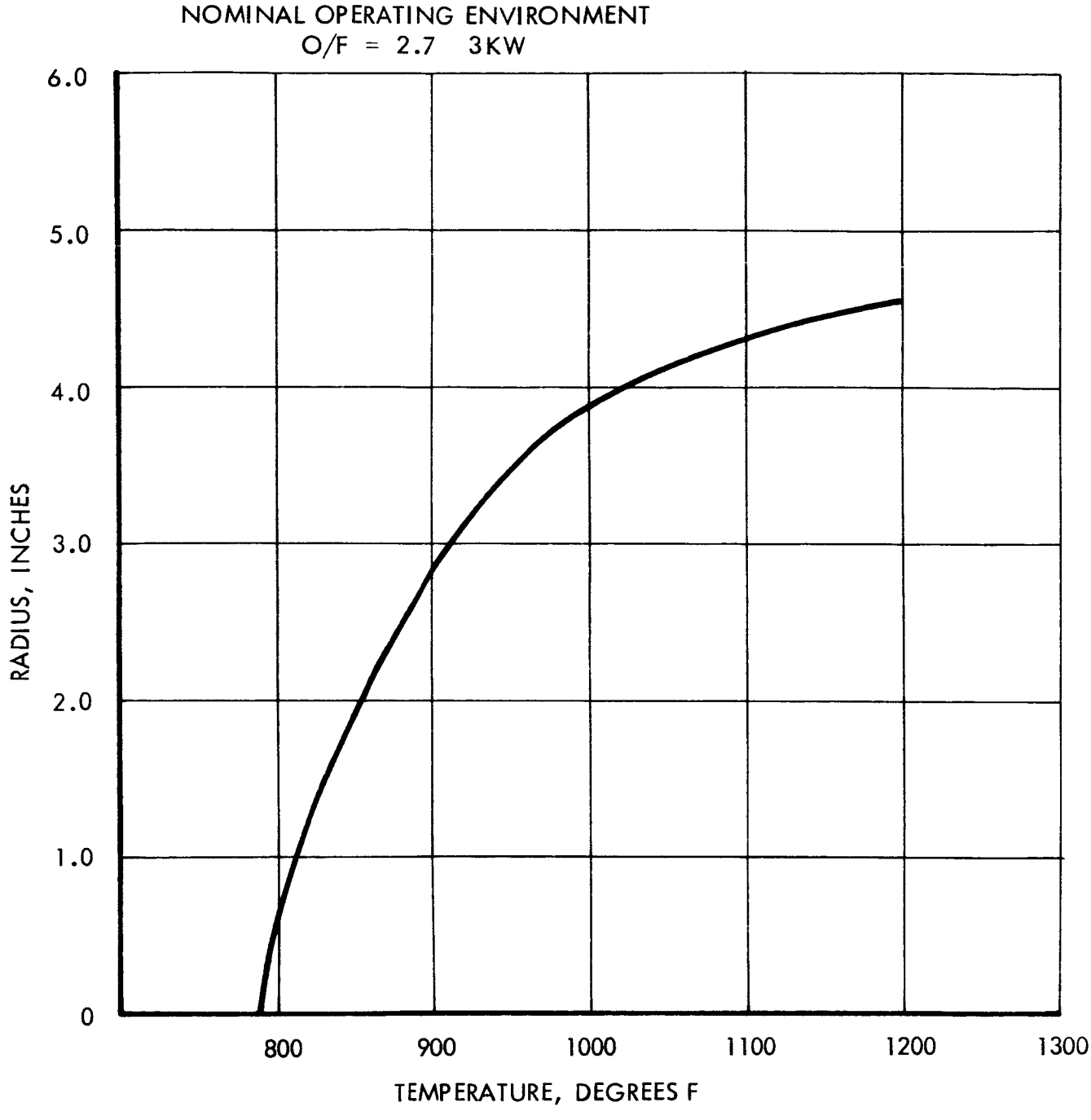

FIGURE 4-2 TEMPERATURE DISTRIBUTION - TURBINE WHEEL

The disk stress analysis was accomplished by a digital computer program based on a solution of finite difference equations of equilibrium and compatibility developed by S.S. Manson.[2] The criteria of failure were the creep and stress rupture properties as expressed by the Larson-Miller parameter for Waspaloy.

The radial and tangential components of stress are shown in Figure 4-3. Also shown is the equivalent stress calculated from the following equations:

$$S_e = \sqrt{S_r^2 + S_t^2 - S_r S_t}$$

where S_e = equivalent stress, psi

S_r = radial stress, psi

S_t = tangential stress, psi

Figure 4-4 shows the margin of safety based on yield where margin of safety is defined as:

$$M.S. = \frac{FT_y}{S_e} - 1$$

where M.S. = margin of safety

FT_y = yield strength of material

The margin of safety is greater than zero at every point on the disk. Therefore, the yield strength is not exceeded.

The long term stress analysis is based on the Larson-Miller parameter for stress rupture. Rupture will be imminent at 3.6 million hours at the neck of the disk between the rim and hub. Negligible creep, .01 micro inches per inch, is expected at the neck after 500 hours of operation. The turbine hub is over-designed to prevent failure in that area.

The disk was also analyzed at an overspeed of 20% or 44,000 rpm. Figure 4-5 shows that most of the turbine wheel is stressed beyond the yield strength, but well below the ultimate tensile strength.

The nominal tensile stress at the blade root developed by the centrifugal force of the blade is 53,500 psi. Superimposed upon this is the bending stress caused by the pulses of hot gas impinging against the blades. This bending stress is 130 psi at the leading edge of the root of the blade. The total stress equals 53,630 psi. Applying a stress concentration factor of 1.7 for the blade root fillet area, the maximum stress is about 91,000 psi. This is well below the ultimate strength of 162,000 psi for the temperature existing at the blade root.

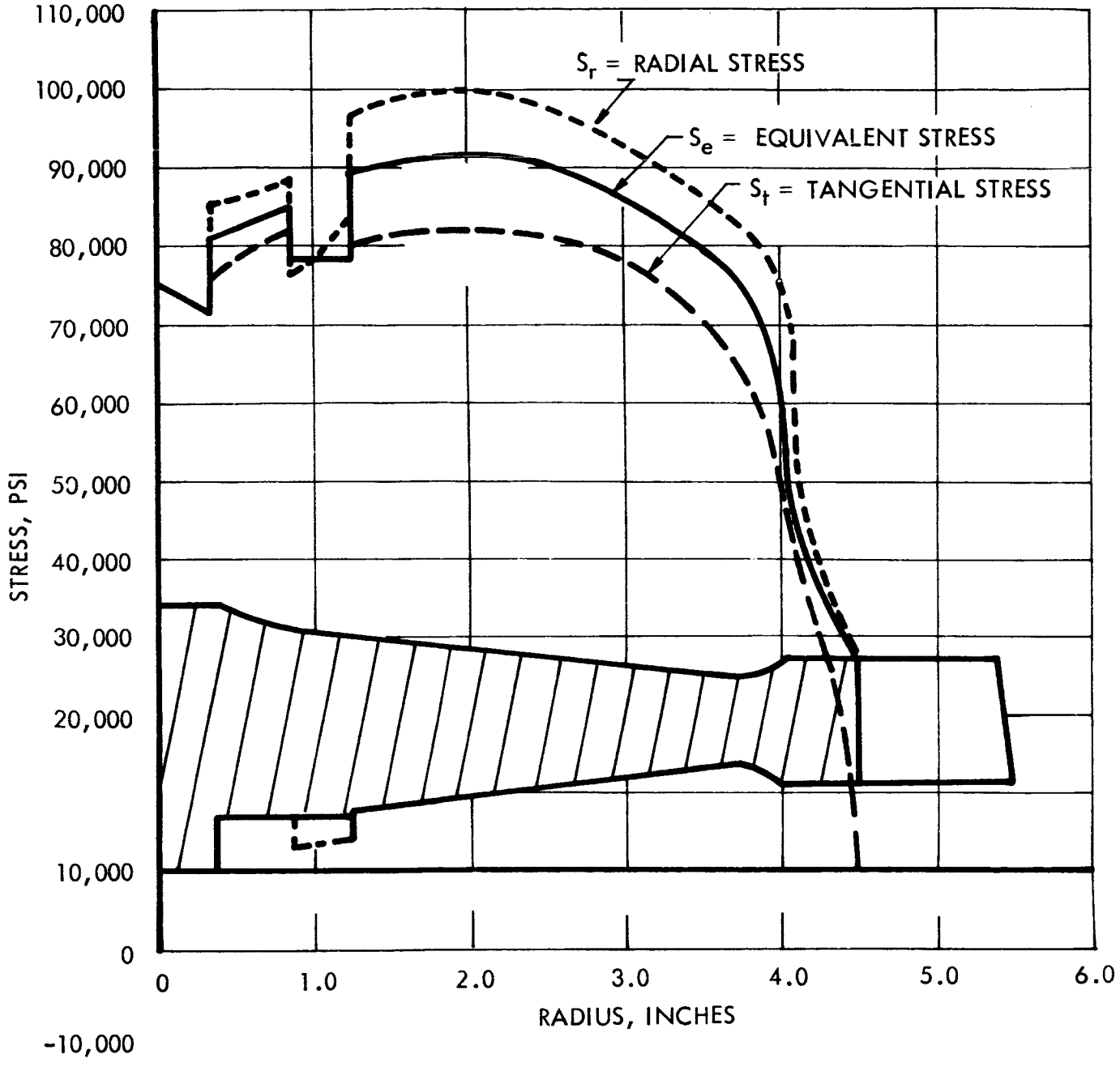

FIGURE 4-3 STATE OF STRESS
TURBINE WHEEL - 36,700 RPM

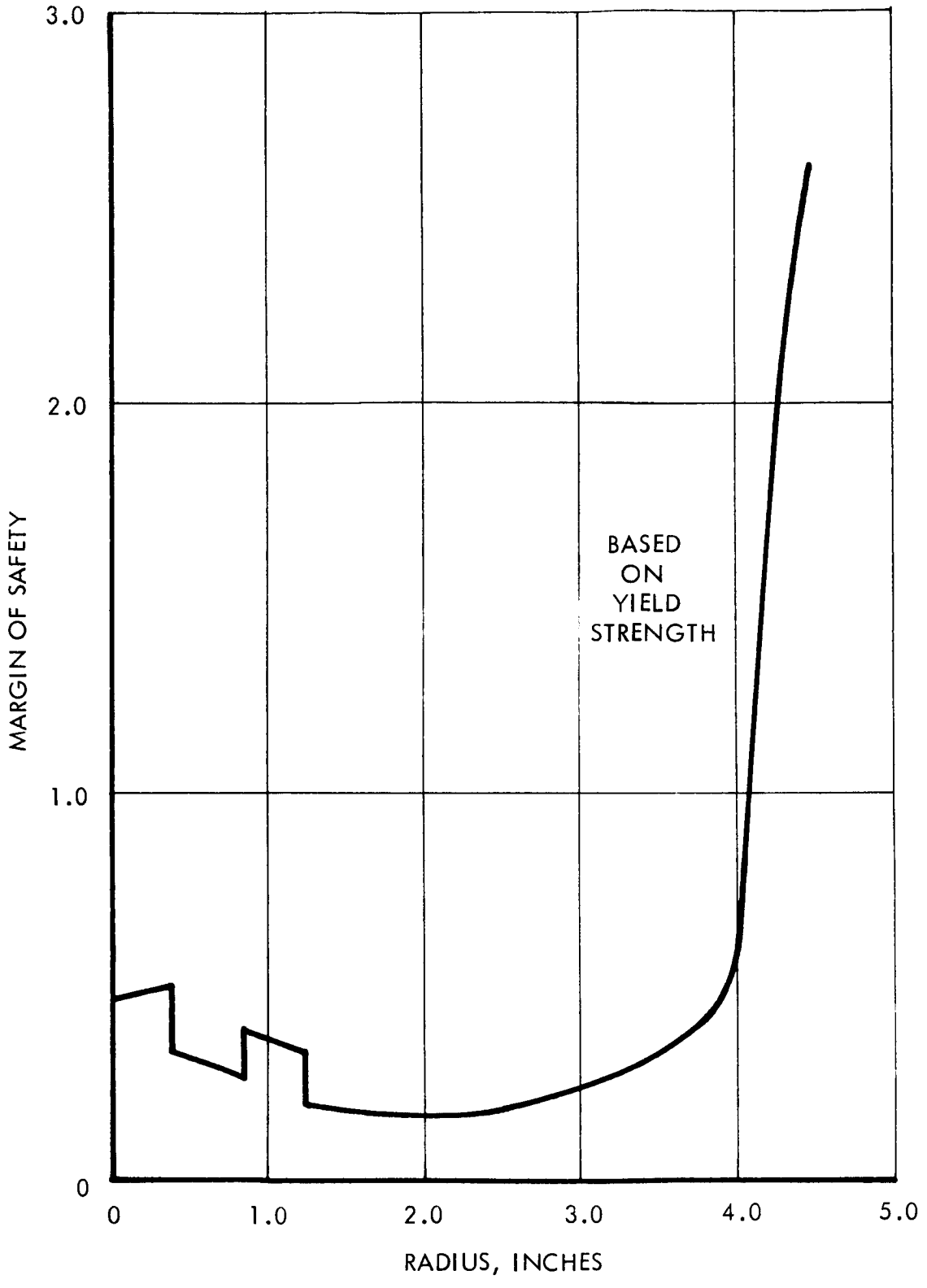

FIGURE 4-4 MARGIN OF SAFETY
TURBINE WHEEL - 36,700 RPM

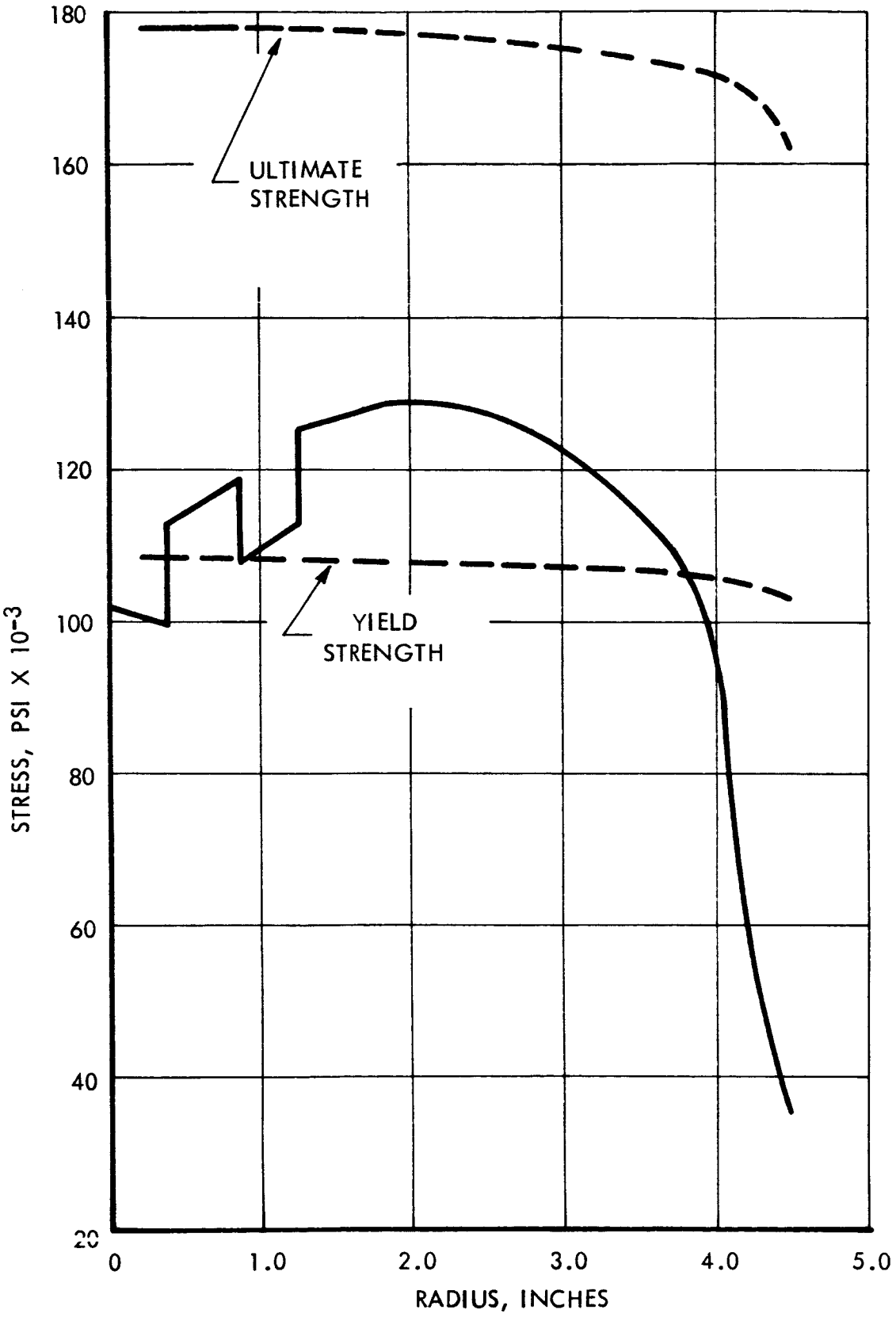

FIGURE 4-5 EQUIVALENT STRESS DISTRIBUTION TURBINE WHEEL 20% OVER SPEED

The blade natural frequency is approximately 7550 cps. This was computed by a numerical integration of the equation for virtual work for the static deflection of the blade. This natural frequency permits the blade to vibrate between 11 and 13 times for every revolution. As a blade passes each nozzle, it receives a pressure fluctuation, which causes a forced vibration of the blade as the turbine rotates. This forced vibration occurs 23 times during each revolution of the blade. The amplification factor for displacement caused by this forced vibration was calculated to be 0.47. Thus, it does not cause a magnification of displacement and stress at the blade root because the frequency of the forced vibration is much greater than the natural frequency of the blade.

Another forcing frequency exerted on the blades arises from the intermittent flow of the gas against the blades. This also may cause an amplification of the blade displacement. For operation in which the value of τ is 30 where

$$\tau = \frac{\text{pulse time + coast time}}{\text{pulse time}}$$

the amplification factor is 1.08. Amplification factor will decrease as τ increases because the log decrement characteristic of the material has a longer time to damp the vibration as the time between pulses increases. This amplification factor was used in computing the bending stress of 130 psi.

4.1.1.2 Critical Speed Analysis

The shaft critical speed was calculated with a computer program based on a finite difference method by M.A. Prohl[3]. Bearing stiffnesses were calculated as a function of load. After using various values of stiffness in the critical speed computation, it was determined that the variation of roller bearing stiffness had little effect on the critical speed. However, the variation of ball bearing stiffness had a marked effect on critical speed. Figure 4-6 shows the variation of critical speed with ball bearing stiffness when the roller bearing stiffness is 2.38×10^6 lb/in. Ball bearing stiffness is approximately 1.3×10^5 lb/in based on expected bearing load while roller bearing stiffness varies insignificantly over the expected bearing load. This results in a critical speed of approximately 12,000 rpm according to Figure 4-6. The rigid support critical speed is seen to occur at approximately 56,000 rpm where the ball bearing stiffness is 7×10^7 lb/in. Since the bearing is never loaded enough to achieve this stiffness, this critical speed will not be reached.

4.1.1.3 Seals

Three types of seals were used in the turboalternator: (1) shaft face seal, (2) 0 ring seals, and (3) piston ring seals.

The alternator and bearing cavities are isolated from the ambient vacuum by a metal bellows seal to prevent the interchange of oil and hot gas between the turbine and bearing areas. One end of the bellows is welded to a cup which is retained in the

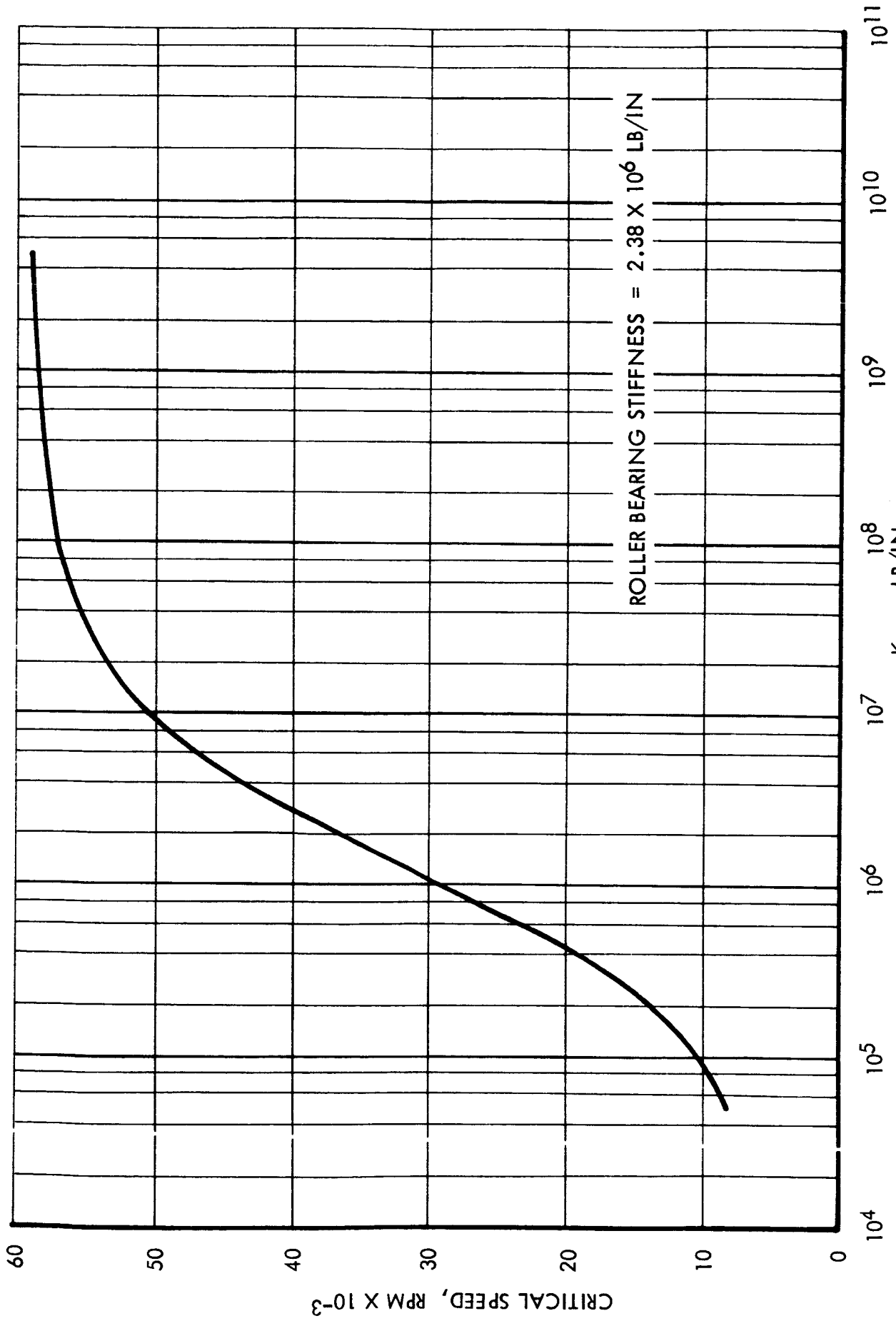

FIGURE 4-6 CRITICAL SPEED VERSUS BALL BEARING STIFFNESS

bearing and seal housing. A carbon insert is attached to the other end of the bellows. The insert seals against the mating ring which is clamped in place on the shaft by the ball bearing inner race. The seal retainer is designed to accept seals made by Sealol Inc. and Koppers Co.

Viton 0 ring seals are used in several areas to prevent oil escaping from inside the alternator housing. An 0 ring seals the path between the seal retainer and the turbine bearing housing. This prevents oil escaping from the ball bearing and seal area to the inlet side of the turbine wheel. Another 0 ring is used in the alternator housing on the roller bearing end to seal the leak path between the alternator end cap and alternator housing. Two 0 rings, one on each side of the roller bearing lube inlet orifices, prevent leakage from the roller bearing area. Finally, 0 rings seal the two ball bearing oil jet inserts, the thermocouple and field coil connectors, and the magnetic pickup.

A piston ring seals the cavity on the inlet side of the turbine wheel from ambient vacuum. There is approximately a .025 in. gap between the alternator front flange and the nozzle-scroll assembly inside diameter. To prevent gas from escaping during each pulse, a high temperature ductile iron piston ring fills the gap. An Inconel X expander ring inserted between the ring inside diameter and the alternator outside diameter forces the piston ring to contact the nozzle-scroll inside diameter.

4.1.1.4 Bearings

A ball and roller bearing suspension supports the rotating assembly. This suspension offers flexibility with regard to differential expansion between the stator and shaft assembly. Thermal analysis indicated that the rotating assembly would expand more than the stator in the axial direction. The roller bearing permits differential expansion without a change in axial load on the ball bearing. Thrust toward the turbine disk end is maintained on the ball bearing by magnetic means during the coast period and by the gas loads on the turbine disk plus the magnetic load during the pulse period. The magnetic thrust is achieved by designing the alternator parasitic gap on the turbine end with a section which provides a .025 in. axial gap between the alternator rotor and housing. On the opposite end no axial gap is used and a .50 in. clearance exists between the rotor and the end cap.

The difference in clearance causes a magnetic attraction of the rotating assembly in the direction of the smaller clearance, i.e. toward the turbine. This force, which is about 15 lbs, exists at all times during alternator operation. The gas force at a calculated nozzle exit pressure of .69 psia existing at the 0.9 0/F ratio is approximately 65 lbs. Thus, the thrust on the ball bearing varies from 15 lbs. to 80 lbs. and is always in the turbine direction.

The ball bearing, located between the turbine wheel and alternator rotor, is a Marlin Rockwell 9205-U-16-ST. This is a split inner ring bearing which is necessary for assembly and provides high load carrying capacity. It is an ABEC 5 bearing with internal looseness of .0014 in. to .0024 in. The balls and races are heat stabilized to 800°F.

The roller bearing is a Marlin Rockwell R-203-E. The bearing conforms to RBEC 5 with an internal looseness of .0006 in. to .0010 in. The crowned rollers are held in the retainer which rides on the outer race. This configuration, rather than an inner race riding retainer, was selected because of its better capability for high speed operation. The retainer riding on the outer race is lubricated by oil introduced in the gap between the retainer and the inner race.

4.1.2 Thermodynamic Design

The turbine is a single stage, full admission impulse type. It is capable of operation at O/F ratios of 0.9 or 2.7 with approximately the same power output at each condition. The conditions to which the turbine was designed appear in Table 4-2.

Table 4-2. Turbine Design Conditions

	O/F = 2.7	O/F = 0.9
Inlet pressure, psia	100	100
Inlet temperature, °R	4820	3700
Exhaust pressure	vacuum	vacuum
Instantaneous propellant flow, lb/sec	0.3	0.3
Pitch line velocity, fps	1600	1600
Calculated nozzle heat loss, Btu/lb	350	350
Calculated rotor heat loss, Btu/lb	204	204

Thermodynamic data for design of the turbine were obtained from a Mollier chart developed from thermochemical calculations described in ER-6630. The turbine geometry was based on the 2.7 O/F ratio conditions, and the performance at the 0.9 O/F ratio was to be satisfactory with this configuration. Equilibrium flow was assumed in the expansion from 100 psi to .69 psia after which frozen composition was assumed to exist.

The calculated thermodynamic parameters appear in Table 4-3.

Table 4-3 Turbine Thermodynamic Parameters

	0/F = 2.7	0/F = 0.9
Pressure ratio	145	210
Ideal available enthalpy, Btu/lb	1150	1190
Actual nozzle exit velocity, fps	7200	7320
Rotor relative inlet velocity, fps	5710	5840
Rotor relative inlet angle, degrees	25.5	25.4
Blade static temperature, °R	2060	1058
Rotor relative Mach. No.	2.63	3.0
Rotor velocity ratio	.22	.22
Turbine efficiency	.38	.36

The turbine nozzles are a transition from circular cross section at the throat to trapezoidal cross section at the exit This configuration conserves space at the nozzle exit and permits more exit area at a given circumference than does the conical nozzle design. In addition, the trapezoidal exit provides better matching of the nozzle exit with the rotor inlet. The nozzle design parameters appear in Table 4-4.

Table 4-4 Nozzle Design Parameters

Number of nozzles	23
Throat diameter, in.	.159
Maximum divergence angle, degrees	30
Area ratio	16.5
Trailing edge thickness, in.	.055
Exit pressure, psia	
0/F = 2.7	.69
0/F = 0.9	.48
Inlet angle, degrees	20

There are 101 impulse blades on a 10 in. pitch diameter. The high relative entering Mach number of 2.6 requires a high solidity (chord/pitch) and thin leading edges for good efficiency. However, heat transfer and fabrication considerations required a compromise on solidity and leading edge thickness. This resulted in a lower turbine efficiency, but increased the capability of the blades to accept the extremely high

temperature gas. To insure that the blade leading edges would not reach too high a temperature during a pulse, the edge thickness was made .030 in. To keep the number of blades to a minimum, which reduced the cost of fabrication, a solidity of 2.4 was used. A summary of turbine rotor dimensions appears in Table 4-5.

Table 4-5 Turbine Rotor Dimensions

Pitch diameter, in.	10.0
Inlet tip diameter, in.	10.875
Inlet root diameter, in.	9.0
Exit tip diameter, in.	11.0
Exit root diameter, in.	9.0
Pitch	.311
Entrance angle, degrees	28
Exit angle, degrees	28
Leading and trailing edge thickness, in.	.030
Axial chord, in.	.75
Number of blades	101

4.1.3 Alternator Design

The basic TRW brushless alternator has been applied to the power system, with a specific design generated for this application. The unit generates three phase AC power in a conventional wye connected stator. A solid four pole rotor is formed by electron beam welding of magnetic pole pieces and a nonmagnetic separator. Field excitation is produced by field coils mounted on the stator. Flux produced by these coils enters the rotor through parasitic air gaps at each end of the stator.

All of the basic design parameters for the alternator can be summarized as follows:

Power Level:	6 KW continuous at unity power factor
Overload:	7.2 KW for two minutes
Short Circuit Capability:	300% current for five seconds
Speed:	33,000 rpm
Output Voltage:	23 volts, line to line
Frequency:	1100 cps at 33,000 rpm
Connection:	3 phase, 4 wire, wye connection

There are several design features incorporated in the alternator to meet the specific demands of the power system. The output voltage level was selected to permit direct rectification for a 29 volt DC output. A margin was included for rectifier drops and the effects of rectifier commutation and waveform distortion. The rotor is hollow to permit assembly to the turbine shaft. The parasitic gaps are designed so that the excitation will produce a forward thrust on the rotor. This force is sufficient to maintain the proper loading on the bearings during the coast period between hot gas pulses. All materials selected for the alternator provide a design compatible with the thermal demands of the unit and the available oil cooling.

4.1.3.1 Alternator Operation

The cross section of thebasic TRW Brushless Alternator is shown in Figure 4-7. A conventional polyphase stator (1) is supported by a magnetic housing (2). DC excitation is provided by coils (3) wound on nonmagnetic spools (4). The excitation coils are also supported by the housing (2). The rotor is constructed from two identical magnetic pole sections (7) and (8) and a nonmagnetic spacer (6). An isometric view of a four-pole rotor is shown in Figure 4-8.

The magnetic flux produced by the excitation coils travels axially in the housing section (2) to the end bell (5) and enters the rotor through the radial parasitic gap (9). The flux then travels axially into the poles of rotor (7) and enters the stator through the radial gap (11). The flux continues circumferentially around the back iron of the stator and then returns radially across the gap (11) to the pole section (8). The magnetic path is completed through the parasitic gap (10) returning the flux to the housing end bells (5). Pole sections (7) and (8) establish the flux distribution in the gap and are opposite in polarity due to the directions of the flux established in the sections. The flux travels with the rotor and generates voltage in the stator winding. It is important to note that the magnetic section of the stator is 100% effective in producing power, as in a conventional salient pole alternator.

The rotor pole pieces are tapered in three directions to provide the minimum section required for the rating, since the flux requirement decreases linearly to zero from the root to the tip of each pole. This limits the leakage flux between poles and reduces the mass of the pole pieces to improve the mechanical design. The solid rotor serves as a damper winding for transient and unbalanced load operation.

Controlled DC excitation power for the alternator is supplied by the static voltage regulator which, in turn, obtains power from the alternator output. The relatively long magnetic path of the housing, end plates, and rotor provides a residual MMF sufficient to produce initial voltage buildup. However, to insure voltage buildup under stringent environmental conditions and to provide the radial magnetic load during starting, a field flash is used in the unit.

The voltage level is a function of the air gap flux and the speed. Any change in the load will automatically change the armature reaction. This, in turn, produces a change in the output voltage. The voltage regulator will then adjust the excitation

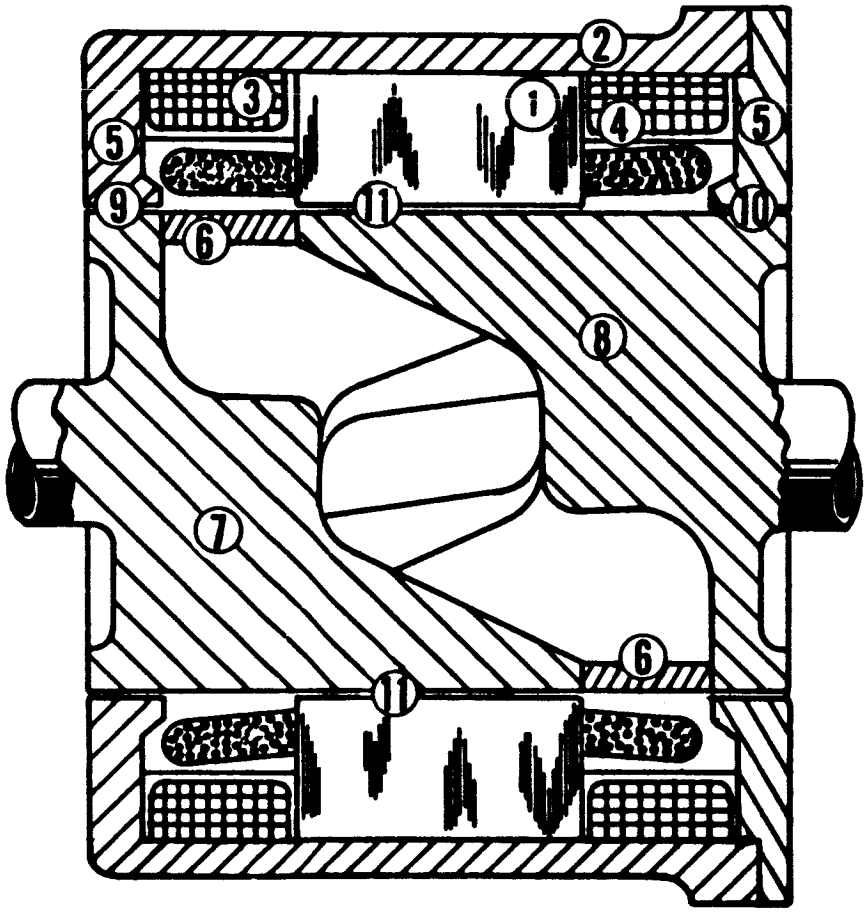

FIGURE 4-7 TRW BRUSHLESS ALTERNATOR

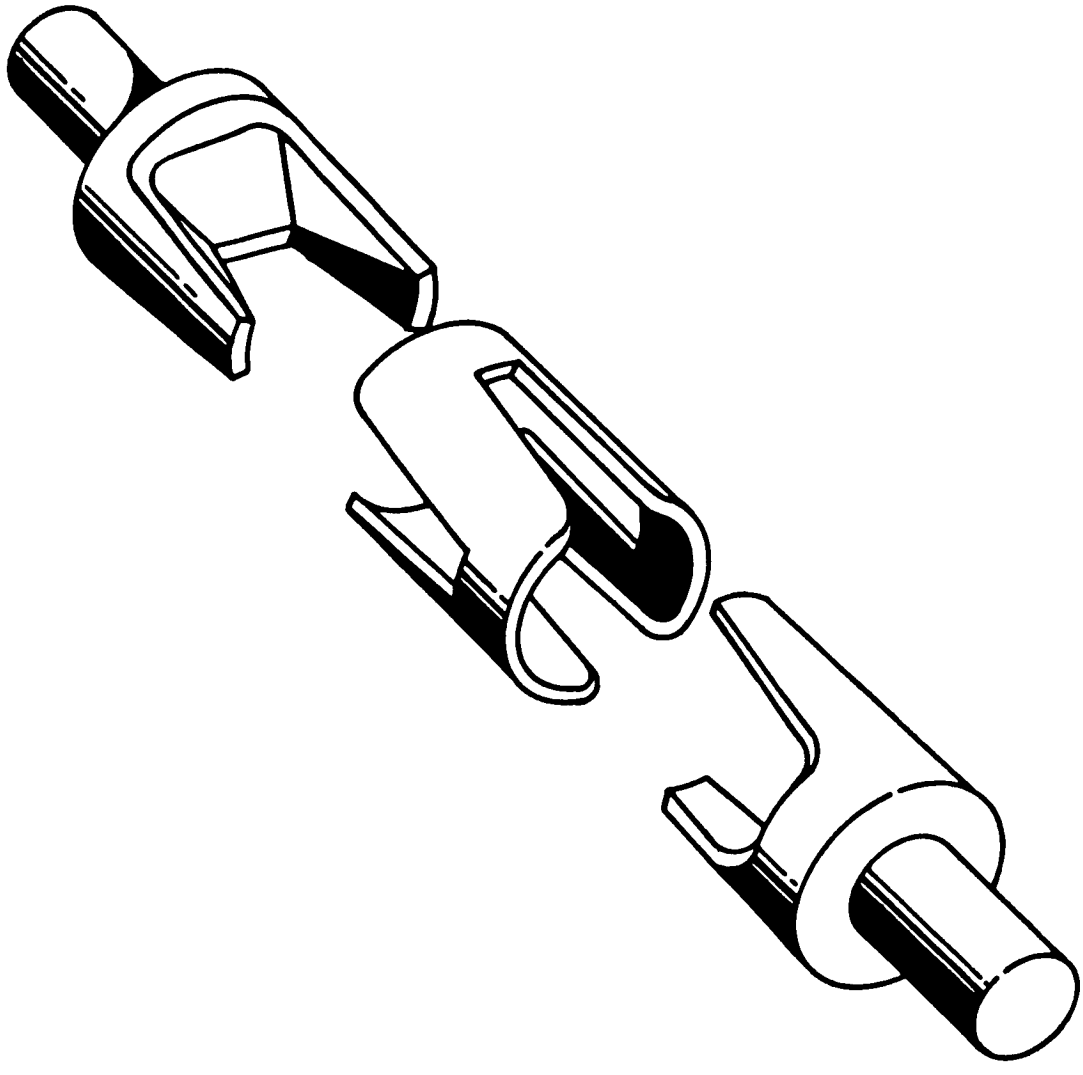

FIGURE 4-8 4 POLE ROTOR CONSTRUCTION SCHEMATIC

power to compensate for the change in armature reaction and return the voltage to the nominal value.

4.1.3.2 Detailed Alternator Design

The details of the alternator design are best shown by the assembly drawing for the complete unit presented in Figure 4-1. The alternator rotor is 2.55 inches in diameter and 4.24 inches long at the outer surface. The magnetic pole pieces are fabricated from 4320 steel, and the nonmagnetic separator is Inconel X. These pieces are formed into a smooth rotor by electron beam welding prior to final machining. The rotor is mounted to the turbine shaft by providing a one inch diameter hole through most of the rotor length. The alternator rotor and turbine shaft are pinned to provide a positive coupling. The turbine shaft extends through the rotor at a smaller diameter. Bearings are mounted to the shaft and a nut is used to retain the rotor. A view of the alternator rotor assembled to the turbine is presented in Figure 4-9. Close examination of this photograph will reveal the configuration of the pole piece and separator.

The stator winding is also indicated on Figure 4-1. The stack assembly is 1.2 inches long with an inner diameter of 2.60 inches and an outer diameter of 4.26 inches. The field coil assemblies are mounted on either side of the stator stack. Both windings contain 95 turns of #16 copper wire. The rear field coil is made longer and narrower to permit easier assembly. Field coil leads are brought out through the sealing gland pointing downward as indicated on Figure 4-1. Five thermocouples were included in the unit and these are shown leaving the unit from the top through a second sealing gland. Output leads from the stator are brought out through four conductor sealing glands at the rear of the assembly. A separate lead is provided for each phase and for the neutral. All stator and field windings use heavy ML insulation. The stator is impregnated with ML varnish.

Passages for cooling oil are provided around the outside of the alternator housing. The end bells contain the parasitic gaps. As indicated on the turbine end in Figure 4-1, the parasitic gap at the end includes a portion on the front surface of the rotor. This gap provides the forward thrust required on the rotor. The overall diameter of the alternator housing is 4.95 inches. The effective length of the alternator housing is 4.312 inches. A view of the housing is provided in Figure 4-9.

In addition to the detailed alternator design, calculated performance characteristics were also determined for the alternator. A complete set of constants were calculated. These constants were used in an analog computer study for the turboalternator. The results of the computer study, along with the alternator constants, are presented in ER-6715, "Analog Computer Analysis of Pulsed Energy Turboalternator."[4]

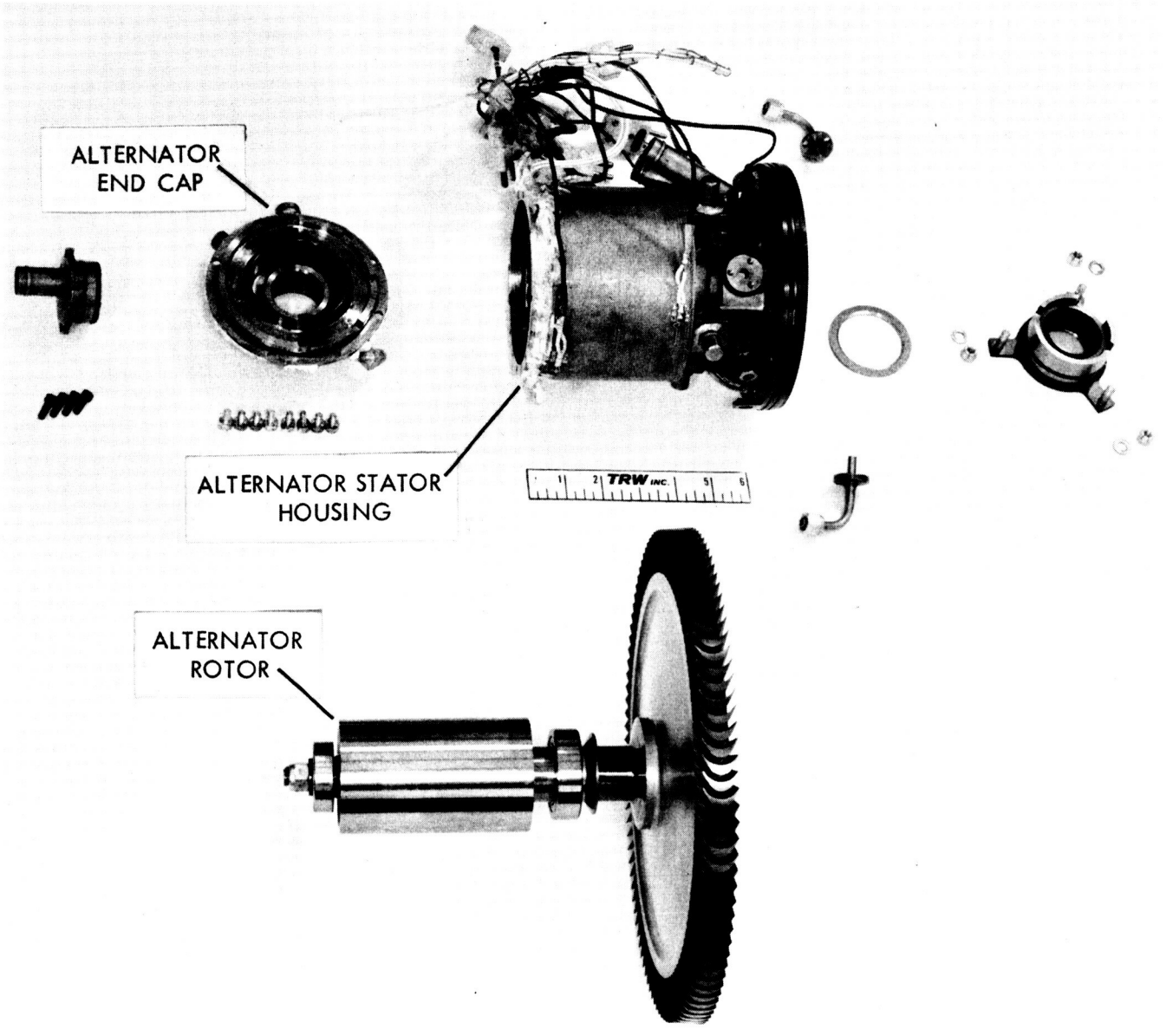

FIGURE 4-9 ALTERNATOR COMPONENTS

4.1.4 Gas Generator

The gas generator assembly consists of the generator chamber, the injector head, and the bipropellant valves. The injector head is welded to the chamber and the bipropellant valves are bolted to flanges on the injector head.

The gas generator operates at an 0/F ratio of 0.9 or 2.7. Two separate sets of oxidizer and fuel orifices and one bipropellant valve for each 0/F ratio permit operation at either condition. A schematic diagram of the gas generator assembly appears in Figure 4-10. Each bipropellant valve feeds oxidizer and fuel to capillary tubes connecting the valve flange to the injector head. The propellants pass through the injector head and meet in a predetermined pattern in the reaction chamber where they react to form the hot gas. The valve mounting flanges are constructed to permit the insertion of different orifice sizes so that compensation may be made for variations in fabrication tolerances of the tubes and orifices.

The orifices are arranged in the injector head in four concentric circles with six holes in each circle. The orifices, moving from the outer to the inner circle, are for the 0.9 0/F oxidizer, 2.7 0/F oxidizer, 0.9 0/F fuel, and 2.7 0/F fuel, respectively. Each orifice, with the exception of the 2.7 0/F fuel orifices, is fed propellant from the bipropellant valve by a single capillary tube. The circle of 2.7 0/F fuel orifices is fed from a cavity to which a single capillary tube is connected. The orifices are drilled at angles such that initial impingement occurs at 0.2 in. from the outlet of the orifice. The momentum of each propellant stream was designed so that the momentum of the mixture after reaching the initial point of impingement would cause each mixed stream to converge at a point further downstream of the injector.

This feature was accomplished by selecting the necessary injection angle stream velocity and stream diameter so that a reimpingement angle of 5° resulted. Thus, mixing and efficient combustion of fuel and oxidizer were assured. Table 4-6 presents the design data for the gas generator.

Tests of small rockets have produced pressure spikes in the rocket chamber when conditions of high vacuum, low propellant temperatures and low metal temperatures exist simultaneously. To avoid this condition, a helium pressurization system is activated for 100 milliseconds during the first pulse of each run. The helium solenoid valve is energized 50 milliseconds prior to energizing the bipropellant valve so that the gas generator chamber is subjected to full design helium pressure by the time the propellants enter the chamber. The helium system is designed to provide 5 psia in the generator chamber. This is adequate to eliminate one of the three necessary conditions, high vacuum, for chamber spiking. On subsequent pulses, the metal temperatures are high enough that the third necessary condition for spiking is eliminated, and chamber pressurization is no longer needed.

A major consideration in the design of the gas generator was control of the propellant and metal temperatures. It was necessary to prevent the propellants from vaporizing

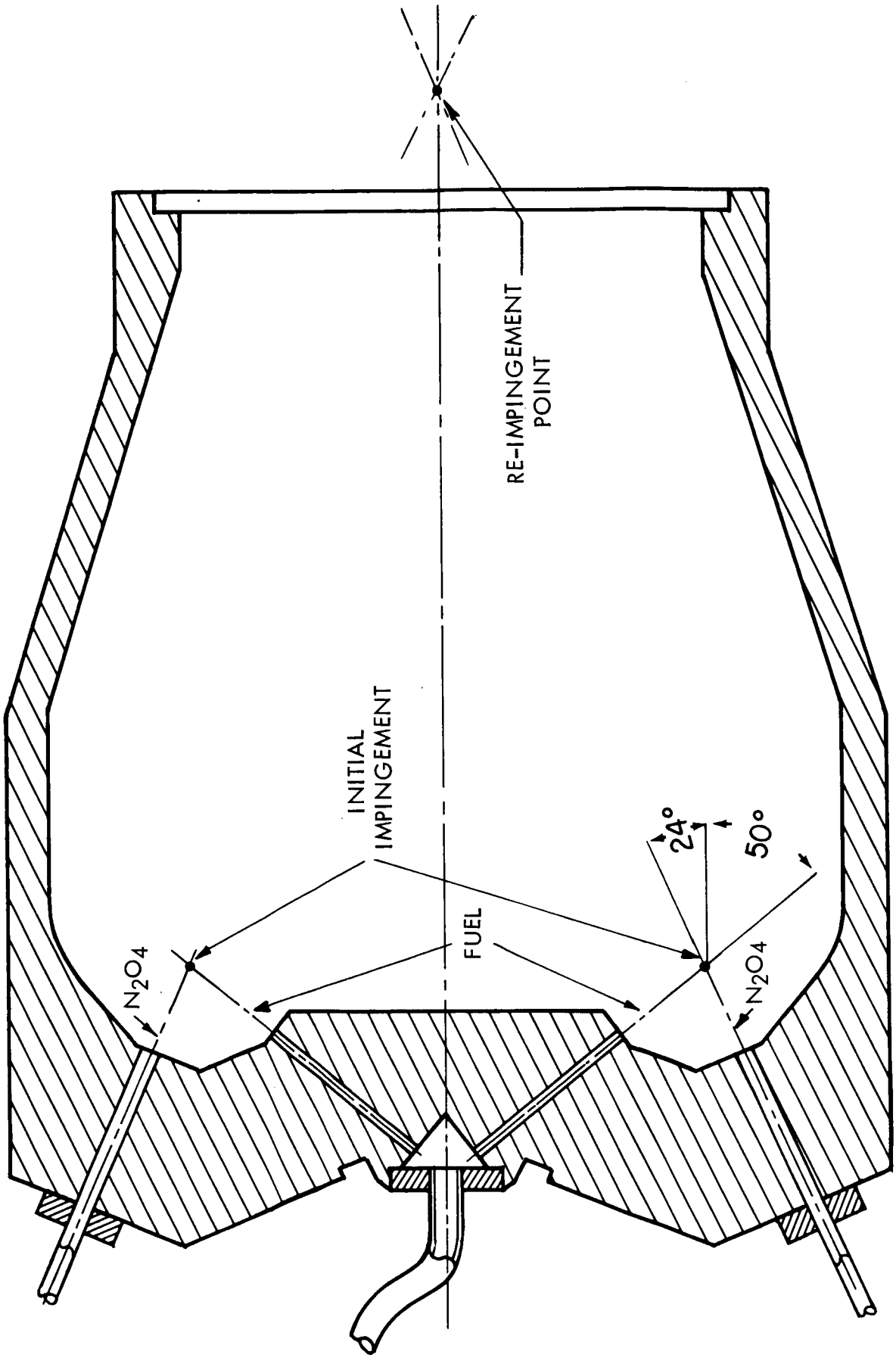

FIGURE 4-10 GAS GENERATOR FOR 2.7 O/F RATIO

Table 4-6 Design Data for Dual Gas Generator

$0/F = 0.9$

	Oxidizer	Fuel
Number of inlet tubes	6	6
Tube inside diameter, in.	.032	.036
Tube length, in.	3.0	2.50
Number of orifices	6	6
Orifice diameter, in.	.035	.041
Orifice velocity, ft/sec	40.4	52.9
Impingement angle	49°	23°
Flow rate, lb/sec	.142	.158
Chamber pressure, psia	100	

$0/F = 2.7$

	Oxidizer	Fuel
Number of inlet tubes	6	1
Tube inside diameter, in.	.041	.059
Tube length, in.	3.5	2.0
Number of orifices	6	6
Orifice diameter, in.	.035	.028
Orifice velocity, ft/sec	58.9	56.1
Impingement angle	23°	49°
Flow rate, lb/sec	.2192	.0808
Chamber pressure, psia	100	

before impingement. Otherwise, inefficient combustion and 0/F ratio shift would occur. This required maintaining propellant temperatures well below the temperature at which vaporization would occur.

To achieve this objective, several items were considered in design. The heat conduction path between the gas generator and the injector head was minimized by reducing the wall thickness as much as possible within safe structural limits. This reduced heat transfer from the hot gas generator to the cooler injector head to a minimum. The injector face area was minimized to reduce the area exposed to heat transfer by convection from the hot gas directly to the injector head. High thermal conductivity silver braze heat sink material was potted behind the injector head and around the propellant inlet tubes. This permitted heat transfer away from the injector head to the outer ring of the injector where it could be transferred to the propellant in the inlet tubes. This heat path was carefully balanced to prevent excessive heat flow into the propellants with resulting vaporization within the tubes.

It was necessary to maintain the bipropellant valve seats below 200°F so that the Teflon seats would not be distorted. Therefore, the valve mounting flanges were isolated from the high conductivity silver braze by an epoxy potting compound which minimized heat soak back from the injector head to the flange. In addition, the epoxy potting served as structural reinforcement to the small capillary tubes in the event of an overpressure within the tubes.

Geometric configuration of the gas generator was also important in preventing propellant vaporization before impingement. The propellant dribble volume, i.e. the volume of propellant between the bipropellant valve and injector face, was minimized by making the inlet tubes as short as possible. This reduced propellant stay-time within the tubes and minimized the possibility of the liquid flashing to vapor before reaching the point of impingement.

A second geometric factor was the injection angle. This factor was optimized so that the distance from the injector face to the impingement point was a minimum within the limitation of minimum heat transfer back to the injector face. As the impingement point approaches the face, heat transfer increases, while an impingement point further from the face increases the possibility of vaporization in transit. A distance of 0.2 in. was determined to be the best compromise.

4.1.5 Controls and Power Conditioning

The electrical controls and power conditioning system are basically the same as those presented in ER-6630, "Optimization Studies". Starting controls and protective or safety circuits were incorporated in the system and during the test phase additional safety circuitry was added to the test facility control panel.

The controls and power conditioning circuits were breadboarded and bench tested using simulated inputs and loads prior to actual testing with the turboalternator.

Pictures of the breadboard control are shown in Figures 4-11 and 4-12.

A simplified block diagram of the electrical system is shown in Figure 4-13. The blocks shown "dotted" are test cell controls external to the system controls. A magnetic pick-up mounted in the end cap of the alternator assembly, senses turbine shaft speed independent of the alternator electrical output. Its signal is used to lock out relays which pass the bipropellant valve signals and alternator field voltage, and to close valves in the fuel and oxidizer lines upstream of the bipropellant valves. An overtemperature trip utilizing an API Sym-Ply-Trol was used to initiate a shutdown in the same manner as above if the turbine scroll temperature exceeded the pre-set level.

A more detailed block diagram of the electrical system is shown in Figure 4-14. The system is started using an external 28 volt DC power supply which is automatically cut out of the system when operating speed is reached and automatic transfer to the speed control has occurred. An external DC voltage source is also used to provide the alternator with sufficient field voltage (about 6 VDC) to allow the initial voltage buildup. The voltage regulator is switched in at transfer from the start up circuit to the speed control and the external source is cut out. The point at which the voltage regulator takes over will be changed to a 90% speed point. This will allow all transients to end before the speed control assumes control. At present the voltage regulator is allowed to take over by reducing the external field flash voltage to zero after the speed control has taken control.

Two electronic safety circuits are provided. One, an undervoltage trip, senses the output voltage level and initiates a shutdown should the voltage drop below a preset level as could occur if one phase of the alternator opens or shorts. The operation of this circuit is delayed for the first several minutes of the start sequence after which it begins to sense the output voltage. If the output voltage is not above the set point at this time it shuts down the system never allowing the start sequence to finish.

The second safety circuit provided is an electronic overspeed sense. This circuit senses the alternator output frequency, which is proportional to speed, and initiates a shutdown should an overspeed occur. This circuit is set slightly below the magnetic pickup set point. Because this circuit would not detect an overspeed should the alternator output be lost, it would be desirable to replace it with the magnetic pickup.

A more detailed description of the individual circuits follows.

4.1.5.1 Voltage Regulator

The voltage regulator is essentially the circuit presented in ER-6630 with only minor modifications. A schematic is shown in Figure 4-15. The power stage of this regulator is a three phase, full wave, half wave control bridge circuit utilizing silicon-controlled rectifiers (SCR's) and silicon diodes. This circuit operates directly from the alternator AC output and supplies the DC excitation voltage to the alternator field. The field excitation voltage is controlled by varying the conduction period of the SCR's.

BOARD #3
TRANSFER AND
PROTECTIVE CIRCUITS

BOARD #2
SPEED CONTROL

BOARD #1
START CIRCUIT

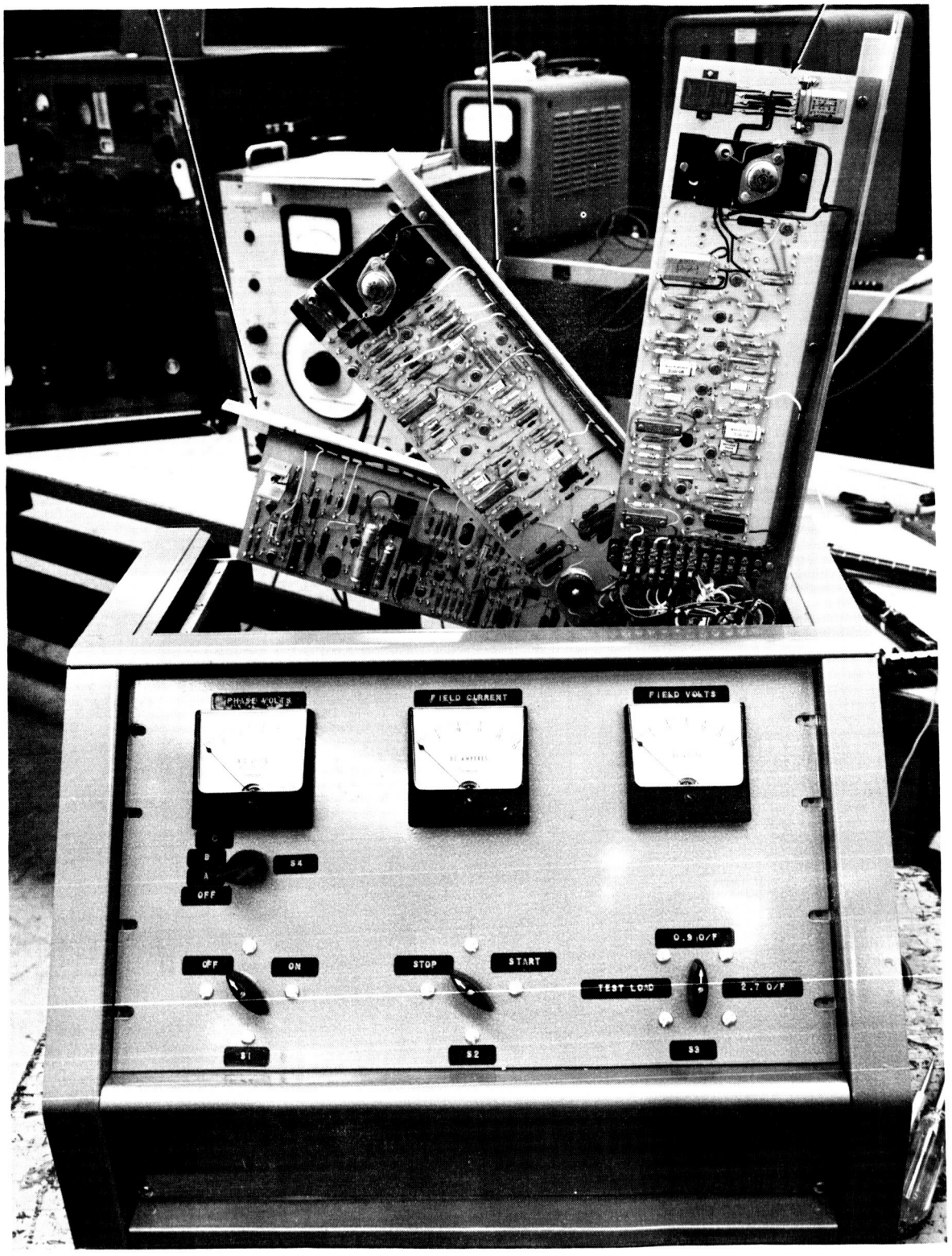

FIGURE 4-11 FRONT VIEW OF BREADBOARD CONTROL CABINET WITH CONTROL CIRCUIT BOARDS EXPOSED

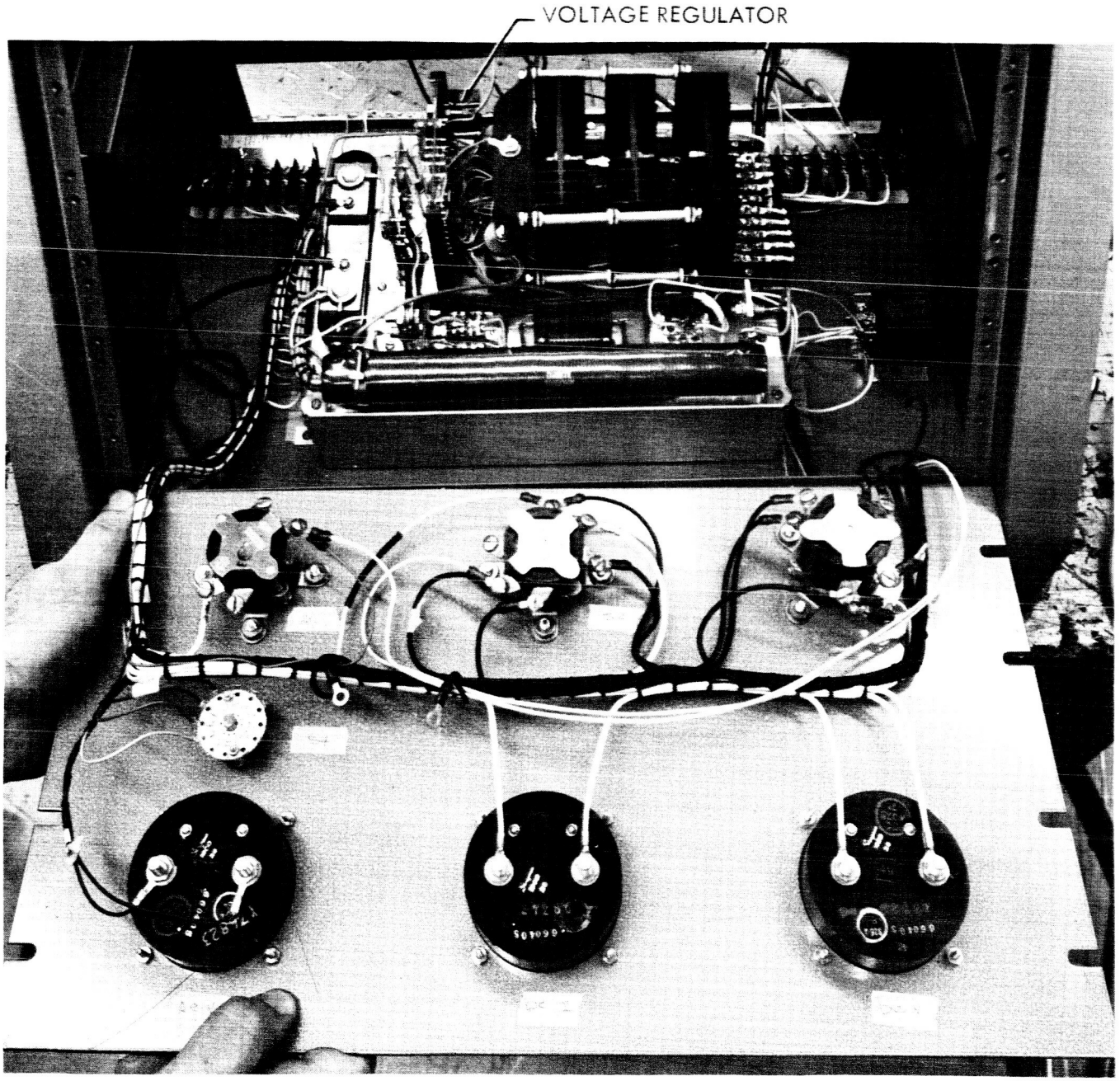

INTERNAL VIEW OF A BREADBOARD CONTROL CABINET SHOWING THE VOLTAGE REGULATOR

FIGURE 4-12

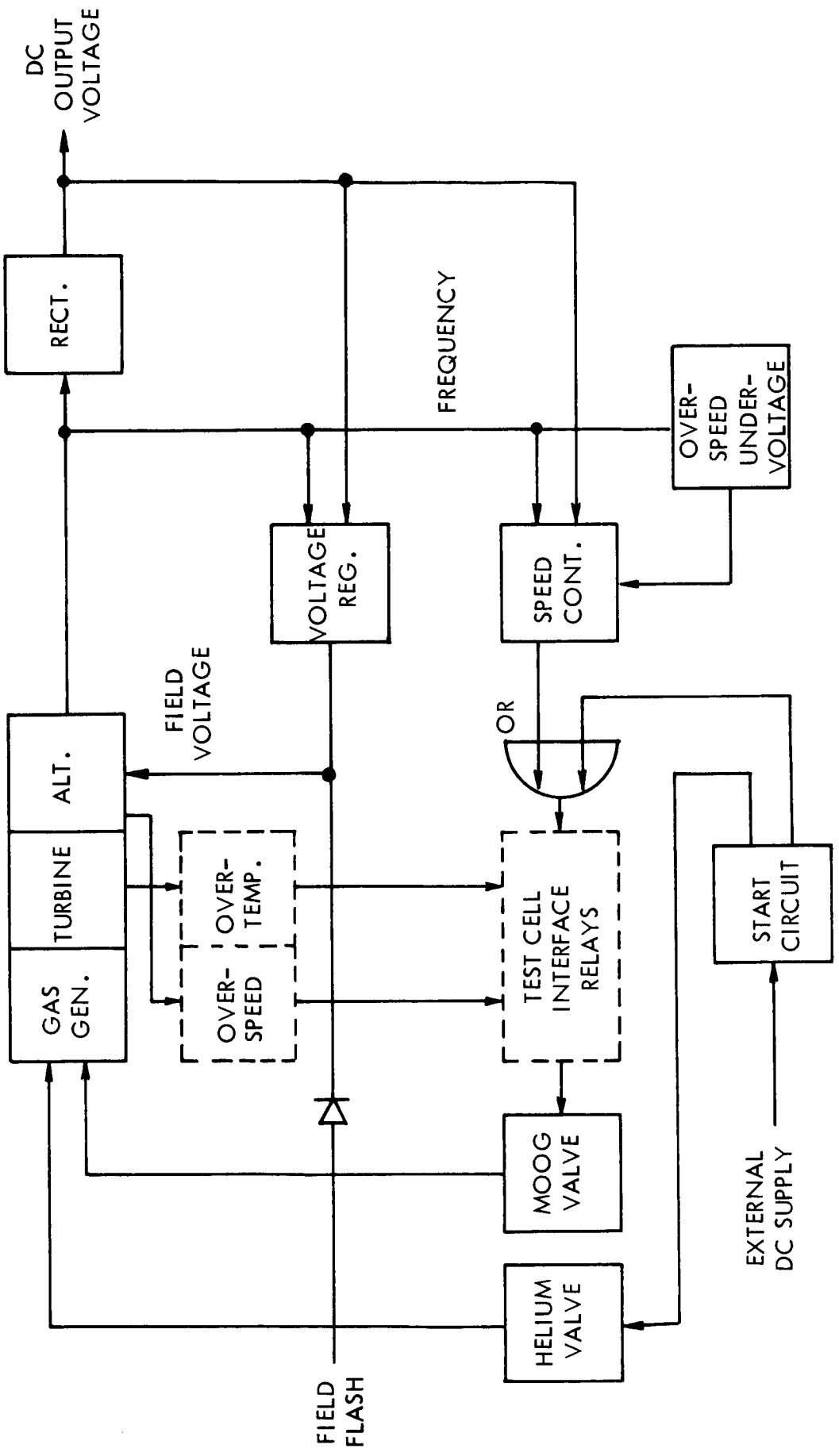

FIGURE 4-13 SIMPLIFIED BLOCK DIAGRAM ELECTRICAL SYSTEM

FIGURE 4-14 DETAILED ELECTRICAL S

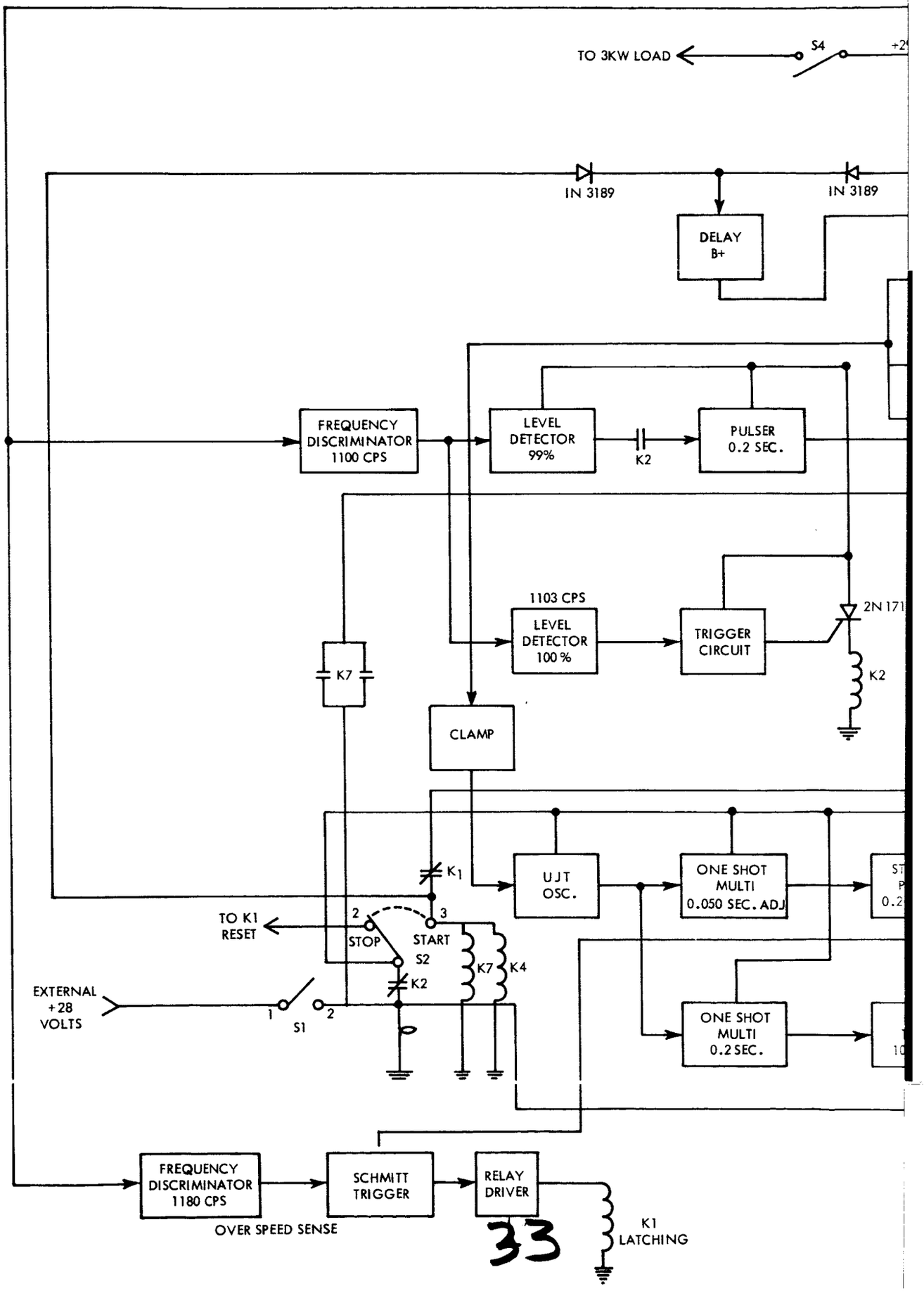

YSTEM DIAGRAM

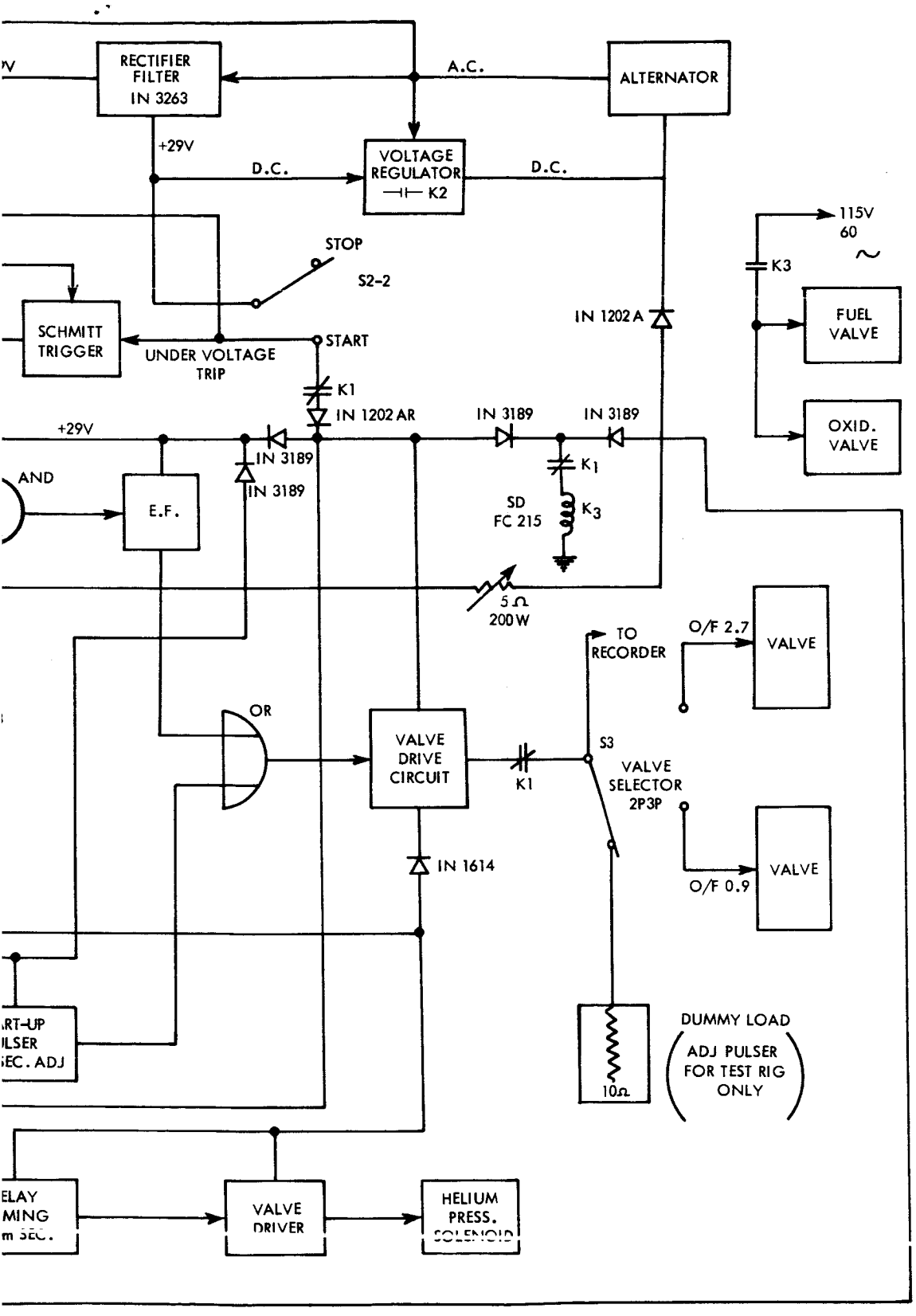

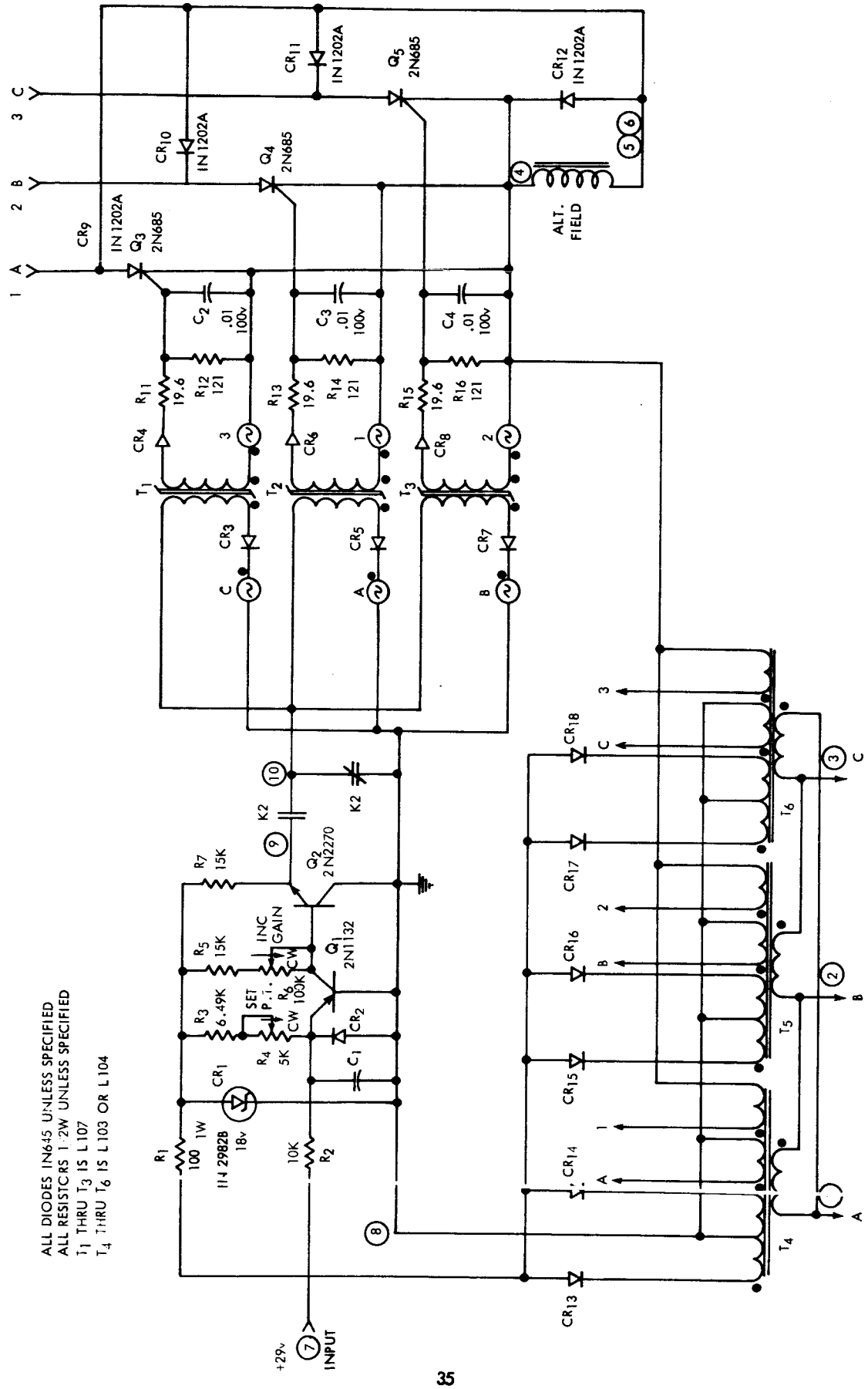

FIGURE 4-15 VOLTAGE REGULATOR SCHEMATIC

Transformers T_4, T_5 and T_6 operate directly from the alternator output and supply the logic power to the phase modulators, T_1 through T_3, as well as the negative bias voltage to the reset control amplifier, Q_1 and Q_2.

The bias voltage for the reset amplifier, Q_1 and Q_2, is obtained from the alternator output by diodes CR 13 through CR 18 connected in a six phase star configuration and regulated to a lower level by CR1.

The phase modulator circuits used to modulate the SCR firing angles are operated by a common reset control amplifier. The set and reset voltages are provided by transformers T_4, T_5 and T_6, thus the voltage for each phase modulator is 120 degrees apart and the reset voltage is 180 degrees out of phase with the set voltage for a given phase modulator. Therefore, the output of each phase modulator has the same pulse width but the leading edge of each output is 120 degrees apart. The reset amplifier controls the reset voltage to each core. Transistor Q_1 is used in the grounded base configuration and therefore provides a current summing point that is very near circuit common. The input current to the emitter is the sum of the currents through R_2 and R_4. As the DC output voltage decreases, the emitter voltage of Q_1 decreases allowing less current to flow through the collector of Q_1 increasing the voltage to the base of Q_2. Q_2 is an emitter follower which provides a low impedance voltage source to the reset windings similar in magnitude to the signal applied to its base. Therefore, the emitter voltage of Q_2, with respect to the circuit common increases. The reset voltage applied to each core is the supply voltage (T_4, T_5 or T_6) minus the voltage on the emitter of Q_2. As the output voltage of the emitter of Q_2 increases, the reset voltage to each phase modulator decreases allowing the core to fire earlier in the cycle. This in turn fires the SCR's earlier in the cycle thus increasing the average DC field excitation voltage.

This type of voltage regulator can be accurately preset to provide the proper DC output voltage and maintain the regulation within the ± 1% limit. The three phase, full wave, half wave control configuration also has the advantage of presenting a balanced load to the alternator.

Figure 4-16 shows the gain characteristics of this regulator and the limits over which it can be adjusted. With the particular values of R_3, R_5, and R_6 shown, the gain can be adjusted from 3 volts/volt to 18 volts/volt. The set point is adjustable by means of R_4 and the gain is adjusted by R_6.

Figure 4-17 shows the voltage regulator gain characteristic during actual operation with the alternator. Its gain is about 8 volts/volt. In order to improve its regulation the gain could be adjusted higher.

Figure 4-18 shows the voltage regulator output voltage change with alternator load. The two curves indicate the band in which the voltage regulator operates during a speed change. When the turbine is pulsed, the regulator output drops to the lower field voltage and as the turboalternator coasts the field voltage increases to the upper curve

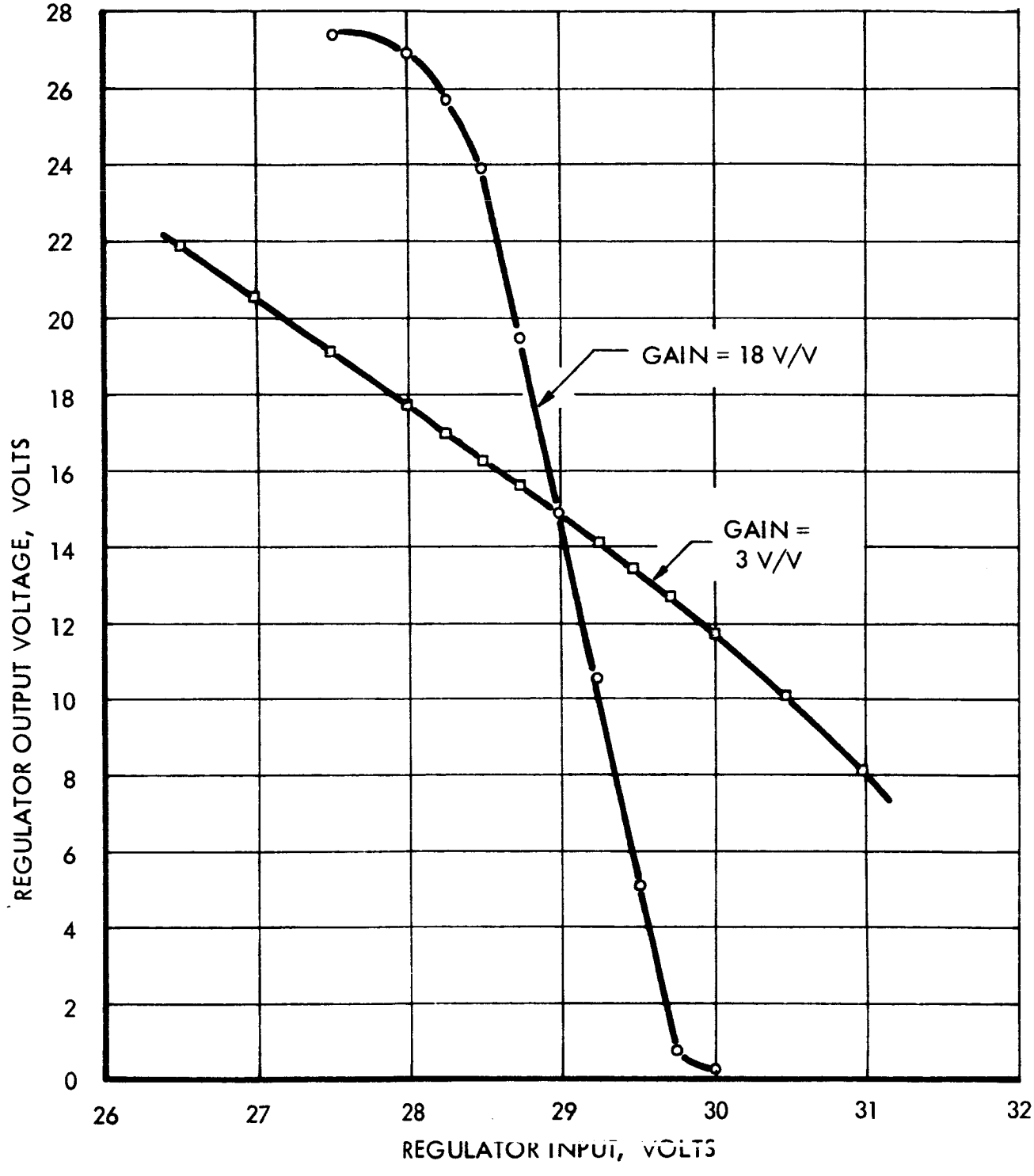

FIGURE 4-16 VOLTAGE REGULATOR GAIN LIMITS

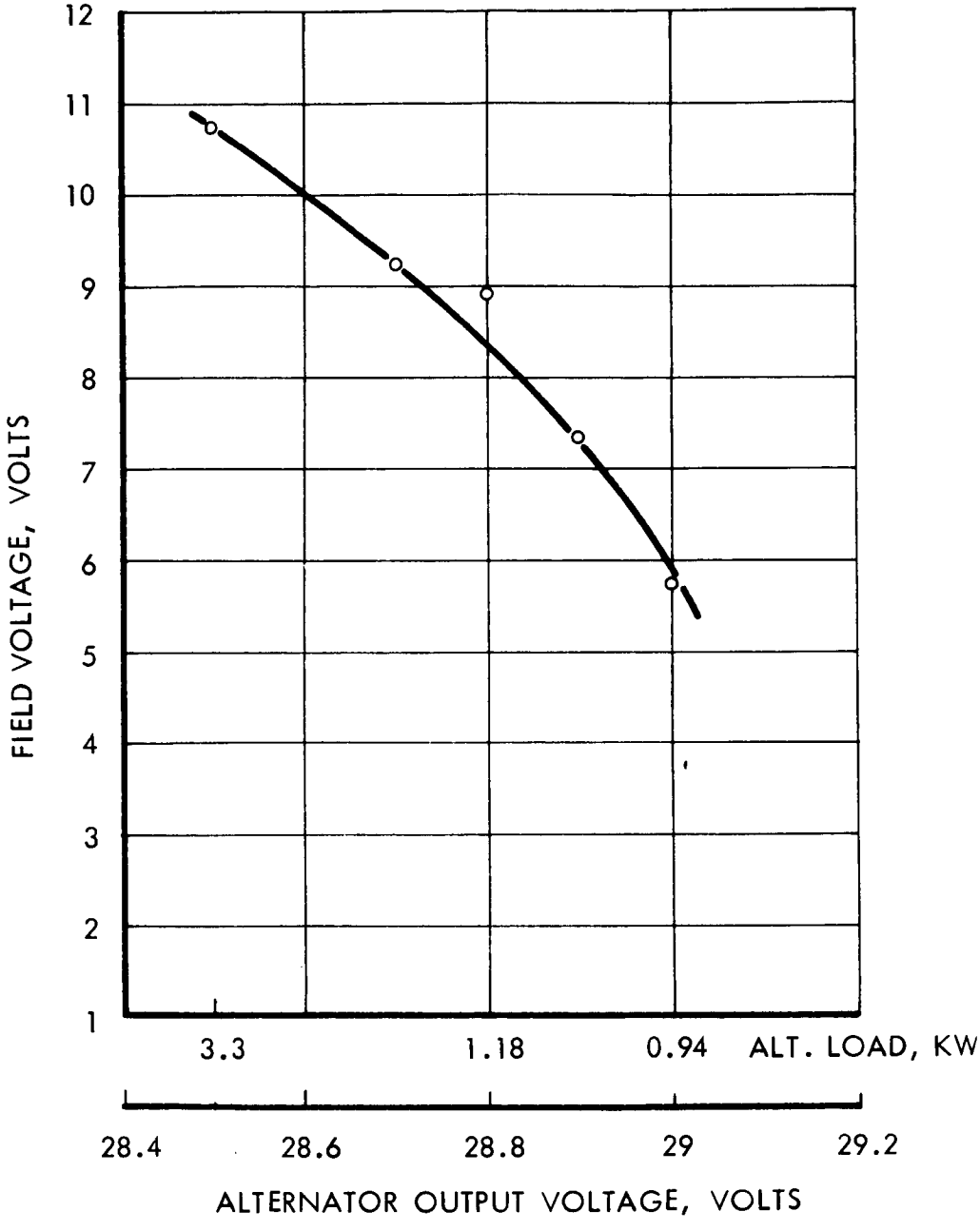

FIGURE 4-17 VOLTAGE REGULATOR CHARACTERISTIC, RUN - 052

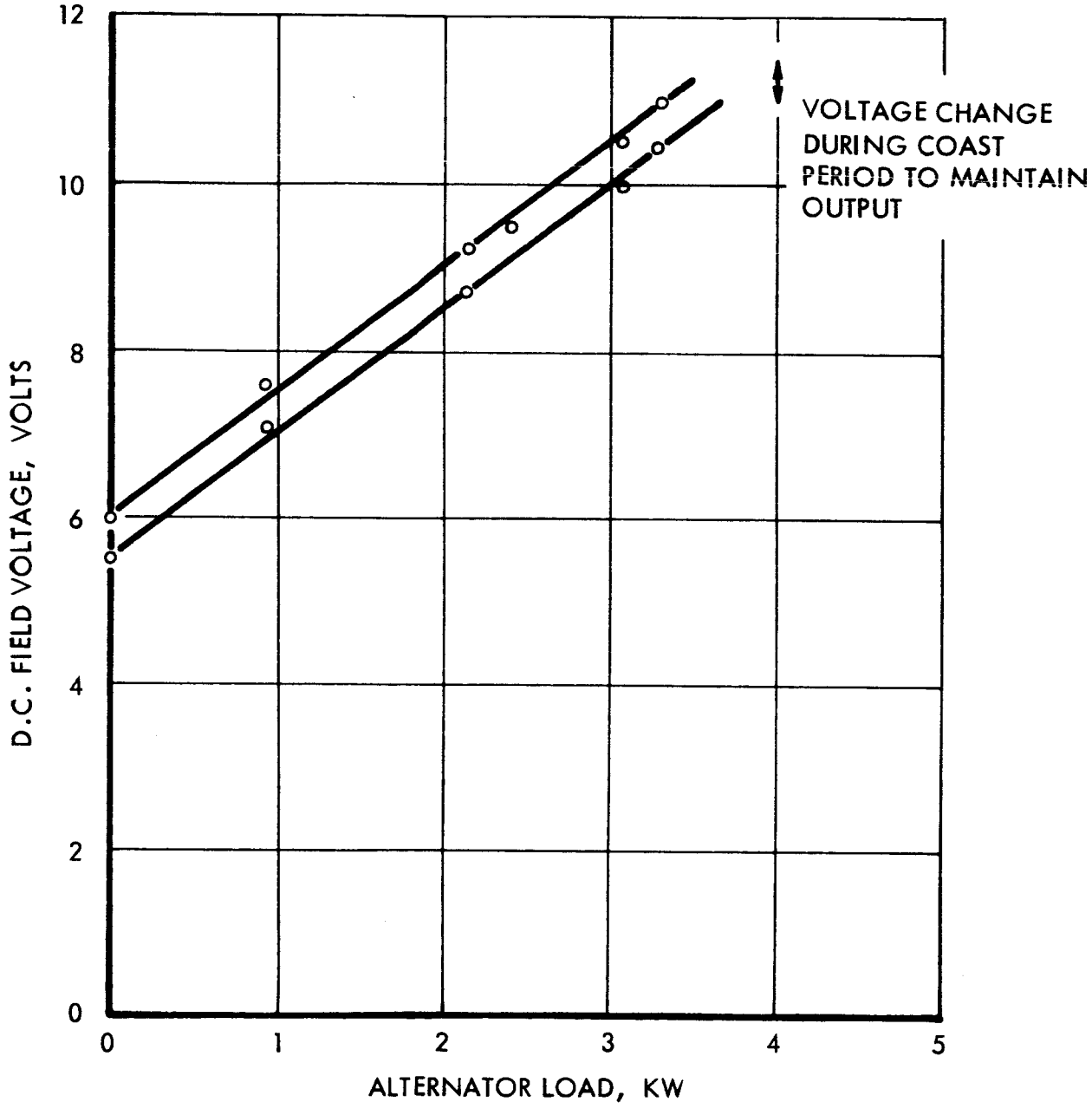

FIGURE 4.19 FIELD VOLTAGE - RUN 052

in order to maintain a constant output voltage. The change in field voltage is approximately 0.5 volts during the coast interval.

Figure 4-19 contains two curves. The top shows output voltage changes with load, and the bottom shows field power requirements with increasing load.

4.1.5.2 Rectifier and Filter

The alternator output is rectified by a three phase full wave bridge circuit. The design power level of the alternator and rectifier circuit is 6 KW with an overload capability of 7.2 KW. The original filter design, a simple L-C filter, proved to be oscillatory during load changes and was eliminated from the developmental turboalternator tests. However, from the developmental test runs, it was observed that the voltage regulator helps to reduce the ripple voltage which will aid in a new filter design.

4.1.5.3 Speed Control, Start and Protective Circuits

A block diagram of the electrical control circuits is shown in Figure 4-14 and its schematic is shown in Figure 4-20. The schematic has been marked to indicate the various circuits and functions. It also indicates on which board in the control box the circuit is located.

The start circuit consists of a UJT oscillator, two one-shots, a hybrid timing circuit using a UJT, a solenoid driver and the helium valve driver.

When switch, S_2, is thrown to the start position, it immediately energizes the UJT oscillator by means of K_4. The oscillator triggers two one-shot multivibrators every six seconds. One is set for 200 milliseconds and the other is set for 50 milliseconds. Figure 4-21 helps describe the chain of events that follows.

When the oscillator triggers the 200 ms one shot, it triggers Q_{30} which energizes K_5 and K_6. Relay K_5 energizes the helium valve drive circuit thus producing a helium pulse as soon as the start switch is thrown. The 50 ms one shot, Q_{23} and Q_{24}, delays triggering the pulser, Q_{26} and Q_{27}, which produces the 200 ms pulse for the bipropellant Moog valve. This 200 ms pulse is "OR'ed" with the speed control and thus drives the same valve driver stage, Q_{15} and Q_{19}. Relay K_6 is an adjustable time delay relay and actuates 100 ms after the first pulse thus cutting the helium pulse to 100 ms. One contact of K_5 is used to latch in both K_5 and K_6 thus preventing any further helium pulses during "start". The Moog valve continues to receive a 200 ms pulse every 6 seconds until the normal operating speed is reached. At this time the output of the frequency discriminator is sufficient to trigger a level detector comprising Q_3, Q_4, Q_5 and SCR Q_6. This level detector energizes relay K_2 which is then latched into the alternator power by one set of contacts. Other contacts of this relay disconnect the external 28 volt start-up supply, and enable the speed control and voltage regulator to operate. As the speed decreases to approximately minus 1 per cent, the point is sensed by a level detector, Q_{11} and Q_{12}. The frequency discriminator characteristic is shown in

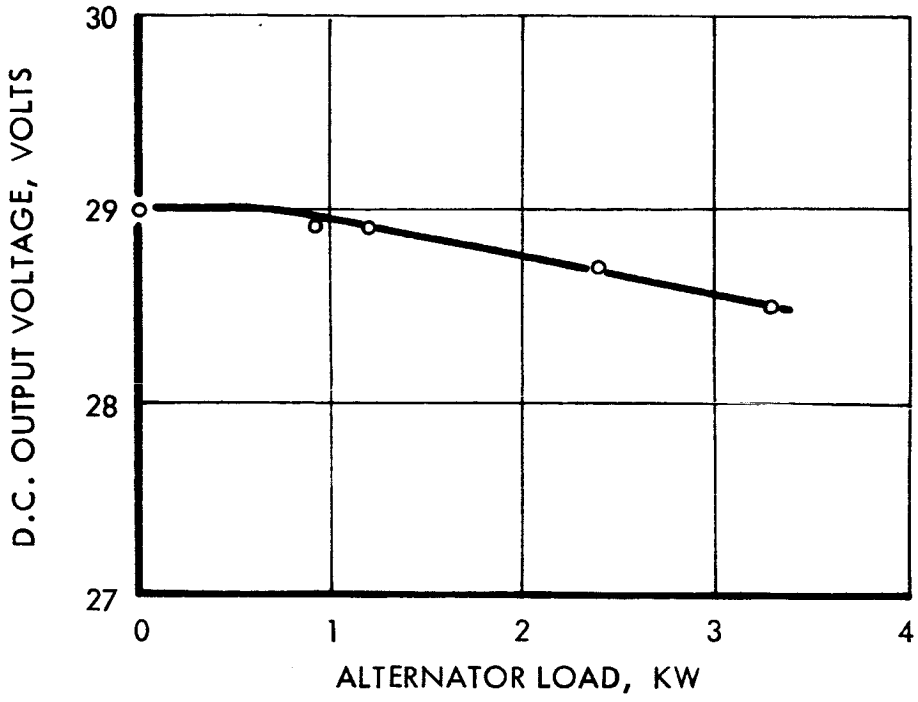

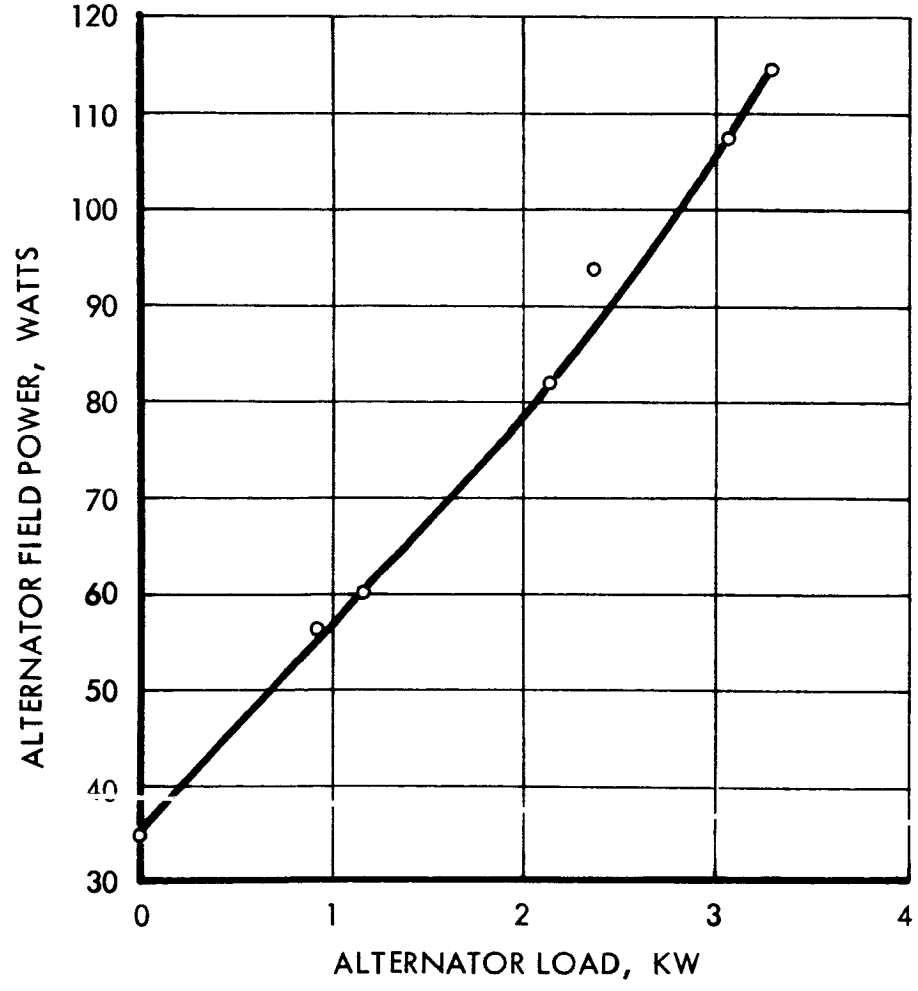

FIGURE 4-19 LOAD REGULATION, RUN - 052

FIGURE 4-20 SPEED CONT

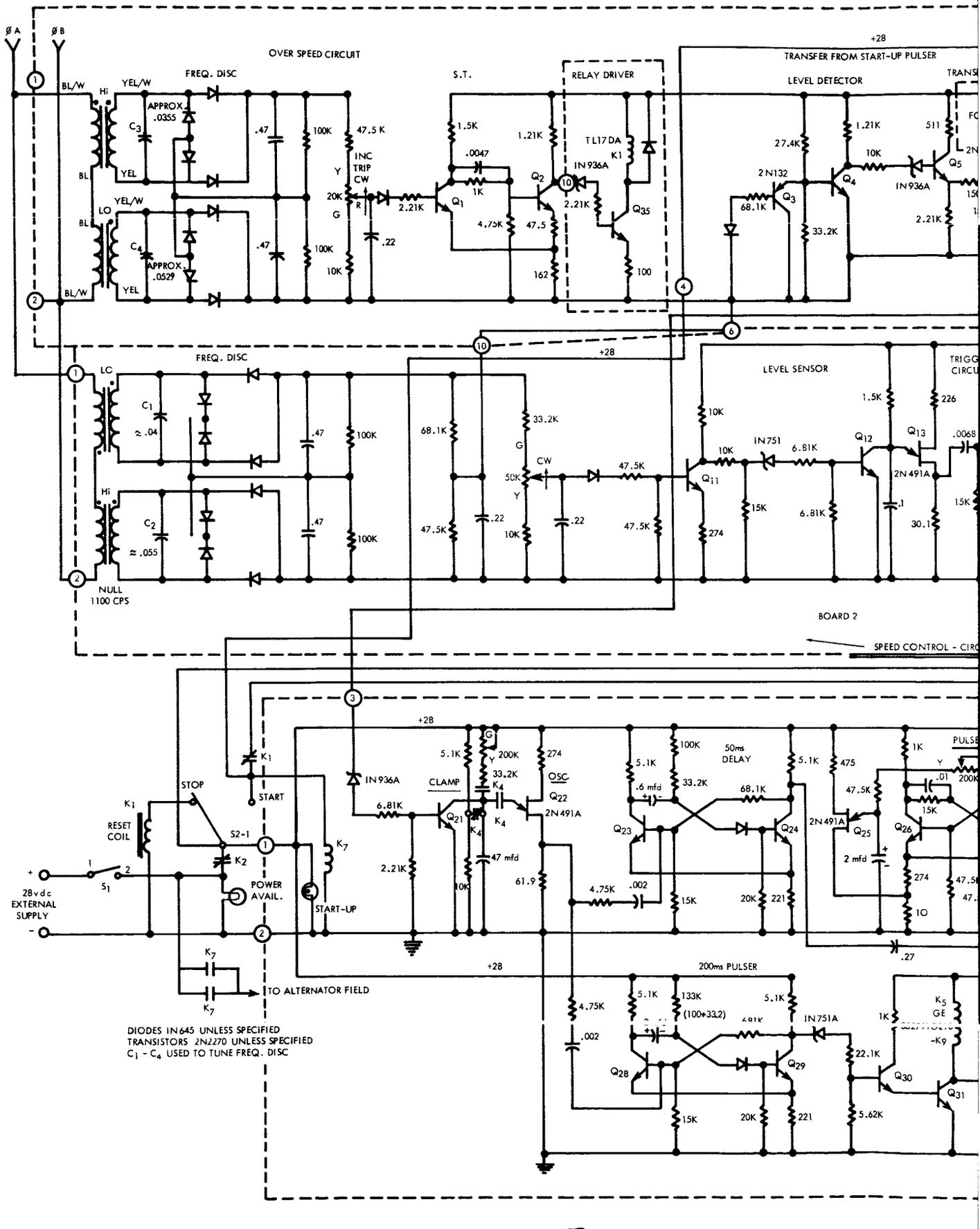

ROL SCHEMATIC

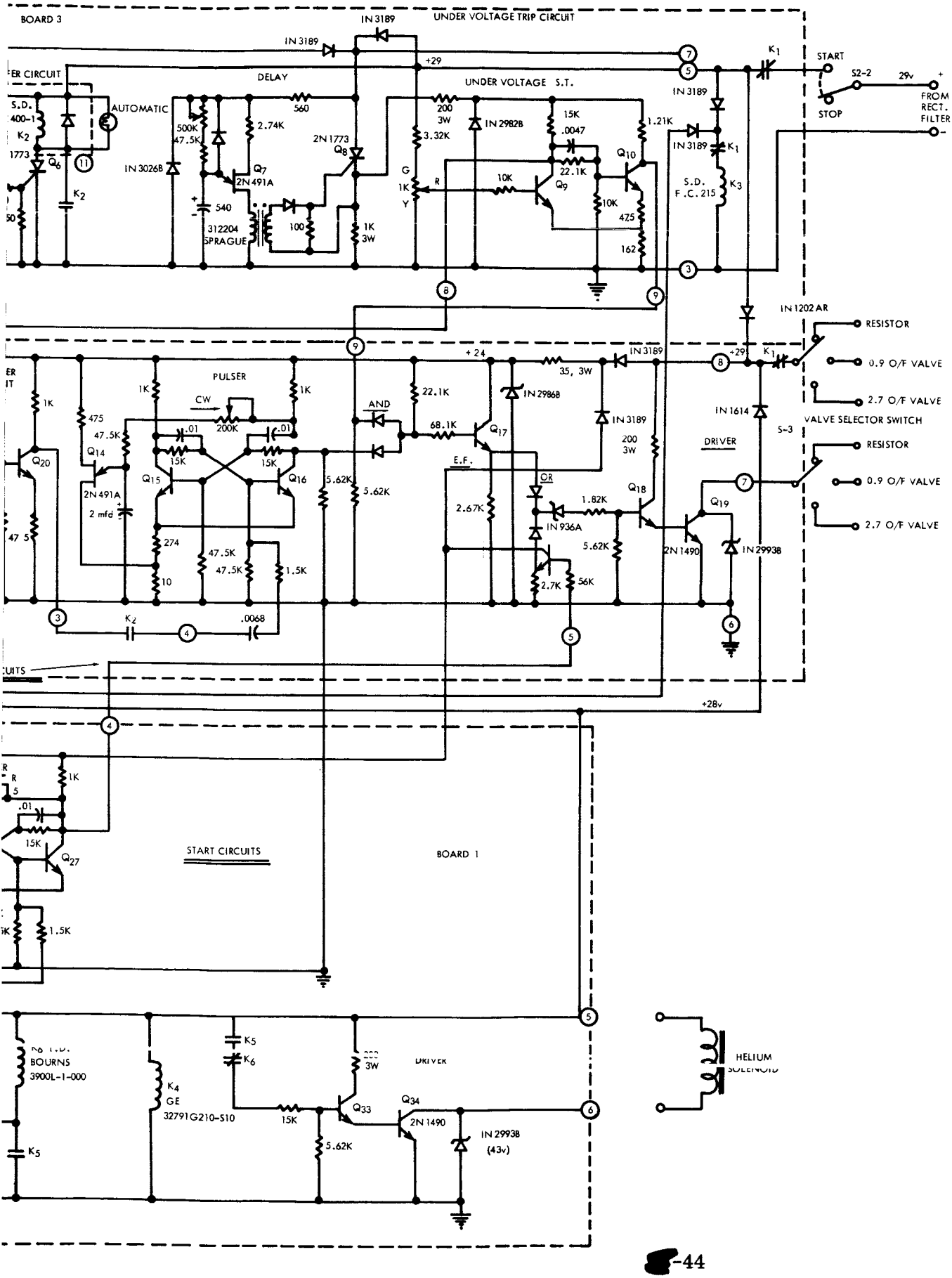

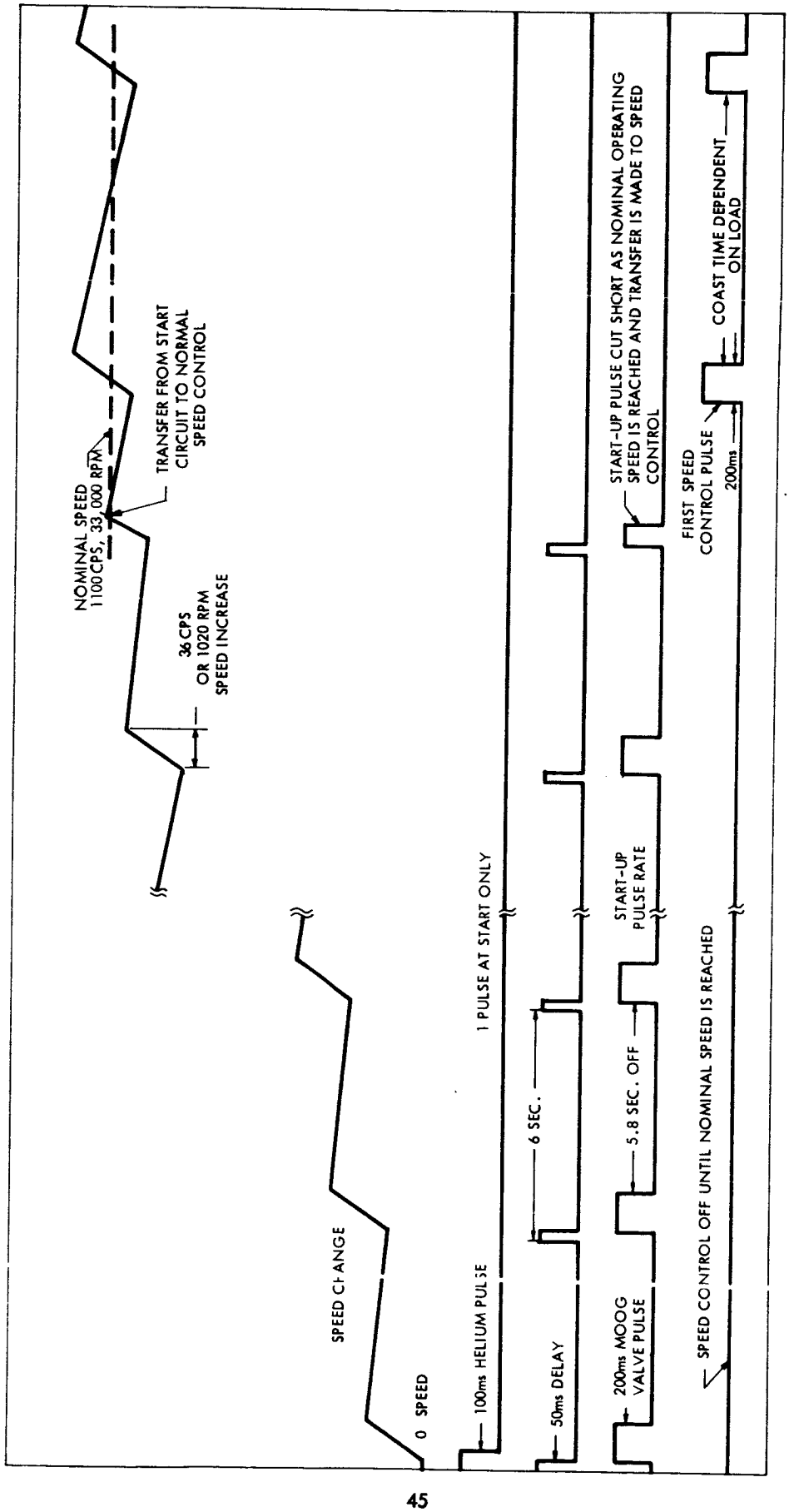

FIGURE 4-21 SPEED CONTROL START AND TRANSFER SEQUENCE

Figure 4-22. When the trigger point, 1089 cps, is sensed Q13 produces several pulses. The first pulse triggers a hybrid timing circuit Q_{14}, Q_{15} and Q_{16} which then triggers the driver stage for 200 ms. The pulses from Q_{13} are cut off again by Q_{12} as soon as the frequency moves several cycles above its trigger point. This usually occurs in 5 to 10 ms. The extra pulses have no effect on the timing circuit but do ensure proper triggering should the first pulse be missed. Each time the turboalternator coasts down to this trigger point the cycle is repeated. The coast time is determined by the turbine inertia and the load applied. This time between pulses is not controlled electrically. In future designs, the time between pulses would be limited electrically to some minimum safe value. This would ensure against too rapid, or continuous pulsing should the load on the turbine suddenly increase beyond its capability. This circuit would be used in conjunction with an underspeed circuit to initiate a shut down should speed continue to decay below some safe value.

In addition to the transfer circuit, board 3 also contains the safety circuits. One, an electronic overspeed, and two, an undervoltage trip. The overspeed circuit consists of a frequency discriminator similar to the one used in the speed control. This frequency discriminator, however, is tuned to a higher null frequency, 1155 cps in this case. Also, the diodes in the output are connected to give a positive characteristic, that is, the output voltage goes more positive for frequencies above null and negative for frequencies below null. A potentiometer is used to select the exact trip point desired. At present this circuit is adjusted to trip at 1180 cps which is equivalent to 35,400 rpm. As the speed increases, the output of the frequency discriminator becomes sufficiently high to trigger a Schmitt Trigger circuit, Q_1 and Q_2. This signal in turn is applied to the base of Q_{35} turning it on. This transistor energizes relay K_1 which initiates the shut down by removing B+ to the speed control and bipropellant valves, and the alternator field excitation voltage. Relay K_1 is a magnetic latching relay, and prevents operation of the system until it is reset.

Because this circuit depends on the electrical output of the power system it is not as fool proof as the magnetic pick-up. Should one phase of the alternator be lost due to either an open or a short, the circuit would become ineffective. For this reason an undervoltage trip circuit was also included as part of the safety circuit design. Future units should include an independent magnetic pick-up to sense overspeed. This pick-up, properly sized, will generate enough power to close a latching relay which would initiate the shutdown. The advantage of this type of overspeed device is that it does not require external power. The output of a magnetic pickup is fed through a tuned circuit and rectified. When the overspeed point is reached, the output of the tuned circuit is high enough to energize the latching relay.

The undervoltage circuit consists of Schmitt Trigger circuit Q_9 and Q_{10}. The rectified output of the alternator is applied to its input and should it drop below a minimum level the circuit would disable the valve drive circuit by means of an "AND" gate connected to the base of Q_{17}. In order to prevent an undervoltage shutdown during the start sequence, the B+ voltage to the Schmitt Trigger circuit is delayed by timing circuit Q_7 and Q_8. B+ is applied to the timing circuit from both the external 28 volt source

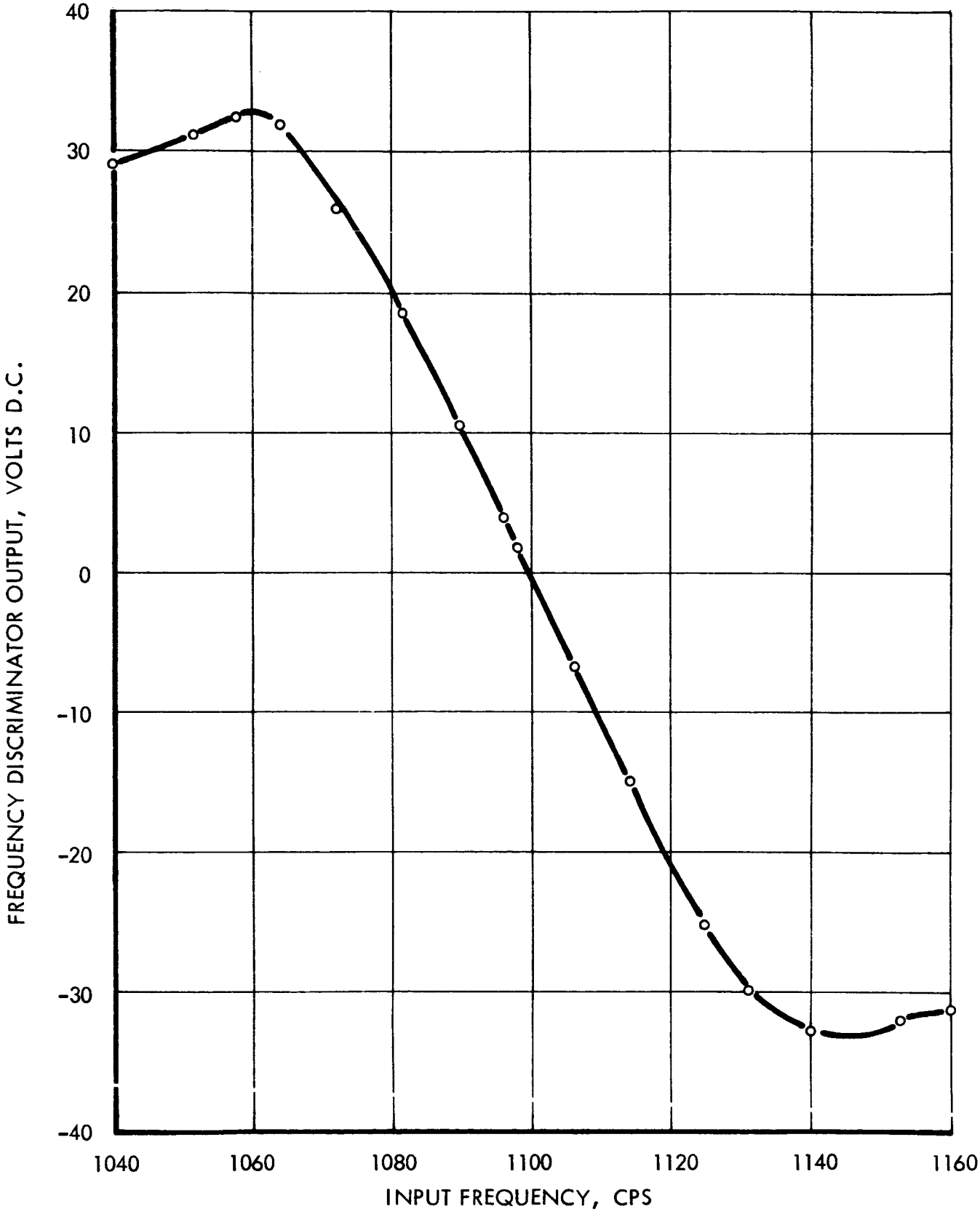

FIGURE 4-22 FREQUENCY DISCRIMINATOR CHARACTERISTIC

and the alternator rectified output. The timing or delay circuit is energized when the start switch is thrown.

When the circuit times out, it applies B+ voltage to the Schmitt Trigger circuit. If the alternator output is high enough, the start sequence is allowed to continue. However, should the alternator output be low, the Schmitt Trigger also shuts down the start sequence. It does this by applying voltage to the base of $Q2_1$ in the start-up oscillator circuit. Q_{21} then clamps the timing capacitor to ground and no further start-up pulses are received. When the external 28 volt source is removed at transfer the undervoltage circuit continues to function on the rectified alternator output. The Schmitt Trigger circuit is designed to operate at a lower B+ voltage as determined by the zener diode so that it will continue to function properly and initiate a shutdown even though the 29 volt alternator rectifier output is not at its full value.

Selection of the desired O/F ratio value is made by means of a selector switch on the control panel. Shutdown is initiated by simply turning switch S_2 from "Start" to "Stop". This removes the bipropellant valve drive voltages, B+ to the speed control, and field excitation to the alternator.

From the development testing accomplished to date, the control circuits have proved to be reliable and to provide the necessary control function. Some desirable modifications became apparent during this test phase and these have been pointed out.

4.1.6 Lubrication and Cooling

Lubrication and cooling are accomplished by a single closed loop system consisting of a scavenge pump, a pressure pump, and a space radiator. The radiator was replaced by two water cooled heat exchangers for development and endurance tests. The system schematic in Figure 4-23 in Section 4.3 shows the integration of the lubrication and cooling system with the power system.

The ball and roller bearings and bellows seal require oil for lubrication and cooling. These are supplied with oil by .030" diameter jets. Each bearing and the seal is sprayed with two jets located 180° apart. The alternator rotor and seal mating ring sling the oil to the outer surface of the bearing and seal cavities where there are scavenge ports leading to the scavenge pump. The scavenge pump sends the oil from the bearing and seal cavities through the oil cooler to the sump. The pressure pump supplies oil to the bearings and seal from the sump.

Oil for cooling the alternator is also supplied by the pressure pump. It flows through an annular passage within the alternator housing and is returned to the cooler and sump by the scavenge pump.

Operating data for the lubrication and cooling system appear in Section 4.3.

4.1.7 Flight System Weight

A list of component weights for a flight system is compiled in Table 4-7 for a 3 KW and 6 KW system. The 6 KW turboalternator and electrical packages are based on actual hardware weights. The 3 KW turboalternator and rectifier-filter weights are calculated weights of flight type hardware based on scaled down versions of these components. The remaining components are also calculated on the basis of flight type hardware. The 6 KW and 3 KW systems weigh 155.8 lb and 99.5 lb, respectively.

The weight of a third system based on an output of 4.5 KW was also estimated. The 6 KW turboalternator with modification for smaller radiation fins due to less heat rejection was assumed. The rectifier-filter and radiator sizes were reduced to a 4.5 KW level. This system would weigh 127.4 lb.

Table 4-7 Weight Summary of 6 KW and 3 KW Flight Systems

Component	Weight (lbs.)	
	6 KW System	3 KW System
Turboalternator	80.0	50.0
Speed control	1.0	1.0
Voltage regulator	0.8	0.8
Rectifier-filter	20.0	12.0
Lube pump and motor	4.5	3.5
Oil reservoir	3.0	2.0
Radiator	20.0	12.0
Cold plate	7.5	4.0
Oil	4.0	3.0
Electrical leads	5.0	3.5
Plumbing	4.0	3.0
Mounting and connections	6.0	4.7
	155.8	99.5

4.2 Fabrication

4.2.1 Materials

The methods and materials used in fabrication of the turboalternator power system are those commonly used in similar machines. A tabulation of the material of each component is shown in Table 4-8.

Table 4-8 Component Materials

Turbine wheel and shaft	Waspaloy
Alternator rotor	
Pole pieces	SAE 4320
Separator	Inconel X 750
Alternator stator	
Laminations	Armco Tran Cor-T
Windings	Oxygen free copper
Insulation	Armco D-1 Max M-22
Alternator housing	AISI 1018
Turbine inlet scroll and nozzle weldment	Hastelloy X
Ball bearing	
Balls and races	440C Modified
Retainer	Silver plated SAE 4340
Roller bearing	
Rollers and races	52100
Retainer	Silver plated iron silicon bronze
Gas generator	
Chamber	Hastelloy X
Injector head	Inconel 600
Injector head potting ring	304 SS
Injector head potting	BTG 130 Premabraze

4.2.2 Methods of Fabrication

Turbine Wheel and Shaft

The turbine disk blank was machined from a forged disk and the shaft was machined from Waspaloy bar. The two pieces were joined with an electron beam weld. The blade passages were cut in the turbine disk by the electrical discharge machining process. The turbine wheel and shaft were then machined to the final configuration.

Alternator Rotor

The two pole pieces and separator were milled from bar stock. The three pieces were joined by electron beam welding and finish machined.

Inlet Scroll and Nozzles

The nozzle scroll assembly is composed of three major pieces: 1) the scroll section, 2) the nozzle block, and 3) the turbine shroud. The scroll section was contour milled from a forged disk. The nozzles were electrical discharge machined in a forged disk. The turbine shroud was machined from a forged ring. The three pieces were electron beam welded together. A later design change was made which incorporated copper fins on the nozzle-scroll assembly. The fins were joined to the nozzle-scroll assembly by electron beam welding.

Alternator Housing

The alternator housing is a weldment made of three pieces: 1) the turbine bearing support, 2) the stator housing, and 3) the cooling passage cover. The turbine bearing support is a casting which was machined prior to welding. The stator housing is a tube which was machined to fit the turbine bearing casting. The cooling passage cover is a tube which was sized to have an interference fit with the stator housing. The three pieces were electron beam welded together, and the weldment was then final machined.

Alternator Stator

Fabrication of the alternator stator was started by assembling the lamination stack in a fixture. The lamination stack was welded along the outside and finish machined to the proper outside diameter. Slot liners were inserted to insulate the stator winding. The stator conductors were forced into hairpin shaped turns in a forming fixture using rectangular cross section wire coated with heavy ML insulating film. These conductors were inserted into the lamination stack along with insulating separators and end turn insulation. Individual turns were silver soldered at the rear end of the alternator to form the proper winding connection. The complete stator winding was impregnated with ML varnish to complete this item.

Field coil spools were machined from beryllium copper. Each coil was wound with 95 turns of 16 gauge wire coated with heavy ML insulation. The assembly was wound with fiberglass tape and impregnated with ML varnish. Lead wires were attached and the assembly was sealed with Sauereisen cement. Finally, the field coil assemblies were machined to the proper outside diameter.

The field coils and the stator winding were assembled into the stator housing after attaching thermocouples to critical points. The field leads and thermocouples wires were brought out through sealing glands. Output leads were attached to the stator windings. When the end cap was put in place, the output leads were brought out axially through individual conductor sealing glands in the end caps.

Controls and Power Conditioning

In the original program plan, it was intended that packaged speed controls, voltage regulators and rectifier-filter units would be fabricated. The optimization studies indicated the need for a broader control effort to include the automatic start and transfer functions and protective circuits. It was also recognized that the controls would be used only as external supporting equipment during turboalternator tests. These conclusions lead to the fabrication of a single control cabinet containing all control functions, packaged as a piece of laboratory equipment.

All of the control circuits were breadboarded and tested to finalize circuit designs. Using these results, circuit boards were designed to provide a neat, yet readily accessible component layout. The boards were fabricated using flight quality components throughout. All boards were mounted in the control cabinet as indicated in Figure 4-11 and 4-12. The switches to perform start and stop, manual transfer, and O/F ratio selection were mounted on the front of the cabinet along with meters to display electrical performance.

The rectifier and filter circuits were fabricated as a separate assembly. This was done to permit this equipment to be mounted close to the power lead exit from the altitude chamber.

Gas Generator

The injector head, chamber and valve mounting flanges were first machined and drilled. The capillary tubes were welded to collars which were then welded to the orifice holes in the injector head. The tubes were formed to fit the valve mounting flanges and furnace brazed in place. The potting ring was electron beam welded to the injector head, and the cavity formed by the back of the injector and ring was filled with potting compound. The valve mounting flange brackets were welded to the potting ring and the flanges to offer support to the flanges and valves. Finally, the generator chamber was electron beam welded to the injector head.

A subsequent design change was incorporated in which additional potting was applied around the capillary tubes between the existing silver braze potting and the valve mounting flanges. This potting was an epoxy compound which gave the tubes structural support in the area where ruptures had been occurring. The exposed surface of the epoxy potting was covered with a silicone rubber compound, Dow Corning RTV 891, to protect the potting from deterioration in the event of an oxidizer leak.

4.3 Test Installation

All system and breadboard tests were conducted in the TRW altitude facility located at Rocky Mount, Virginia. This facility is designed and arranged specifically for liquid propellant turboalternator power system testing at altitudes up to 100,000 feet. A three stage steam ejector, using the steam flow from a 40,000 lb/hr. boiler provides the altitude capability. The altitude chamber itself is 6 ft. in diameter and 9 ft. long A 22" diameter exhaust pipe connects the chamber to the ejector system. This pipe replaces two 5.5" diameter pipes which were originally used. Altitude pressure variation during pulsing was excessive with these small pipes.

The installation of the power system in this facility is shown schematically in Figure 4-23. Details of the electrical system installation are shown in Figure 4-14.

The turboalternator is mounted from cantilevered struts at approximately the center of the chamber with the turbine exhaust directed toward the center of the 22" diameter exhaust pipe. All connections to the turboalternator are made through bulkheads in the altitude chamber wall, as shown in the schematic.

For convenience in testing, the automatic control box, consisting of the speed control and voltage regulator, were located at the control console. The rectifier-filter package was located just outside the chamber in the test cell area. This was done to minimize the voltage drop in the electrical output leads.

The lubrication system, consisting of a pressure pump, scavenge pump, two oil-to-water heat exchangers and the reservoir, was installed outside the chamber in a convenient location. Manual control of oil pressure and oil temperature was provided.

Primary sub-systems in the test installation are described below:

Propellant Systems

The oxidizer and fuel supply systems are similar with the exception that nitrogen is used to pressurize the Aerozine- 50 and helium is used to pressurize the $N_2 O_4$.

Both systems are arranged for manual pressure regulation by means of Grove regulators installed on the control panel which regulate the supply pressure leaving the gas bottles.

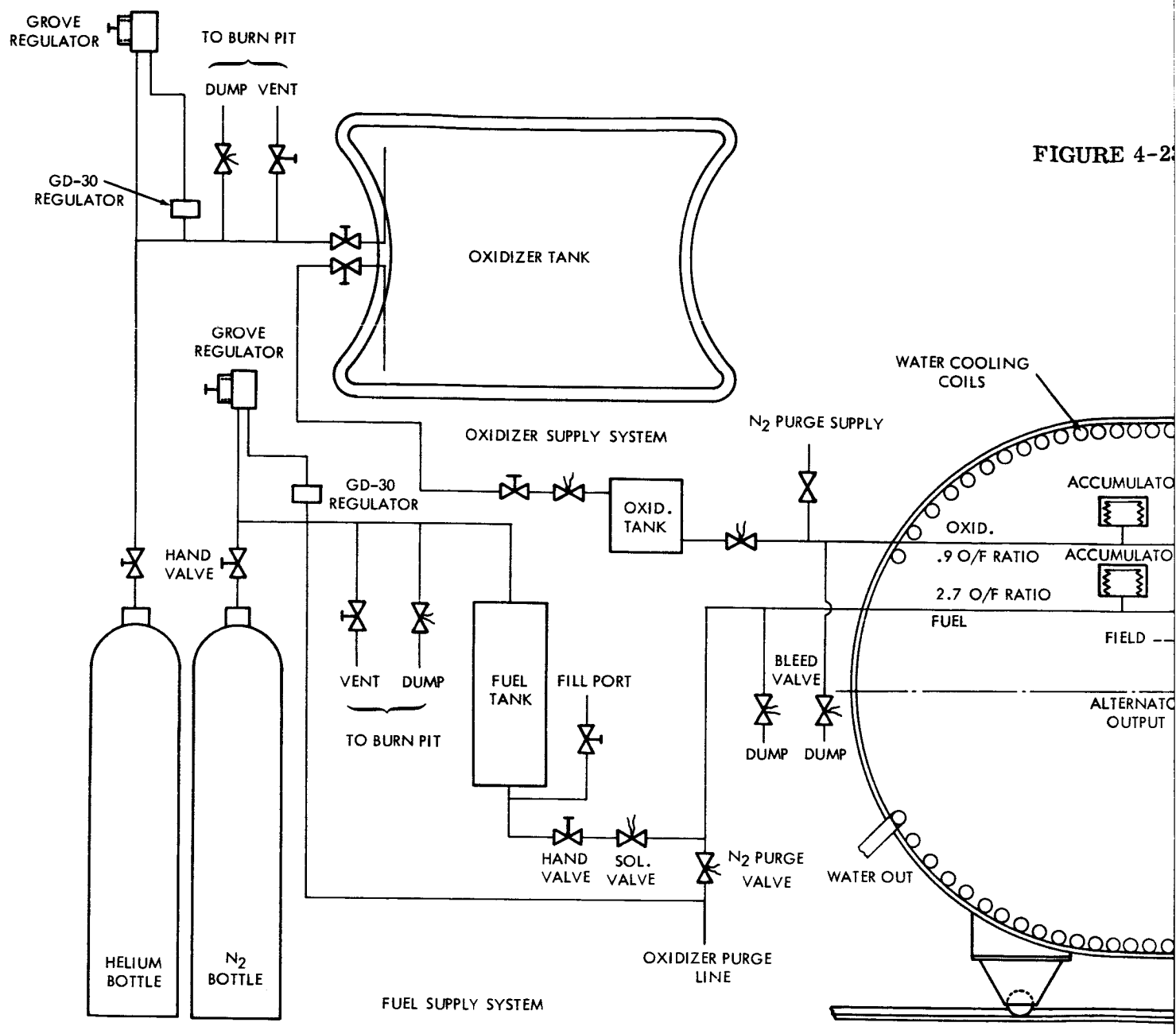
GROVE REGULATOR
TO BURN PIT
DUMP VENT
GD-30 REGULATOR
OXIDIZER TANK
GROVE REGULATOR
WATER COOLING COILS
OXIDIZER SUPPLY SYSTEM
N_2 PURGE SUPPLY
GD-30 REGULATOR
OXID. TANK
ACCUMULATO
OXID.
.9 O/F RATIO
ACCUMULATO
2.7 O/F RATIO
FUEL
FIELD
HAND VALVE
VENT DUMP
FUEL TANK
FILL PORT
BLEED VALVE
ALTERNATO OUTPUT
TO BURN PIT
DUMP DUMP
HAND VALVE
SOL. VALVE
N_2 PURGE VALVE
WATER OUT
HELIUM BOTTLE
N_2 BOTTLE
OXIDIZER PURGE LINE
FUEL SUPPLY SYSTEM

FIGURE 4-2

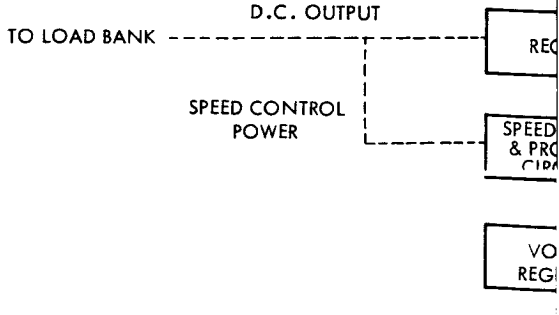
D.C. OUTPUT
TO LOAD BANK
REC
SPEED CONTROL POWER
SPEED & PRO
VO REG

3 POWER SYSTEM SCHEMATIC DIAGRAM

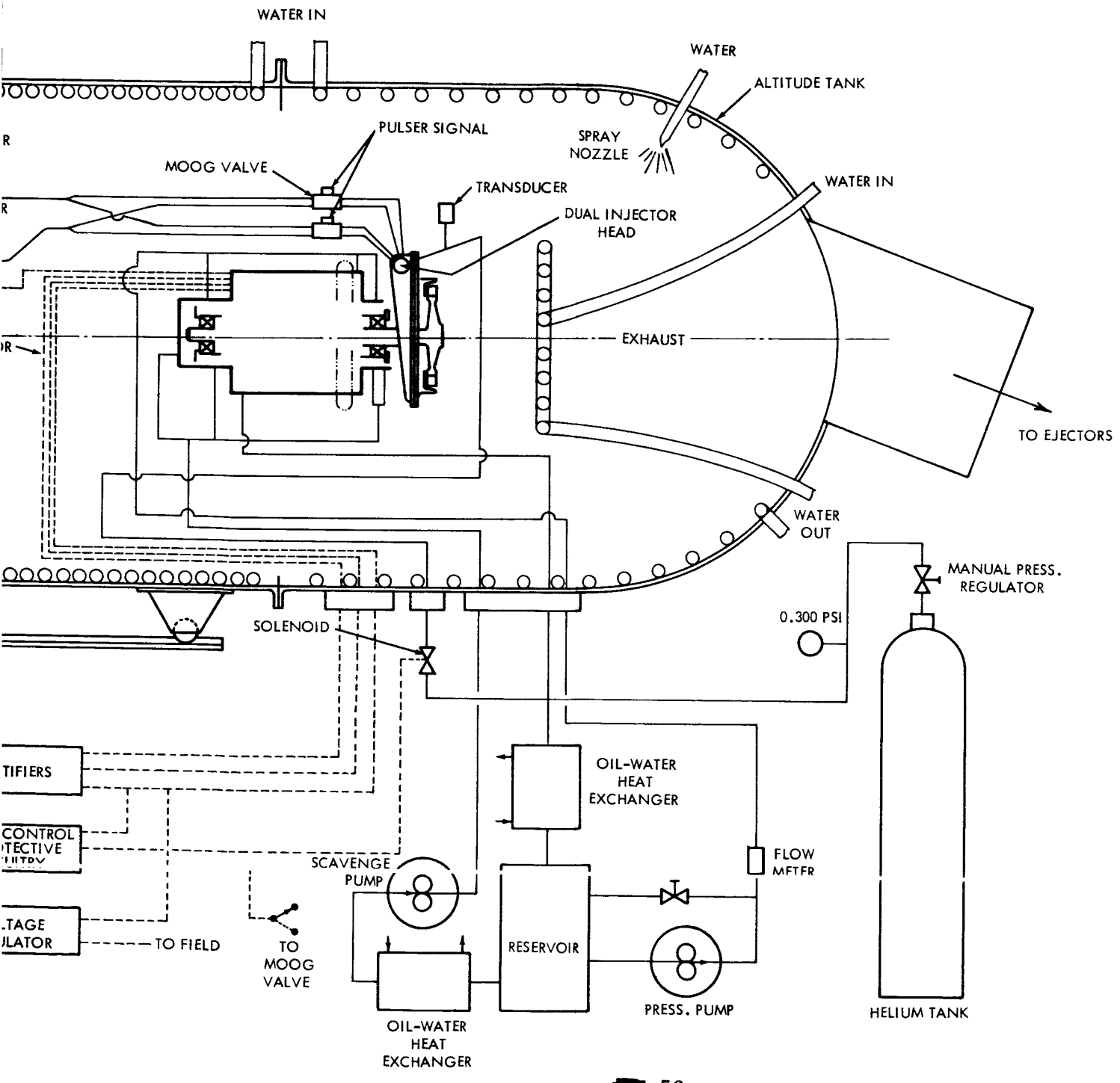

Fuel and oxidizer tanks located outside the altitude chamber are then directly pressurized. Hand and solenoid control valves are provided external to the chamber to provide on/off control, N_2 purge and dump capability. The propellant supply lines pass through the chamber to the Moog valve. During the test program, propellant supply pressures were held within ± 2 psig of normal setting. This setting depended upon the injector used and was usually 190 or 195 psig. Cooling of the propellant supply lines within the chamber was provided by water coils wound around the lines in earlier testing. In later testing the oxidizer was cooled by a water jacketed tube. This revision was required for endurance testing when altitude chamber temperatures at times exceeded 200°F.

Lubrication System

For this test program a breadboard type lubrication system was used. This system consisted of a pressure pump, a scavenge pump, two oil-to-water heat exchangers and means of manually controlling oil pressure and temperature. Pressure pump output was provided to three points on the turboalternator:

a) The ball bearing and seal

b) The roller bearing,

c) The alternator cooling jacket

Redundant jets were used for both bearings. Scavenging from the ball bearing and roller bearing areas was direct to the scavenge pump inlet. The alternator cooling jacket scavenge line returns to the oil reservoir through a separate oil-to-water heat exchanger. After some development and enlargement of oil jets, the following flow conditions were maintained for the majority of testing:

Total oil flow	.7 G. P. M.
Stabilized oil temperature to unit	150°F
Oil temperature to unit at start-up	80° to 120°
Pump discharge pressure	30 - 45 psia
Ball bearing and seal flow	.24 to .30 GPM
Roller bearing flow	.04 to .08 GPM
Alternator cooling jacket flow	.30 to .40 GPM
Ball bearing and seal supply pressure	20 to 35 psia
Roller bearing supply pressure	25 to 40 psia
Alternator cooling jacket supply pressure	25 to 40 psia
Scavenge pressure	0 to 4 psia

The previous pressure and flow relationships are a function of the installation and will be altered if, for example, oil feed lines are shortened. Oil pressures were measured outside the altitude chamber. Flow rates to the turboalternator are not critical and can be varied considerably with no resultant damage to the machine. The rates are given to show relative flows to the three pressure connections.

Altitude Chamber Cooling System

During the test program, overheating of the altitude chamber was a constant and recurring problem. During the early tests a water cooled shroud ducted the exhaust gas to the altitude chamber exhaust. This proved to be totally ineffective and was removed. Copper coils were then installed to line the chamber walls with a water cooled surface. This helped considerably but was not sufficient since some surface could not be covered due to the interferences of connections, supports, etc. A flat coil of copper tubing was then installed for direct exhaust gas impingement on a water cooled surface. This again helped but was not sufficient. The two 5.5" diameter altitude chamber exhaust pipes were then replaced by a single 22" diameter pipe. This reduced chamber temperatures appreciably and permitted continuous endurance type running. Chamber temperatures reached and occasionally exceeded 200°F. External insulation from the exhaust end dome was removed with a resultant minor effect. An interior water spray at the exhaust end of the chamber was used in some runs and reduced chamber temperature somewhat. However, ice tended to form and was objectionable. Further cooling will be required for testing at higher load levels for long periods.

Electrical System

The electrical system consists of the voltage regulator, speed control and rectifier filter package, which is described schematically in Figure 4-14, and is discussed in Section 4.1.5. The electrical system is designed to provide fully automatic control after the start-up switch S-2 is energized. Helium pressurization of the gas generator for positive ignition is first triggered. A signal for the Moog valve to open is given 0.05 sec. later. The helium pressurization is removed following an additional 0.05 sec. delay. Pulse signals every 6 secs. are then given until the turboalternator reaches speed at which time transfer to automatic control takes place. Operation at 33,000 rpm is then automatically maintained within the ± 1.5% variance caused by pulsing. In the event of overspeed or overtemperature automatic shutdown occurs. In addition, a DC resistive load bank was installed outside the altitude chamber to absorb rectified alternator output. A series of switches located at the control panel permitted load addition and removal without entering the test cell.

Start-Up Procedure

A formal start-up procedure was developed and is included to further explain actual system operation.

Start-Up Procedure

PRELIMINARY

(a) Kindle charcoal fires in the oxidizer and fuel vent pits.

(b) Make certain all panel switches are in the off position.

(c) Check stand installation to make sure that all system lines (propellant, cooling, instrumentation and electrical) are properly connected.

(d) Check Groove Pressure Regulators (oxidizer and fuel) on top of panel to see that they are in the closed (counterclockwise) position.

(e) Check hand valves in fuel and oxidizer vent lines to pits to see that they are in the closed position.

(f) Open hand valve in oxidizer fill line.

(g) Open Helium Bank valves to G. D. 30 Regulator and check for sufficient operating pressure (at least 600 psig).

(h) Open Nitrogen Bank Valves to G. D. 30 Regulator and check for sufficient operating pressure (approximately 1000 psig).

(i) Check hand valve in Fuel Fill Line inside cell to make sure it is in closed position.

(j) Check all hand valves in lines leading from fuel and oxidizer tanks to main fuel and oxidizer valves to insure that they are in the open position.

(k) Check for steam ejection system capability.

(l) Open cell doors.

(m) Turn oil heaters on.

PRESSURIZATION - FUEL SYSTEM

(a) Turn on blinking lights, sound alarm and erect warning sign at outside entrance to cell.

(b) Turn on panel power by actuating switch in upper left inside corner of console.

(c) Turn fuel pressure switch to on position.

(d) Turn main fuel valve to on position.

(e) Pressurize fuel system to 75 - 100 psig by turning the left hand Grove regulator in a clockwise direction and monitoring the tank pressure gage on the left hand side of the cell window.

(f) Make a visual check of stand for possible leaks.

(g) Open fuel bleed valve for 10 seconds. Then close.

Start-Up Procedure - Continued

(e) Turn Grove regulator on oxidizer side counterclockwise to full close position.

(f) Turn oxidizer dump switch to open position. Pressure should decrease in both propellant tanks to zero in 3 or 4 minutes.

TO PURGE SYSTEM

(a) Turn both oxidizer and fuel bleed valve switch to the on position.

(b) Turn both oxidizer and fuel system purge valve switches to on position for 3 minutes.

NOTE: If unit is to be removed from test stand then the bipropellant (Moog) valve and unit must be purged thoroughly. Also unit must be purged after shutdown in order to prevent heat soak back into the injector.

(c) After system is purged, close both oxidizer and fuel bleed valves keeping both fuel and oxidizer purge valves in the open position.

(d) Open Moog valve and unit will purge completely. Purge time depends on how hot unit is at completion of run.

Instrumentation

The basic instrumentation used in the program is described in Table 4-9, entitled "Instrumentation Requirements." This listing was used in the selection and procurement of required instrumentation.

TABLE 4-9
INSTRUMENTATION REQUIREMENTS

Item	Parameter	Units	Expected Operating Range	Transducer or Instrument Range	Recorder	Recorder Parameter Range	Record. Deflect. Range	Readable Increment	1/4 Cycle Response Time	Transd. Reproducability	Completed by Instrumentation: Galvo Type	Resp. Rate	P.S.	Remarks
1	Chamber Pressure	Psia	125 Psia	0-300 Psia	Century #1	0-150 Psia	4 inches	1 Psia	.001 sec	0.1% F.S. 0.3 Psia		600 cps	10 in/ sec	Buy new P_c transducer with temp. compensation and vacuum operation.
2	Oxidizer Pressure	Psia	206 Psia	0-300 Psia	Century #1	0-300 Psia (175-225) with suppression)	4 inches	1.5 Psia (0.25 Psia with suppression)	.001	0.1%F.S. 0.3 Psia		600 cps	10 in/ sec	Buy new P_c transducer w/ temp. compensation. Buy new trim pressure regulator. Note: If greater readability is required, i.e. 4.5 PSI →1.5 PSI, a system of suppressed zero is reqd.
3	Fuel Pressure	Psia	206 Psia	0-300 Psia	Century #1	0-300 Psia (175-225) with suppression)	4 inches	1.5 Psia (0.25 Psia with suppression)	.001	0.3 Psia		600 cps	10 in/ sec	Buy new P_{fuel} transducer Note: If greater readability is required, i.e. 1.5 PSI → 0.25 PSI, a system of suppressed zero is reqd.
4	Oxidizer Tank Pressure	Psia	0-600 Psi	Visual Gauge 6" Dial	Not Recorded	0-600 Psi	6" Dial	2 Psi	--	2% = 12 Psi	--	NA	--	
5	Fuel Tank Pressure	Psia	0-600 Psi	Visual Gauge	Not Recorded	0-600 Psi	6" Dial	2 Psi	--	2% = 12 Psi	--		--	
6	Turbine Exit (Vacuum Chamber Pressure)	Inches Hg	0.3 in. Hg	30-0 in. Hg	Century #1	0-30 in.	4 in.	.15 in.	0.10	1%F.S. .3 in.		100 cps	1 in/ sec.	0-100 PSI transd. calibrated in negative direction Transd. on hand. Prefer vacuum transd. if poss.
7	Helium Start-up Tank Pressure	Psig	0-600 Psi	Visual Gauge	Not Recorded Note: Start pressure observed on P_c transducer.	0-600 Psi	6" Dial	2 Psi	--	2% = 12 Psi	--	--	--	Buy pressure gauge (or procure from other source.
8	Altitude Chamber Pressure Visual	in. Hg	0.3 in. Hg	30-0 in. Hg	Visual Monometer	30-0 in. Hg	30" Hgt.	0.1 in.	--	.01 in.	--	--	--	Manometer on hand.

TABLE 4-9 (Cont.)
INSTRUMENTATION REQUIREMENTS

Item	Parameter	Units	Expected Operating Range	Transducer or Instrument Range	Recorder	Recorder Parameter Range	Record. Deflect. Range	Readable Increment	1/4 Cycle Response Time	Transd. Reproducability	Completed by Instrumentation: Galvo Type	Resp. Rate	P.S.	Remarks
9	Roller Bearing Supply Pressure	Psia	30 Psia	0-50 Psia	Visual	0-50 Psia	0-50 Psia	2 Psi	--	2% = 1 Psi	--	--	--	Buy pressure gauge.
10	Ball Bearing and Seal Supply Pressure	Psia	50 Psia	0-100 Psia	Visual	0-100 Psia	0-100 Psia	2 Psi	--	2% = 2 Psi				Buy pressure gauge.
11	Alternator Oil Cooling Supply Pressure	Psia	10 Psia	0-25 Psia	Visual	0-25 Psia	0-25 Psia 6"Dial	0.5 Psia	--	2% = 0.5 Psia	--	--	--	Buy pressure gauge.
12	Scavenge Bearing Drain Pressure	Psia	10 Psia	0-25 Psia	Visual	0-25 Psia	0-25 6" Dial	1 Psia	--	2% = .5 Psia	--	--	--	Buy pressure gauge.
13	Alternating Cooling Line Exit Pressure	Psia	10 Psia	0-25 Psia	Visual	0-25 Psia	6"Dial	0.5 Psia	--	2% = 0.5 Psia	--	--	--	Buy pressure gauge.
14	Lub Pressure Pump Discharge Pressure	Psia	65 Psia	0-100 Psia	Visual	0-100 Psia	6"Dial	2 Psia	--	2% = 2 Psia				
15	Fuel Flow Rate	Cps (Lbs/sec)	.1574 lbs/(.9) sec. (200 cps) .0808 lbs/sec (2.7) (125 cps)	0-600 cps	Century #1	0 -.3 lbs/sec	0-300 cps	1/2 Cycle	Basic 600 cps	0.1% F.S. 1.2 cps		600 cps	10 in/sec	Buy flowmeter. D.C. amplifier reqd. & on-hand. High source impedance >10 MEG OHM. Expected flow measurement accuracy:2-4%
16	Oxidizer Flow Rate	Cps (Lbs/sec)	.1416 lbs/sec(0.9) (175 cps) .2182 lbs/sec(260cps)	0-600 cps	Century #1		0-300 cps	1/2 Cycle	Basic 600 cps	0.1% F.S. 1.2 cps		600 cps	10 in/sec	Buy flowmeter. D.C. amplifier reqd. & on-hand. High source impedance > 10 MEG OHM. Expected flow measurement accuracy:2-4%
17	Oil Flow Rate a) Roller Bearing c) Alternator	GPM	a) .05 c) 0.18	0 -.5 GPM	Visual Flowmeter Integrator	0 -.5 GPM	--	.02 GPM		4% F.S. .02 GPM	--	--	--	Measure roller brg. flow as function of items 9 & 10. (inlet pressure. Flowmeter & integrators on hand at Roanoke.)

TABLE 4-9 (Cont.)
INSTRUMENTATION REQUIREMENTS

Item	Parameter	Units	Expected Operating Range	Transducer or Instrument Range	Recorder	Recorder Parameter Range	Record. Deflect. Range	Readable Increment	1/4 Cycle Response Time	Transd. Reproductability	Completed by Instrumentation			Remarks
											Galvo Type	Resp. Rate	P.S.	
18	Oil Flow Rate Ball Bearing and Seal Supply	GPM	0.40	0.5 GPM	Visual Flowmeter Integrator	0 -.5 GPM	--	.02 GPM	4% F.S. .02 GPM		--	--	--	See above.
19	Oxidizer Supply Temperature	°F	70°F	30-120°F I.C. Thermocouple	Century #1	30°-120°F	4 in.	.06°F	.020	4% 4.8°F		100 cps		If possible, use electrical reference junction
20	Fuel Supply Temp.	°F	70°	30°-120°F I.C. Thermocouple	Century #1	30°-120°	4"	.06°F	.020	4.8°F		100 cps		Same as above
21	Field Voltage - D.C.	VDC	10V	Direct to Galvo	Century #1	0-30	4 in.	.6V	.001	2% F.S.		600 cps		Filtering?
22	Moog Valve Voltage	VDC	28	Galvo	Century #1	0-35 VDC	4 in.	0.150 VDC	.001	0.5% = 0.14VDC		600 cps		Secure amplifiers -Galvos
23	Moog Valve Current	Amps	1.0	Galvo	Century #1	0-3.5 Amps	4 in.	.006 Amps	.001	0.5% .05 Amps		600 cps		Secure amplifiers -Galvos
24	Oxidizer Tank Temperature	°F	40-80°F	0-250°F	Visual Tempera. Prob.	--	3"Dial	5°	--	5%	--	--	--	
25	Fuel Tank Temp.	°F	40-80°F	0-250°F	Visual Tempera. Prob.	--	3" Dial	5°	--	5%	--	--	--	
26	Alternator Frequency	cps or rpm	0-30,000 rpm 0-12,000 cps	E-put COUNTER	Visual					0.01%				
27	Alt. D.C. Output Volts	VDC	28 VDC	0-30 VDC	Visual Voltmeter	0-50VDC	4"Dial	0.24	Visual S.S.	.05 VDC 0.1%	--	--	--	Buy or loan from Cleveland
28	Alt. D.C. Output Amps	ADC	103-206 Amps	0-300 Amps DC	Visual Ammeter	Multiple 0-100 0-300	4"Dial	1 Amp	Visual S.S.	1.5 Amps 0.5%	--	--	--	Buy or loan from Cleveland
29	A.C. Volts @ 1100 cps	VAC	20 VAC 1100 cps	0-50 VAC	Visual Voltmeter	0-50 VAC	4"Dial	0.25 VAC	Visual S.S.	1.0 VAC 2%				Buy or loan from Cleveland
30	Waveform + Pulse Setting	Scope		Visual Scope	Visual Scope	--	--	--	--	--	--	--	--	

TABLE 4-9 (Cont.)
INSTRUMENTATION REQUIREMENTS

Item	Parameter	Units	Expected Operating Range	Transducer or Instrument Range	Recorder	Recorder Parameter Range	Record. Deflect. Range	Readable Increment	1/4 Cycle Response Time	Transd. Reproductability	Completed by Instrumentation: Galvo Type	Completed by Instrumentation: Resp. Rate	Completed by Instrumentation: P.S.	Remarks
31	Helium Valve Voltage	VDC	28 VDC	0-30 VDC	Century #1	0-30 VDC	3/4"	1.5 VDC	.004	0.5% Galvo		100 cps		Amplifier probably not reqd. for this channel.
32	Ripple Voltage	VRMS	1.5 VRMS	V.T.V.M.	Visual	Multiple		0.5 VRMS	Slow	3%	--	--	--	
33	Moog Valve Temp.	°F	200°F	Logger I.C. #1	Leeds	0-600°F	10" Paper	2°F	40 Sec	1-1/2% 10°F				①
34	Face Seal Housing	°F	500°F	Logger I.C. #1	Leeds	0-600°F	10" Paper	2°F	40 Sec	1-1/2% 10°F			2 in/Min	①
35	Turbine Bearing Race Outer	°F	350°F	Logger I.C. #1	Leeds	0-600°F	10" Paper	2°F	40 Sec	1-1/2% 10°F				②
36	Alternator Turbine End Housing	°F	400°F	Logger I.C. #1	Leeds	0-600°F	10" Paper	2°F	40 Sec	1-1/2% 10°F				②
37	Alternator Outboard End Housing	°F	300°F	Logger I.C. #1	Leeds	0-600°F	10" Paper	2°F	40 Sec	1-1/2% 10°F				②
38	Roller Bearing Outer Race	°F	275°F	Logger I.C. #1	Leeds	0-600°F	10" Paper	2°F	40 Sec	1-1/2% 10°F				②
39	Oil Inlet Temp.	°F	150-250°F	Logger I.C. #1	Leeds	0-600°F	10" Paper	2°F	40 Sec	1-1/2% 10°F				②
40	Voltage Regulator Temp.	°F	200°F	Logger I.C. #1	Leeds	0-600°F	10" Paper	2°F	40 Sec	1-1/2% 10°F				①
41	Power Conditioning	°F	325°	Logger I.C. #1	Leeds	0-600°F	10" Paper	2°F	40 Sec	1-1/2% 10°F				②
42	Pulser Temperature	°F	200°F	Logger I.C. #1	Leeds	0-600°F	10" Paper	2°F	40 Sec	1-1/2% 10°F				①
43	Alternator-Turbine End, End Turns	°F	475	Logger I.C. #1	Leeds	0-600°F	10" Paper	2°F	40 Sec	1-1/2% 10°F				②
44	Field Coil-Turbine End	°F	475	Logger I.C. #1	Leeds	0-600°F	10" Paper	2°F	40 Sec	1-1/2% 10°F				①
45	Reaction Chamber	°F	800-1400°	Logger C.A. #2	Leeds +N.	0-2400°F	10" Paper	10°F	40 Sec	--	--	--	2 in/min	②
46	Scroll Temperature	°F	800-1400°	Logger C.A. #2	Leeds +N.	0-2400°F	10" Paper	10°F	40 Sec	25°F				②

TABLE 4-9 (Cont.)
INSTRUMENTATION REQUIREMENTS

Item	Parameter	Units	Expected Operating Range	Transducer or Instrument Range	Recorder	Recorder Parameter Range	Record. Deflect. Range	Readable Increment	1/4 Cycle Response Time	Transd. Reproductability	Completed by Instrumentation			Remarks
											Galvo Type	Resp. Rate	P.S.	
47	Nozzle Temperature	°F	800-1400°	Logger C.A. #2	Leeds + N.	0-2400°F	10" Paper	10°F	40 Sec	25°F				②
48	Nozzle Plate	°F	800-1400°	Logger C.A. #2	Leeds + N.	0-2400°F	10" Paper	10°F	40 Sec	25°F				②
49	Water Cooled Duct	°F	90°F	Logger I.C. #1	Leeds + N.	0-2400°F	10" Paper	10°F	40 Sec	25°F				②
50	Injector Head Temp.	°F	250°F	Logger I.C. #1	Leeds + N.	0-2400°F	10" Paper	10°F	40 Sec	25°F				②

4.4 System Performance

This section is based upon the testing of Unit No. 1.

4.4.1 Coast Time

The coast time between pulses depends essentially on two factors: (1) the various loads applied to the unit and (2) the speed increase during the previous pulse. The speed increase is a function of the turbine inlet conditions. If these conditions are not equivalent to the design conditions, the speed increase and subsequent coast time will decrease. Such factors as propellant pressure and temperature had a measurable effect on coast time. As propellant temperature increases, the density decreases and the resultant mass flow in each pulse decreases. Reduced propellant inlet pressures caused by pressurization system tolerances also result in smaller mass flows. In either case, reduced mass flow imparts less energy to the turbine and reduces the speed increase and coast time. Thus, it becomes important to maintain conditions of the propellants within close tolerances for repeatable performance.

The loads imposed on the turbine consist of the electrical load of the alternator, the mechanical losses of the bearings and seals, and the windage on the rotating assembly with the major windage loss being that of the turbine disk. The coast time is basically a function of electrical load because windage and mechanical losses are constant with change in electrical load. Figure 4-24 shows the relationship between coast time and equivalent output. The slope of this curve curve changes as output increases. This occurs because alternator efficiency increases as load increases from zero to 2/3 load. Thus, an increase in useful output in this range causes a less than proportional increase in electrical losses, and a less than proportional decrease in coast time. However, the alternator efficiency is nearly constant above 2/3 load and the decrease in coast time is approximately proportional to the increase in load. Therefore, the slope of the curve is nearly constant in this load range. Tests at O/F ratios of 0.9 and 2.7 showed that the coast time is approximately the same for both ratios.

Figure 4-24 is expressed in terms of equivalent output. Equivalent output consists of two loads: (1) useful electrical output and (2) windage. Windage is included in equivalent output because it is a loss due to a limitation of the altitude facility rather than a function of any part of the power system, itself. This limitation will not exist in the actual vacuum application and, therefore, should not penalize the performance of the unit in tests simulating the vacuum environment.

To avoid the performance penalty; the windage value is treated as equivalent electrical output by adjusting it for alternator efficiency and adding it to the actual alternator output. The windage power is adjusted by multiplying by the incremental alternator efficiency i.e. the efficiency with which the alternator would have converted that increment of shaft power available if there were no windage to electrical power. This factor is approximately 0.9. The adjusted windage power is then added to the alternator output.

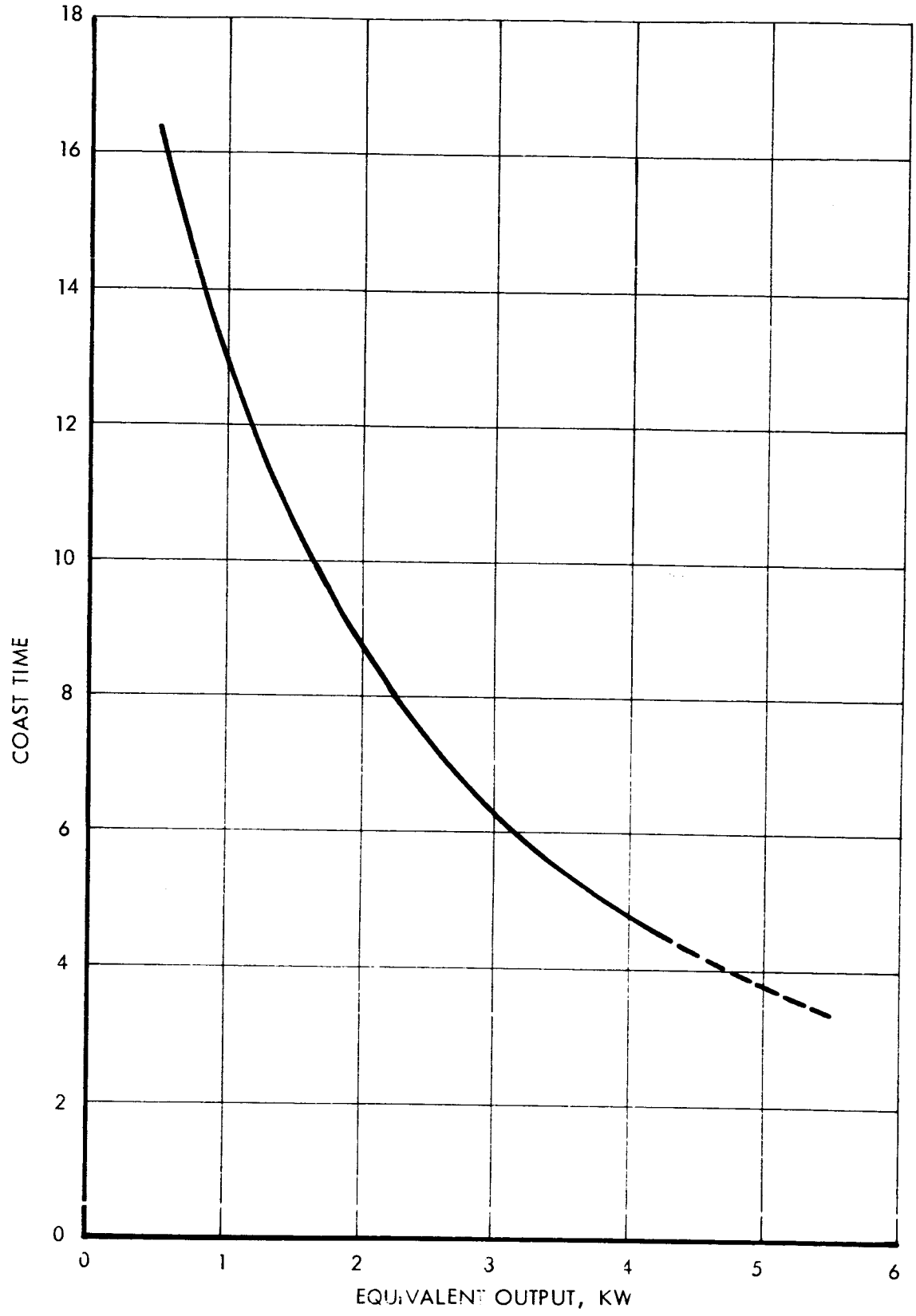

FIGURE 4-24 COAST TIME VERSUS EQUIVALENT OUTPUT FOR O/F = 0.9 & 2.7

The windage was experimentally determined by obtaining the coast time at a range of altitude cell pressures corresponding to the range of 70,000 ft. to 100,000 ft. altitude. The results are plotted in Figure 4-25. If the curve is extrapolated to zero psia, the power losses remaining are the fixed mechanical and electrical losses in the machine. The total drag horsepower at each altitude was computed by multiplying the polar moment of inertia of the rotating assembly by the angular deceleration determined from the coast time. The power attributed to windage is the power in excess of the power existing at an ambient pressure of absolute zero.

4.4.2 Specific Propellant Consumption

The specific propellant consumption (SPC) was determined at various loads at the 0.9 and 2.7 O/F ratios. The results are shown in Figures 4-26 and 4-27. Figure 4-26 shows that the best SPC achieved was 8.35 lb/BHP-HR with an equivalent output of 4.3 KW at the DC terminals. The SPC is based on the equivalent output which includes windage referred to the DC terminals. The SPC may be referred back to the shaft output by adjusting the SPC and equivalent power output for the electrical conversion efficiency. This is shown in Figure 4-27 as an SPC of 6.60 lb/BHP-HR at a shaft output of 7.20 hp. A second curve showing the SPC generated by the turbine wheel itself, neglecting bearing and seal friction is included for comparative purposes.

In either case, the SPC decreases with increased load because fixed loads such as mechanical losses in the seals and bearings become a smaller portion of the output power. Tests indicated that SPC was approximately the same for both the 0.9 and 2.7 O/F ratios.

4.4.3 System Temperatures

Temperature data from the tests of Unit No. 1 with the copper finned scroll indicated that the extremely high temperatures were kept largely within the scroll area. Curves of the variation of maximum scroll temperature and turbine shroud temperature with equivalent output in Figures 4-28 and 4-29 show the relationship of temperature and load. The maximum temperature recorded was 1350°F on inlet to the scroll. As was expected, the O/F ratio had a noticeable effect on the temperature of these parts. The temperatures at the same equivalent loads were approximately 200°F higher at the 2.7 O/F ratio.

The face seal and bearing temperatures were maintained well below the safe limits of operation. Ball bearing and face seal temperatures are plotted against load in Figures 4-30 and 4-31. The ball bearing temperature was measured by a shielded thermocouple in contact with the bearing outer race, and the seal temperature was measured by a shielded thermocouple in contact with the outside diameter of the seal retainer. These temperatures were controlled to low values by the oil sprayed directly on these parts. The maximum seal temperature was approximately 320°F and the maximum ball bearing temperature was about 300°F. The typical roller bearing temperature was 200°F to 245°F. The fact that the ball bearing was located nearer the turbine than the roller bearing caused it to receive more heat by conduction from the turbine area resulting in a higher bearing temperature. The face seal and ball bearing temperatures were 60° and 25° higher, respectively, at the 2.7 O/F ratio for the same equivalent load. The increase

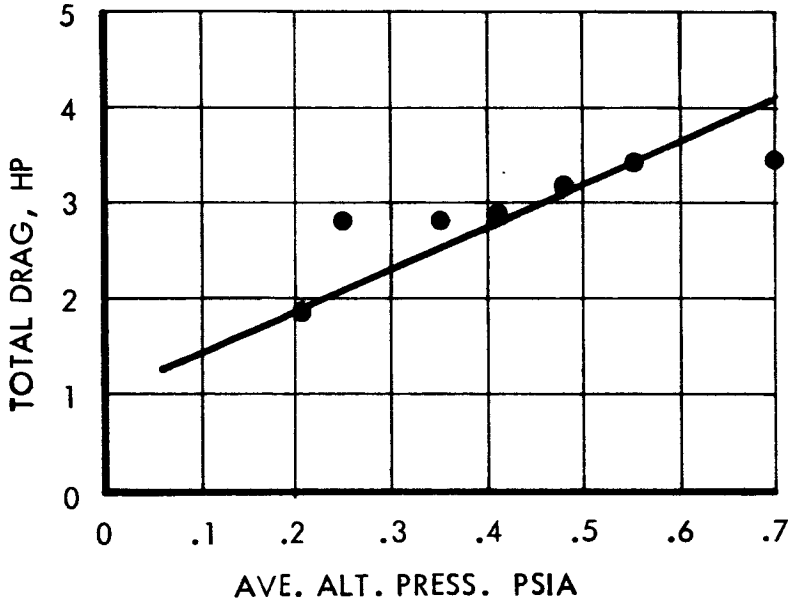

FIGURE 4-25 TOTAL DRAG POWER VERSUS AVERAGE ALTITUDE CHAMBER PRESSURE

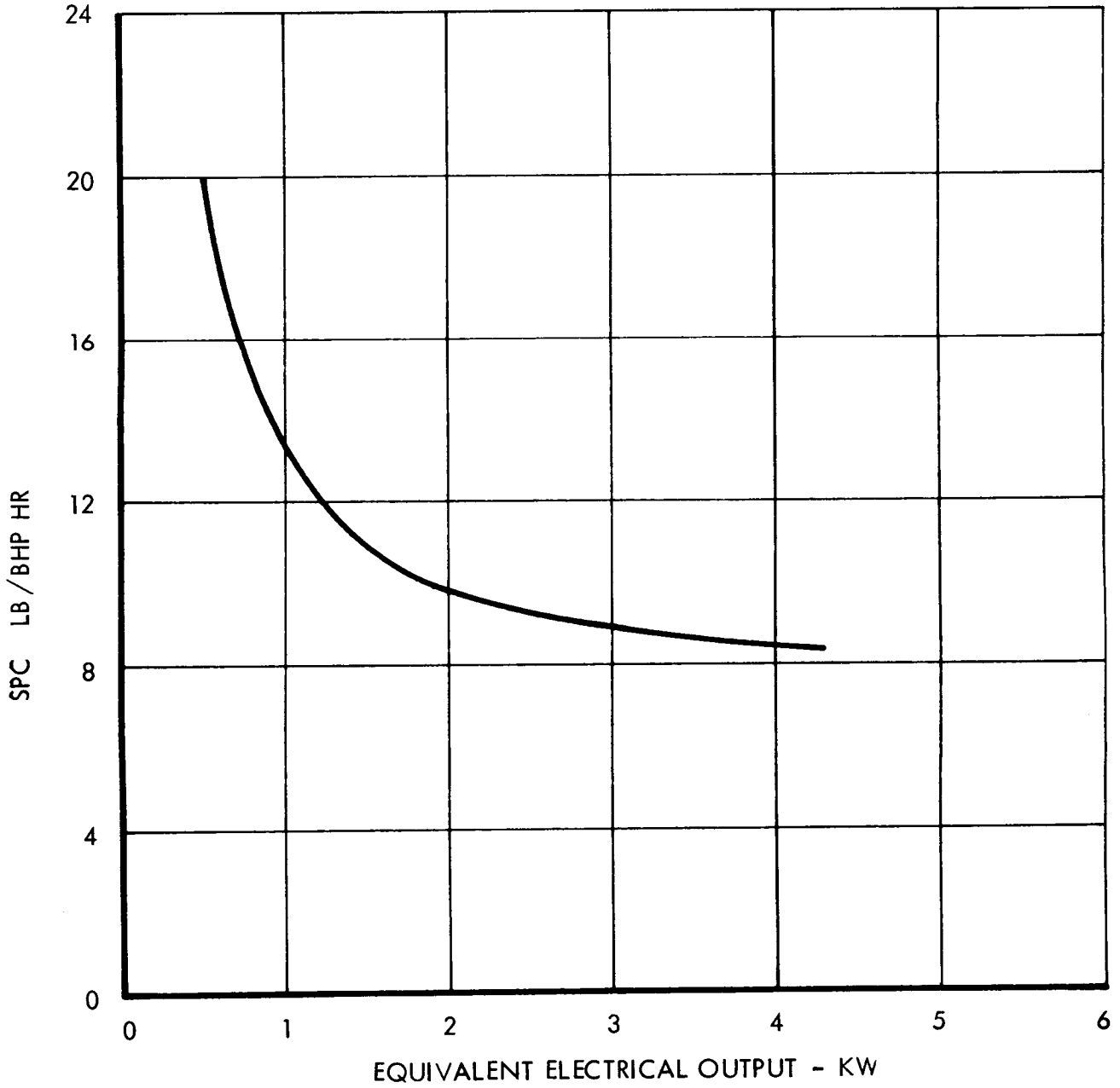

FIGURE 4-26 SPECIFIC PROPELLANT CONSUMPTION VERSUS EQUIVALENT DC ELECTRICAL OUTPUT

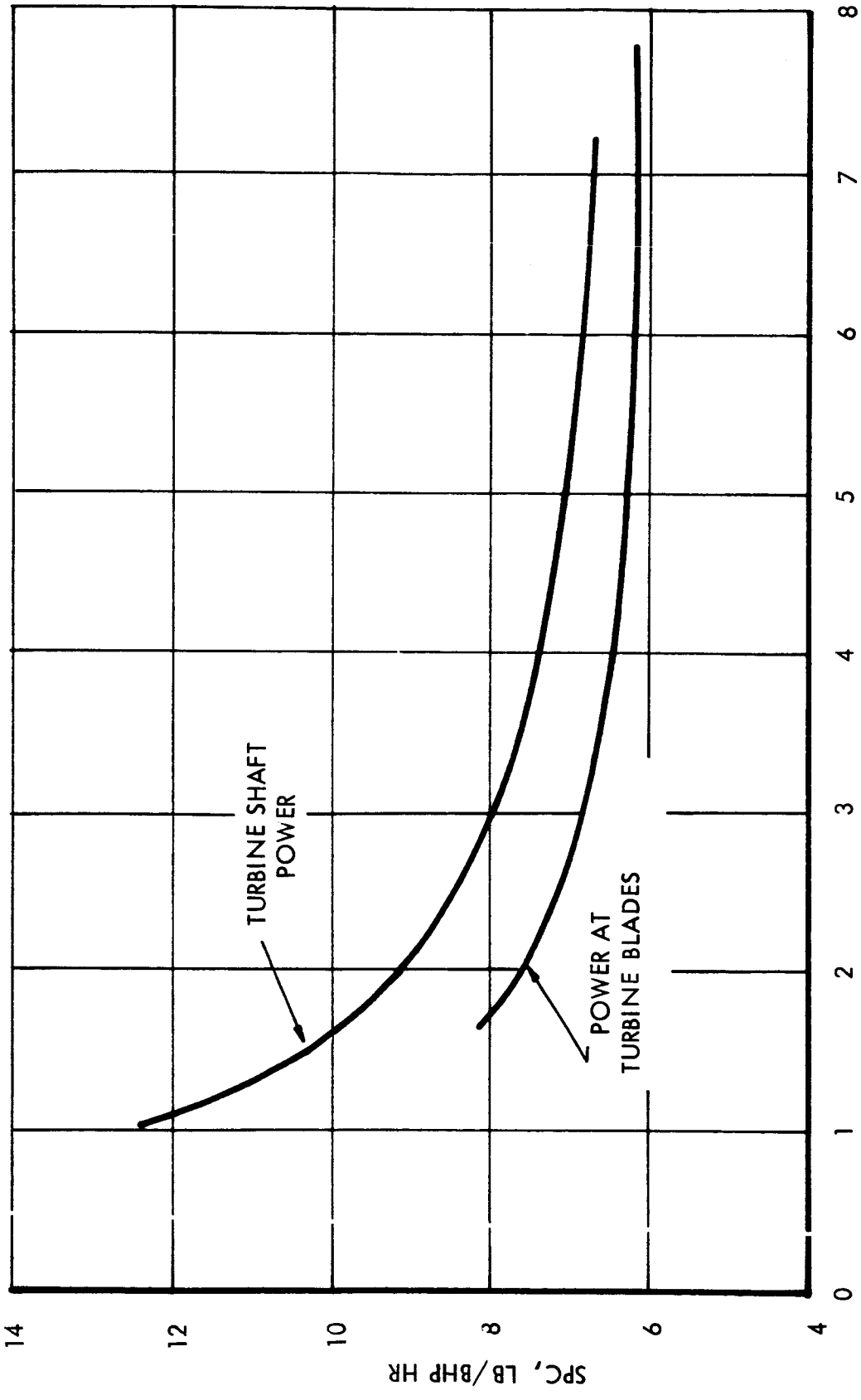

FIGURE 4-27 SPECIFIC PROPELLANT CONSUMPTION VERSUS TURBINE OUTPUT POWER

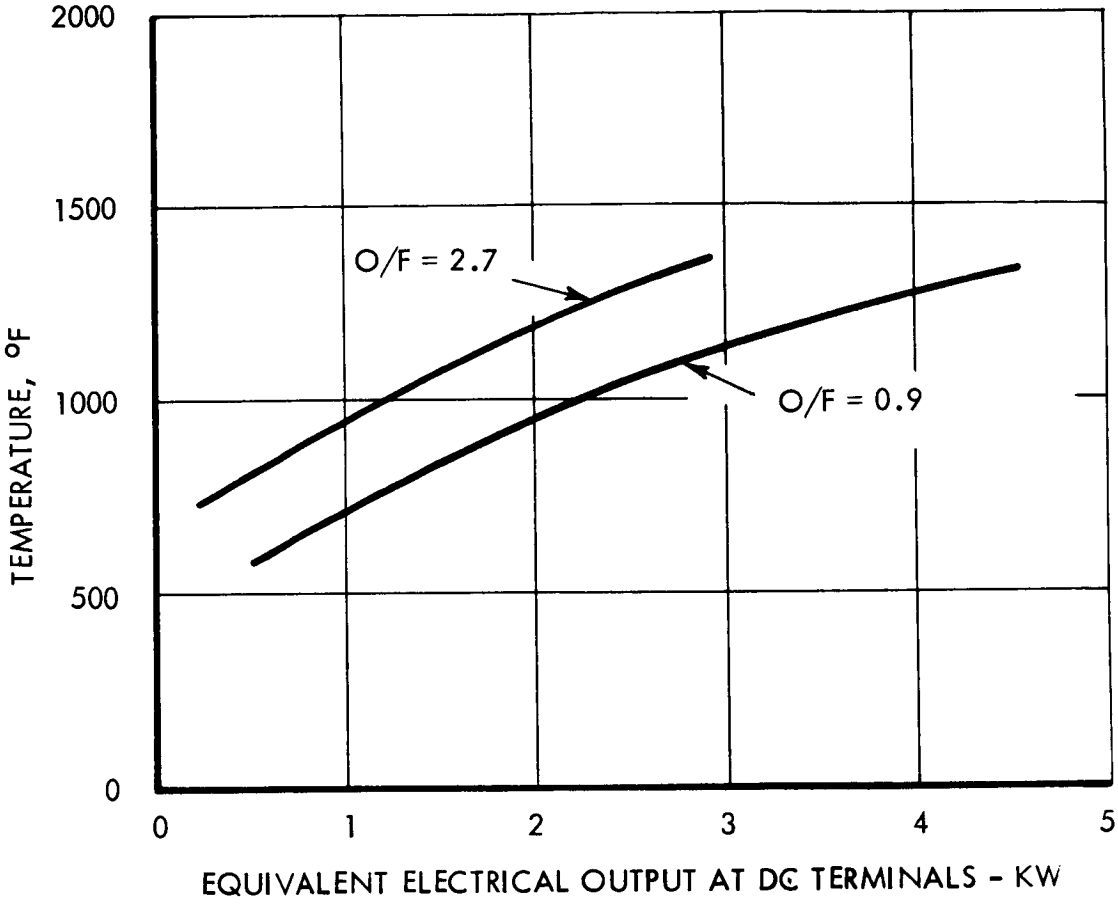

FIGURE 4-28 MAXIMUM TURBINE SCROLL TEMPERATURE VERSUS EQUIVALENT DC ELECTRICAL OUTPUT

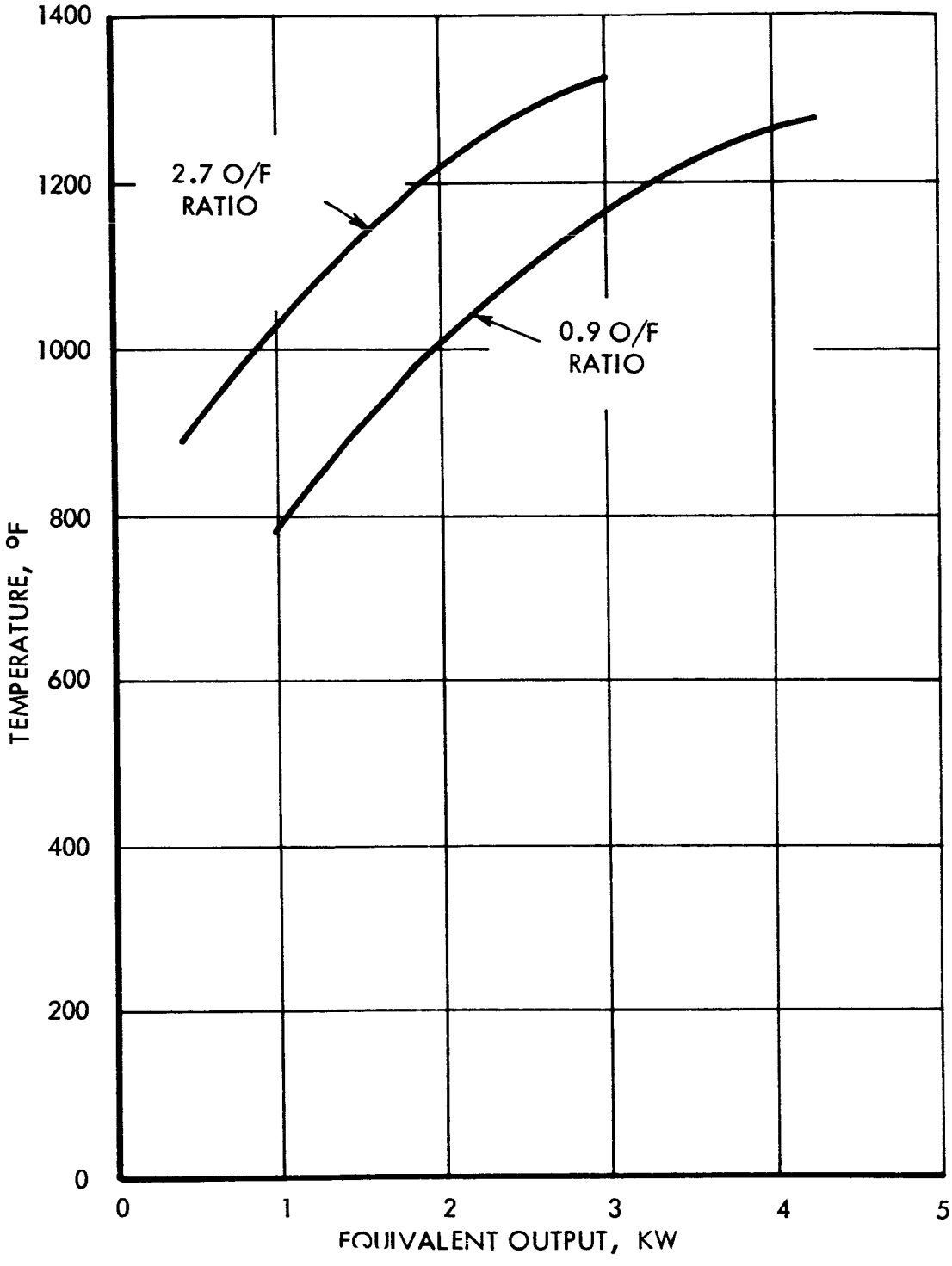

FIGURE 4-29 TURBINE SHROUD TEMPERATURE VERSUS EQUIVALENT OUTPUT

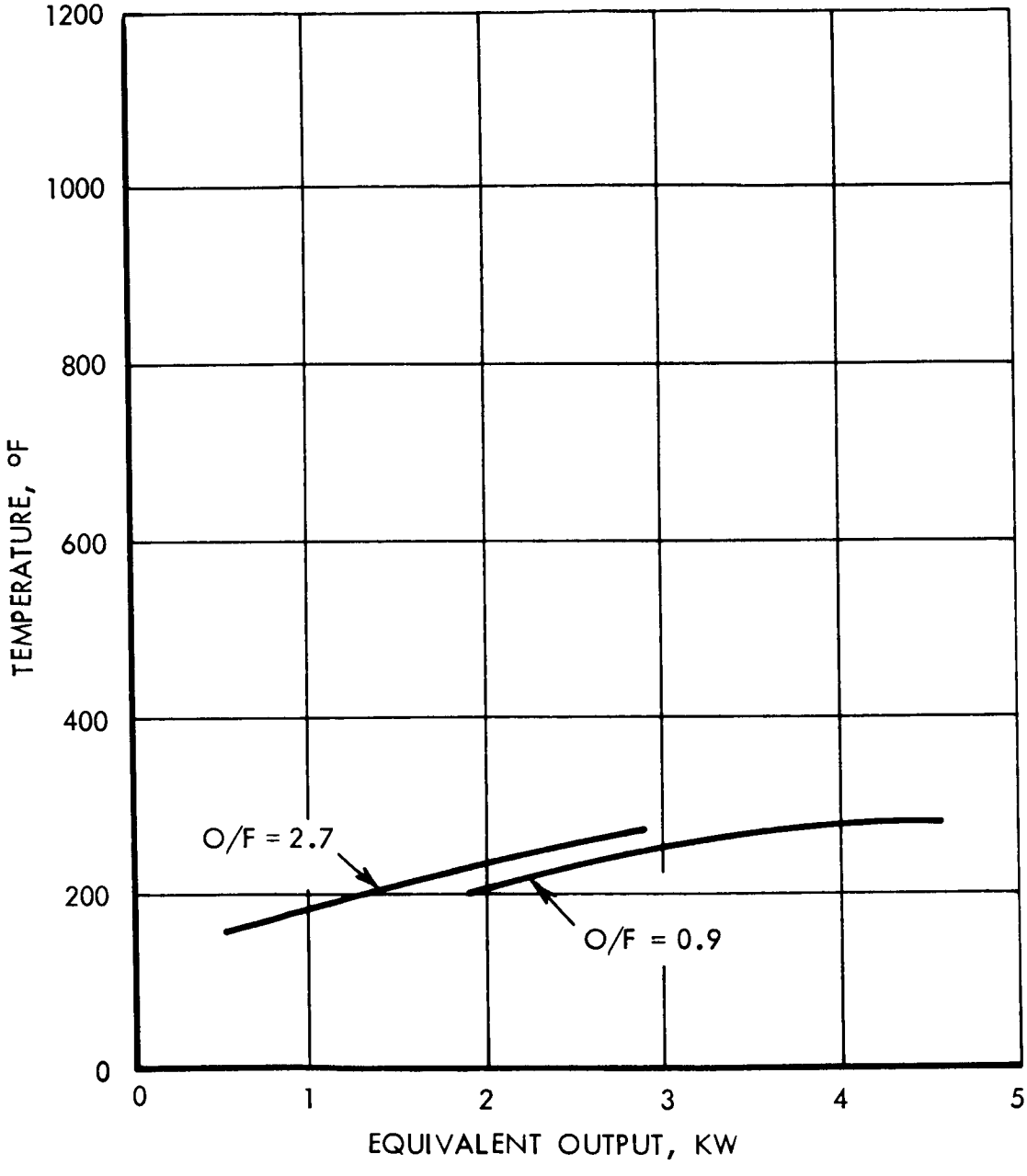

FIGURE 4-30 BALL BEARING OUTER RACE TEMPERATURE VERSUS EQUIVALENT OUTPUT O/F = 0.9 & 2.7

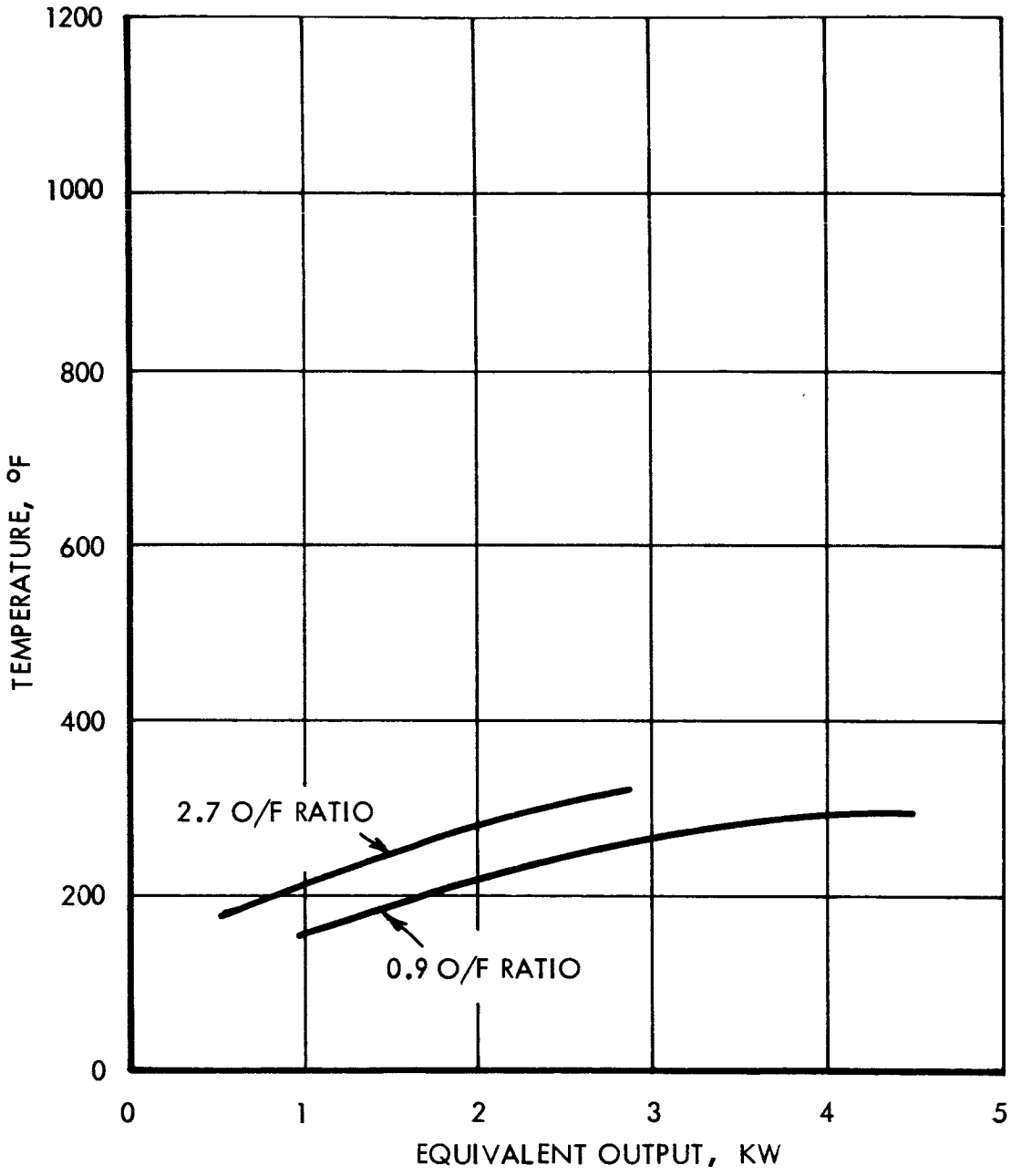

FIGURE 4-31 FACE SEAL TEMPERATURE VERSUS EQUIVALENT OUTPUT

was lower in these areas than in the scroll because of the poor conduction paths connecting the two areas and the ability of the oil to carry away the additional heat at the higher 0/F ratio.

The gas generator differed from other components in that the temperatures were lower at the 2.7 0/F ratio than at the 0.9 0/F ratio. It is believed that this was caused by the high vapor pressure of the oxidizer. For example, the vapor pressure of N_2O_4 is 100 psia at a temperature of 155°F. Thus, when the oxidizer temperature is above 155°F, which is possible in the injector head, the vapor pressure is greater than the gas generator pressure. This promotes vaporization of some of the N_2O_4 as it leaves the injector orifices with consequent possible freezing of some of the nonvaporized liquid because of the cooling effect of the heat of vaporization. This phenomenon tends to reduce the gas generator metal temperature at the 2.7 0/F ratio because the flow of oxidizer is higher at that condition than at the 0.9 0/F ratio.

Although the turbine blade temperatures were not measured, they may be estimated from the temperature of the shroud around the turbine. The thermal analysis has shown that the turbine blade temperatures are approximately 150°F less than the shroud temperature. Figure 4-29 shows the maximum shroud temperature was 1325°F at an 0/F ratio of 2.7. Therefore, the blade temperatures reached approximately 1175°F.

Normal temperatures of the components at maximum loads at both 0/F ratios appear in Table 4-10. An area of concern is the alternator front flange. The temperature here, which reached 700°F at the 2.7 0/F ratio, is indicative of the amount of heat being transferred into the alternator housing near the bearing and seal area. Thus, in spite of efforts to isolate the alternator from the scroll by restricting the heat conduction with a piston ring, the flange reached 700°F. The 0.9 0/F ratio temperature of 535°F was maintained at a satisfactory level. Future units will be modified in this area to reduce alternator flange temperature.

Table 4-10 Normal Component Operating Temperatures

	0/F = 0.9	0/F = 2.7
Equivalent load-KW	4.0 - 4.5	2.5 - 3.0
Temperatures - °F		
Maximum scroll	1325	1375
Gas generator	1240	990
Turbine shroud	1280	1325
Average fin	650	700
Alternator front flange	535	700
Ball bearing	270	270
Roller bearing	200	245
Face seal	300	310
Alternator housing	170	180
Alternator stator	231	226
Inlet-lube oil heat exchanger	170	160
Exit-lube oil heat exchanger	140	100

4.4.4 System Energy Balance

Data from tests on Unit No. 1 were used to calculate major losses in the operating cycle at each 0/F ratio for 3 KW equivalent output. Where data were not available to calculate losses, they were estimated for the component actually used. The mechanical losses consist of the seal and bearing losses. The seal loss was obtained from the manufacturer, and the bearing losses were estimated for the particular types selected. The power conditioning loss was estimated from the final electrical circuits. The heat losses to the scroll and fins, turbine, and oil were calculated from metal and oil temperatures, and oil flow. The combustion efficiency loss for constant combustion efficiency is a linear function of the heating value, and the heat loss to the exhaust is the difference between the heating value and the sum of the other losses. The results appear in Table 4-11.

The heating value of the propellants at the 0.9 0/F ratio was not available. Thus, the combustion efficiency and the energy loss to the exhaust could not be calculated.

As anticipated, the heat rejected to the scroll, fin, and turbine is higher for the 2.7 0/F ratio because of the higher gas temperature. Heat loss to the oil is greater for the 2.7 0/F ratio because more heat is conducted to the turbine bearing from the scroll area through the alternator flange. In future units the heat conducted to the oil by this means will be reduced by revisions in the alternator flange area.

4.5 Test Results

Early in the program, tests were run using an SIV B gas generator reworked to provide an 0/F ratio of 2.7. Operating data were obtained first with a tube and single nozzle having an L* of 100, and second with a full admission turbine scroll having eleven nozzles. Ignition characteristics, pulse dynamics, and metal temperatures were acceptable. The results of these breadboard tests were then applied to the detailed design of the prototype.

A prototype system including the turboalternator, lubrication system, speed control, voltage regulator and rectifier filter package was then built and after a brief period of development testing was operated at rated load in an endurance test. A second turboalternator was assembled and tested at rated loads in an acceptance test.

The results of the testing program are presented in this section.

4.5.1 Breadboard Tests

4.5.1.1 Test Hardware Description

The capillary tube injector head used for the breadboard gas generator was a reworked SIV B unit. Alternate doublets of the SIV B injector head were plugged to accommodate the weight flow requirements of the breadboard injector; therefore, the breadboard

Table 4-11 Cycle Performance

	0/F Ratio 0.9	0/F Ratio 2.7
Equivalent Output at DC Terminal, BTU/hr	10,250	10,250
Combustion Efficiency Loss, BTU/hr	-	3,900
Mechanical Losses, BTU/hr	1,550	1,550
Power Conditioning Loss, BTU/hr	2,100	2,100
Heat Loss to Oil, BTU/hr	4,450	9,500
Heat Loss from Scroll and Fins, BTU/hr	18,130	29,900
Heat Loss from Turbine Wheel, BTU/hr	3,740	6,300
Heat Loss to Exhaust, BTU/hr	-	34,700
		98,200

% Losses	0/F Ratio 0.9	0/F Ratio 2.7
Theoretical Energy Content		2,950 BTU/lb
Combustion Efficiency	96%	96%
Mechanical Efficiency	87%	87%
% of Combustion Energy Lost to Exhaust		35.4%
% of Combustion Energy Lost to Oil		9.7%
Alternator Efficiency	89%	89%
Power Conditioning Efficiency	92%	92%
S. P. C., lbs/BHP-HR	8.9	8.9
Off/On Ratio	31.5	31.5

injector head consisted of six pairs of unlike impinging doublets such that the propellant streams were injected from two concentric circles; the fuel on the inside and the oxidizer on the outside.

The breadboard injector head was fabricated in accordance with the following design specifications:

Oxidizer Orifices (6)	.0355 in.
Fuel Orifices (6)	.0283 in.
Oxidizer Orifice Velocity	58.9 ft/sec
Fuel Orifice Velocity	34.33 ft/sec
Oxidizer Impingement Angle	44°
Fuel Impingement Angle	39°
Oxidizer Tube (Steady State) Velocity	58.87 ft/sec
Oxidizer Tube (Steady State) Total Flow	.2182 lbs/sec
Oxidizer Transient Flow	.2756 lbs/sec
Fuel Tube (Steady State) Velocity	11.65 ft/sec
Fuel Tube (Steady State) Total Flow	.0808 lbs/sec
Fuel Transient Flow	.118 lbs/sec
Resultant Momentum Angle	31°
Fuel Fill Volume	.0675 cu. in.
Oxidizer Fill Volume	.04335 cu. in.

In order to adapt the Moog valve (Model 52 x 108) to the existing injector head valve flanges, it was necessary to utilize two adapter sections. The adapter tubes were sized to provide a fuel lead of approximately .005 seconds. Injector dribble volume was minimized by minimizing the inside diameter of the adapter tubes consistent with available tubing.

To accomplish early testing of the injector head, a single throat nozzle was utilized in lieu of the multi-throat nozzle block/scroll design. The area of the single throat nozzle approximated the total area of the eleven .232 diameter nozzles of the nozzle block/scroll assembly which was used in the second phase of the test program.

The test hardware with the single throat nozzle had an L* of approximately 100; whereas the test hardware utilizing the nozzle block/scroll assembly had an L* of approximately 158.

Included in the test set-up was a breadboard electronic pulser. This unit was utilized in tests of significant duration to automatically provide pulses of equal duration and consistent periods.

4.5.1.2 Test Program Description

The breadboard test program was conducted to evaluate the performance of an SIV B gas generator, reworked to approximate the prototype gas generator. Temperature profile tests were run to obtain thermal data applicable to the design of the prototype hardware. In addition, the tests provided an opportunity to evaluate the test set up.

The breadboard tests were conducted in two phases. Phase I utilized a single nozzle having a throat area approximately that of the total area of the eleven nozzles in the nozzle block. Phase II utilized the breadboard nozzle block/scroll assembly.

As an adjunct to the above test program, tests were run on two test specimens which simulated the turbine wheel blades. This addition to the test program was conducted to obtain an early insight into the ability of the turbine blades to withstand the environment of the hot gases.

Table 4-12 is a tabulation of the individual tests. Table 4-13 is a tabulation of the pulsing history for the duration of the breadboard test program. Data and curves for tests of specific interest are also presented.

4.5.1.3 Discussion of Test Results

Figures 4-32 through 4-37 are the results of the breadboard temperature profile tests with the nozzle-scroll attached to the reworked SIV B injector and generator. Tests 023-1, 023-2, and 024 were conducted at a simulated altitude of 100,000 feet. Test 023-1 was run at a τ of 60. Tests 023-2 and 024 were run at τ values of 40 and 30 respectively. Figure 4-33 shows the temperature variation of the inlet side of the injector. The maximum temperature measured was 295°F for a $\tau = 40$. However, for $\tau = 30$ there was an indication that the maximum temperature would have exceeded 295°F. The run was terminated before the injector temperature was stabilized. Runs 023-1 and 023-2 showed that the injector stabilization temperature was between 250-300°F. However, this did not necessarily imply that the surface-mounted thermocouple on the injector was indicating heat soak-back from the chamber because the altitude cell temperature stabilized at 300-350°F as shown in Figure 4-38. Plans have been initiated to reduce the cell temperature during altitude firings for prototype tests so that unbiased injector temperature measurements can be accomplished.

Tabulated below in Table 4-14 are the maximum temperatures that were obtained during tests 023-1, 023-2, and 024 which also includes the corresponding time during the test that these maximum temperatures were recorded. The thermocouple locations are shown in Figure 4-39.

TABLE 4-12

TEST HISTORY

PHASE I (Tests with Single Throat Nozzle)

Run	Pulsing Method	Sea Level/Altitude	Purpose
006	Manual	Sea Level	Rig checkout
007	Manual	Sea Level	Rig checkout
008	Manual	Sea Level	Establish supply pressures
009	Pulser	Sea Level	Pulser checkout
010	Manual	Sea Level	Supply pressure check
011	Pulser	Altitude	Temperature profile, τ = 30
012	Pulser	Altitude	Temperature profile, τ = 40
013	Pulser	Altitude	Temperature profile, τ = 20
014-1	Manual	Sea Level	Recheck rig
014-2	Pulser	Sea Level	Test simulated turbine blades
015	Manual	Altitude	Thrust test
016	Pulser	Altitude	Temperature profile, τ = 40
017	Pulser	Altitude	Repeat temperature profile, τ = 40
018	Pulser	Altitude	Retest simulated turbine blades Temperature profile, τ = 30
019	Pulser	Altitude	Temperature profile, τ = 20

PHASE II (Tests with Nozzle Block/Scroll)

020	Pulser	Sea Level	Check supply pressures, τ = 40
021	Pulser	Sea Level	Recheck supply pressures
022-1	Manual	Altitude	Test revised turb. blade simulator
022-2	Manual	Altitude	Continue turbine blade test, τ = 40
022-3	Pulser	Altitude	Continue turbine blade test, τ = 40
023-1	Pulser	Altitude	Temperature profile test, τ = 60
023-2	Pulser	Altitude	Temperature profile test, τ = 40
024	Pulser	Altitude	Temperature profile test, τ = 30

TABLE 4-13

PULSING HISTORY

Run	No. of Pulses	Programmed Pulse Duration (Sec)	Programmed Total on Time (Sec)
006	4	1.0	4.0
007	1	2.6	2.6
008	1	1.0	1.0
	1	1.5	1.5
009	3	.2	.6
	3	.1	.3
	3	.2	.6
	3	.1	.3
010	2	2.0	4.0
011	125	.2	25.0
012	150	.2	30.0
013	135	.2	27.0
014	2	1.0	2.0
	3	.2	.6
015	3	3.0	9.0
016	19	.2	3.8
017	90	.2	18.0
018	100	.2	20.0
019	120	.2	24.0
020	10	.2	2.0
	10	.2	2.0
021	10	.2	2.0
022-1	1	.1	.1
022-2	5	.2	1.0
022-3	10	.2	2.0
023-1	100	.2	20.0
023-2	75	.2	15.0
024	80	.2	16.0
	1169	Accumulated on time =	233.4

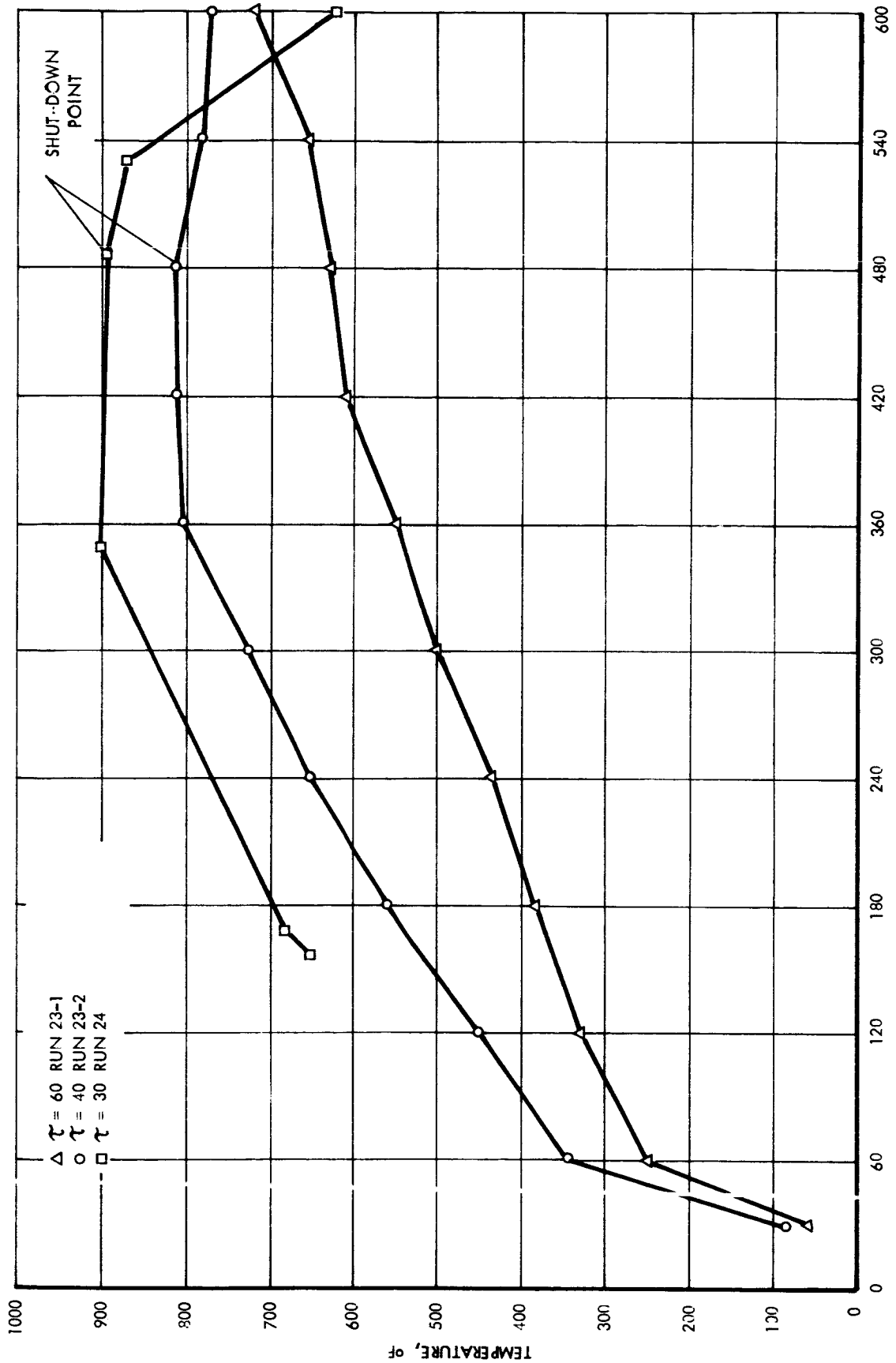

FIGURE 4-32 TEMPERATURE VERSUS RUN TIME (WITH NOZZLE SCROLL) FOR THERMOCOUPLE NO. 3
(SEE FIGURE 4-39)

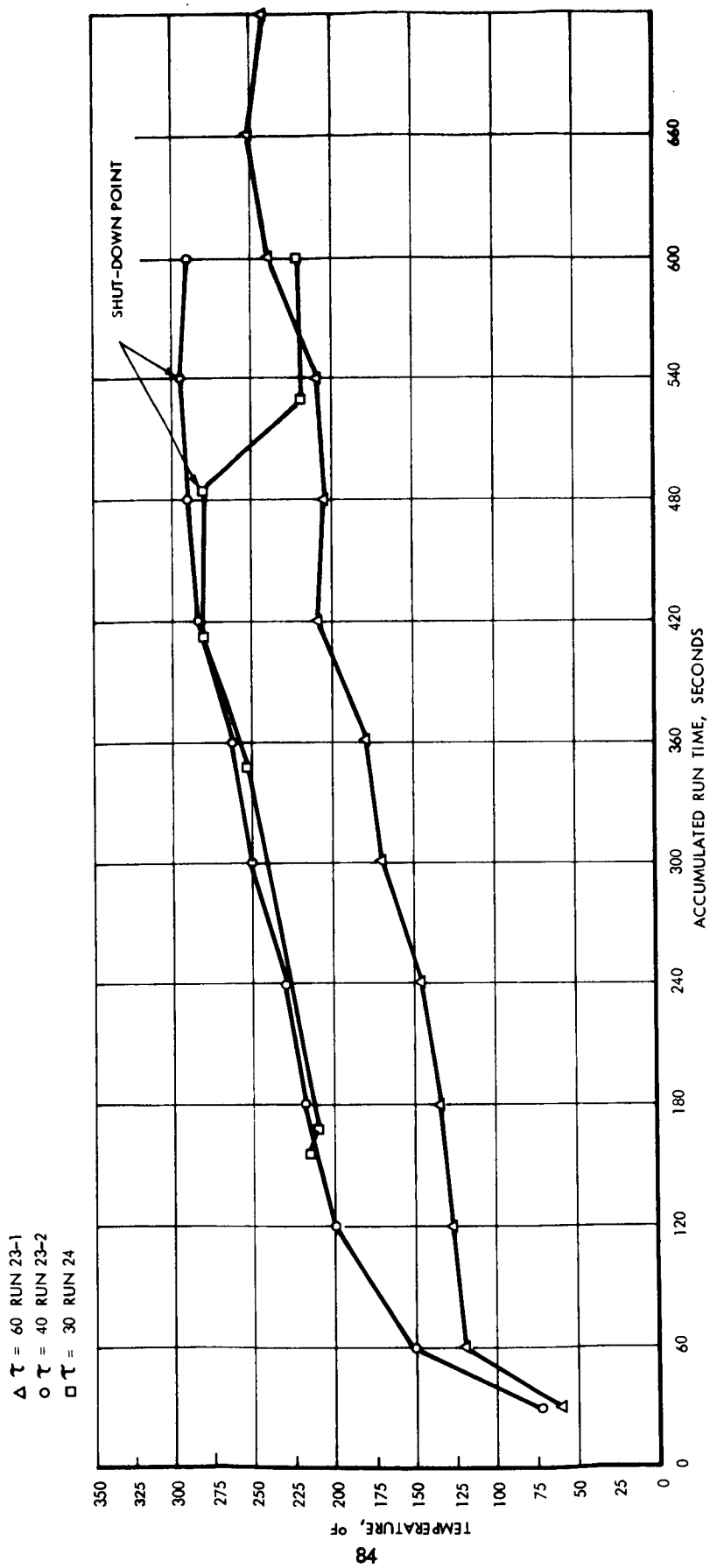

FIGURE 4-33 TEMPERATURE VERSUS RUN TIME (WITH NOZZLE SCROLL) FOR THERMOCOUPLE NO. 4
(SEE FIGURE 4-39)

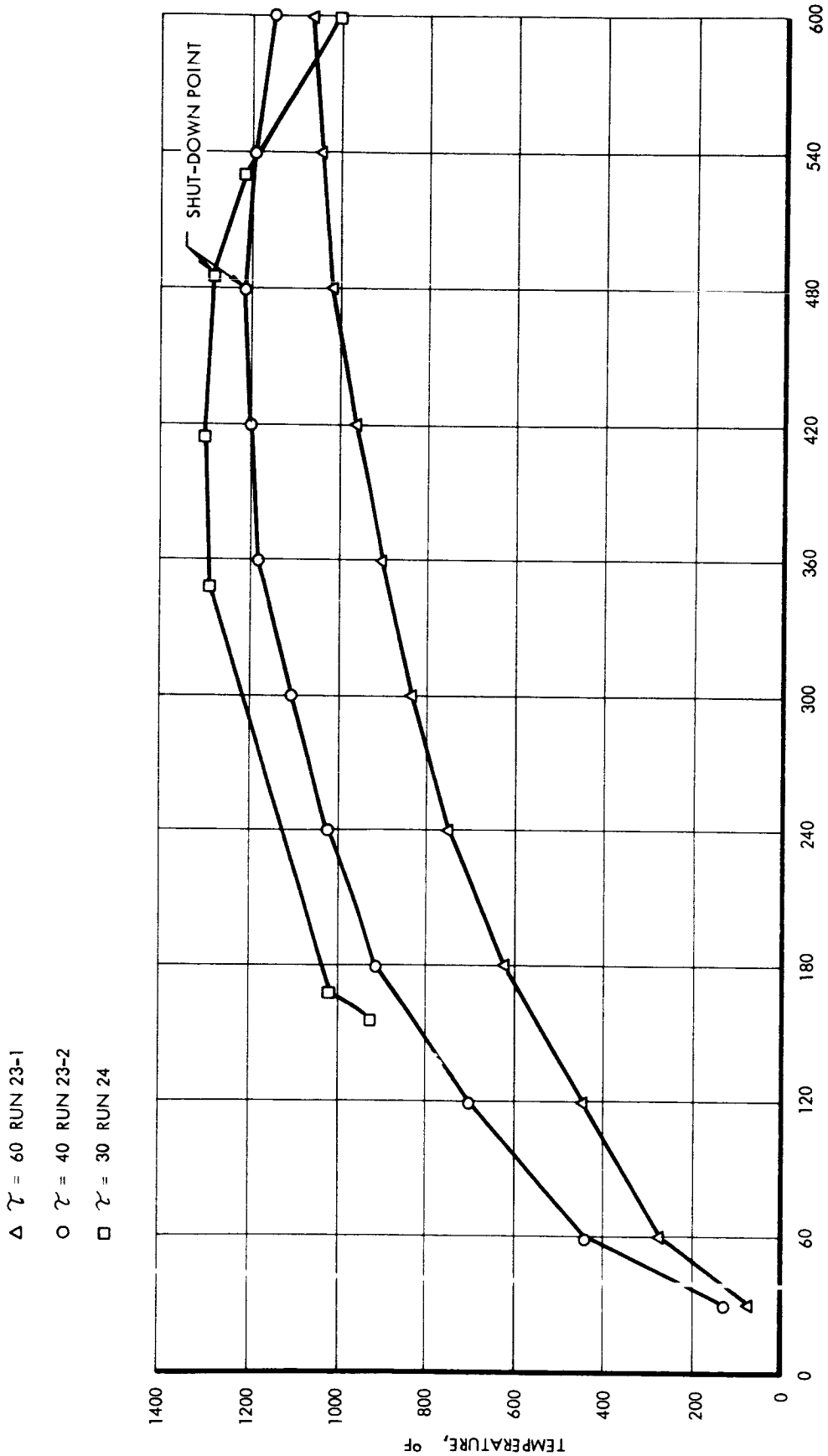

FIGURE 4-34 TEMPERATURE VERSUS RUN TIME (WITH NOZZLE SCROLL) FOR THERMOCOUPLE NO. 7
(SEE FIGURE 4-39)

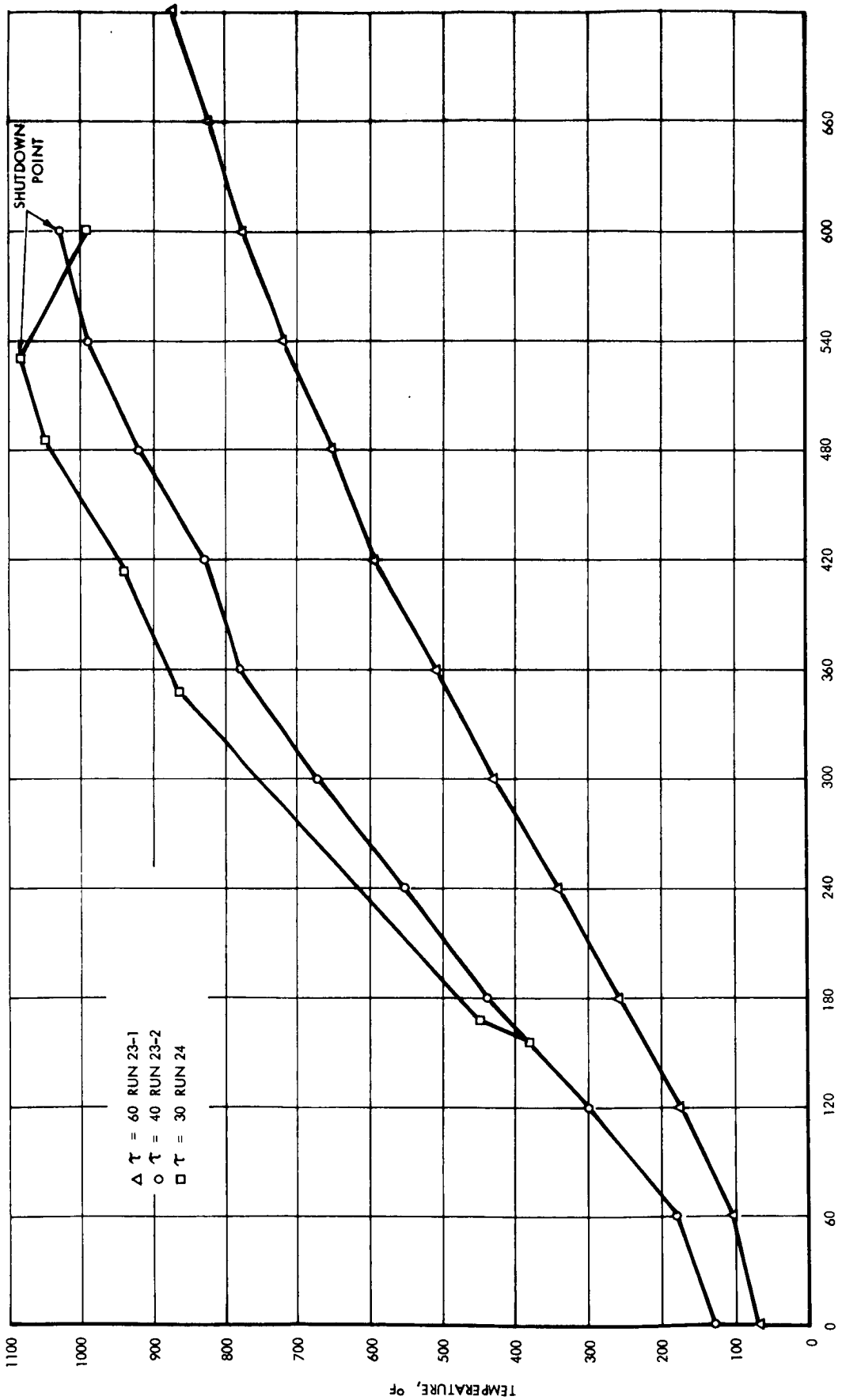

FIGURE 4-35 TEMPERATURE VERSUS RUN TIME (WITH NOZZLE SCROLL) FOR THERMOCOUPLE NO. 11
(SEE FIGURE 4-39)

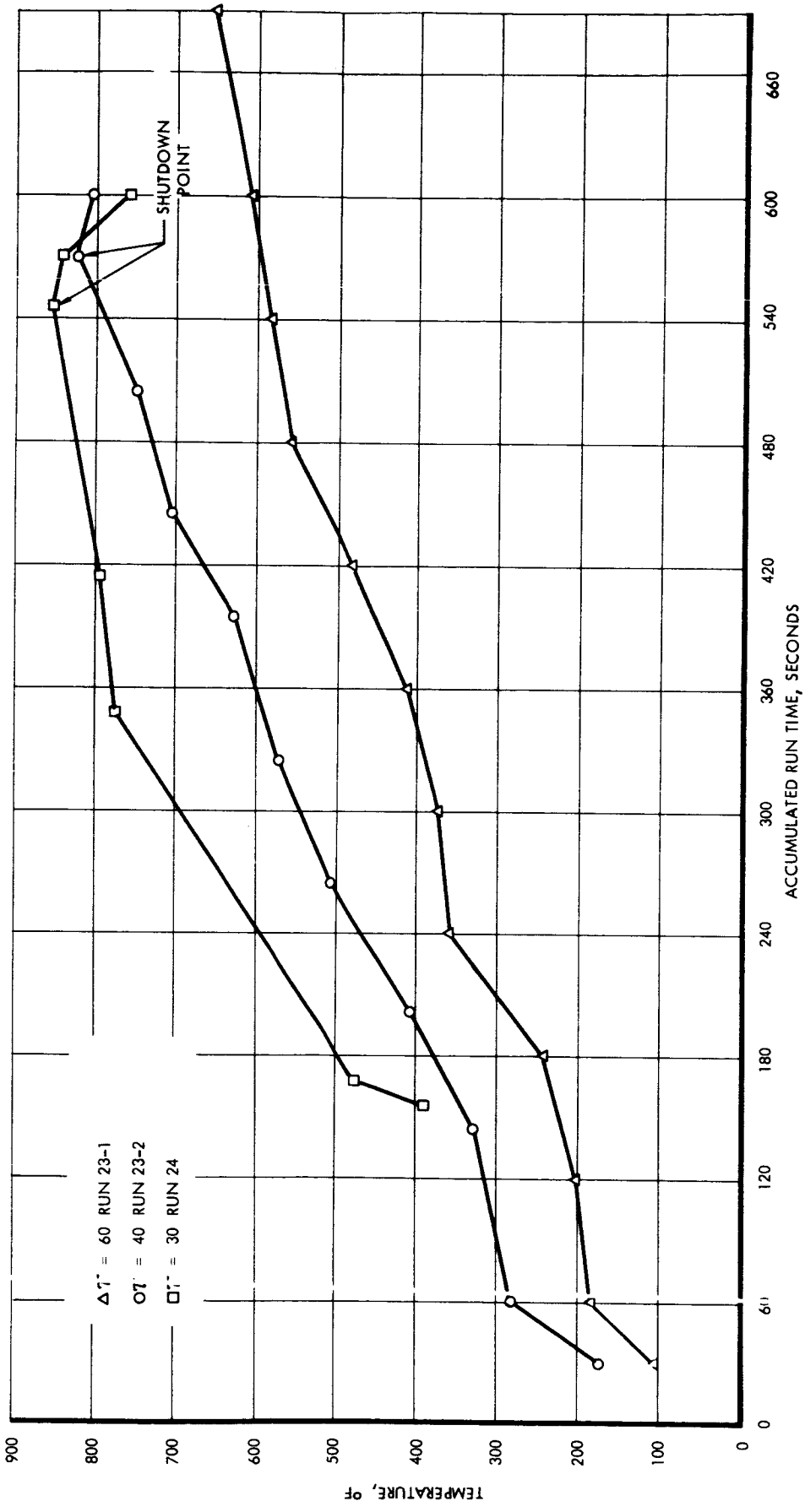

FIGURE 4-36 TEMPERATURE VERSUS RUN TIME (WITH NOZZLE SCROLL) FOR THERMOCOUPLE NO. 13 (SEE FIGURE 4-39_

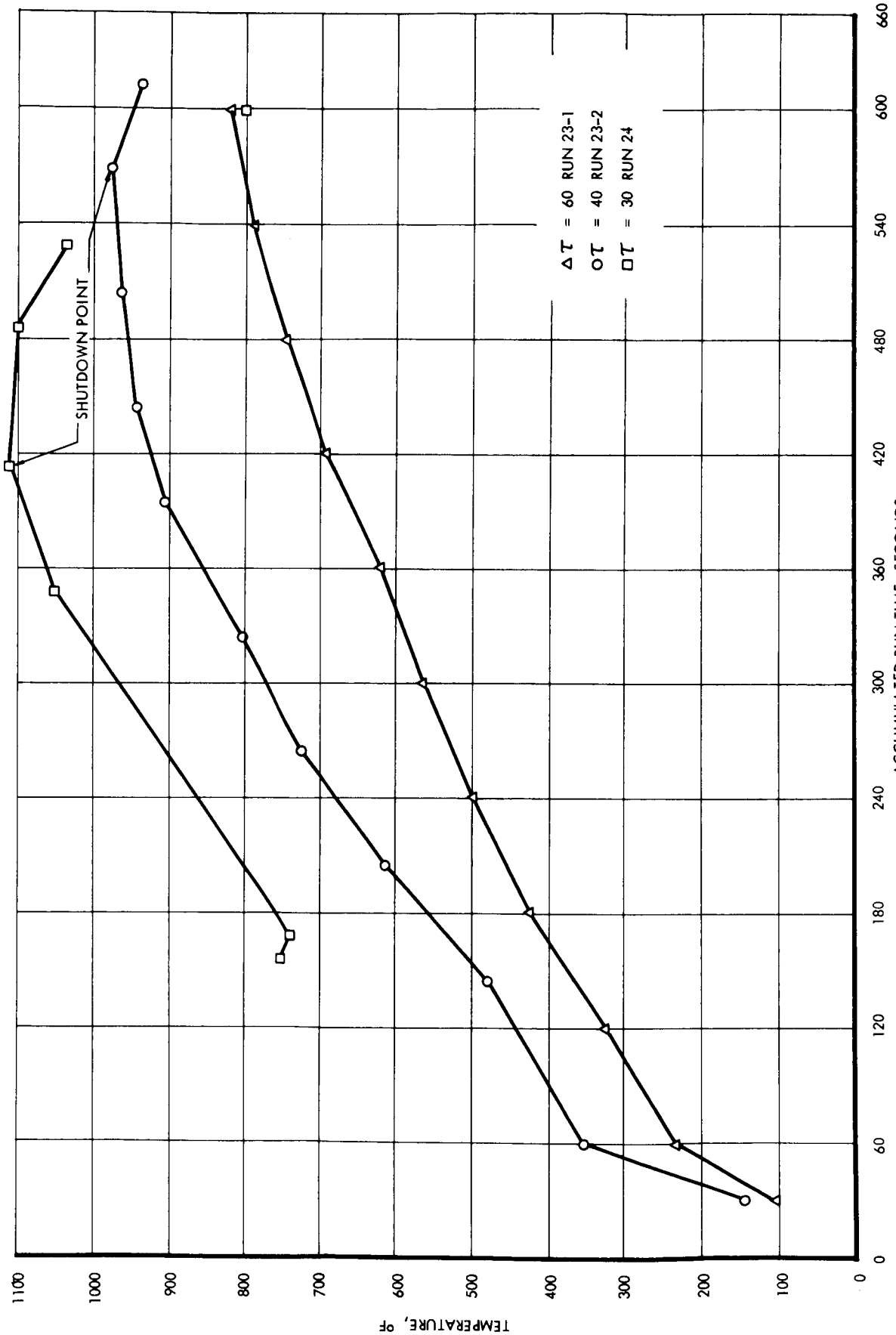

FIGURE 4-37 TEMPERATURE VERSUS RUN TIME (WITH NOZZLE SCROLL) FOR THERMOCOUPLE NO. 14
(SEE FIGURE 4-39)

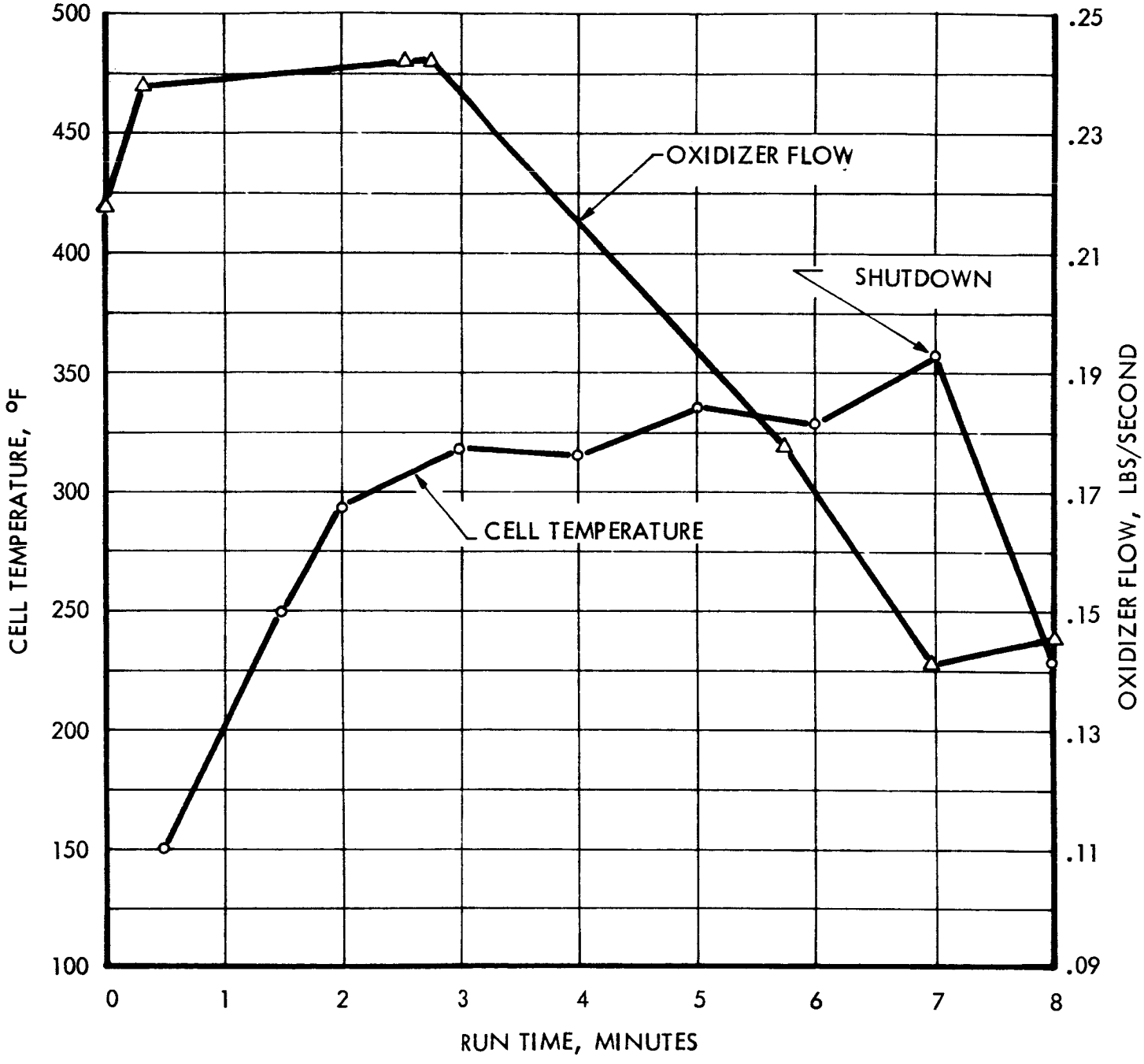

FIGURE 4-38 CELL TEMPERATURE AND OXIDIZER FLOW VERSUS RUN TIME
TEST NO. 24

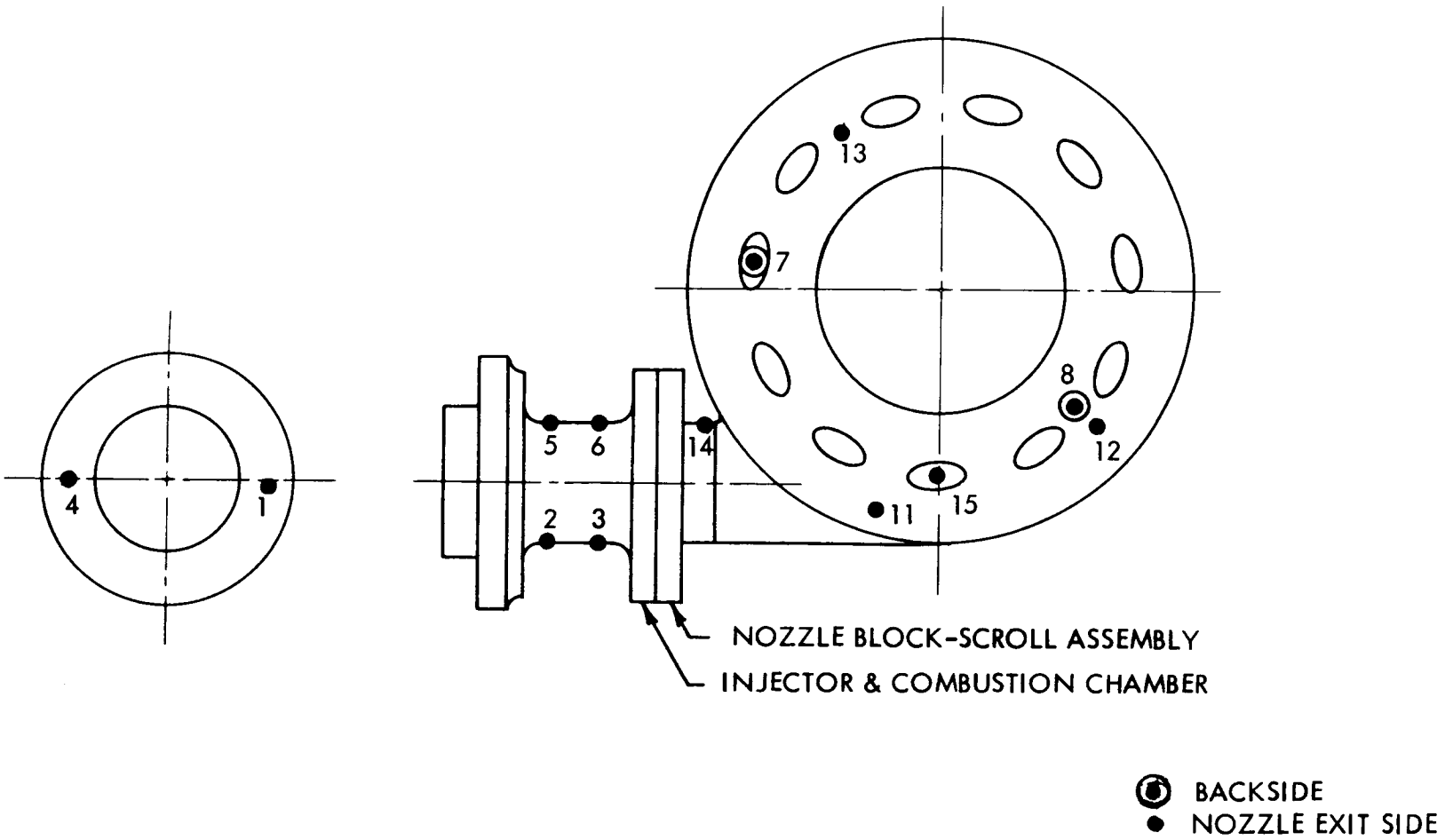

FIGURE 4-39 BREADBOARD GAS GENERATOR WITH NOZZLE BLOCK - SCROLL ASSEMBLY T/C LOCATIONS

TABLE 4-14

Thermocouple	τ = 30 Max. Temp. °F	Time Minutes	τ = 40 Max. Temp °F	Time Minutes	τ=60 Max. Temp. °F	Time Minutes
3	900	5.8	813	8.0	835	20.0
4	282	6.9	293	9.0	270	16.0
7	1300	6.9	1210	8.0	1110	14.0
11	1082	8.8	030	10.0	1030	20.0
13	855	9.1	825	9.5	865	18.0
14	1110	6.9	975	9.5	945	18.0

All of the temperature profile curves show that for longer off-times the rate of temperature rise was lower as was expected. However, for the shortest off-time pulses, temperature stabilization occurred much sooner than for the longer off-time pulses.

The first phase of testing for temperature profile data was with the reworked SIV B injector and generator welded to a test nozzle which simulated the condition of an L* = 100. The nozzle had a 3/4" throat diameter with a 2/1 expansion ratio. The results of tests 011, 012, and 013 are shown in Figures 4-40 through 4-42 for τ's of 20, 30 and 40. The thermocouple locations are shown on Figures 4-43. Listed below in Table 4-15 are the maximum temperatures recorded with the corresponding time of occurrence. These three tests were conducted at a simulated altitude of 100,000 feet.

TABLE 4-15

Thermocouple	τ = 20 Max. Temp. °F	Time Minutes	τ = 30 Max. Temp. °F	Time Minutes	τ = 40 Max. Temp. °F	Time Minutes
3	1030	8.0	920	10.0	940	11.0
4	300	8.0	305	10.0	305	12.0
11	1320	8.0	1235	10.0	890	11.0

Figure 4-41 shows that the nozzle throat section temperature had begun to stabilize at shutdown. The criteria used to determine test termination was injector temperatures in excess of 300°F. This is shown in Figure 4-40 where injector temperatures were still rising when the tests were terminated. Data from run 011 indicated an erroneous thermocouple reading at the combustion chamber wall as shown in Figure 4-39 at the 300 second mark. Figure 4-39 also shows that after approximately 420 seconds the combustion chamber wall temperature was beginning to stabilize.

The performance data for the breadboard tests are tabulated in Table 4-16. Tests 015 and 016 were run to determine the thrust performance characteristics of the injector, generator, and nozzle. The following average performance values were obtained from runs 015 and 016:

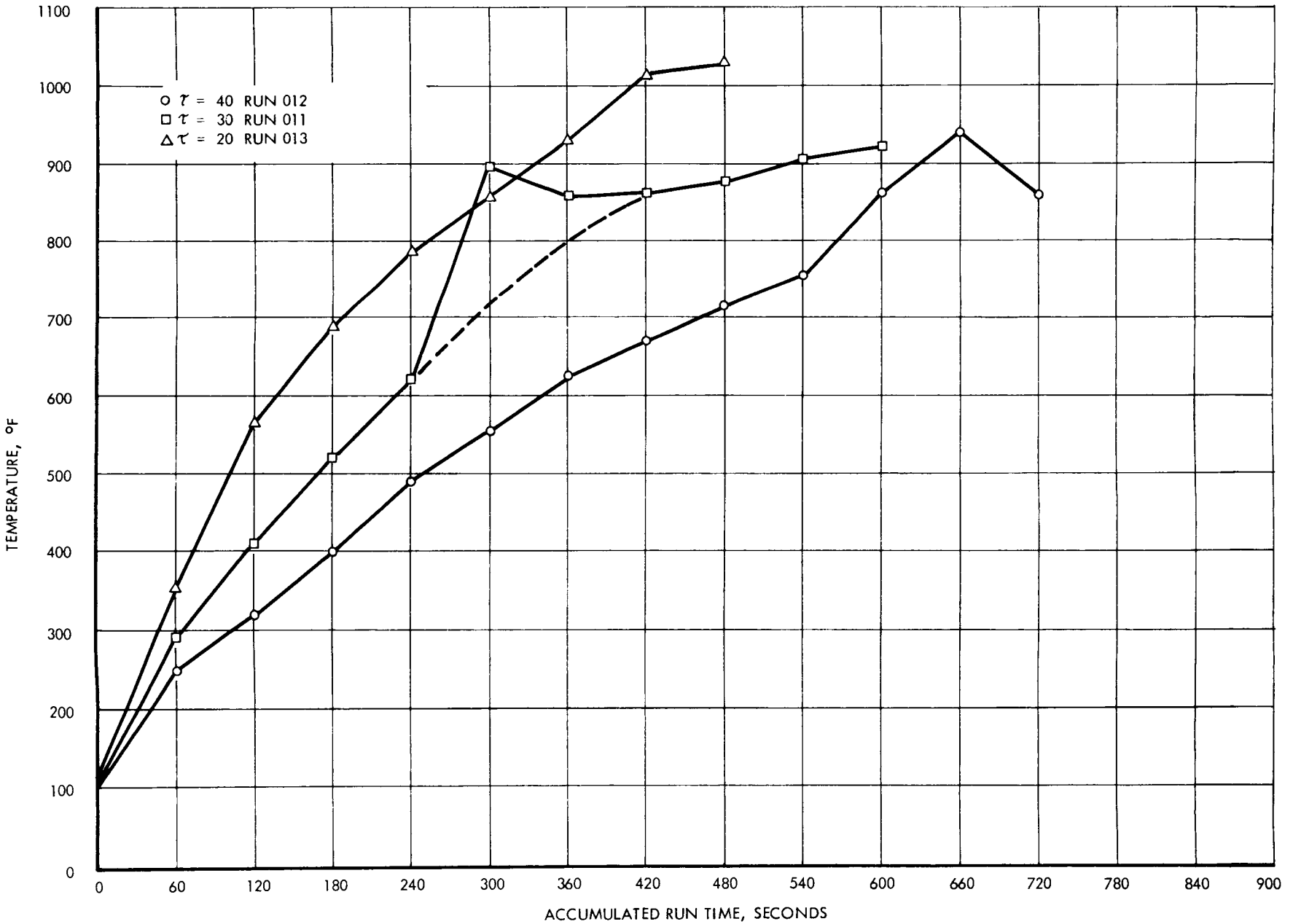

FIGURE 4-40 TEMPERATURE VERSUS RUN TIME (WITH TEST NOZZLE) FOR THERMOCOUPLE NO. 3 (COMBUSTION CHAMBER WALL)
SEE FIGURE 4-43

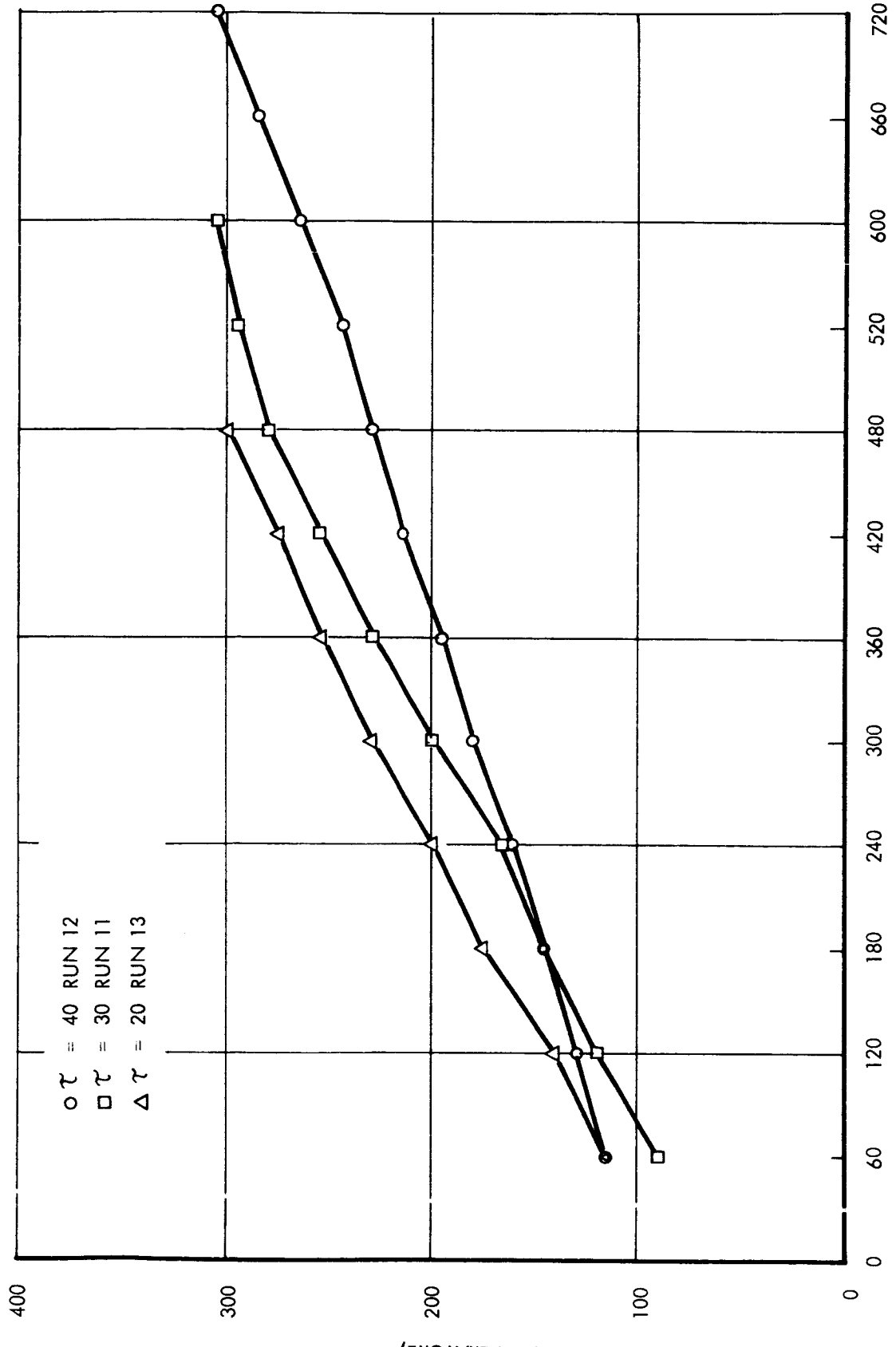

FIGURE 4-41 TEMPERATURE VERSUS RUN TIME (WITH TEST NOZZLE) FOR THERMOCOUPLE NO. 4 (BACKSIDE OF INJECTOR) (SEE FIGURE 4-43)

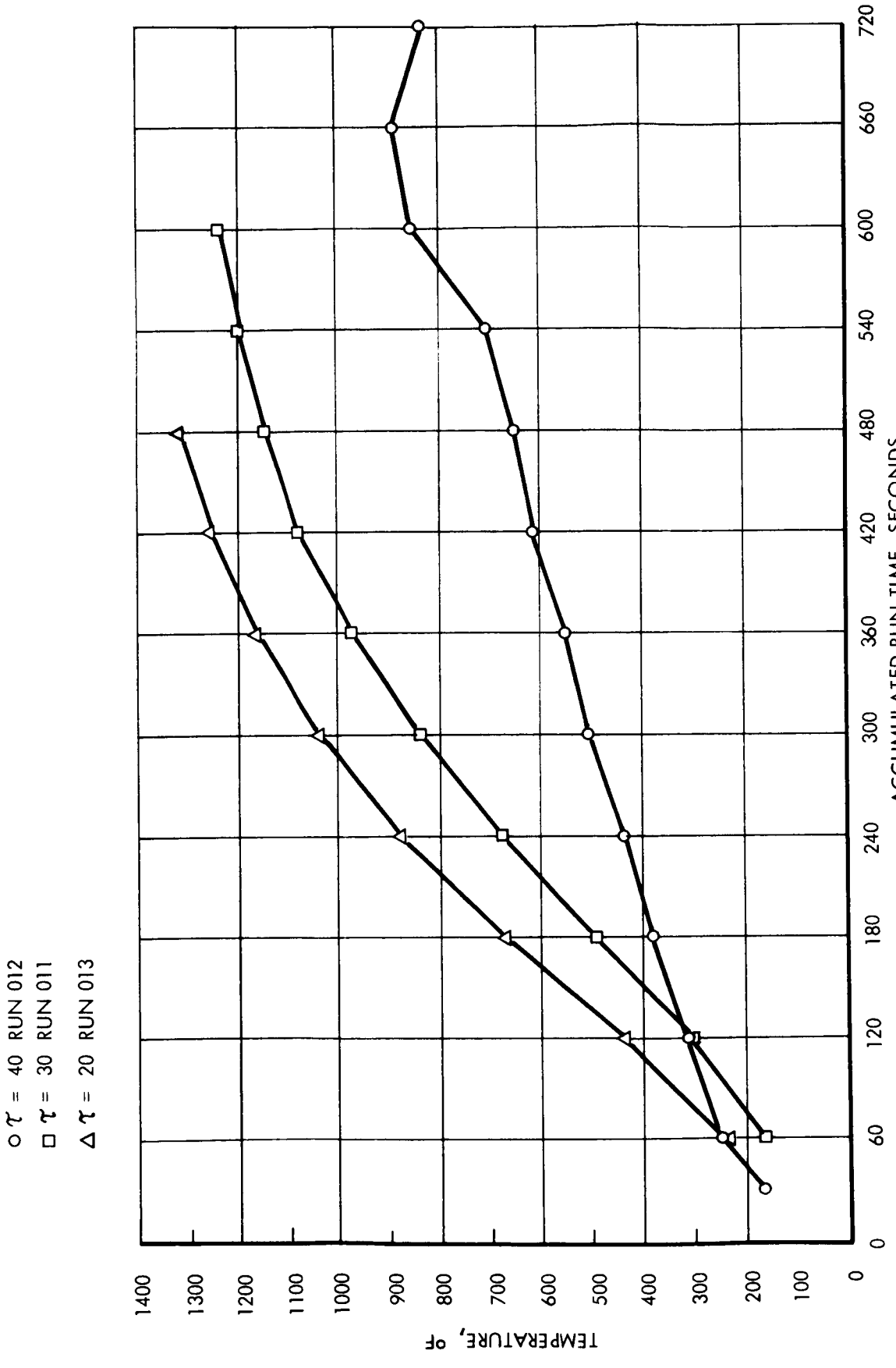

FIGURE 4-42 TEMPERATURE VERSUS RUN TIME (WITH TEST NOZZLE) FOR THERMOCOUPLE NO. 11 (NOZZLE THROAT AREA)
(SEE FIGURE 4-43)

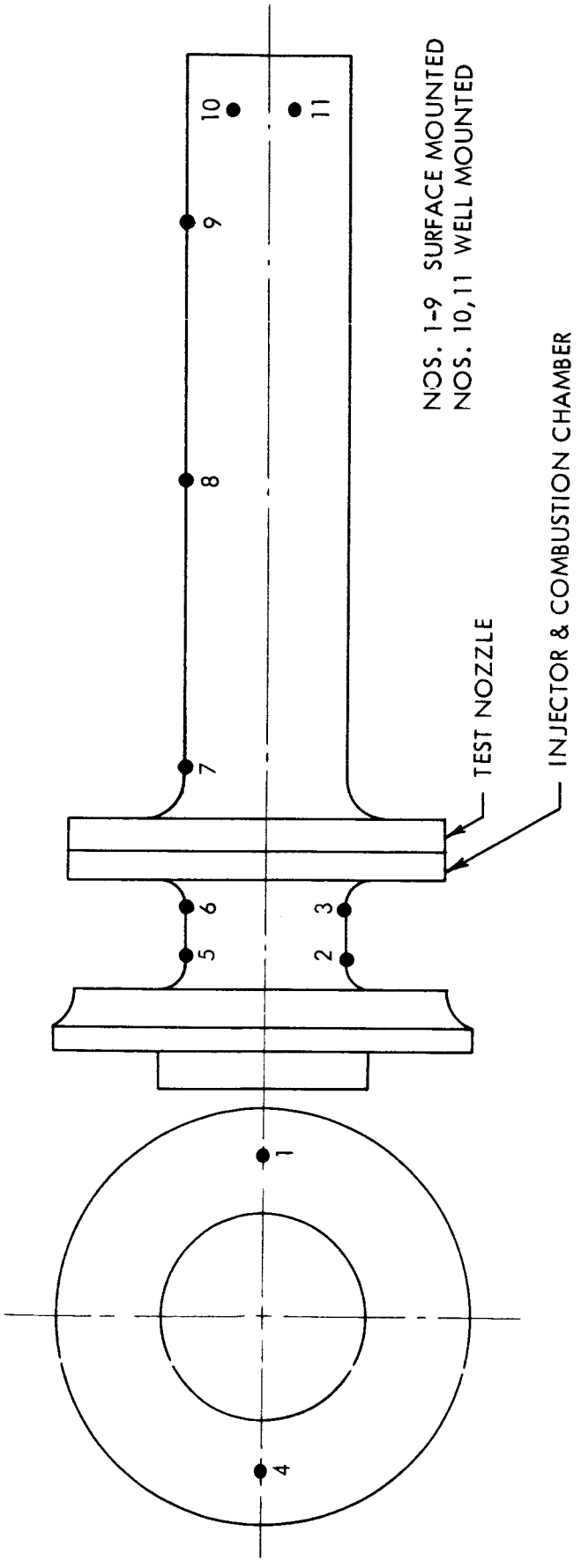

FIGURE 4-43 BREADBOARD GAS GENERATOR WITH TEST NOZZLE T/C LOCATIONS

TABLE 4-16
Gas Generator Data Tabulation

Test No.	Pulse No.	(Sec) Pulse Width Actual	Off Time Actual	P_f	P_{ox}	P_c	P_f	P_{ox}	$\dot{W}_f$ (lb/sec)	$\dot{W}_{ox}$ (lb/sec)	$\dot{W}_t$ (lb/sec)	P_o	F	F_{vac}	I_{sp}	I_f (°F)	T_{ox} (°F)	O/F	C*	Valve Voltage
015	1	1.475	NA	172.7	335.7	112.3	60.4	223.4	.0776	.2308	.3084	1.31	65.94	67.15	218.0	71.0	71.5	2.974	5170.0	28
015	2	2.808	NA	172.8	317.9	114.8	58.0	203.1	.0775	.2219	.2994	1.31	61.23	62.44	208.5	71.0	71.5	2.864	5460.0	28
015	3	2.477	NA	167.9	323.1	112.4	55.5	210.7	.0758	.2217	.2975	1.31	56.50	57.71	194.0	71.0	71.5	2.925	5385.0	28
016	4	.234	NA	182.7	348.8	114.8	67.9	234.0	.0777	.2608	.3385	1.39	56.50	57.77	170.5	71.0	71.5	3.356	4820.0	28
016	5	.198	NA	182.8	353.8	119.70	63.0	234.0	.0754	.2515	.3269	.266	65.90	66.14	202.5	71.0	71.5	3.34	5210.0	28
018	58	.206	NA	197.5	343.7	115.6	81.9	228.1	.0769	.197	.2739	.19	NA	NA	NA	65	66	2.65	6000	28
018	59	.203	NA	197.7	343.7	116.7	81.1	227.0	.0779	.207	.2799	.19	NA	NA	NA	65	66	2.66	5930	28
018	60	.2075	NA	197.5	343.7	115.4	82.1	228.3	.0771	.215	.2871	.28	NA	NA	NA	65	66	2.79	5720	28
018	92	.206	NA	211.5	379.7	117.7	93.8	262	.0766	.2135	.2901	.172	NA	NA	NA	65	66	2.79	5760	28
018	93	.206	NA	213.7	378.7	115.4	98.3	263.3	.0798	.2110	.2908	.172	NA	NA	NA	65	66	2.65	5650	28
018	94	.204	NA	213.7	378.7	117.7	96.0	261	.0813	.2160	.2973	.172	NA	NA	NA	65	66	2.66	5630	28
022	2	.208	NA	216.5	304.7	121.7	94.8	183.0	.0727	.2495	.3222	.2062	NA	NA	NA	60	60	3.43	5365	28

T_f = Fuel Temperature, Valve Inlet

T_{ox} = Oxidizer Temperature, Valve Inlet

$\dot{W}_f$ = Fuel Flow Rate

$\dot{W}_{ox}$ = Oxidizer Flow Rate

$\dot{W}_t$ = Propellant Flow Rate

O/F = Oxidizer to Fuel Weight Ratio

P_c = Chamber Pressure (PSIA)

C^* = Characteristic Velocity Ft/Sec.

P_o = Altitude Cell Pressure (Avg) (Psia)

F = Thrust as Measured (Lbs)

F_{vac} = Thrust Corrected to Vacuum Conditions (lbs) $F \; P_o A_e$

I_{sp} = Instantaneous Specific Impulse (Sec) $\frac{F_{vac}}{W_t}$

P_f = Fuel Injector Inlet Pressure (PSIA)

P_{ox} = Oxidizer Injector Inlet pressure (PSIA)

ΔP_{ox} = Oxidizer Injector Differential Pressure (PSI) $P_{ox} - P_c$

ΔP_f = Fuel Injector Differential Pressure (PsI) $P_f - P_c$

NA = Not Applicable

Average Thrust, F_{vac} = 62.24 lbs

Average Oxidizer Flow Rate = .2373 lbs/second

Average Fuel Flow Rate = .0768 lbs/second

Average Total Flow Rate = .3141 lbs/second

Average Chamber Pressure = 114.8 psia

Average Specific Impulse = $F_{vac,\ ave.}$ = 62.24 = 198.15 sec.

Average Characteristic Velocity, $C^*_{ave} = \frac{P_{c,\ ave} A_{tg}}{\dot{w}_{T,\ ave}} = \frac{114.8 \times .442 \times 32.2}{.3141}$

C^*_{ave} = 5202 ft/sec

Consistent performance data were unattainable during the breadboard testing because of the inadequacies of the instrumentation while subjected to the severe environment of the tests. One of the main problems encountered was excessively high temperatures obtained in the altitude chamber during runs. The pressure transducers were adversely affected by the chamber temperature because of their temperature sensitivity.

Figure 4-44 is a sketch of the two tests specimens which were used to simulate the turbine blades. These specimens were placed in the hot gas stream to appraise the ability of the blades to withstand the temperature environment of the hot gases. Specimen #1 was tested during Phase I of the breadboard tests which utilized the single nozzle. After three one-second bursts at sea level condition, it was evident that the leading edges of the blades were badly burned. Since this particular test was considered to be unrealistic because of the test conditions, specimen #2 was fabricated and subsequently tested during Phase II of the program. During this phase of the test schedule, the nozzle block scroll assembly was attached to the gas generator. The pulse width was the normal .2 seconds and the test was conducted at altitude conditions (approximately 100,000 feet). Specimen #2 was included in tests 022 through 024. Visual examination of the specimen showed no deterioration of the blades. Figure 4-44 also shows the temperature readings at various points along a segment of the simulated turbine wheel. These temperatures were recorded at the end of each run. No temperature data were available on test specimen #1, since the thermocouples were burned and/or blown off the specimen.

4.5.1.4 Conclusions

1. Confidence in the structural integrity of the prototype hardware was advanced since the design and fabrication techniques utilized for the breadboard unit are being used for the prototype hardware.

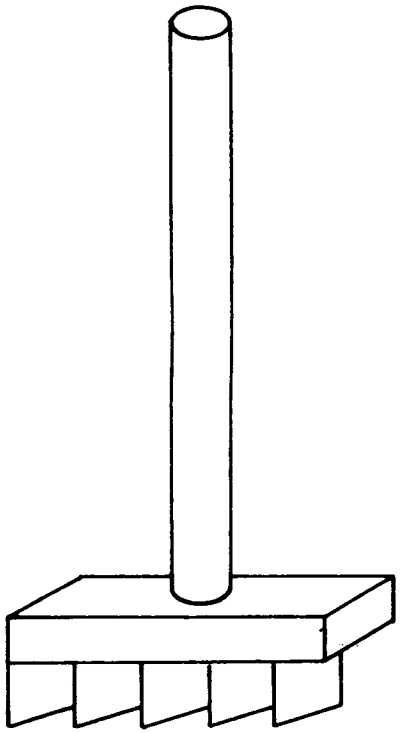

SPECIMEN #1

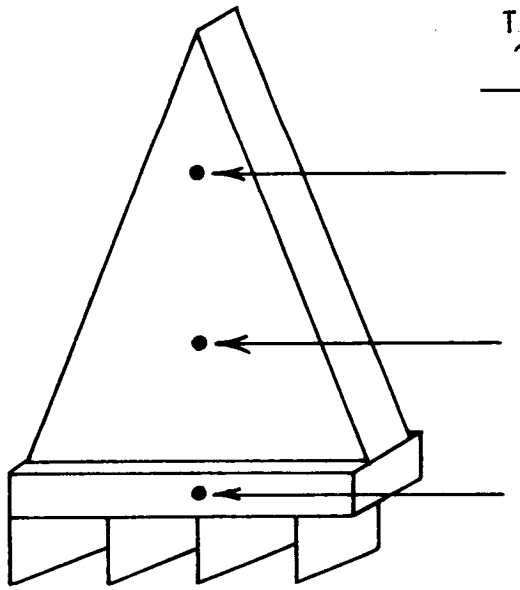

SPECIMEN #2

	TEST 024 $\tau = 30$	TEST 023-2 $\tau = 40$	TEST 023-1 $\tau = 60$
	255°F	278°F	390°F
	365°F	375°F	460°F
	510°F	475°F	510°F

SCALE ≅ 1/2

FIGURE 4-44 TURBINE BLADE SIMULATORS

2. Test hardware temperatures were not excessive and no hot spots were evidenced. Some tests were terminated when the back face of the injector head reached approximately 300° F. However it is felt that this temperature rise was due to the combination of thermal soak back and the excessive thermal environment of the altitude chamber and not just the thermal soak back from the gas generator combustion chamber.

3. The data accumulated during the thrust tests, which were considered to be the most reliable during the test program, indicate an average C* of 5200 ft/sec, which results in a C* efficiency in excess of 95%. This, plus the average Isp of 198 sec. was within the realm of pretest predictions.

4. The tests using turbine blade simulator specimen #1 were considered invalid since the test conditions were unrealistic. Tests with specimen #2 show that, at least for the duration of these tests, the blades withstood the environment of the hot gases.

5. The test rig requires modifications which will allow for more accurate and consistent data during prototype system tests.

6. Results of the temperature profile tests and subsequent preliminary thermal and stress analyses on the nozzle block scroll assembly indicate that the combination of stresses in the area of the interface of the relatively thick nozzle block and relatively thin scroll do not present a problem.

4.5.2 Prototype Tests of Unit #1 (013-055) for Purpose of System Development

These tests were conducted on the first assembled unit with the complete system installed in the altitude chamber at the Roanoke Laboratory. The electrical system was checked out prior to installation at the Electronics Laboratory in Cleveland. The lubrication system was assembled at Roanoke and checked out in the test cell prior to initial start-up. For a description of the installation, refer to the schematic, Figure 4-23, and Figure 4-14.

Since this was the first time a complete system of this type had been run, many of the tests were exploratory. In particular this applies to the start-up tests, the control system tests and the initial operation of the unit under load.

4.5.2.1 Start-up Tests of Unit #1 (013-019)

The purpose of these tests was to develop a pulsing rate sequence capable of accelerating the unit to speed in a reasonably short time period without exceeding normal metal temperature limits. With this objective in mind, the unit was accelerated to speed (33,000 rpm) in gradual steps starting with 10 pulses for test 013 and proceeding to 41 pulses for test 019. The initial pulsing rate corresponded to τ of 40, which proved to be conservative. Starting with test 017, the pulsing rate was reset to provide a τ of 30. Test results are presented in Table 4-17.

Test 016 and test 017 compare the acceleration characteristics at $\tau = 40$ and $\tau = 30$, respectively. Twenty-five pulses were applied in both cases. At $\tau = 30$, 24,000 rpm was reached while at $\tau = 40$, 21,700 rpm was obtained. Metal temperatures were the same 990°F in both cases. After running Test 017, $\tau = 30$ was selected as the start-up pulsing rate. In test 019 the unit was accelerated to speed using 41 pulses. Figures 4-45 and 4-46 show acceleration rate and scroll temperature comparisons for the two pulsing rates.

Table 4-17 Start-up Test Results

Test No.	No. of Pulses	τ	Speed Attained rpm	Max. Scroll Temp.-°F	Elapsed Time-Secs.
013	10	40	10,000	470	80
014	15	40	15,000	600	120
015	20	40	17,700	860	160
016	25	40	21,700	990	200
017	25	30	24,000	990	150
018	33	30	30,000	1130	198
019	41	30	33,000	1260	246

The unit can be accelerated to speed more rapidly than was done in this program due to improvements now incorporated to increase heat dissipation. Acceleration time is approximately four minutes.

4.5.2.2 Speed Control and Power Conditioning (020-035)

Reference: Schematic Figure 4-14

These tests were run to integrate the speed control, voltage regulator and rectifier-filter with the turboalternator and its output. At the completion of these tests, all components, with the exception of the filter, operated successfully permitting application of rated load on the D. C. terminals. Numerous minor problems were encountered and resolved. No major problems developed.

During these tests, several modifications were made to the controls. The first modification was to incorporate a signal light which would indicate when transfer had been made from the start-up circuit to the speed control. Several areas were rewired to prevent "sneak" paths from keeping the start circuit energized after transfer had been made. In addition, the oscillator circuit was modified to start as soon as the "start" switch was thrown. Previously, there was a 7 or 8 second delay until the first pulse occurred. The undervoltage delay circuit had to be readjusted to a shorter delay time.

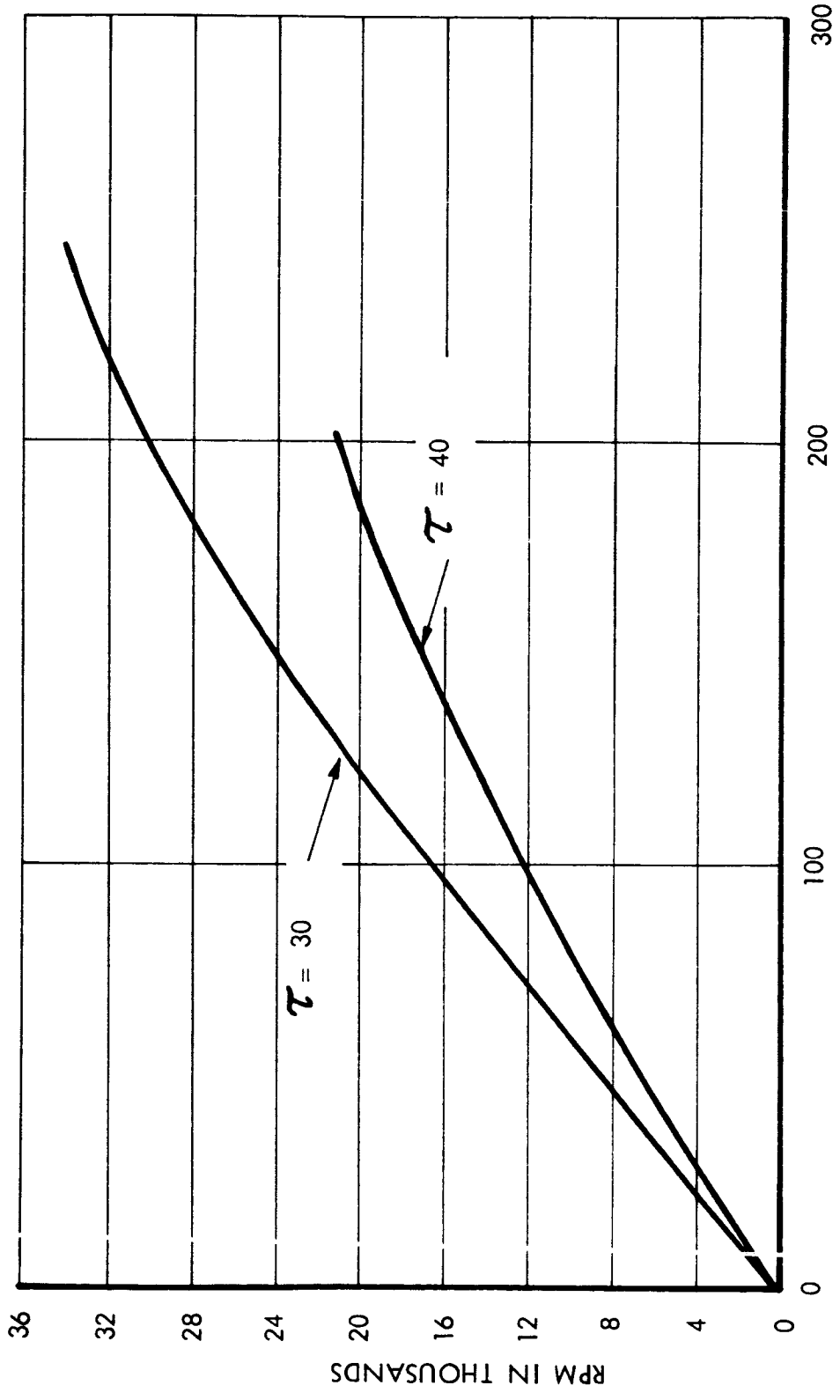

FIGURE 4-45 ACCELERATION CHARACTERISTICS
RPM VERSUS TIME

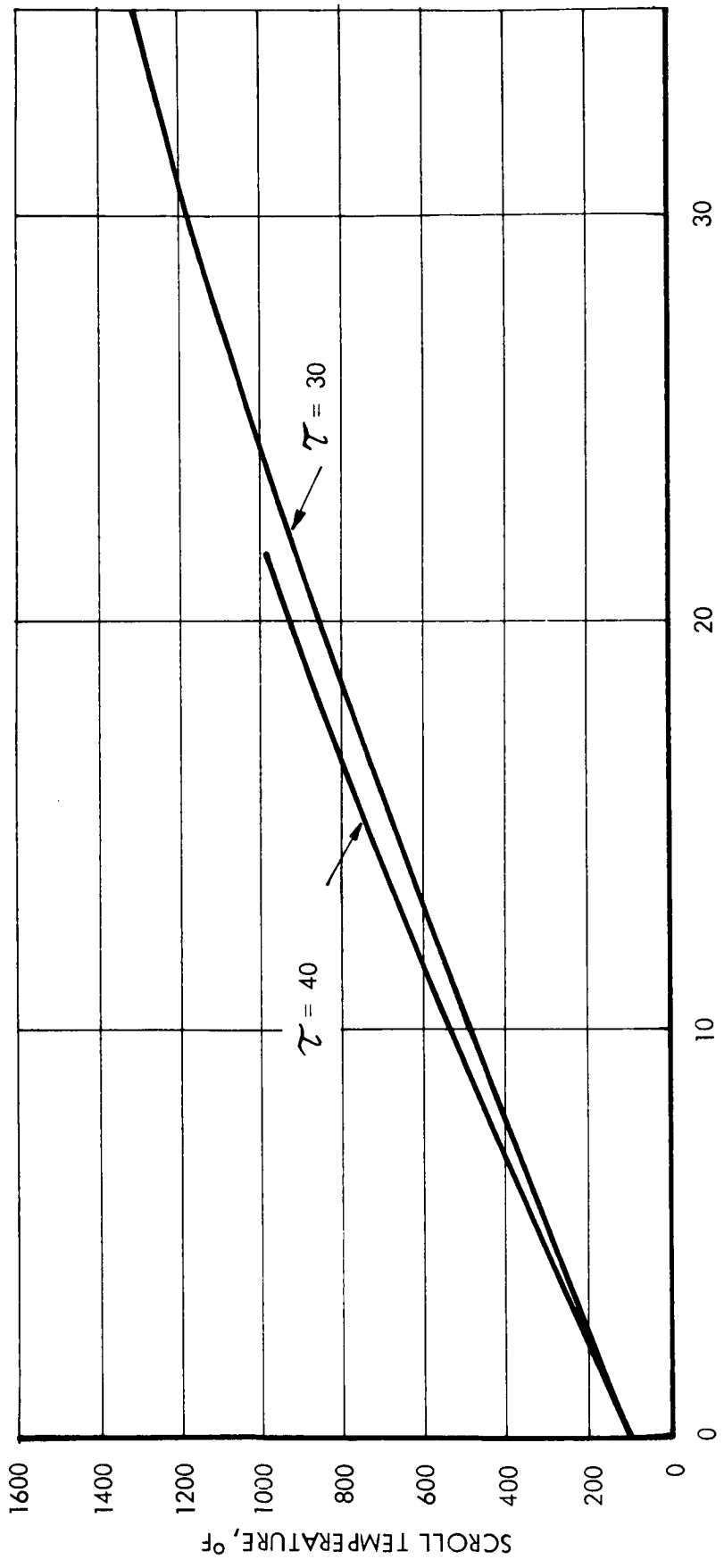

FIGURE 4-46 ACCELERATION CHARACTERISTICS SCROLL TEMPERATURE VERSUS RPM

During several of the first runs, the unit came up to speed and transferred to the speed control normally. However, it coasted down below its trigger point and then gave a 330 ms pulse which brought it up to speed. It was found that the delay was set too long and thus disabled the driver stage longer than is desired. When the delay circuit had timed out, it allowed approximately the last half of a trigger pulse to energize the valve. Because the unit was still below its normal operating range, a second pulse was immediately applied. This brought the unit into its operating range and normal control followed. Reducing the delay time on the undervoltage circuit corrected this problem.

During this test phase, it was determined that energizing the voltage regulator at 90 or 95% point would eliminate potential unstable conditions. For the remainder of the test program, the voltage regulator was brought into control manually after transfer to the speed control had been automatically completed.

This was accomplished by gradually reducing the external field excitation voltage to zero. This could not be done at an under speed point as contacts of relay K_2 enable the voltage regulator to operate when it is energized. Relay K_2 is energized at transfer. It has been found that this type of regulator can maintain a high output voltage even at 50 or 60 percent of rated speed. This would stress or burn out wound components designed to operate at a higher frequency. For this reason, it is desirable to keep the voltage regulator inoperative until the operating region is neared. This can easily be done by replacing the K_2 contacts with those of another relay operated by a different sensing circuit.

When load was first applied to the system, filter oscillations caused an overspeed shutdown. For purposes of development tests, the filter was eliminated and not redesigned at this time. It was felt that conditioned power was a second order problem and not necessary to prove feasibility. The voltage regulator was nearly adequate to meet the ripple voltage specification itself without the filter.

At this time, the external overspeed shutdown was added to the system as a back-up for the electronic overspeed circuit. The magnetic pickup used in this system does not require a voltage output from the alternator in order to operate. The main reason this was added was that the altitude chamber heating problems posed the possibility of losing some of the wiring between the turboalternator and the control room in which the controls and safety circuits were located. As stated previously, this pickup could initiate a shutdown by interrupting all power to the bipropellant valves and the alternator field. It also de-energized solenoid valves in the fuel and oxidizer lines running to the bipropellant valves.

In conclusion the modifications made to the electrical system during the testing phase were small. Several desirable features were analyzed, but the design changes were not implemented as they did not contribute appreciably to the end goals.

4.5.2.3 Altitude Chamber Temperature Problems

Throughout the program, altitude chamber temperature over-heating continued and proved difficult to cure. Many fixes were tried and each reduced the temperature somewhat. (See Section 4.3 for a description.) The problem was most evident at 0.9 0/F ratio where chamber temperature during early testing under load exceeded 500°F. Ultimately, with all the fixes built in, this temperature dropped to 200°F and was acceptable for the endurance test conditions. At higher power levels, further cooling must be provided.

The extremely high temperatures during early testing were detrimental to insulation on electrical leads, tended to deteriorate oil hoses and had an adverse effect on injector head, Moog valve and propellant temperatures. Injector head heat soak back is directly related to the chamber temperatures. All endurance testing was run at conditions more severe than encountered in the actual environment. It is desirable, in future tests, to duplicate actual conditions by controlling the chamber temperature at the proper level. Performance of the system itself and, in particular, the operation of the injector head will be improved under those conditions.

4.5.2.4 Scroll Temperature - Various Configurations

It was evident in very early tests on Unit No. 1 that the temperature of the turbine scroll was a problem. For example, during acceleration and stabilization at speed, the maximum scroll temperature showed the following trend during Test 023:

Time Secs.	Maximum Scroll Temperature °F	Stabilized Temperature (windage load only)
0	190	
40	550	
80	750	
120	960	
160	1060	
200	1150	
240	1260	
8 mins.		1260°F

During operation with no external electrical load, the maximum temperature stabilized at 1260°F (0.9 0/F ratio). At 3 KW equivalent load, the estimated temperature was above 1600°F thus precluding full load testing. The scroll configuration, at that time, was bare Hastelloy with no fin or emissivity coating. The scroll was then spray coated with a titanium oxide emissivity coating and the temperature results in Test 025 were was follows:

Time Secs.	Maximum Scroll Temperature °F	Stabilized Temperature (windage load only)
0	80	
40	400	
80	680	
120	800	
160	940	
200	1020	
240	1000	
8 mins.		960°F

This represented a sizable improvement with a predicted temperature at 3 KW equivalent load of 1260°F and at 4.5 KW equivalent load of 1420°F. Further improvement was desirable. At the next build an aluminum oxide emissivity coating, having superior metal adherence, was applied and a Hastelloy fin was added. Test 046 showed the following temperatures:

Time Secs.	Maximum Scroll Temperature °F	Stabilized Temperature (windage load only)
0	100	
40	430	
80	680	
120	830	
160	1000	
200	1060	
240	1060	
8 mins.		990°F

This obviously showed no improvement over the previous configuration. It was concluded that the conductivity of the Hastelloy fin was so low that the fin effectiveness was negligible.

At the next build a copper fin was used in place of the Hastelloy fin. In Test 054 the following temperatures were recorded:

Time Secs.	Maximum Scroll Temperature °F	Stabilized Temperature (windage load only)
0	120	
40	400	
80	580	
120	700	
160	800	
200	880	
240	820	
8 mins.		800°F

In Test 057, accelerating to speed and stabilizing at 2.7 °/F ratio, temperatures were as follows:

Time Secs.	Maximum Scroll Temperature °F	Stabilized Temperature (windage load only)
0	130	
40	370	
80	550	
120	730	
160	830	
200	890	
240	900	
8 mins.		850°F

Due to the sizable improvement with the copper fin, it was now possible to operate at rated loads with temperature margin remaining. Figure 4-47 graphically shows a comparison of the four configurations.

Further analysis shows that considerable improvement is possible with a better fin design and location. This is being explored relative to a continuous rating of 6 KW.

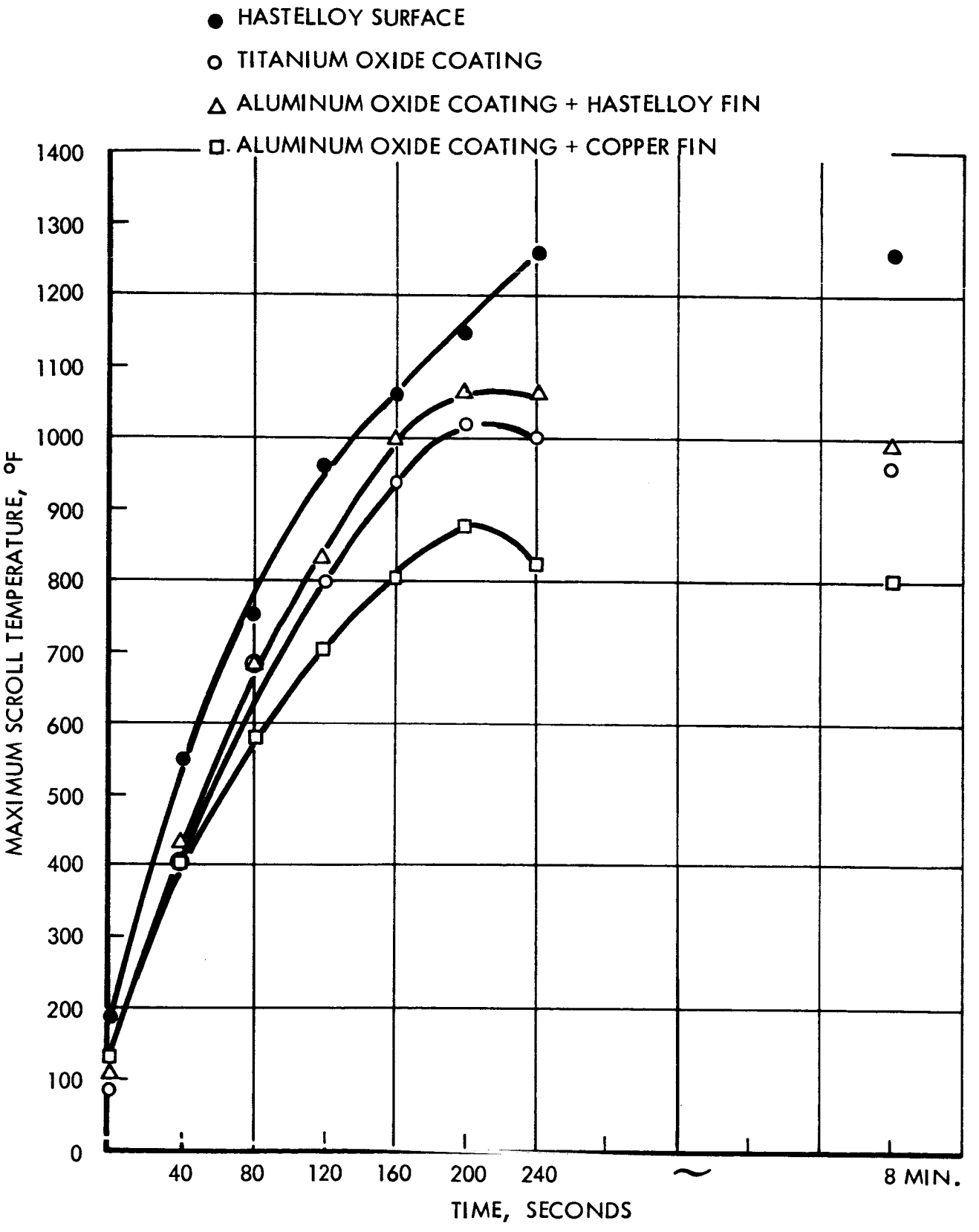

FIGURE 4-47 SCROLL TEMPERATURE COMPARISON
0.9 O/F RATIO

4.5.2.5 Gas Generator Failures

During the entire program, two failures occurred in the gas generator oxidizer tubes. The first failure occurred on April 18 during Test 047. While running at 2 KW electrical load at 0.9 0/F ratio, the scroll temperature suddenly increased from 1200°F to 1500°F. After shutdown a 0.9 0/F oxidizer tube was found to be ruptured and the 2.7 0/F fuel valve port and 0.9 0/F oxidizer valve port were leaking. Analysis of the failure showed a weakened tube area caused by a nick at the point of failure. It was concluded that fuel leaking from the 2.7 fuel port dribbled into the 0.9 oxidizer tubes causing explosions which could not be contained by weakened tubes. On disassembly, the valve seats were found to be cracked and small portions of the seats had ruptured. It was established that combustion occurred during the coast period and was apparently supported by fuel leaking from the 2.7 valve and oxidizer leaking from the 0.9 valve. This continuous combustion was verified from the coast times which lengthened during the last three pulses from 7 seconds to 10.2 seconds.

Moog valve failures were caused by inadvertent overtemperaturing of the seats during an earlier run.

The second failure occurred on May 24 during Test 056. In this case, a 2.7 0/F oxidizer tube failed while running at 0.9 0/F ratio. The tube failure became evident after switching to 2.7 0/F ratio when valve flange temperatures dropped to less than 30°F. The time of failure was precisely determined by analysis of the 2.7 0/F valve flange temperatures which increased after 3:55 p.m. while still operating at 0.9 0/F ratio. Upon switching to the 2.7 0/F ratio, the valve flange temperature dropped abruptly. A ball of oxidizer ice was found surrounding the injector tube area at shutdown.

Examination of the failed tube again indicated a weakened area at the point of failure. A thin tube wall existed in the area brazed to the valve flange. It was concluded that mild explosions had occurred due to propellant mixing in the tubes. This caused a failure at the weakest point.

It was well known that altitude pressure variations occurred in the altitude chamber during each pulse and the theory was advanced that this pressure increase caused propellants to back-flow after a pulse into the injector head ports and tubes. For Test 057 the altitude chamber exhaust area was increased from 47 in^2 to 380 in^2. Injector tubes were strengthened by adding epoxy potting. Since making these changes, no injector tube failures have occurred.

4.5.3 Endurance Tests (056-072)

The endurance program was accomplished on a 10 hour/day basis in a total of 10 days of testing. Accumulated running time was 56.75 hours for this period with a total running time on Unit No. 1 of 80.24 hours. The maximum running time in any one day was 8.75 hours and the minimum was 1.34 hours. A summary of the endurance testing is shown in Table 4-18.

TABLE 4-18

PROGRAM ENDURANCE SUMMARY

Date	Test No.	Remarks	Running Time Hrs.	Running Time/ Day
5/24	056	Started Endurance. Scavenge pump stopped. 5 pulses, 1 second apart. Started again. Injector tube failure.	3.22	3.22
6/23	057	Brief test to check 0/F ratio.	.08	
	058	Trimmed 0/F ratio. Ran to check system.	1.26	1.34
6/24	059	Endurance test. Total time at load 7.25 hours.	8.10	8.10
6/27	060	Endurance test. Scavenge pump stopped. 4 pulses 1 second apart.	4.28	4.28
6/28	061	Brief run to check lubrication system.	.08	
	062	Endurance test. Shutdown by thunderstorm. Lost electrical power.	3.67	4.75
6/29	063	Endurance test. Automatic shutdown inadvertently occurred.	4.17	
	064	Start-up. No pulses after No. 32	.05	
	065	Start-up. Ran to 7:20 p.m.	.33	4.55
6/30	066	Endurance test. Automatic shutdown after a few hours.	3.93	
	067	Endurance test. Automatic shutdown caused by temp. trip	.92	
	068	Reset automatic over-temp. trip. Endurance test.	2.47	7.32
7/1	069	Endurance test. Shutdown due to marginal heat soak back.	3.25	
	070	Endurance test. Cooled altitude chamber with water spray. Reduced injector temp.	5.00	8.25
7/5	071	Endurance test.	7.17	7.17
7/6	072	Endurance test.	8.75	8.75

Endurance was first begun on May 24 on Unit No. 1 using the dual injector head copper finned scroll configuration. The load schedule specified operation at 4.5 KW at 0.9 0/F ratio, and 3.0 KW at 0.9 and 2.7 0/F ratios. The 0.9 0/F ratio endurance was under way when the oil scavenge pump stopped, causing the unit to pulse 5 pulses 1 second apart before manual shutdown could be initiated. This thermally severe operating condition caused no damage to the turbine. After correcting the scavenge pump coupling binding, endurance was continued. After a short period of running on the 2.7 valve, the valve flange temperatures slowly dropped to less than 30°F. After shutdown, a ruptured 2.7 0/F ratio oxidizer tube was found. This was the second oxidizer tube rupture with the dual injector head. The first occurred on the 0.9 0/F ratio tubing.

The cause of the failure was thought to be fuel dribble draining or back-flowing into the oxidizer tubes with resultant explosions. Also it was known that the capillary tubing used in the injector head was unnecessarily fragile (.009" wall thickness) and was further weakened in manufacturing processing. A combination of mild explosions and weakened tubes was suspected. Unit No. 1 was then rebuilt with the following changes to minimize the possibility of tube failure:

a) Epoxy potting to structurally support tubes was used.

b) The scroll was rotated 60° relative to the alternator housing to provide gravity draining of the injector.

c) At the 0.9 0/F flange, a transducer was installed to measure pressure in the 0.9 oxidizer tubing.

d) The altitude chamber exhaust system was enlarged by installing a 22" diameter outlet to reduce altitude pressure variation.

e) The unit was assembled for 2.7 0/F ratio running only to minimize fuel dribble volume.

Endurance was then continued on June 23 and completed on July 6. During this period the unit operated stably and consistently from day to day with virtually no change in temperature levels or pulsing rates. A typical operating condition is shown below for Test 070:

Maximum Scroll Temperature	1350°F
Copper Fin Temperature	810°F
Seal Temperature	340°F
Maximum Ball Bearing Temperature	280°F
Roller Bearing Temperature	220°F
Oil Flow	0.7 GPM
Injector Temperature	265°F
Pulse Period	6.9 secs.

Actual Electrical Output	2.0 KW
0/F Ratio	2.7
Altitude	104,000 ft.
Probable Equivalent Electrical Load	2.6 KW

It should be noted that this test may have been run at an equivalent electrical output less than 3 KW. This was caused by a probable error of 0.06 psia in reading the absolute altitude pressure. This resulted from the use of brass scale and temperature corrections for the barometer reading but not using these same corrections for the manometer reading. During the Acceptance Test of Unit No.2, a sensitive vacuum gage was used as a check. This gage was then calibrated and it became apparent that the windage corrections for earlier tests were in doubt. This uncertainty applies to tests run with the 22" diameter pipe installed. Tests run earlier with the two 5.5" diameter exhaust pipes are not in question as the windage corrections were evolved with that configuration. There is still doubt concerning the true answer to this problem since only one pressure tap was used. In the future a series of averaging taps will be used with sensitive vacuum gages.

A typical dynamic pressure trace is shown in Figure 4-48. From initial valve opening to full gas generator pressure, a period of approximately 30 milliseconds elapses. Decay time from the cut-off of valve signal to 90% generator pressure decay is also approximately 30 milliseconds. Dwell time at pressure is 170 milliseconds. Century trace calibrations are included at the end of this section.

Appreciable variations in fuel and oxidizer pressures occur at opening and closing of the Moog valve. This is caused by the length of line from the tanks to the Moog valve (approximately 12 feet for the fuel line and 8 feet for the oxidizer line). Accumulators are installed just upstream of the Moog valve which reduce but do not eliminate these pressure variations. A dynamic analysis is needed to more precisely match the accumulators to the line dynamics.

At the completion of the test the unit was disassembled and inspected. The condition of all parts was excellent showing no evidence of deterioration. Carbon deposits on the seal cartridge were traced to the "O" ring seal used on the O.D. of the cartridge to seal against the alternator housing bore. This "O" ring is standard size for the groove but provides insufficient interference to properly seal, especially when slight deformation occurs from running at temperature. In the future a slightly larger "O" ring will be used. Condition of the parts is shown in the following figures:

Figure 4-49	Disassembled Turboalternator
Figure 4-50	Turbine Scroll and Gas Generator - Alternator Side
Figure 4-51	Turbine Scroll and Gas Generator - Turbine Side
Figure 4-52	Turbine Wheel - Exhaust Side
Figure 4-53	Turbine Wheel - Inlet Side

FIGURE 4-48 TYPICAL SYSTEM DYN

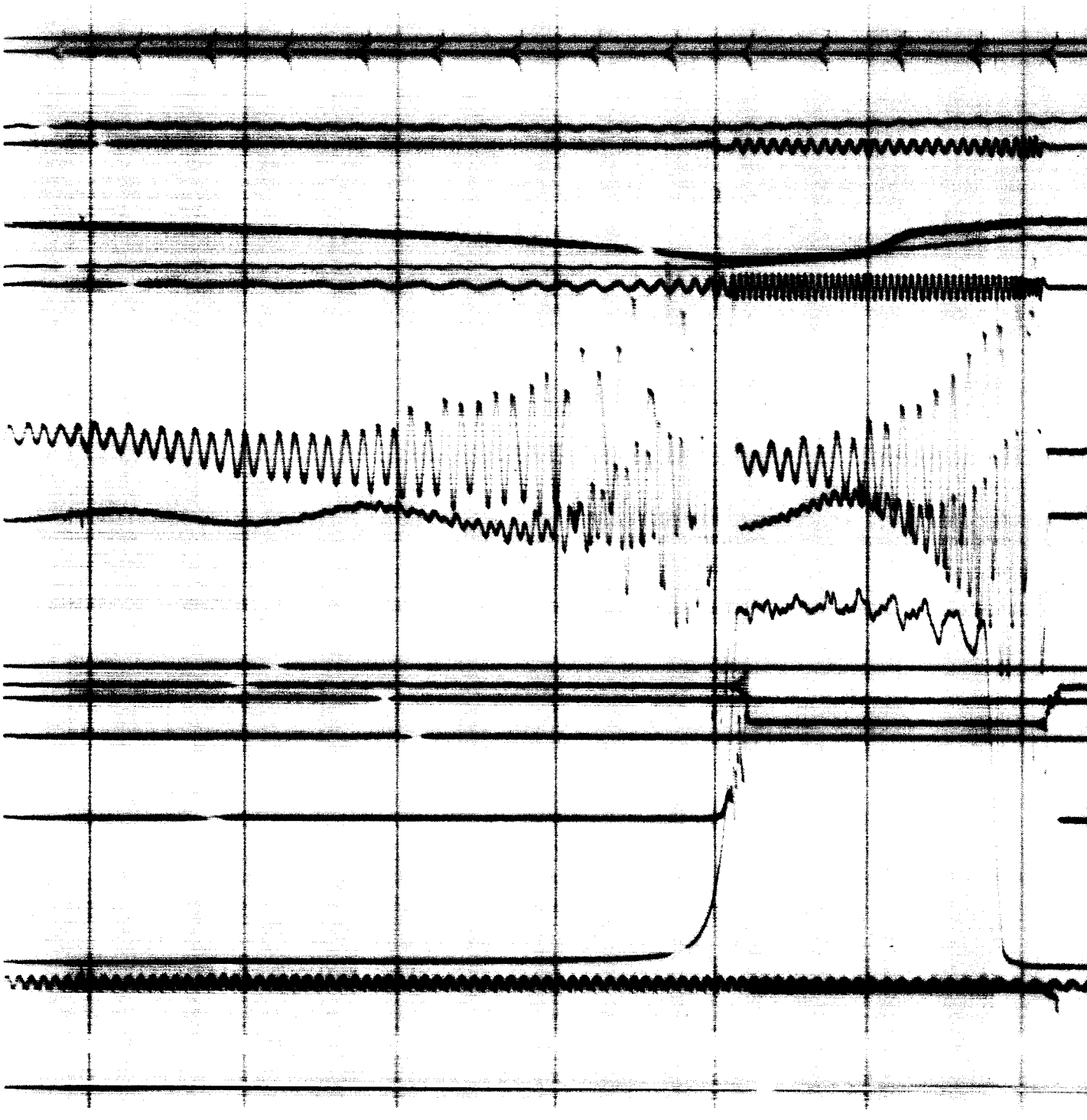

AMIC DATA DURING PULSE

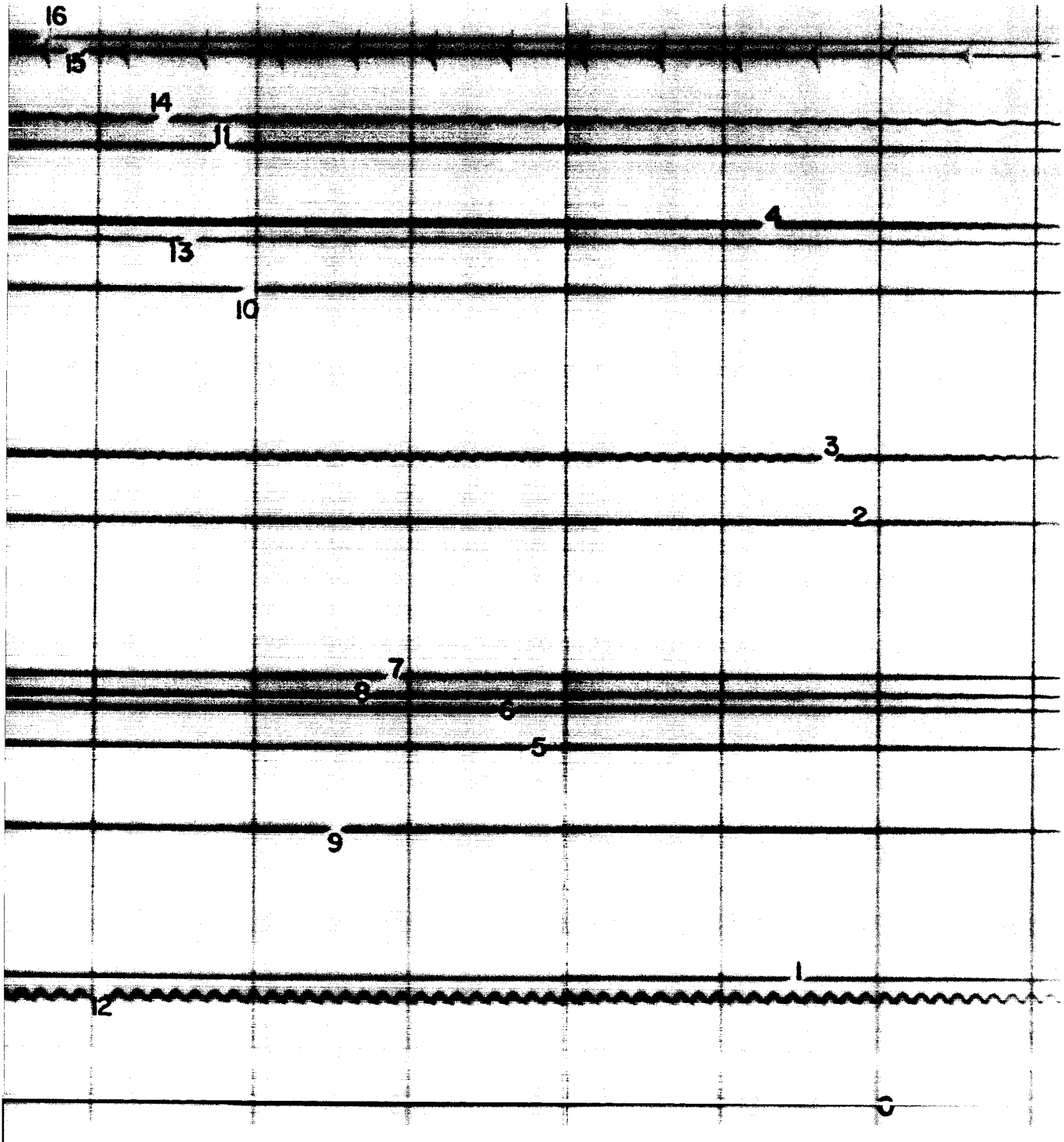

Figure 4-54	Close-up of Turbine Wheel and Shaft
Figure 4-55	Turbine Blade Leading Edges
Figure 4-56	Turbine Blade and Rim
Figure 4-57	Alternator Rotor
Figure 4-58	Scroll Support Pins
Figure 4-59	Seal Cartridge Showing Carbon Seal Face
Figure 4-60	Seal Wear Ring
Figure 4-61	Close-up of Carbon Seal Face
Figure 4-62	Seal Cartridge Showing Oil Leak
Figure 4-63	Roller Bearing Inner Race
Figure 4-64	Roller Bearing Rollers, Retainer and Outer Race
Figure 4-65	Ball Bearing Inner Race
Figure 4-66	Ball Bearing Outer Race
Figure 4-67	Ball Bearing Retainer and Ball Complement.

The Century trace parameters for Test 056 are as follows:

Century Trace No.	Parameter
0	Base
1	Gas Generator Pressure
2	Oxidizer Inlet Pressure
3	Fuel Inlet Pressure
4	Vacuum Chamber Pressure
5	Fuel Inlet Temperature
6	Oxidizer Inlet Temperature
7	Helium Valve Voltage
8	Moog Valve Current
9	Moog Valve Voltage
10	Fuel Flow
11	Oxidizer Flow
12	Alternator Field Voltage
13	Alternator Speed
14	Alternator Voltage AC
15	Timing Lines
16	No. 2 reference

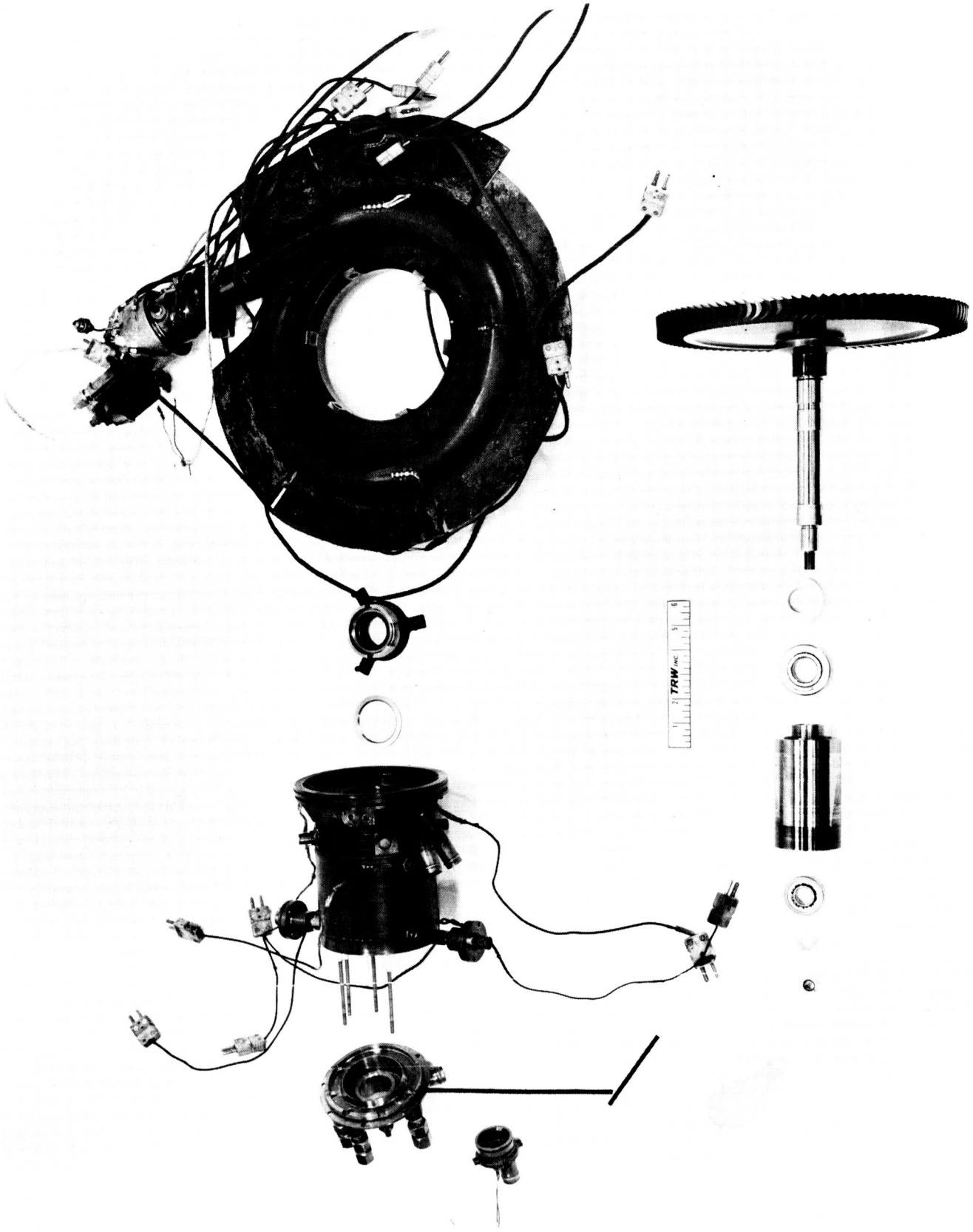

FIGURE 4-49 DISASSEMBLED TURBO-ALTERNATOR

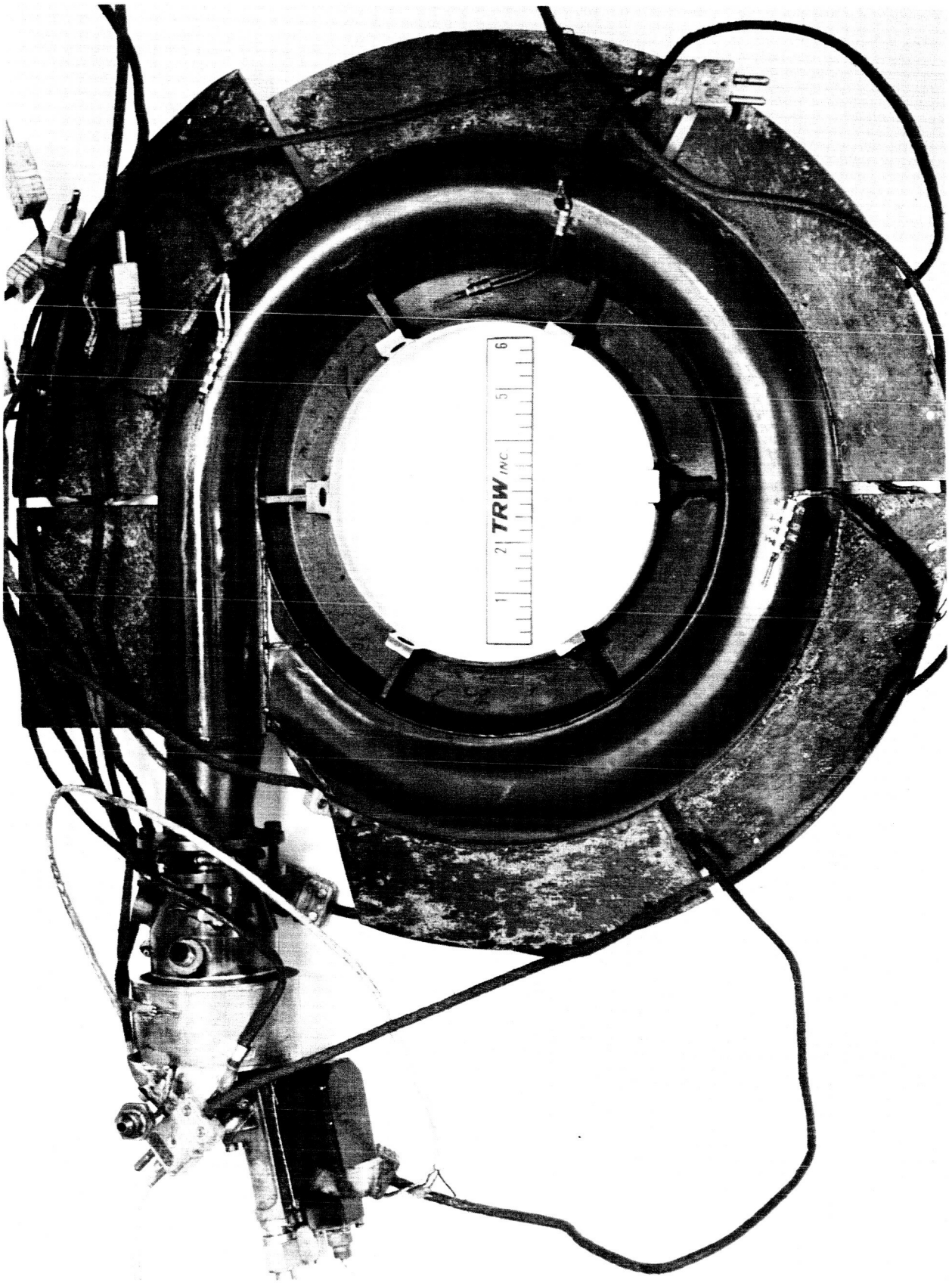

FIGURE 4-50 TURBINE SCROLL AND GAS GENERATOR - ALTERNATOR SIDE

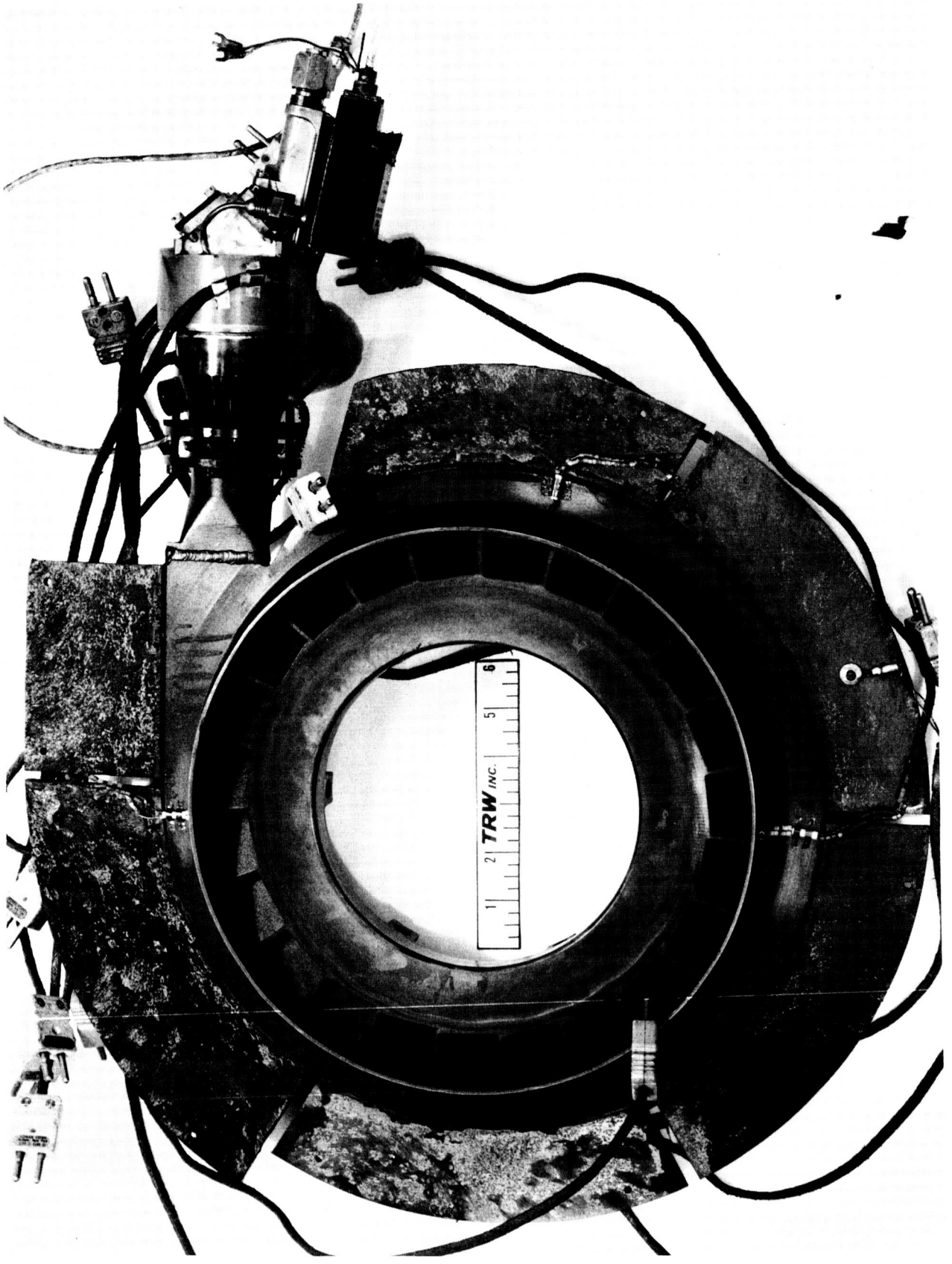

FIGURE 4-51 TURBINE SCROLL AND GAS GENERATOR - TURBINE SIDE

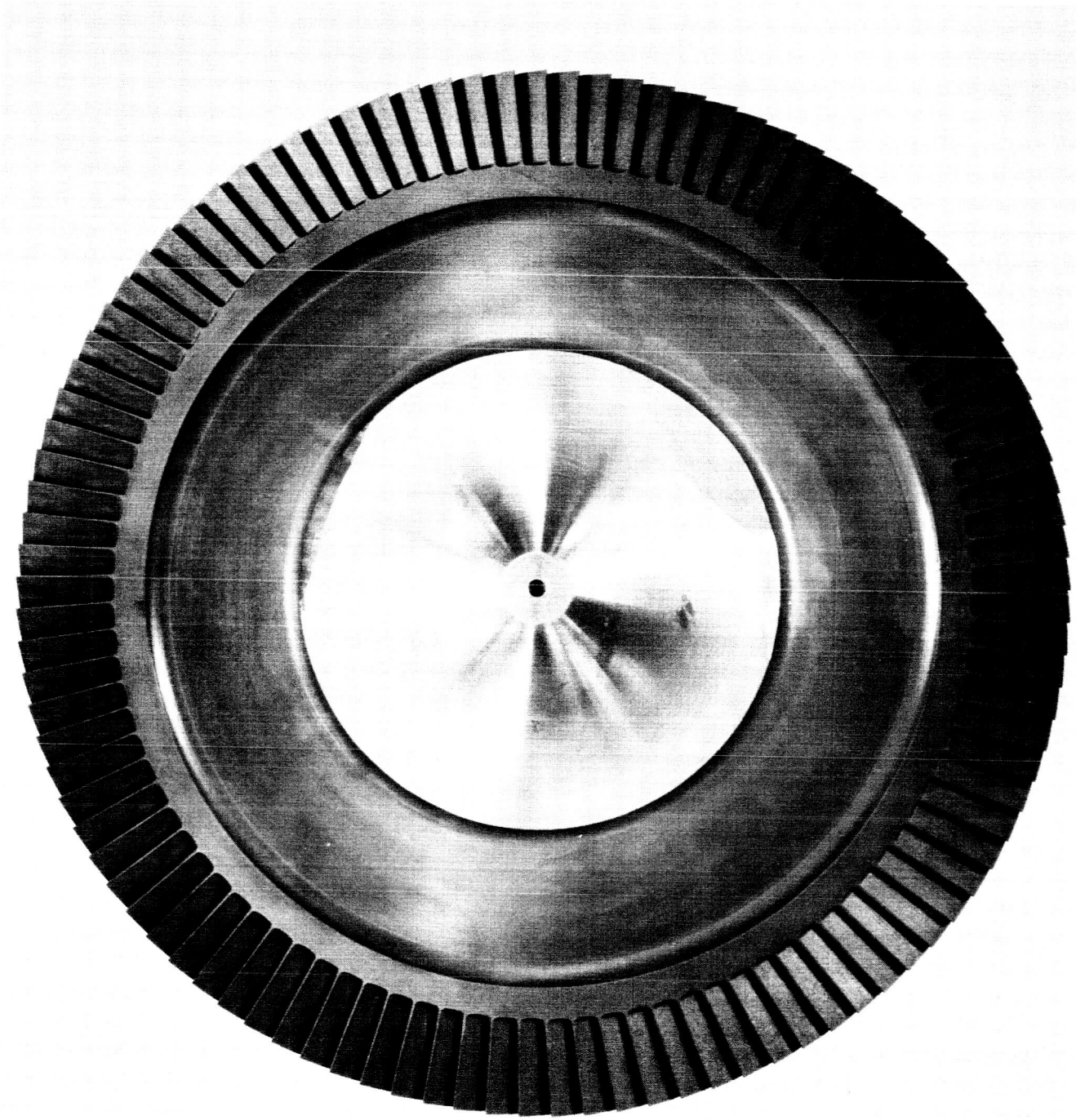

FIGURE 4-52 TURBINE WHEEL - EXHAUST SIDE

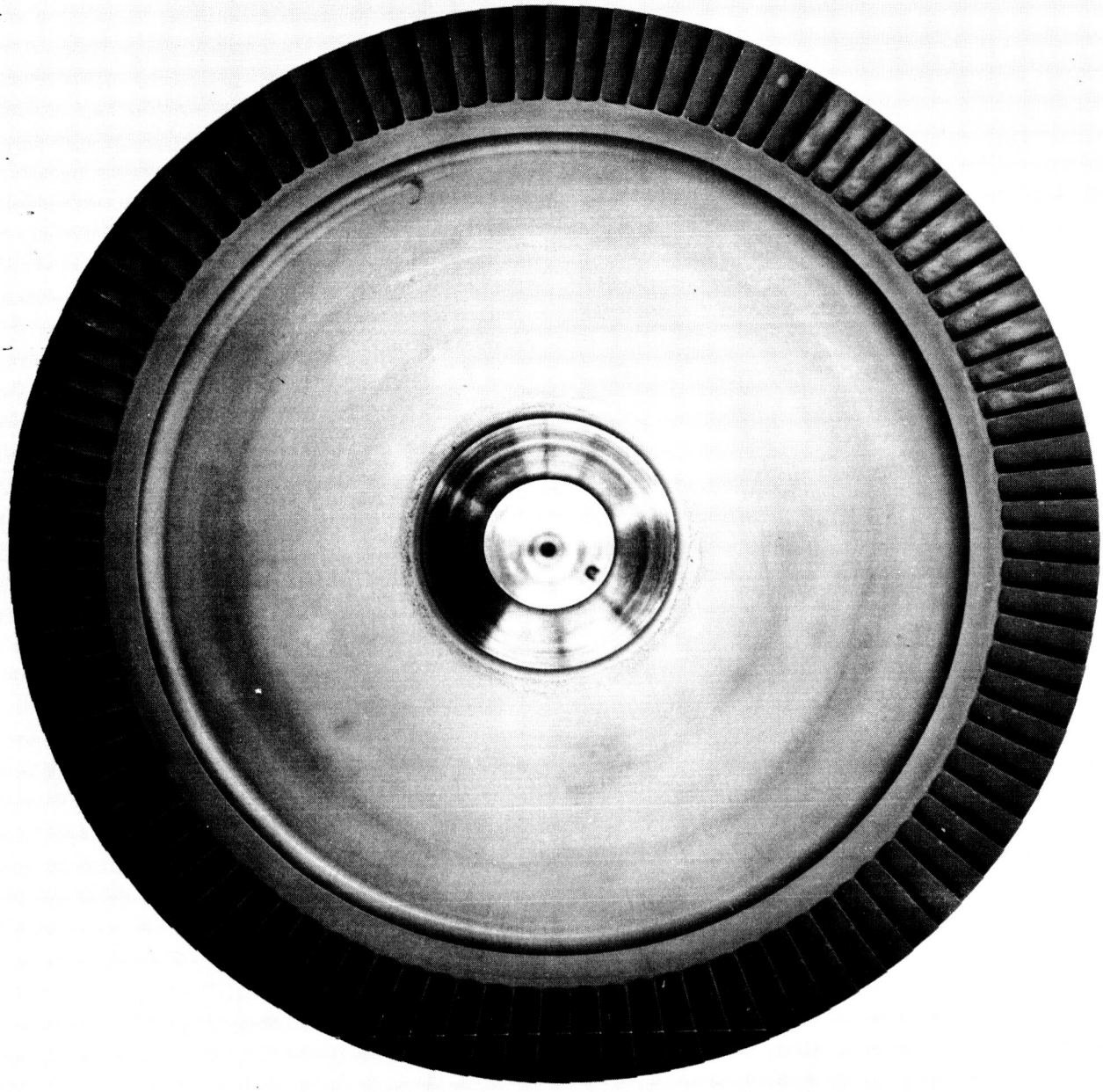

FIGURE 4-53 TURBINE WHEEL - INLET SIDE

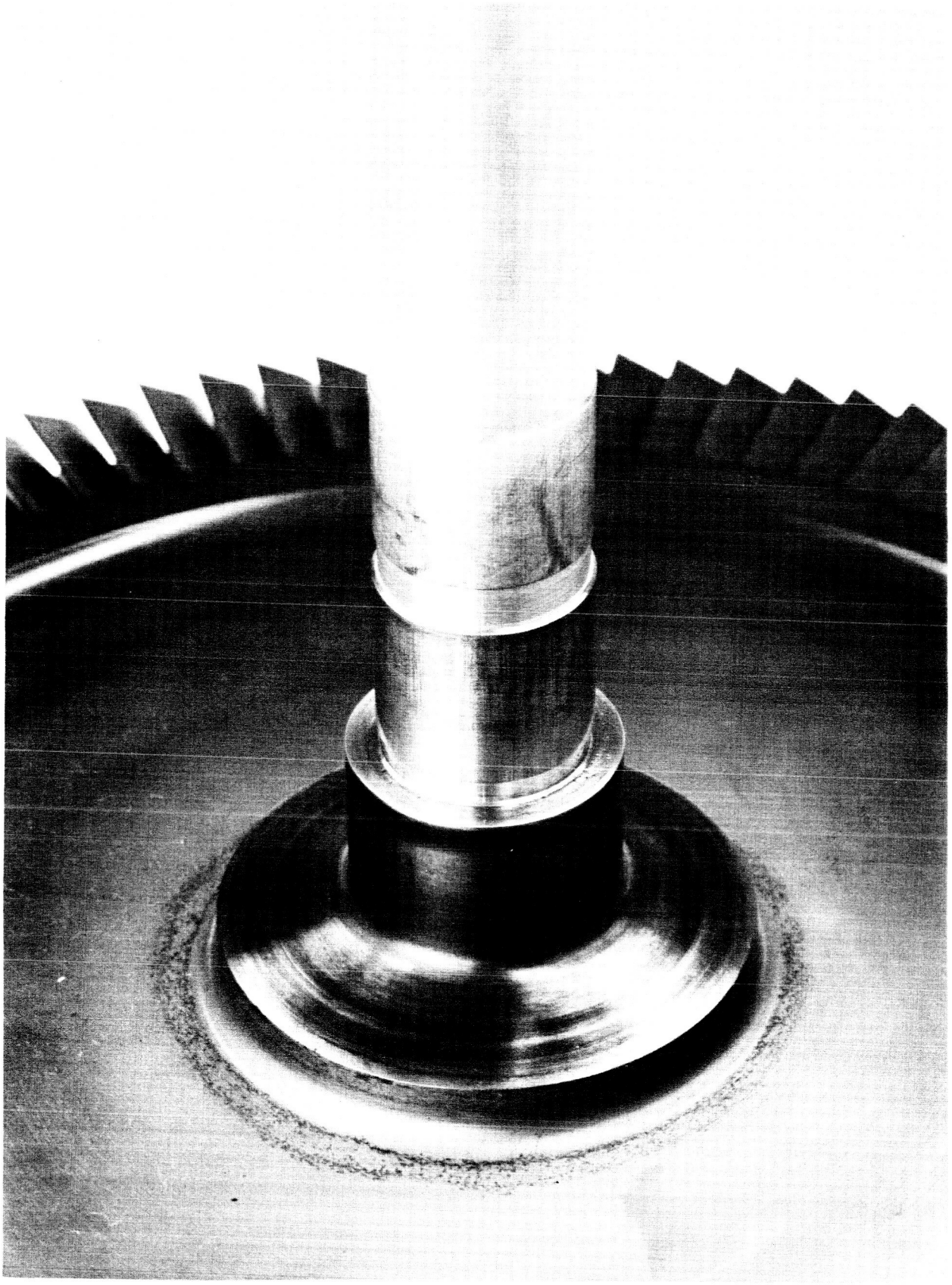

FIGURE 4-54 CLOSE-UP OF TURBINE WHEEL AND SHAFT

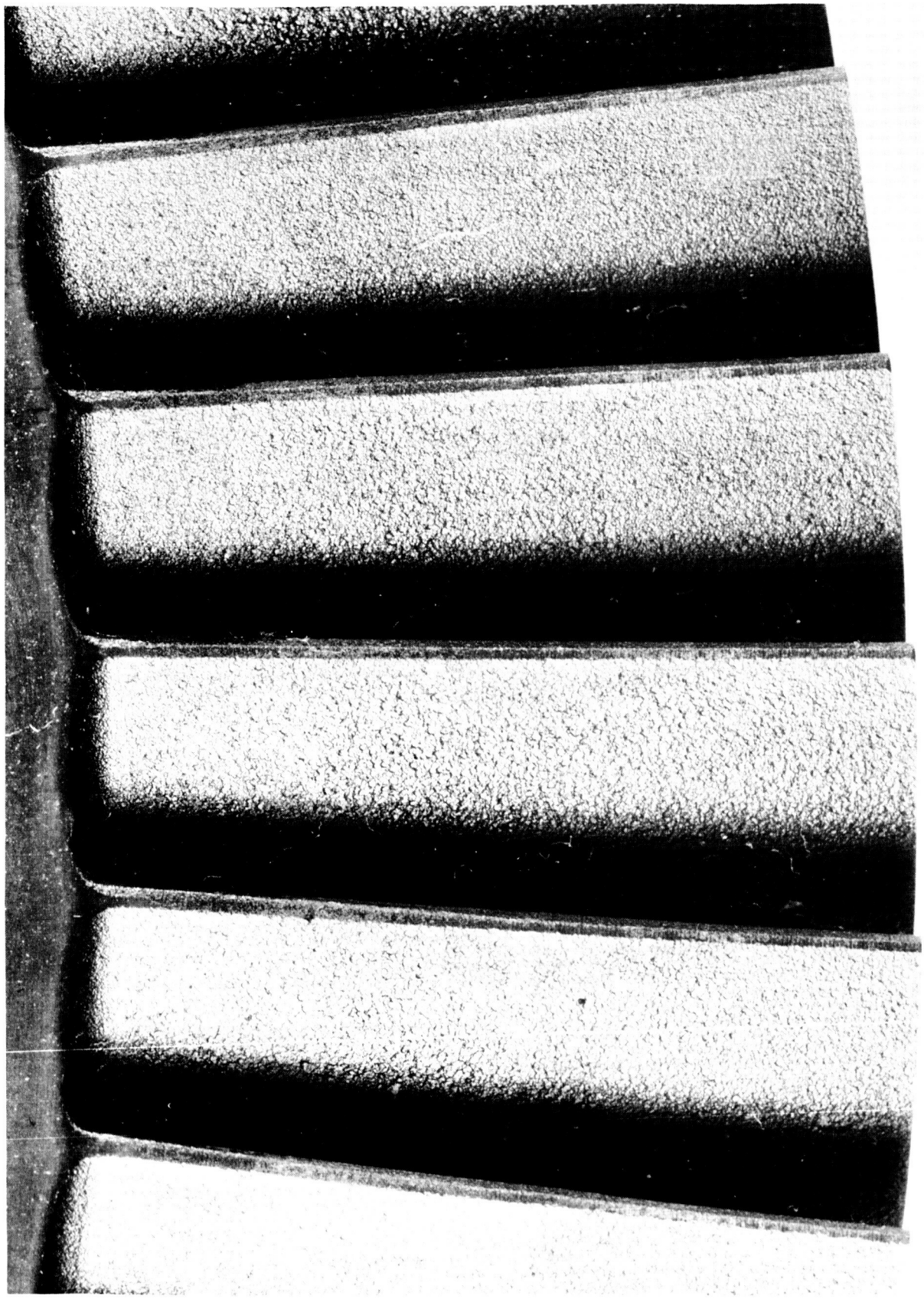

FIGURE 4-55 TURBINE BLADE LEADING EDGES

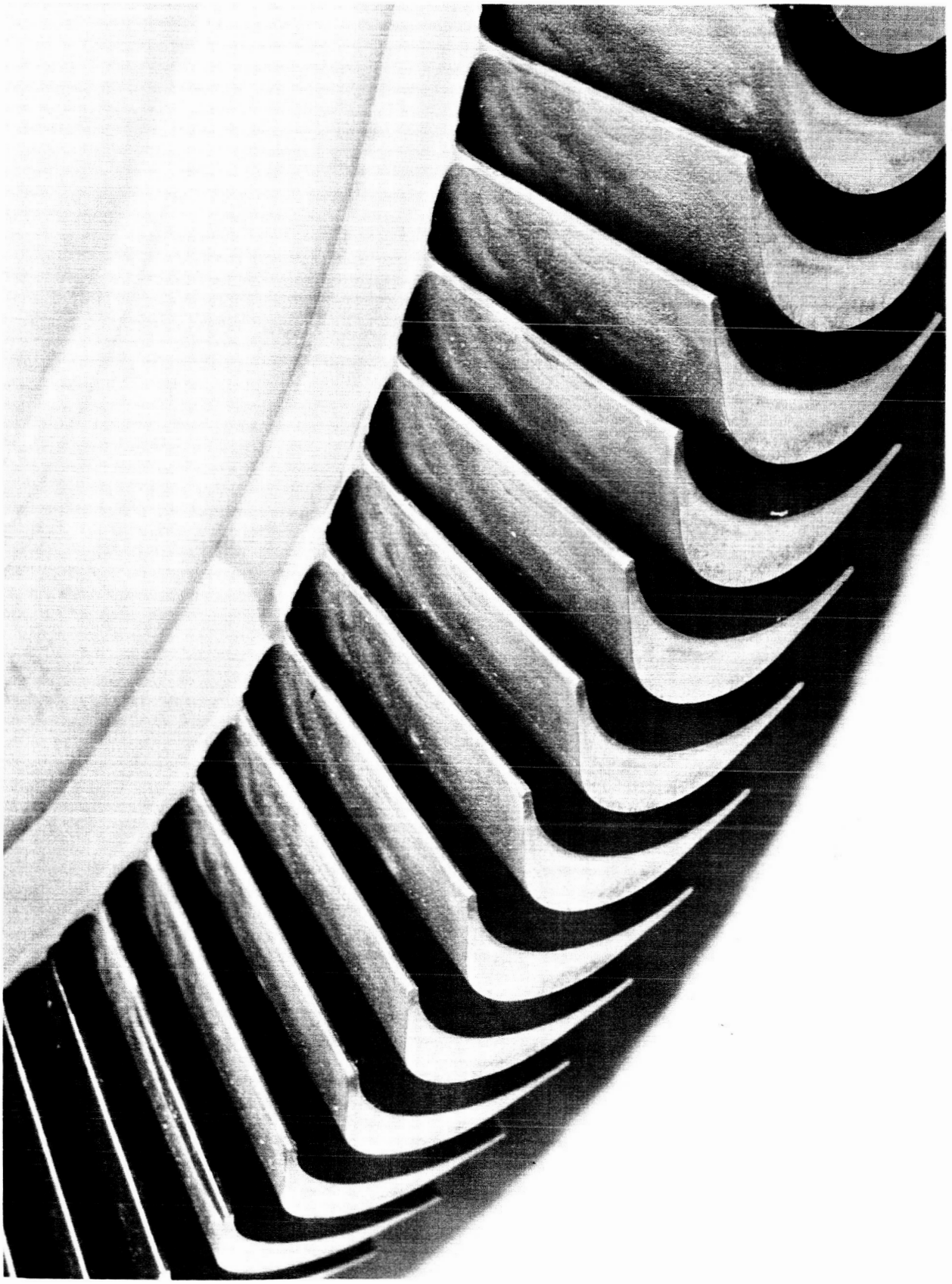

FIGURE 4-56 TURBINE BLADES AND RIM

FIGURE 4-57 ALTERNATOR ROTOR

FIGURE 4-58 SCROLL SUPPORT PINS

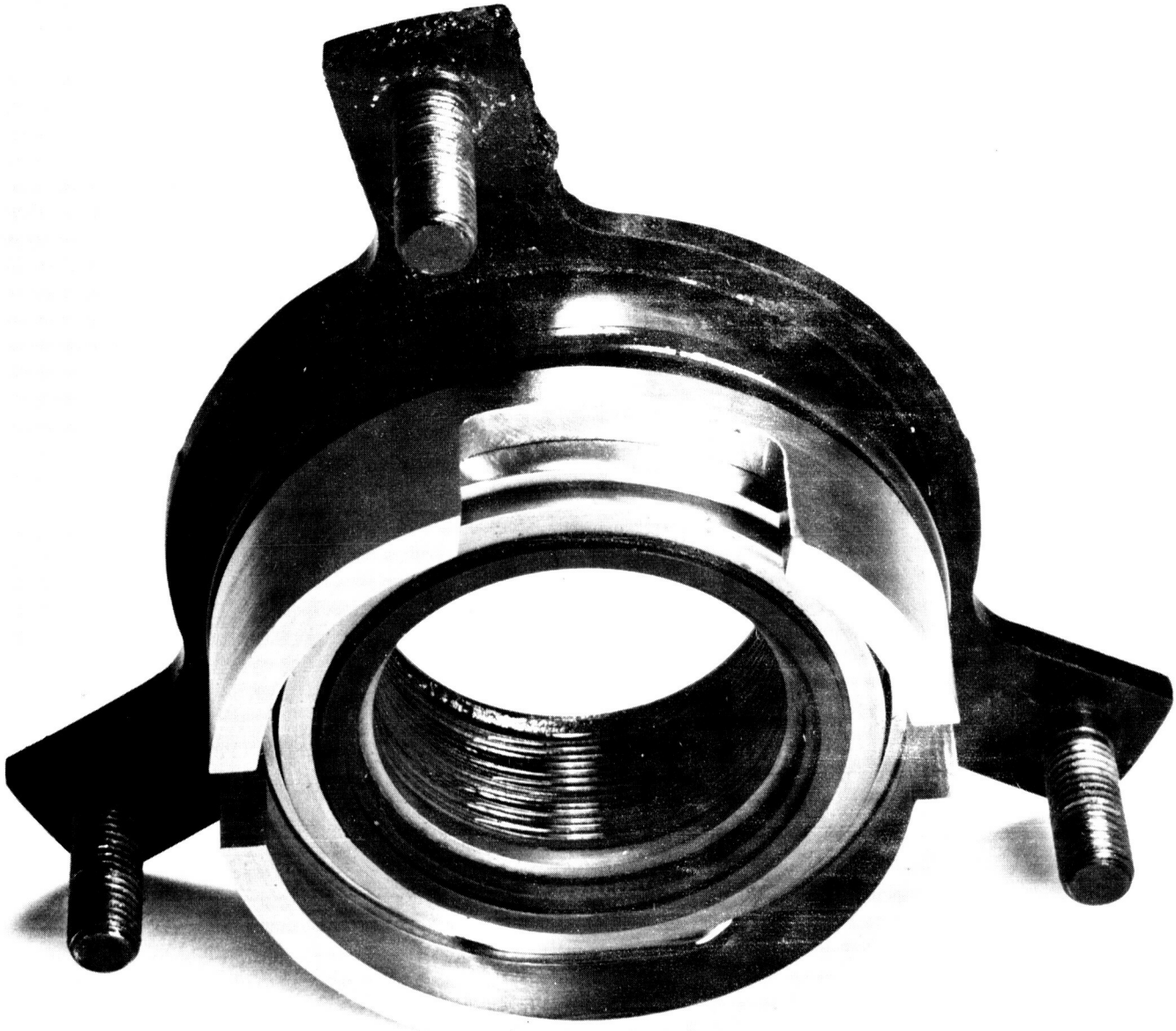

FIGURE 4-59 SEAL CARTRIDGE SHOWING CARBON SEAL FACE

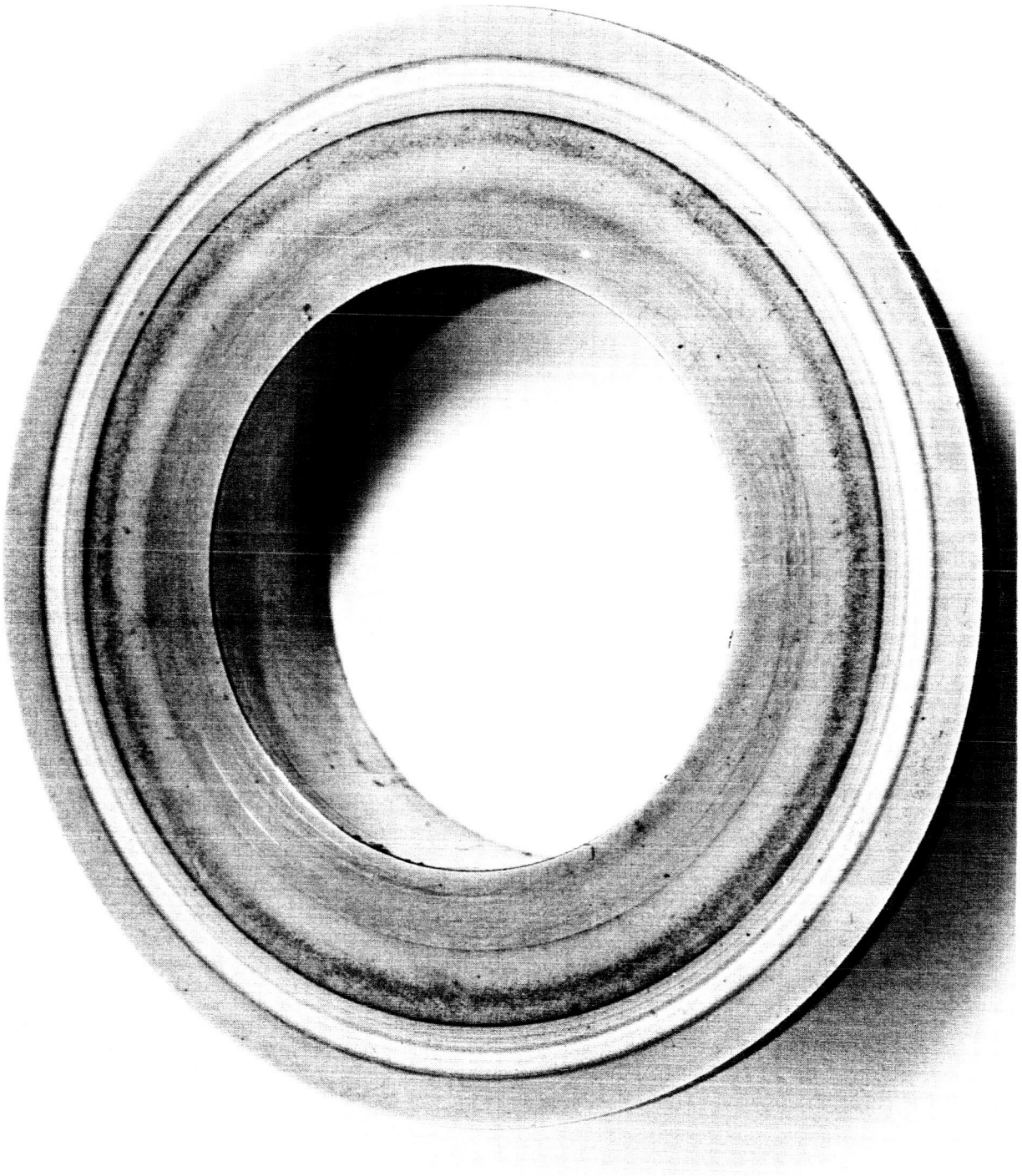

FIGURE 4-60 SEAL WEAR RING

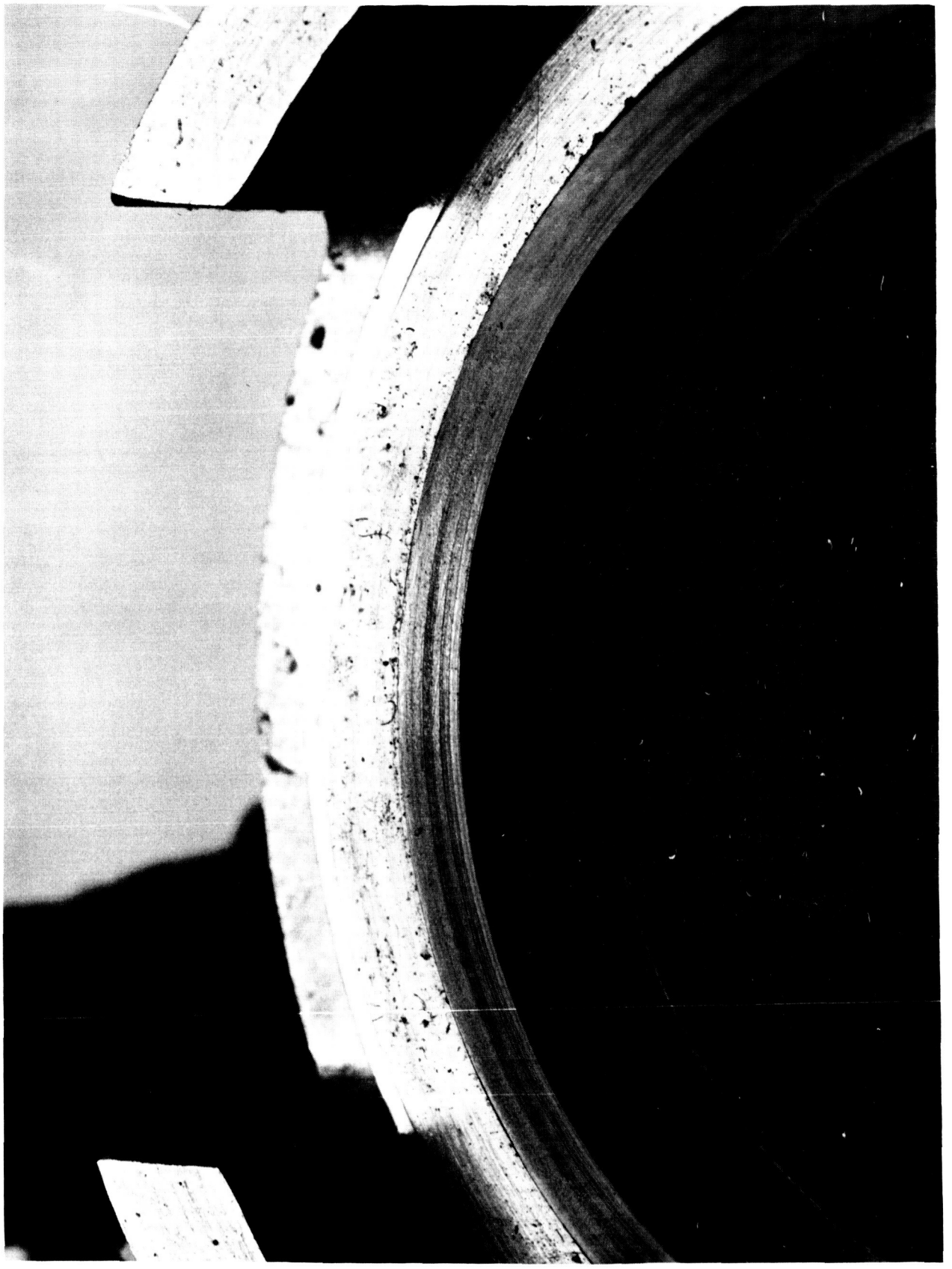

FIGURE 4-61 CLOSE-UP OF CARBON SEAL FACE

FIGURE 4-62 SEAL CARTRIDGE SHOWING OIL LEAK

FIGURE 4-63 ROLLER BEARING INNER RACE

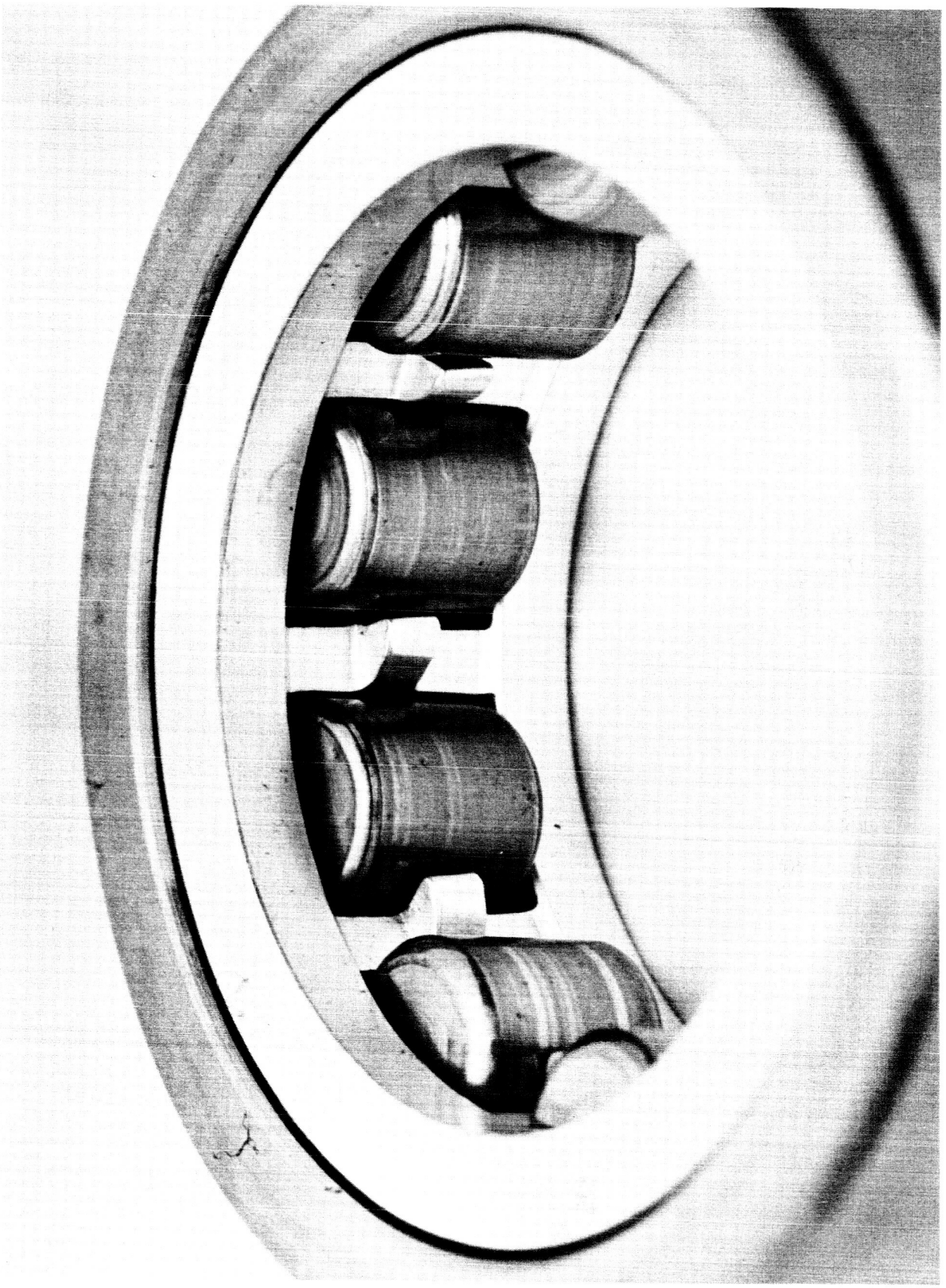

FIGURE 4-64 ROLLER BEARING ROLLERS, RETAINER AND OUTER RACE

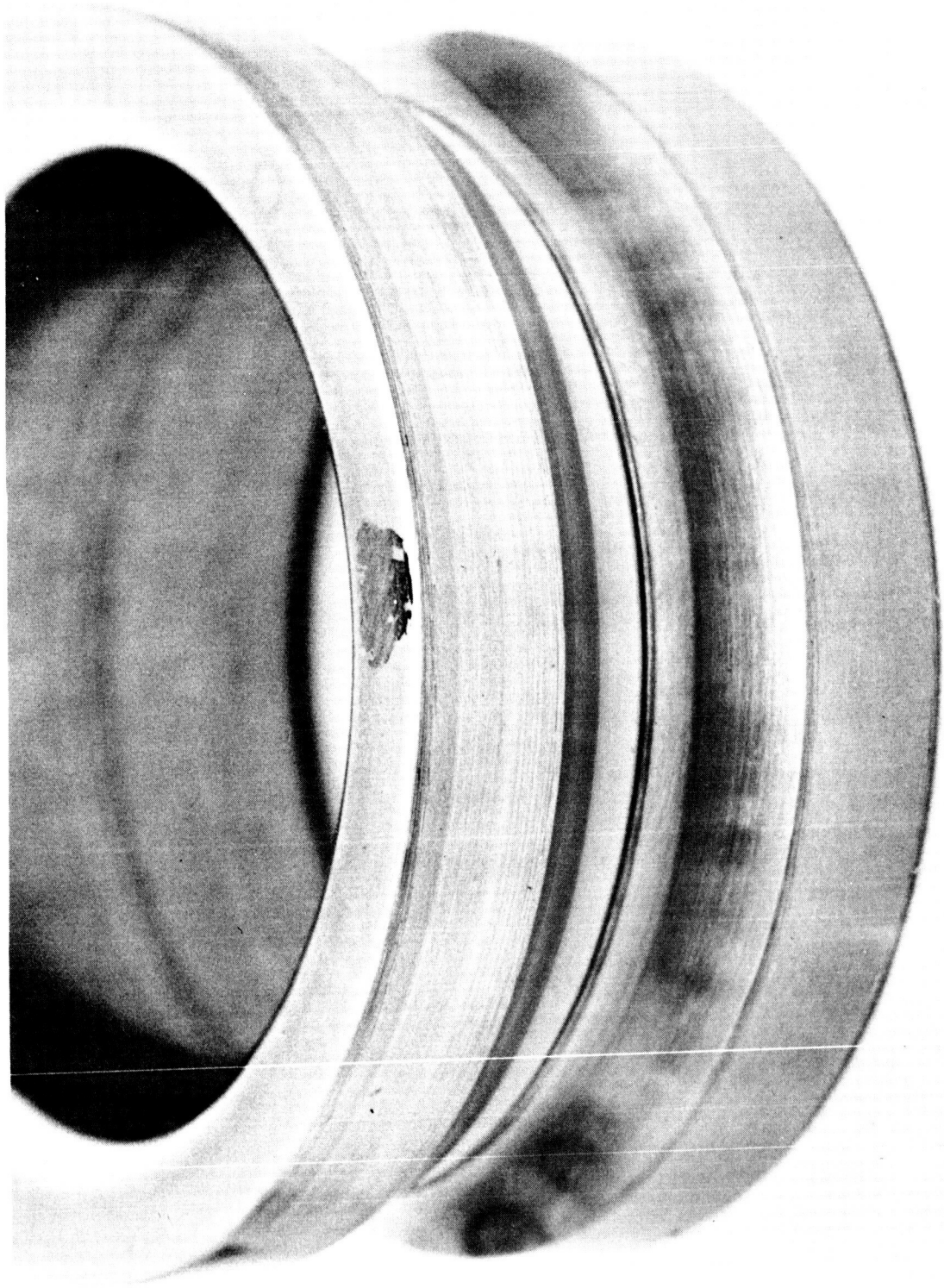

FIGURE 4-65 BALL BEARING INNER RACE

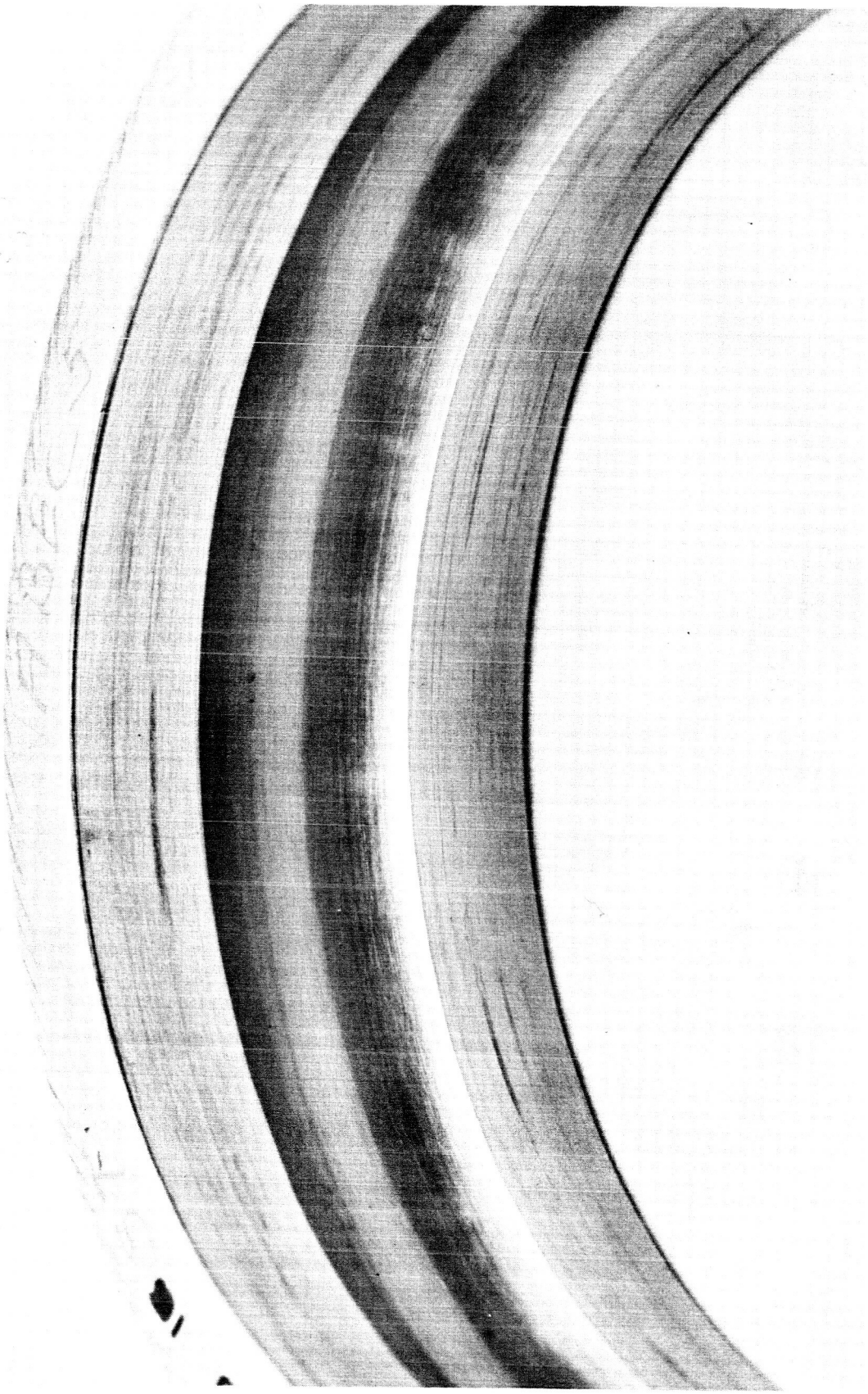

FIGURE 4-66 BALL BEARING OUTER RACE

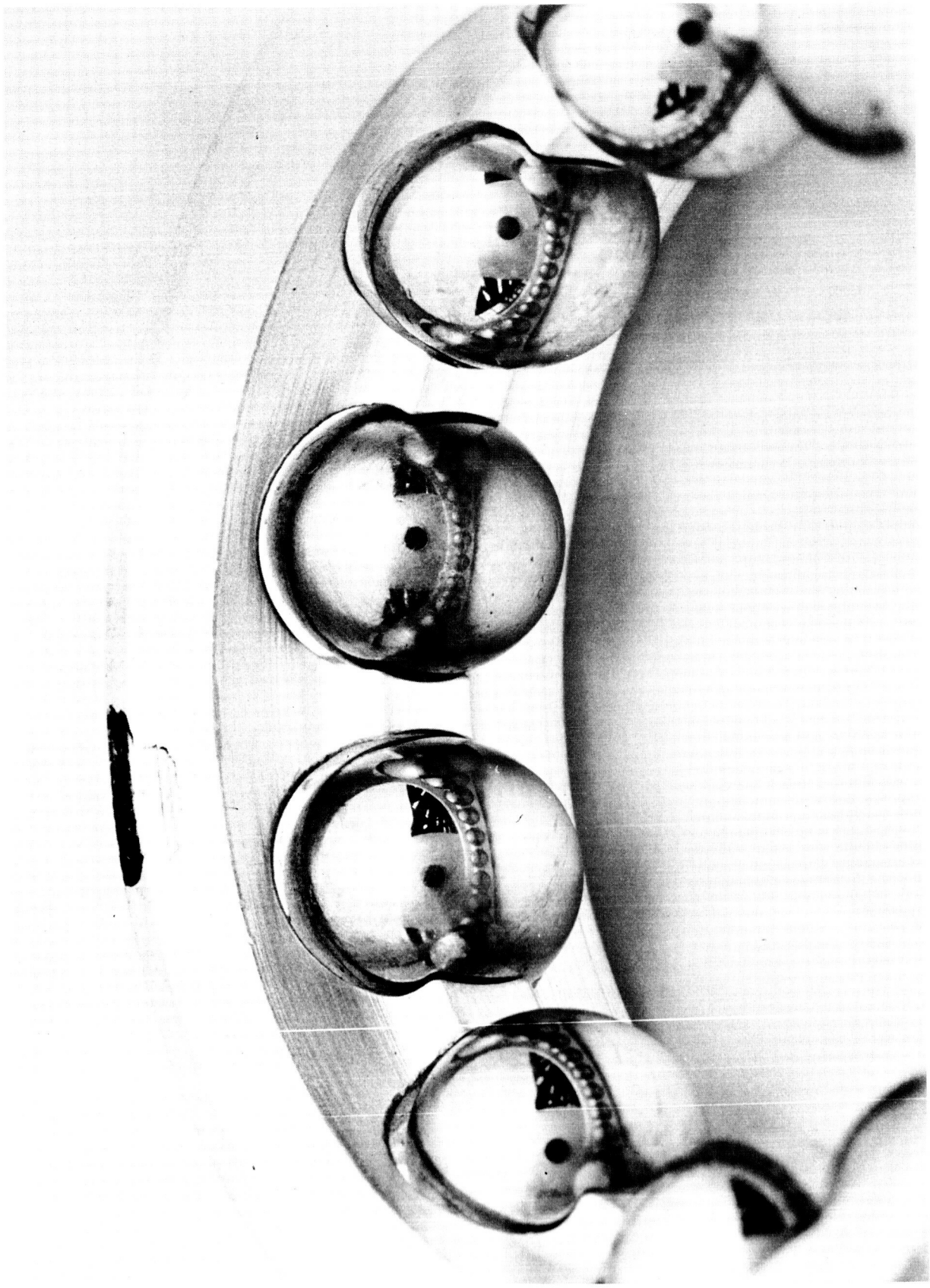

FIGURE 4-67 BALL BEARING RETAINER AND BALL COMPLEMENT

1. Gas Generator Pressure Calibration.

Deflection from Base Inches	Gas Generator Pressure Psia
0	10.8
1.0	41.0
2.0	71.0
3.0	101.5
4.0	131.0

2. Oxidizer Inlet Pressure Calibration.

Deflection from Base Inches	Oxidizer Pressure Psia
0	
1.0	50.0
2.0	105.0
3.0	160.0
4.0	214.0

3. Fuel Inlet Pressure Calibration.

Deflection from Base Inches	Fuel Inlet Pressure Psia
1.0	28.0
2.0	82.0
3.0	137.0
4.0	193.0

4. Vacuum Chamber Pressure.

Deflection from Base Inches	Vacuum Chamber Pressure Ins. Hg. Abs.
1.0	0.6
2.0	7.2
3.0	14.0
4.0	20.8
5.0	27.5

5. Fuel Inlet Temperature Calibration.

Deflection from Base Inches	Fuel Inlet Temperature °F.
2.0	35.5
2.5	79.0
3.0	119.5
3.4	152.5

6. Oxidizer Inlet Temperature Calibration.

Deflection from Base Inches	Oxidizer Inlet Temperature °F.
2.4	48.0
2.7	74.8
3.0	99.8
3.4	132.5

7. Helium Valve Voltage Calibration.

Not Available.

8. Moog Valve Current Calibration.

Deflection from Base Inches	Moog Valve Current Amperes
2.60	2.25
2.80	1.44
3.00	.64
3.10	.24

9. Moog Valve Voltage Calibration.

Deflection from Base Inches	Moog Valve Voltage Volts
3.6	4.0
4.0	13.0
4.4	22.2
4.8	31.0

10. Fuel Flow Calibration.

Frequency cps	Volumetric Flow Gals/sec
80	.007
120	.0105
160	.0141
200	.0177
240	.02125

11. Oxidizer Flow Calibration.

Frequency cps	Volumetric Flow Gals/sec
100	.0090
140	.0125
180	.0160
220	.01962
260	.0231

12. Alternator Field Voltage Calibration.

    Not Available.

13. Alternator Speed Calibration.

Deflection from Base Inches	Frequency Cycles/sec (Expanded Scale)	RPM (Expanded Scale)
1.0	995	29,900
2.0	1068	31,980
3.0	1140	34,220
4.0	1215	36,520

14. Alternator AC Voltage.

    Not Available.

4.5.4 Acceptance Test of Unit #2

An acceptance test of Unit #2 was conducted to prove satisfactory operation and determine system performance.

The acceptance test consisted of the following steps:

1) startup at 0.9 O/F ratio

* 2) operation at 2.7 O/F ratio at equivalent load of 3.0 KW for 25 minutes

* 3) operation at 0.9 O/F ratio at equivalent load of 3.0 KW for 25 minutes

* 4) operation at 0.9 O/F ratio at equivalent load of 4.5 KW for 10 minutes

* Note: Due to uncertainty in determining windage correction factors, loads may have been .40 KW less.

After running for 18 minutes at 0.9 O/F ratio at condition 3 above the injector head temperature reached 440°F. Load was removed for a period of 1/2 hours. Injector head temperature slowly dropped to 320°F. Unit was then shutdown to install water to the cooling coils in the injector. The unit was restarted and the remainder of the acceptance was completed. Total running time, including runs for O/F ratio adjustments, was 2.00 hours.

The second unit was very similar in operation to unit #1 with the exception of scroll and gas generator temperatures. Table 4-19 shows a comparison between Unit #1 and Unit #2 at the 2.7 O/F ratio and an equivalent load of 2.61 KW.

Table 4-19 Comparison of Performance of Unit #1 and Unit #2 at 2.7 0/F Ratio

	Unit#2	Unit #1
SPC lb/BHP-HR DC terminals	9.5	9.2
Coast time, sec	6.6	6.6
Temperatures - °F		
Injector head-rear	223	230
Injector head-front	232	211
Gas generator-rear	618	726
Gas generator-front	1190	1021
Turbine shroud	1130	1270
Scroll support flange	1126	1059
Alternator support flange	626	715
Ball bearing	200	270
Roller bearing	250	155
Face seal	330	320
Average fin	870	780
Alternator stator	233	208

The SPC for Unit #2 was slightly more than for Unit #1. This was probably due to the slightly larger turbine tip clearance of Unit #2, .045 in., compared to .038 in. for Unit #1. The component temperatures on Unit #2 at the 2.7 0/F ratio do not show a consistent variation either high or low from Unit #1. The temperatures of the scroll and exit end of the gas generator are 60 to 170°F higher than Unit #1, but the temperature of the injector end of the gas generator is slightly more than 100° lower than Unit #1. This may be due to slightly different placement of thermocouples from unit to unit or a small change in location of the initial point of propellant impingement.

Operation at 0.9 0/F ratio resulted in appreciably higher metal temperatures in the gas generator area. Comparison of the component temperatures of Unit #2 at both 0/F ratios appears in Table 4-20. These data show that injector and gas generator temperatures are hotter at the 0.9 0/F ratio, but temperatures around the scroll are lower, which is consistent with Unit #1 results. Tests of Unit #1 have brought out the fact that when injector head temperatures exceed 260°F, the 0/F ratio begins to shift and system performance declines with resultant higher metal temperatures. This chain of events occurred in Unit #2, and made it necessary to water cool the injector head before completion of the test at the 0.9 0/F ratio.

Table 4-20 Comparison of Unit #2 Temperatures at 0/F Ratios of 0.9 and 2.7 Without Injector Cooling

	2.7 0/F	0.9 0/F
Equivalent load, KW	2.61	2.61
Temperatures, °F		
Injector head-rear	223	337
Injector head-front	232	440
Gas generator-rear	618	1004
Gas generator-front	1190	1465
Turbine shroud	1330	1130
Scroll support flange	1126	962
Alternator support flange	626	574

Temperatures in the unit after addition of injector head cooling are shown in Table 4-21. They are compared with similar temperatures of Unit #1 at a slightly greater electrical output. In general, Unit #2 temperatures in the gas generator and scroll areas were higher than Unit #1. This was due in part to the amount of cooling applied to the injector head of each unit. Water was flowed continuously through the injector of Unit #1 in the test being compared resulting in a temperature of 125°F. Water was passed through the Unit #2 injector to maintain the temperature of approximately 200°F by flowing water into the injector head about once every five minutes for a fifteen seconds period. If cooling had been equivalent for each unit, the temperature differences would have been less.

Table 4-21 Comparison of Component Temperatures of Unit #1 and #2 at 0.9 0/F Ratio With Injector Cooling

	Unit #1	Unit #2
Equivalent load, KW	4.47	4.11
Temperatures - °F		
Injector head	125	210
Gas generator	1245	1300
Turbine shroud	1230	1405
Ball bearing	265	225
Roller bearing	200	200
Face seal	300	220
Average fin	700	910

It may be concluded that Unit #2 performed satisfactorily and in a manner similar to Unit #1. Fuel consumption was 3% higher probably due to larger turbine tip clearance. Turbine shroud and gas generator temperatures exhibited a slightly different pattern, and a higher level. This is partially explained by the 3% higher SPC. It has also been noted in previous testing on Unit #1 that the second scroll, now installed on Unit #2 tends to operate at a somewhat higher temperature than the first scroll. It is thought that differences in emissivity exist in the three turbine housings. This must be more fully investigated.

4.6 Comparison of Test Results with Preliminary Analysis

A preliminary analysis of turbine performance and scroll temperatures was presented in ER-6630, "Optimization Studies, Preliminary Design and Program Definition, Turbine-Alternator Power Generation System." Those results are compared with test results of Unit #1 at a 3 KW equivalent output.

4.6.1 Coast Time and SPC

Test results indicate the coast time at 3 KW equivalent output was 6.3 seconds, and SPC was 8.9 lb/BHP-HR computed at the DC terminals. The same performance was recorded at both 0/F ratios. The theoretical performance at the 2.7 0/F ratio was an SPC of 7.2 lb/BHP-HR and a coast time of 7.8 seconds. The theoretical performance at the 0.9 0/F ratio was slightly lower. These comparisons are summarized in Table 4-22.

Table 4-22 Comparison of Theoretical and Actual Performance

Performance	Theoretical		Actual
	2.7 0/F	0.9 0/F	Both 0/F
Coast time, sec.	7.4	7.0	6.3
SPC, lb/BHP-HR at DC terminals	7.2	7.6	8.9

The actual SPC is higher than the predicted values given in ER-6630, Page 3-32. There were several changes in the actual design from the theoretical which account for part of this discrepancy.

To design, build and successfully endurance test a space power system within a period of one year required that some conservatism in design and operation be employed. In the turbine, three design features accomplished this objective:

a) The operating speed was 33,200 RPM rather than the actual design speed of 36,600 RPM.

b) The turbine blade leading and trailing edges were .030 in. thick instead of .015 in. originally considered.

c) The turbine tip clearance was .040 in. which is considered high for a turbine of 10 in. pitch diameter. This insured the prevention of turbine wheel rubbing.

Mechanically and thermally, these features provided trouble-free operation although each introduced a performance penalty.

The amount of improved performance that may be achieved in each area is listed below:

a)	Increase turbine speed to 36,600 RPM	7%
b)	Decrease blade edge thicknesses to .015 in.	5%
c)	Reduce turbine tip clearance to .030 in.	2%

If the actual SPC is adjusted for these improvements, its value closely approaches the predicted value.

4.6.2 Nozzle-Scroll Assembly Temperatures

As previously explained, the SPC values from tests were approximately the same for both 0/F ratios whereas theoretically at 2.7 0/F ratio, SPC is lower. This is believed due to three factors; 1) the inaccuracy of instrumentation measuring fuel flow tended to partially conceal the difference between the two 0/F ratios, 2) the actual temperatures of the scroll at the 2.7 0/F ratio are generally higher than theoretically calculated and 3) fins were added to actual scroll with consequent increase in radiating area. The last two items indicate that more heat was transferred to the scroll than calculated, and, correspondingly, less energy was available to the turbine. This reduced the 2.7 0/F ratio SPC closer to the 0.9 0/F ratio value. Table 4-23 shows a comparison of the theoretical and actual thermal conditions at the 2.7 0/F ratio.

Table 4-23 Comparison of Theoretical and Actual Scroll Thermal Conditions at the 2.7 0/F Ratio

Component	Theoretical	Actual
Scroll support flange temperature - °F	920	1090
Turbine shroud temperature - °F	1140 - 1350	1255 - 1330
Scroll temperature - °F	1020	1160 - 1350
Turbine blade temperature - °F	1200	1150 (estimated)
Heat transferred to metal (including turbine blades) Btu/hr	23,980	36,200 (calculated from temp. data)

4.6.3 Energy Balance

The values of major losses in the system were estimated in the preliminary analysis. These values are compared to values obtained from testing at the 2.7 O/F ratio in Table 4-24. Whereas the theoretical losses were preliminary design estimates, the actual losses are more accurate estimates based on actual hardware used and data obtained as explained in Section 4.4.4. Table 4-25 compares the theoretical and actual component efficiencies and energy losses as percentages of the heating value of the propellants.

Table 4-24 Comparison of Theoretical and Actual Major Losses at 2.7 O/F Ratio

Item	Theoretical Loss (Btu/hr)	Actual Loss (Btu/hr)
Equivalent output at DC terminals	10,250	10,250
Combustion efficiency loss	3,400	3,900
Mechanical losses	1,710	1,550
Power conditioning loss (rectifier-filter)	1,100	680
Heat loss to coolant	5,760	9,500
Heat loss to metal	23,980	—
Scroll and fins	—	29,900
Turbine	—	6,300
Heat loss to exhaust	38,800	36,120
	85,000	98,200

4.6.4 Alternator performance

Data on alternator performance were obtained from tests of the complete system. These tests confirmed the ability of the alternator to provide the required output up to the level of approximately 3.3 KW at the DC terminals. Information was obtained on the field requirements of the alternator over this load range. The actual test results are presented in Figure 4-68 and are compared to the calculated field requirements predicted in the design study. As shown by Figure 4-68, the field power requirements are significantly lower than predicted at the no load condition. The measured field requirements do increase rather rapidly as the power level is raised. At the maximum test point, the actual field requirements were somewhat higher than those calculated. The type of result obtained would indicate generally that the magnetic material was harder than predicted in a magnetic sense. This type of characteristic would provide a high

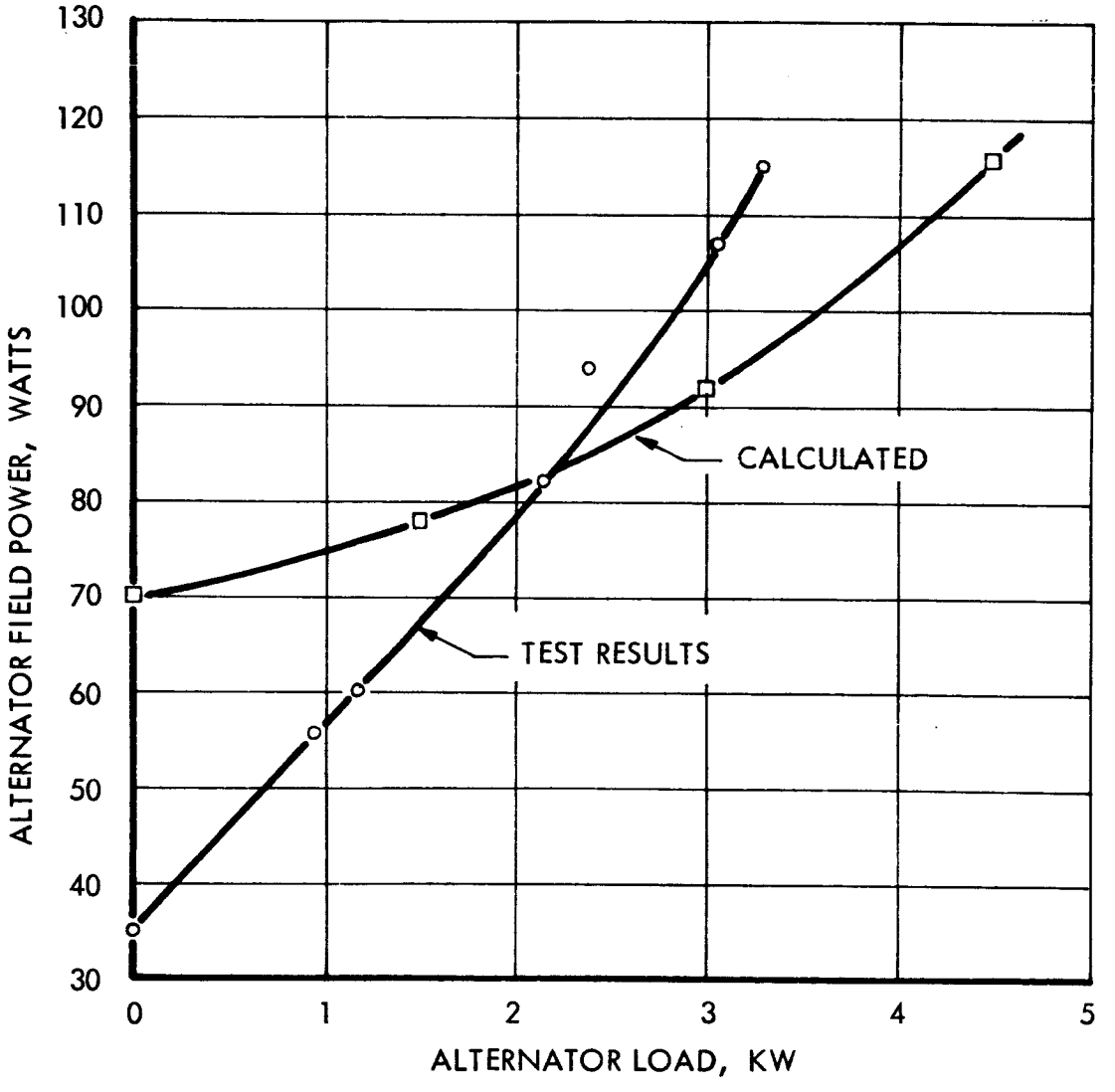

FIGURE 4-68 COMPARISON OF CALCULATED AND ACTUAL FIELD POWER REQUIREMENTS

residual magnetic effect at no load. As field requirement is increased, a greater MMF is needed to produce the required flux. This result again emphasized the desirability of conducting more extensive tests on the alternator as a part of any future efforts.

Table 4-25 Energy Losses as Percentages of Heating Value and Efficiencies (at 2.7 O/F Ratio)

Item	Estimated Value	Actual Value
Theoretical energy content	2950 Btu/lb(est.)	2950 Btu/lb (est.)
Combustion efficiency	96%	96%
Mechanical efficiency	87%	87%
Percentage of combustion energy lost to exhaust	46.8%	36.8%
Percentage of combustion energy lost to coolant	6.8%	9.7%
Percentage of combustion energy lost to metal	28.1%	37.0%
Alternator efficiency	88%	89%
Power conditioning efficiency (rectifier filter)	90%	94%
Average power level	3.0 KW	3.0 KW
Off/on ratio	37.0	31.5

4.6.5 Turbine Horsepower

The design turbine output power at 36,600 rpm was estimated to be 182 hp. Test data plotted in Figure 4-69 compare the actual instantaneous turbine power with the theoretical value.

The actual turbine horsepower is 165 for 33,000 rpm and a pulse width of .200 secs. This lower than theoretical output is due to the lower turbine speed and thicker blade leading edges as discussed in Section 4.6.1.

The lower turbine performance does not completely account for the total difference between actual and predicted SPC. It is believed that instrumentation inaccuracy in measuring propellant flow, altitude chamber pressure, and duration of speed increase are responsible for the remaining discrepancy between SPC and turbine performance.

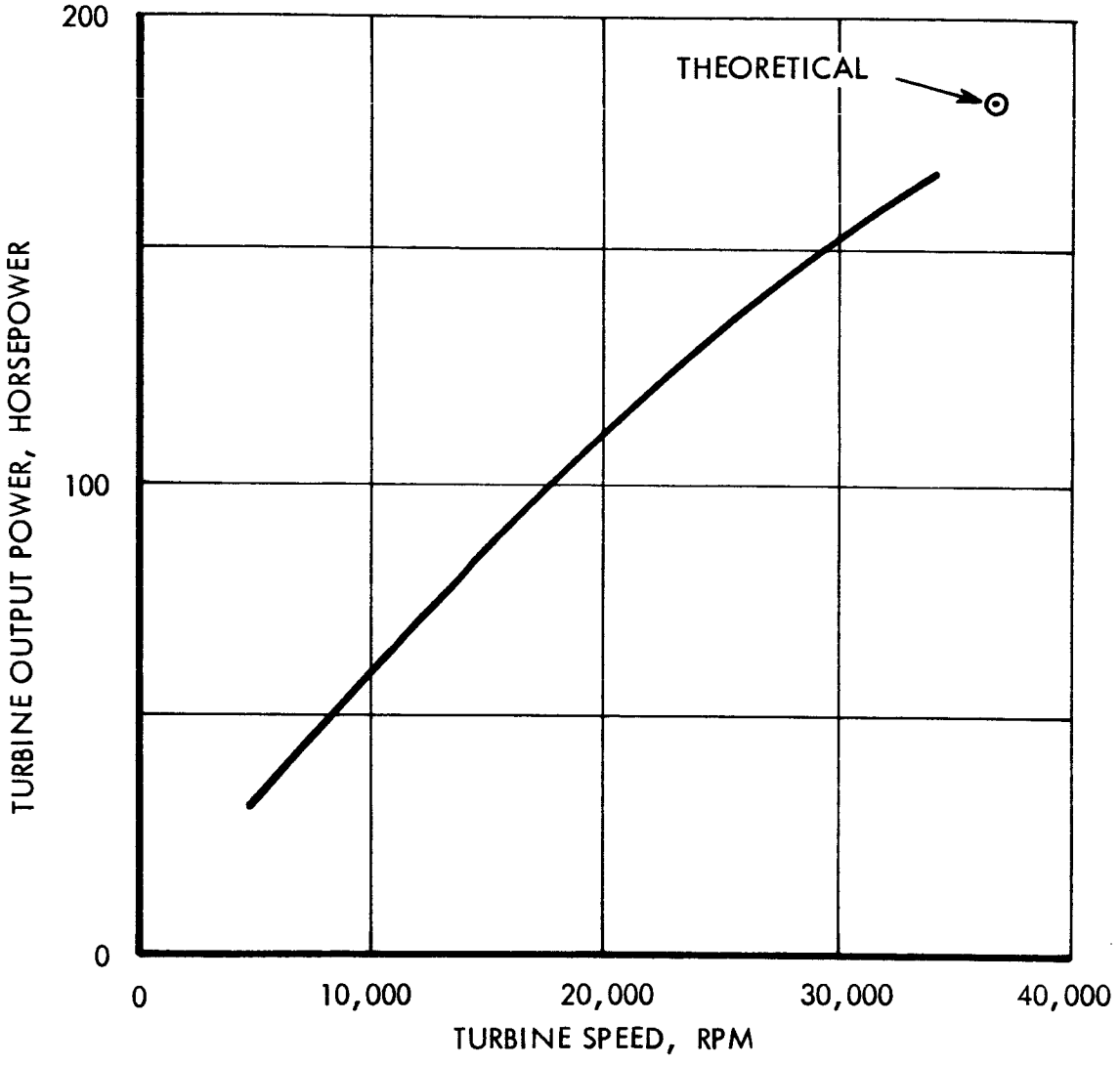

FIGURE 4-69 TURBINE OUTPUT POWER VERSUS TURBINE SPEED

4.7 Materials Analysis of Gas Generator Failure

Failures occurred in two gas generators in the oxidizer inlet tubes to the injectors. These failures consisted of ruptures in the tube walls close to the area where the tubes were gold brazed to the valve mounting flange. These ruptures were metallurgically examined to determine type and cause of failure.

Examination of the first failed tube under low magnification showed the tube wall to be elongated at the point of fracture. This is characteristic of a ductile failure. Under high magnification, an intergranular penetration was observed on the outside diameter of the tube.

To determine if gold alloy could be attacking the Inconel, a tube-to-flange braze sample was examined under high magnification. Figure 4-70 shows the presence of intergranular penetration into both the tube and flange by the gold alloy braze in the middle.

To further investigate the action of the gold alloy braze on Inconel, a gold alloy ring was attached to an Inconel tube and the sample was subjected to the standard brazing cycle. Figure 4-71 shows the sample after brazing. The sample was arranged so that gold alloy was deposited heavily on one side of the tube while no gold alloy was deposited on the area 180° opposite. This enabled a direct comparison of the Inconel tube with and without the effect of gold alloy. There is a heavy deposit of gold braze on the bottom and no deposit on the top in Figure 4-71. It can be observed that the tube thickness reduces from .0087 in. where there is no gold alloy to .0035 in. where the heaviest deposit of gold alloy exists. Thus, it is evident that the gold braze alloy in the oxidizer inlet tube corroded and weakened the tube at the flange-tube braze joint.

The failure of the tube was probably due to an overpressure, and may have occurred even in the absence of tube weakening by the gold braze. However, tube corrosion and intergranular attack both contributed to weakening the tube so that the ruptures took place at the weakest points in the area of the braze. In the future heavy walled tubes will be used to minimize the detrimental effects of the brazing operation.

4.8 Installation of Power System Within Spacecraft

The power system, as now designed, is best suited to an exterior mounting arrangement in which the turbine wheel and scroll reject heat by direct radiation to space. With this arrangement all required cooling is provided by the oil radiator and by cold plates for electronic component mounting. Interior mounting of the turboalternator within the spacecraft itself has only been analyzed in a preliminary way. Alternate methods of removing heat from the turbine scroll and turbine wheel have been studied. With minor revision to the present scroll design, a coolant loop could be added to the outside diameter of the fins and turbine shroud. This loop would circulate a mixture of 80% Dowtherm A and 20% Dowtherm E and would operate at an average radiator temperature of 550°F. Assuming a 100°F temperature rise in the fluid, the required flow is 1.5 GPM for 3 KW at 2.7 O/F ratio and 4.5 KW at 0.9 O/F ratio. Pumping power is less than

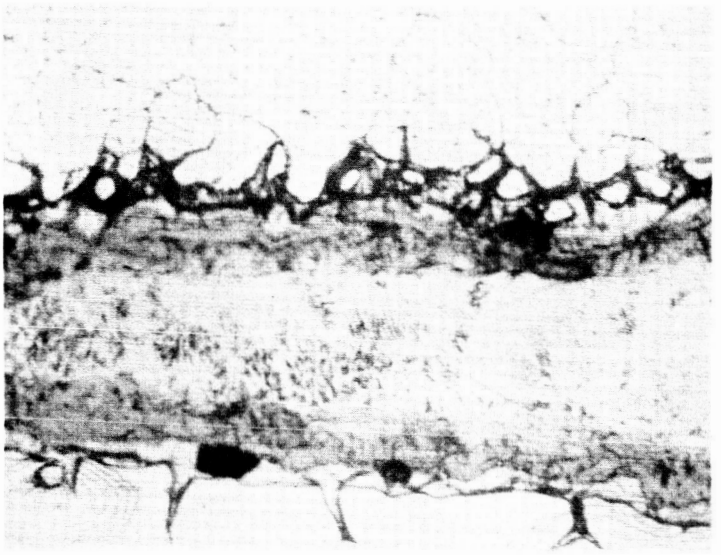

530 X

FIGURE 4-70 TUBE TO FLANGE BRAZED JOINT. INCONEL AT TOP AND BOTTOM. GOLD ALLOY AT CENTER.

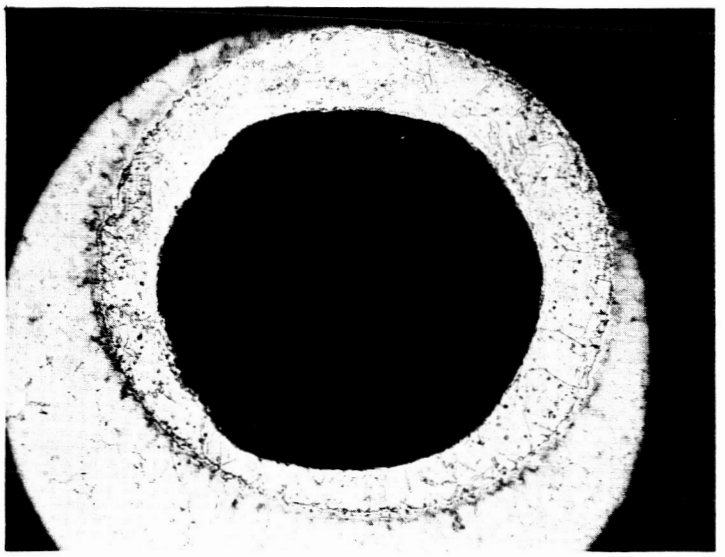

50 X

FIGURE 4-71 INCONEL TUBE WITH GOLD ALLOY BRAZE.

50 watts. The above estimates are based upon removal of scroll and turbine wheel radiated heat, estimated to be:

at 0.9 0/F ratio	Scroll	27,200 BTU/hr
4.5 KW	Turbine	5,600 BTU/hr
	TOTAL	32,800 BTU/hr
at 2.7 0/F ratio	Scroll	29,900 BTU/hr
3.0 KW	Turbine	6,300 BTU/hr
	TOTAL	36,200 BTU/hr

This would be a constant flow type system with radiator temperature varying with load. Required radiator area, for an emissivity of 0.85, is 27.0 ft^2. (Radiating from one side only.)

It is believed necessary to maintain a minimum 8 inch diameter exhaust duct to the point of exhaust from the spacecraft. This duct, as well as the turbine scroll, will require insulation to minimize spacecraft heating.

As an alternate to the Dowtherm coolant loop, the lubricant pump can be increased in capacity and the lubricating oil itself used as a coolant, in which case, average radiator temperatures will probably not exceed 500°F and radiator area will be approximately 32 ft^2.

A reduction in radiator area to 10.1 ft^2 can be achieved by using a mercury cooling loop and operating at 800°F average radiator temperature. The technology for this approach is well developed and no state-of-the-art advances are required. This system may offer little weight saving as compared with the Dowtherm system, however, due to the lower specific heat and higher density of the mercury.

An arrangement of the turboalternator mounted inside the spacecraft is shown in Figure 4-72.

For submerged installation, revisions to the present turboalternator should be made in order to reduce the heat input to the scroll assembly. This can be accomplished by using a double walled shroud in which the inner portion is allowed to operate at a higher temperature, and the outer structural portion operates at more normal temperatures. Revisions to the nozzle plate to reduce the heat transfer rate from the nozzles to the nozzle plate can be accomplished by making the nozzle entrance, through and beyond the throat area, as a separate piece of high temperature material. Small areas of contact between these separate nozzles and the nozzle plate will reduce heat flow considerably. These revisions offer potential for a reduction in fuel consumption as well as a sizable reduction in scroll heat loss.

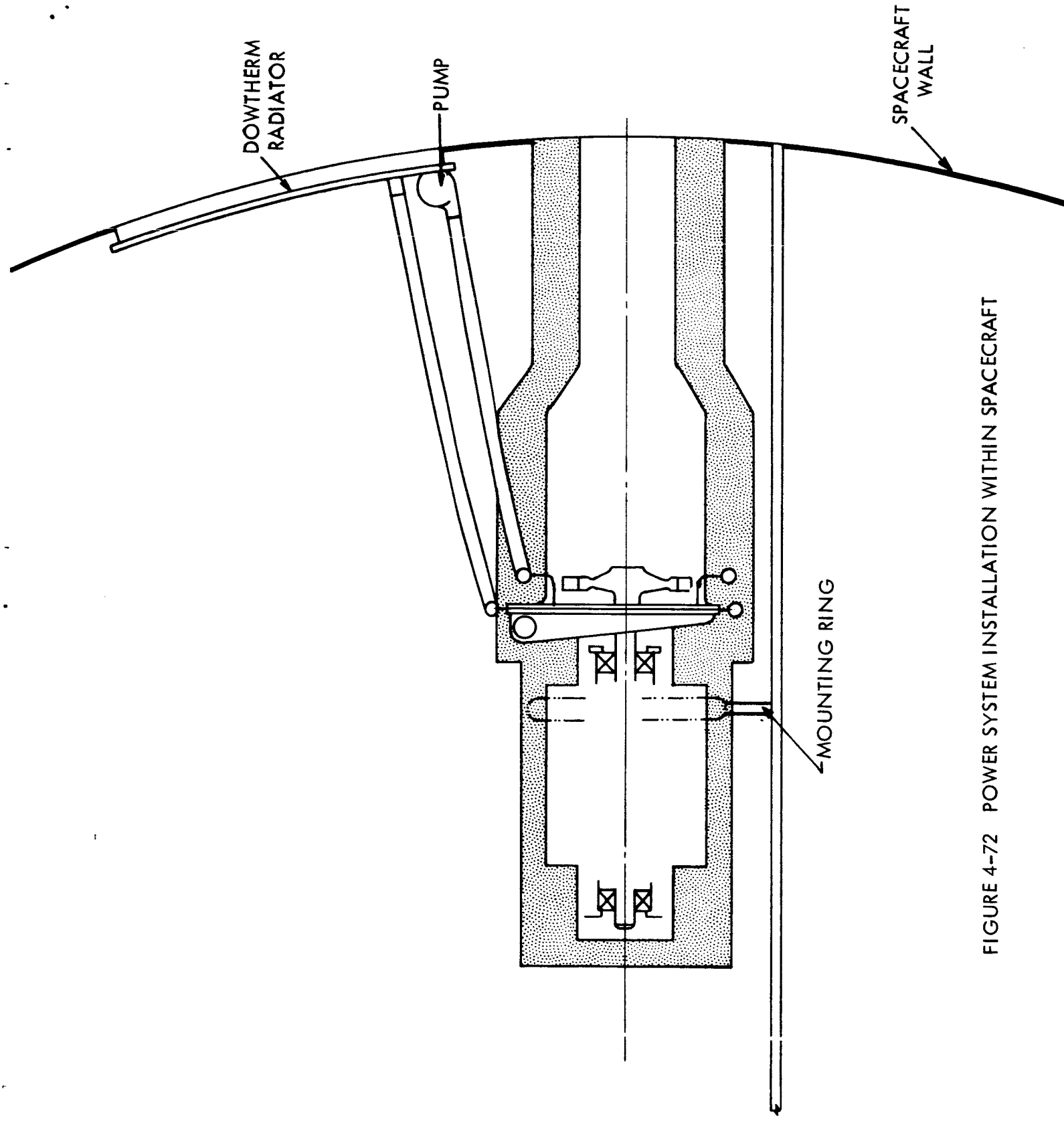

FIGURE 4-72 POWER SYSTEM INSTALLATION WITHIN SPACECRAFT

If mounting within the spacecraft becomes a requirement, an optimization analysis must be performed. This should include,

a) a thermal analysis of the heat rejection rates to the turbine scroll, turbine wheel and exhaust ducting,

b) coolant system trade-offs to determine size, weight and configuration using various coolant fluids,

c) analysis of various arrangements and locations of system components both within and outside the spacecraft and

d) recommendations of practical system and component configurations for the specific application.

REFERENCES

1. ER-6630, "Optimization Studies, Preliminary Design and Program Definition, Turbine-Alternator Power Generation System," TRW Equipment Laboratories, September 8, 1965.

2. Manson, S. S., "Determination of Elastic Stresses in Gas Turbine Disks," National Advisory Committee for Aeronautics, Cleveland, Ohio, Report No. 871, February 27, 1947.

3. Prohl, M. A., "A General Method for Calculating Speeds of Flexible Rotors;" ASME Transactions; Vol. 67, 1945, pp 142-148.

4. ER-6715, "Analog Computer Analysis of Pulsed Energy Turboalternator," TRW Equipment Laboratories, December 9, 1965.

APPENDIX "A"

TEST LOG

I. Breadboard Test Program (conducted in September and October 1965)

Tests 001 through 005. These consisted of Potter flowmeter calibrations using water. Instrument calibrations and rig check-out were also performed.

Test 006. The reworked SIV B injector head, modified to operate at 2.7 0/F ratio, was installed with the 100 L* single throat nozzle.

Four 1.0 sec. pulses were fired manually at sea level to check out the rig.

Pulse On Time 4.0 secs.

Test 007. One 2.6 sec. pulse at sea level was fired manually to check out the rig.

Pulse On Time 2.6 secs.

Test 008. One 1.0 sec. pulse and one 1.5 sec. pulse were fired manually at sea level. Propellant flow readings were taken and supply pressures to provide design flow rates were calculated.

Pulse On Time 2.5 secs.

Test 009. The breadboard pulser was installed. Three .2 sec. pulses, three .1 sec. pulses, three .2 sec. pulses and three .1 sec. pulses were fired at sea level to check pulser operation.

Pulse On Time 1.8 secs.

Test 010. After adjusting propellant supply pressures, two 2.0 sec. pulses were fired manually at sea level to check design flow rates. These were satisfactory.

Pulse On Time 4.0 secs.

Test 011. One hundred twenty-five .20 sec. pulses were fired at 100,000 feet altitude at a τ of 30 (5.8 sec. off time). The nozzle throat temperature reached 1230°F at 100 pulses and was leveling off. Shutdown to analyze data. Altitude cell temperature and injector head temperature exceeded 300°F.

Pulse On Time 25.0 secs.

Test 012. One hundred fifty .2 sec. pulses were fired at altitude at a τ of 40 (7.8 secs. off time). After the 80th pulse the nozzle throat temperature leveled off at 900°F. Injector head temperature and altitude cell temperature again exceeded 300°F.

Pulse On Time 30.0 secs.

Test 013. One hundred thirty-five .20 sec. pulses were fired at altitude at a τ of 20 (3.8 secs. off time). After 120 pulses nozzle throat temperature reached 1310°F. Altitude cell temperature and injector head temperature exceeded 300°F.

Valves, pulser, and injector all functioned well. An injector heat soak back problem, aggravated by excessive altitude chamber temperature was the only deficiency observed.

Pulse On Time 27.0 secs.

Test 014. Two 1.0 sec. manual pulses and three .2 sec. pulses were fired at sea level to recheck rig and propellant flows.

Pulse On Time 2.6 secs.

Test 015. Three 3.0 sec. pulses were fired manually at altitude for the purpose of measuring thrust and specific impulse. Analysis of data indicated 198 specific impulse.

Pulse On Time 9.0 secs.

Test 016. Nineteen .2 sec. pulses were fired at altitude at a τ of 40 for the purpose of measuring thrust. Again specific impulse at the stabilized point during the pulse reached 198 secs. Thrust measurements are only approximate due to non-precise instrumentation.

Pulse On Time 3.8 secs.

Test 017. Ninety .20 sec. pulses were fired at altitude at a τ of 40 as a re-check of metal temperature profiles obtained during Test 012. Results were repeated.

Pulse On Time 18.0 secs.

Test 018. One hundred .2 sec. pulses were fired at altitude at a τ of 30 as a re-check of Test 011. A simulated turbine blade row was installed in the gas stream for this test. Turbine blades did not burn.

Pulse On Time 20 secs.

Test 019. One hundred twenty .20 sec. pulses were fired at altitude at a τ of 20 as a recheck of Test 013. The results repeated.

Pulse On Time 24 secs.

The above tests completed the breadboard program with the 100 L* tube. It was concluded that the gas generator, valves, pulser and nozzle performed well. No excessive metal temperatures were reached. An injector heat soak back problem, aggravated by altitude chamber overheating existed.

The gas generator and 100 L* tube were removed from the test cell. The breadboard scroll (using 11 full admission nozzles) was assembled to the gas generator and installed for test.

Test 020. Twenty .2 sec. pulses at τ = 40 were fired at sea level to check propellant flow rates.

Pulse On Time 4.0 secs.

Test 021. Ten .2 sec. pulses at a τ of 40 were fired with fuel and oxidizer pressures adjusted to provide design flow rates.

Pulse On Time 2.0 secs.

Test 022-1. One .1 sec. pulse was fired at altitude with a simulated turbine blade row installed in a nozzle exit, to determine turbine blade resistance to oxidation and burning.

The blade row contained 4 blades having .015, .030, .045 and .060 leading edge thicknesses respectively. This test was so mild that turbine simulator temperature showed only slight change from room temperature.

Pulse On Time .10 secs.

Test 022-2. Five .2 sec pulses at a τ of 40 were fired at altitude to determine turbine blade heating. Turbine disk temperatures increased only slightly.

Pulse On Time 1.0 secs.

Test 022-3. Ten .2 sec. pulses were fired at altitude at a τ of 40. Turbine disk temperature increased slightly and blades showed no deterioration.

Pulse On Time 2.0 secs.

Test 023-1. One hundred .2 sec. pulses were fired at altitude at a τ of 60.

Total Running Time 20 min.

Turbine disk temperature reached 510°F at the rim. Turbine blades showed no deterioration. Maximum scroll temperature reached 1110°F.

Pulse On Time 20.0 secs.

Test 023-2. Seventy-five .2 sec. pulses were fired at altitude at a τ of 40.

Total Running Time 10 min.

Turbine disk temperature reached 475°F at the rim. Turbine blades showed no deterioration. Maximum scroll temperature reached 1210°F.

Pulse On Time 15.0 secs.

Test 024. Eighty .2 sec. pulses were fired at a τ of 30.

Running Time 480 secs.

Turbine disk temperature reached 510°F. Turbine blades showed no deterioration. Maximum scroll temperature reached 1300°F. Injector head temperature reached 290°F. The effects of heat soak back were aggravated by test cell temperature which exceeded 300°F.

Pulse On Time 16.0 secs.

It was concluded that the valves, pulser, gas generator, turbine scroll and turbine blading operated acceptably except for the heat soak back problem. The breadboard unit was removed from the stand, and test cell revision to accommodate the prototype hardware was begun.

Total Pulse On Time
for Breadboard Test Program 233.4 secs.

II. Prototype Test Program

The first prototype gas generator designed for 0.9 O/F ratio operation was installed in the altitude chamber for test, with the 100 L* tube and nozzle.

Test 001. - January 27, 1966
Three 1.0 sec. pulses were fired manually at sea level to check propellant flow rates. The oxidizer filter element ignited internally during this test due to the incompatibility of the material. Oxidizer flowmeter malfunctioned due to the filter failure, and it was hand-carried to Flocon for repairs.

Pulse On Time 3.0 secs.

It was decided to run Tests 002, 003, and 004 without the oxidizer flowmeter.

Test 002. - January 28, 1966
Three 1.0 sec. pulses were fired at sea level to check operation of the system.

Pulse On Time 3.0 secs.

Test 003. - January 28, 1966
Four 1 sec. pulses were fired at altitude to check the helium start-up pressurization system. Helium pressure was turned on 2 secs. before the 1st pulse and 7 secs. before the 4th pulse. No helium was used for the 2nd and 3rd pulses.

Pulse On Time 4.0 secs.

Test 004. - January 28, 1966
Replaced helium bottle and repeated Test 003. Helium pressurization in gas generator reached full pressure in 90 milliseconds. With 1400 psi helium pressure the gas generator pressure reached 22 psia.

Pulse On Time 4.0 secs.

Test 005. - January 28, 1966
Two manual pulses at altitude were fired with helium pressurization.

Pulse On Time 1.5 secs.

Test 006. - January 28, 1966
.2 sec. pulses at a τ of 60 were run at altitude for a total period of 21.3 minutes to obtain temperature stabilization data.

Pulse On Time 21.2 secs.

Test 007. - January 28, 1966
.2 sec. pulses at a τ of 40 were run at altitude to obtain temperature stabilization data. After a few pulses an apparent oxidizer starvation occurred and unit was shutdown. Oxidizer tank was found to be nearly empty. The gas generator and tube were returned to Cleveland.

Pulse On Time 2.0 secs. (est.)

The first prototype turbine scroll was assembled with the 0.9 O/F ratio gas generator and returned to the Roanoke Laboratory for test. The oxidizer flowmeter was repaired and reinstalled.

Test 008. - February 9, 1966

Three 1 sec. pulses at sea level and three at altitude were fired to determine propellant flows.

Test 009. - February 9, 1966
Propellant pressures were adjusted to 190 psig and three 1 sec. pulses were fired at altitude to obtain propellant flow data. Flocon meters did not operate.

Pulse On Time	3.0 secs.

Disassembled and cleaned both flowmeters.

Test 010. - February 9, 1966
Three 1 sec. pulses were fired at altitude to obtain propellant flow readings.

Pulse On Time	3.0 secs.

Test 011. - February 9, 1966
Increased accumulator charge pressure from 210 psig to 315 psia in an attempt to reduce fuel and oxidizer fuel inlet pressure fluctuations. Fired several pulses at altitude to obtain dynamic data. Pressure fluctuations were not improved.

Pulse On Time	1.0 secs. (est.)

Test 012. - Feburary 9, 1966
.2 sec. pulses at a τ of 60 were fired for a period of 12 minutes to obtain temperature stabilization data. Injector head and scroll temperatures stabilized.

Pulse On Time	12 secs.

The scroll-gas generator assembly was removed from the test cell for installation on the first Prototype turboalternator.

Prototype System Tests

The first Prototype System was installed in the altitude chamber for test. The lubrication system and automatic start-up and control system were checked out.

Test 013. - February 15, 1966
Unit No. 1 was started up for the first time. Ten .2 sec. pulses were fired at a τ of 40. (7.8 secs. off time). The unit accelerated to 10,800 rpm in 1.3 minutes. Unit was shutdown to check data; in particular propellant flow rates.

Running Time	1.3 min.
Accumulated Time	.02 hrs.

Test 014. - February 16, 1966
Start-up was initiated by applying fifteen .2 sec. pulses at a τ of 40. Unit accelerated to 15,000 rpm in 2.0 minutes. Manual shutdown was performed to check data.

Running Time	2.0 min.
Accumulated Time	.05 hrs.

Test 015. - February 17, 1966
System performance seemed normal so proceeded with next start-up. Fired twenty .2 sec. pulses at a $\tau = 40$. Unit accelerated to 17,700 rpm. Shutdown to analyze data.

Running Time	2.7 min.
Accumulated Time	.09 hrs.

Test 016. - February 17, 1966
The unit was accelerated by 25 pulses at a τ of 40. Speed reached 21,000 rpm. Shutdown to check data.

Running Time	3.3 min.
Accumulated Time	.14 hrs.

Test 017. - February 17, 1966
The unit was accelerated to 24,000 rpm by applying 25 pulses of .2 sec. duration, at a $\tau = 30$. Shutdown to check data. The system operated normally.

Running Time	2.5 min.
Accumulated Time	.18 hrs.

Test 018. - February 17, 1966
Thirty-three .2 sec. pulses were fired and unit accelerated to 30,000 rpm. Shutdown to check data.

Running Time	3.3 min.
Accumulated Time	.24 hrs.

Test 019. - February 17, 1966
The automatic speed control was adjusted to transfer at 33,000 rpm (1100 cycles). The unit was accelerated up to speed by applying 41 pulses. No transfer occurred. The unit was shutdown manually to determine the cause of malfunction.

Running Time	4.0 min.
Accumulated Time	.31 hrs.

It was decided to transfer to automatic speed control manually.

Test 020. - February 17, 1966
The unit was accelerated to speed (33,000 rpm) and transferred to automatic speed control manually. Ran at no load for 10 minutes.

Running Time	14 min.
Accumulated Time	.54 hrs.

Test 021. - February 18, 1966
Accelerated unit to speed, manually transferred to automatic speed control. Ran for 10 minutes at no load. When voltage regulator was put in the alternator circuit, the automatic overspeed trip shut the unit down.

Running Time	14 min.
Accumulated Time	.77 hrs.

Trouble-shooting of the electrical system did not reveal the cause of malfunction. Decided to run again at no load and trouble-shoot during running.

Test 022. - February 18, 1966
Accelerated unit to speed and ran at no load for 41 minutes. Pressure oil pump was inadvertently shutoff. Shutdown.

Running Time	45 min.
Accumulated Time	1.52 hrs.

Test 023. - February 18, 1966
Accelerated unit to speed and operated at no load for 27 minutes. Scroll temperature stabilized at 1190°F. Alternator was leaking oil severely around terminals, field connection and thermocouple connections. Could not determine the cause of voltage regulator malfunction. Decided to shutdown and return the turboalternator and electrical system to Cleveland for diagnosis and revision.

Running Time	31 min.
Accumulated Time	2.04 hrs.

The speed control and voltage regulator were checked out on the bench. The voltage regulator was redesigned and rebuilt to accept higher alternator step voltages. It was found that the alternator leads had not been installed to the proper phase outputs thus causing the voltage regulator to malfunction. The alternator was reworked to bring the terminals through the end cap to permit easier oil sealing. Conax connections were installed on the field, alternator and thermocouple connections to prevent oil leaks.

An emissivity coating (Titanium Oxide) was sprayed on the turbine scroll to improve heat dissipation. Examination of the turboalternator indicated it was in excellent condition.

The system was rebuilt and reinstalled in the altitude chamber.

Test 024. - March 9, 1966
Prior to installation of the turboalternator, the turbine scroll-gas generator assembly was installed and checked out separately. Four pulses were fired.

Test 025. - March 11, 1966
The turboalternator was reinstalled in the altitude chamber.

Accelerated unit up to speed. A 31 minute run was made at no load. Speed control operation using a separate DC power supply was normal. Electrical oscillations occurred when the voltage regulator was placed on the line. Unit was shutdown to check voltage regulator.

Running Time	31 min.
Accumulated Time	2.55 hrs.

Could find no problem in voltage regulator circuit.

Test 026. - March 14, 1966
The unit accelerated to speed and the speed control transferred to automatic. Speed then dropped below the 1089 cps and pulsed for .3 sec. at 1060 cps. Shutdown manually to trouble-shoot.

Running Time	5 min.
Accumulated Time	2.63 hrs.

Test 027. - March 14, 1966
Could find no problem in speed control circuit. Started up again and the .3 sec. pulse occurred as before. Shutdown to diagnose problem. It was discovered that the speed control start-up delay circuit setting of four minutes was excessively long and should be reduced to 3.5 minutes. Reset the time delay.

Running Time	4 min.
Accumulated Time	2.70 hrs.

Test 028. - March 14, 1966
Started up and speed control operation was normal. Frequency read-out measurement was fluctuating and in doubt. Shutdown and reduced sensitivity setting on meter.

Running Time	20 min.
Accumulated Time	3.02 hrs.

Test 029. - March 15, 1966
Started up and ran at no load under automatic control normally. Shutdown to prepare for operation at load.

Running Time	26 min.
Accumulated Time	3.45 hrs.

Test 030. - March 15, 1966
Accelerated unit up to speed and applied load for the first time. The Moog valve pulsed in short .08 sec. pulses, apparently caused by DC filter oscillation. Shutdown to delete filter from the system.

Running Time	11 min.
Accumulated Time	3.63 hrs.

Test 031. - March 16, 1966
Accelerated unit up to speed at 0.9 0/F ratio. Speed control power was supplied from a separate DC supply. The voltage regulator was not in the circuit. Applied 1.2 KW load manually and operated there for 40 minutes. Scroll temperature reached 1130°F which is 60° lower than scroll temperature at no load without emissivity coating. Pulsing rate 9 sec. Shutdown to check for oil leaks and to prepare for run with automatic voltage regulation.

Running Time	61 min.
Accumulated Time	4.65 hrs.

Test 032. - March 16, 1966
Started up and applied load with voltage regulator in the circuit. The frequency meter pegged. Shutdown to check voltage regulator circuit. Reduced sensitivity of frequency meter:

Running Time	31 min.
Accumulated Time	5.17 hrs.

Test 033. - March 17, 1966
Could find no problem in voltage regulator circuit. Accelerated unit up to speed. Checked pulse width and adjusted to precisely .200 secs. Time between pulses at no load 15.25 to 15.50 secs. Operated at no load for 1 hour, 26 minutes while trouble-shooting electrical system. Shutdown.

Running Time	1.50 hrs.
Accumulated Time	6.67 hrs.

Test 034. - March 17, 1966
Accelerated to speed. Transferred to automatic speed control. Switched speed control to alternator power and frequency meter pegged.

Running Time	15 min.
Accumulated Time	6.92 hrs.

Decided to ignore frequency meter readings.

Test 035. - March 17, 1966
Accelerated to speed and operated on automatic speed control and automatic voltage regulation. Applied step loads of .25 to .40 KW. Maximum load reached 2.15 KW output. At that point voltage regulator power was 101 watts and speed control power 8 watts. Windage correction approximately 1.0 KW. Equivalent output 3.25 KW. At end of test dropped entire electrical load in one step with no effect on voltage regulator performance. Shutdown due to altitude chamber overheating.

Running Time	1.0 hrs.
Accumulated Time	7.92 hrs.

Test 036. - March 18, 1966

Revised altitude chamber installation to provide better cooling. Removed water cooled shroud to prevent flame flash back over the unit. Added 1" diameter ventilation hole in cool end of the chamber.

Accelerated unit to speed and operated on automatic control and voltage regulation at various loads up to 1.50 KW. Altitude chamber overheated as before. Shutdown to install positive altitude chamber cooling, and to install dual injector head.

Running Time	2.03 hrs.
Accumulated Time	9.95 hrs.

The altitude chamber was lined with copper tubing for water cooling. Unit #1 was reassembled with the dual injector. A Hastelloy fin was welded to the #2 scroll and used to provide improved dissipation. The titanium oxide coating was removed and an aluminum oxide emissivity coating was applied to provide better surface adherence. A magnetic overspeed trip circuit and an over-temperature trip circuit were added for operational safety. The unit was then reinstalled in the altitude chamber.

Test 037. - April 7, 1966
Unit was accelerated to speed. 41 start-up pulses were required. Maximum scroll temperature reached 1060°F then leveled out to 1000°F at no load. Roller bearing temperature reached 190°F. Vibration level - 8 g's on alternator housing. Unit was shutdown due to an erroneous injector head temperature of 315°F. Thermocouple was loosened from injector head. No oil leakage was observed.

Running Time	11 min.
Accumulated Time	10.13 hrs.

Test 038. - April 7, 1966
Accelerated unit up to speed. Shutdown due to water system problems in the de-aerating tank. Found boiler feed-water filters plugged with sediment. Cleaned filters.

Running Time	5 min.
Accumulated Time	10.21 hrs.

Test 039. - April 7, 1966
Accelerated unit up to speed. Altitude pressure dropped to 24" Hg gage. Coast time dropped to 3 secs. Shutdown. Found sediment in water filters.

Running Time	9 min.
Accumulated Time	10.36 hrs.

Test 040. - April 11, 1966
Accelerated unit to speed. Shutdown due to extraneous noise which was later traced to the vibration test cell.

Running Time	9 min.
Accumulated Time	10.51 hrs.

Test 041. - April 11, 1966
Accelerated unit to speed on 0.9 O/F ratio and switched to 2.7 O/F ratio. The purpose of the test was to determine and adjust the O/F ratios. O/F ratios were 0.9 and 2.58 respectively.

Running Time	25 min.
Accumulated Time	10.93 hrs.

Test 042. - April 11, 1966
The previous run was made at 190 psig fuel pressure and 185 psig oxidizer pressure. It was decided to adjust the 2.58 O/F ratio by increasing the oxidizer pressure to 190 psig. A run was made to determine the effect of this change.

The unit was accelerated to speed and five pulses at each of the following conditions were obtained:

Condition	Fuel Pressure psig	Oxidizer Pressure psig	Moog Valve Selected
1	190	185	0.9 0/F
2	190	185	2.7 0/F
3	190	190	2.7 0/F
4	190	190	0.9 0/F

Shutdown due to altitude vacuum loss. Found boiler feedwater filters plugged with sediment. Traced problem to mud accumulation in the river pump house. Engaged contractor to pump out the mud.

Analysis of data indicated the following 0/F ratios for condition 1 through 4 above.

Condition 1	.891 0/F
Condition 2	2.61 0/F
Condition 3	2.80 0/F
Condition 4	0.95 0/F

It was decided to use 190 psig pressure for both oxidizer and fuel in future tests.

Test 043. - April 14, 1966
Two and one-half days were required to diagnose and solve the water contamination problem. After pumping out the mud and thoroughly flushing the water system, tests were resumed.

The unit was accelerated to speed on 0.9 0/F ratio and then operated at 2.7 0/F ratio at 1 KW electrical load (2.25 KW equivalent load). After running for about 1/2 hour the incremental speed change during a pulse decreased and after 1 hour of running this increment became 840 rpm rather than 1050 rpm initially. Coast time was proportionately reduced. No injector head cooling water was used during this test. The unit was shut-down and analysis of data indicated a reduction in oxidizer flow due to heating of the oxidizer.

Running Time	1.13 hrs.
Accumulated Time	12.23 hrs.

Test 044. - April 15, 1966
The unit was accelerated to speed at 0.9 0/F ratio and switched to 2.7 0/F ratio. A load of 1.2 KW was applied (2.25 KW equivalent load). Scroll tem-

perature reached 1400°F at hottest point and 1200°F at the coolest point. Injector head temperature reached 260°F. Bearing temperatures reached 280°F (ball bearing) and 220°F (roller bearing). Seal temperature reached 320°F. Alternator flange temperature reached 700°F and was still increasing. Turbine blades glowed red to orange. Speed increment and coast time gradually decreased. Switched to 0.9 0/F ratio for a short time and shutdown. No injector head water was used for this test.

Running Time	1.4 hrs.
Accumulated Time	13.63 hrs.

Test 045. - April 15, 1966
Accelerated unit to speed at 0.9 0/F ratio. Applied loads up to 2.4 KW electrical (3.36 KW equivalent). Scroll temperature reached 1300°F at hottest point and 1125°F at coolest. Injector head temperature reached 260°F. The scroll glowed but turbine blades did not. Speed increment and coast time gradually decreased. Ran a short time at no load and speed increment and coast time gradually returned to normal. Unit was shutdown. It was concluded from this test that injector head cooling or more effective propellant cooling should be used in future tests.

Running Time	.85 hrs.
Accumulated Time	14.48 hrs.

Test 046. - April 16, 1966
Injector head cooling water was used for this test. The unit was started and run at 0.9 0/F ratio. Loads of 1.0 KW, 2.0 KW and 2.75 KW electrical were applied. (Equivalent loads 1.85 KW, 2.85 KW and 3.60 KW).

Pulsing rate:	no load	13 secs.
	2.85 KW	6 secs.
	3.60 KW	5 secs.

At 2.85 KW approximately 1/2 of blade length glowed during a pulse and then cooled to a dull red after a pulse. Inner radial half of blades did not glow. At 3.60 KW blades glowed more brightly approximately to the rim. The rim did not glow. After running for 11 minutes at 3.6 KW the coast time decreased from 5 secs. to 3 secs. The unit was shutdown and propellant flow traces analyzed. Considerable reduction in oxidizer flow (to .655 0/F ratio) had occurred. It was concluded that a positive control over oxidizer temperature increase was required.

Running Time	1.2 hrs.
Accumulated Time	15.68 hrs.

It was decided to fabricate a water jacketed oxidizer flow line for installation at the attachment to the Moog valves. This was completed and installed.

Test 047. - April 18, 1966
Oxidizer and fuel lines were insulated with asbestos tape. A water coil was installed for exhaust gas impingement cooling. A radiation heat shield was installed around the gas generator to shield the Moog valves. The unit was operated for 1.02 hours at 1 KW and 2 KW electrical load. Oxidizer temperature and fuel temperature remained below 115°F. Speed increment and coast time did not decrease during run indicating proper control of propellant temperatures. Suddenly the scroll temperature increased to 1500°F. (at hottest point) and view through window was obscured by oxidizer vapor. The unit was shut down. Inspection revealed the following:

a. An oxidizer tube in the 0.9 O/F ratio head had ruptured.

b. The oxidizer port in the 0.9 O/F ratio valve was leaking.

c. The fuel port in the 2.7 O/F ratio valve was leaking.

The unit was removed from the cell and brought to Cleveland for repair.

Running time	1.02 hrs.
Accumulated time	16.70 hrs.

The second dual injector head was installed on No. 3 scroll. A copper fin was welded to this scroll to provide improved heat dissipation. It was thought that the oxidizer tube failure was caused by the leaking Moog valves which had been inadvertently overtemperatured during test. New valves were installed and the unit was returned to Roanoke for test.

Test 048. - May 17
The unit was accelerated to speed at 0.9 O/F ratio. After transfer to automatic speed control, the magnetic pick-up overspeed trip shut the unit down. The setting was then readjusted to a slightly higher speed, 36,000 RPM.

Running time	4 min.
Accumulated time	16.77 hrs.

Test 049. - May 17
Unit was accelerated to speed at 0.9 O/F ratio and then operated at 0.9 and 2.7 O/F ratios to obtain fuel and oxidizer flow readings. Altitude pressure .28 psia. Coast time at no load 12 seconds at both O/F ratios. Scroll temperature reached 980°F during startup and then dropped below 900°F. Shutdown to analyze oxidizer-fuel traces.

Running time	16 min.
Accumulated time	17.04 hrs.

Test 050. - May 18
Slightly smaller fuel trim orifices were installed for adjustment to proper 0/F ratios. The unit was then accelerated to speed at 0.9 0/F ratio. 1 KW of electrical load was applied and the unit was automatically shutdown by the magnetic pick-up circuit. This was reset to 36,000 RPM+. 0/F ratio = 0.92.

Running time	22 min.
Accumulated time	17.41 hrs.

Test 051. - May 18
Accelerated unit up to speed at 0.90 0/F ratio. Electrical load was applied and the magnetic pickup circuit shut the unit down. This circuit was then reset to 37,500 RPM.

Running time	11 min.
Accumulated time	17.59 hrs.

Test 052. - May 18
Accelerated up to speed at 0.90 0/F ratio. Applied load up to 3.45 KW electrical (4.5 KW equivalent load) 0/F ratio was 0.87.

Pulsing rate	4.8 sec.
Scroll temperature	1270°F max.
Seal temperature	310°F
Ball bearing temperature	270°F
Roller bearing temperature	260°F

The unit was shutdown due to altitude chamber overheating. After shutdown, the altitude chamber metal was excessively hot. It was decided to paint the interior of the chamber with black paint and to install a water spray at the exhaust end of the chamber.

Running time	41 min. 40 sec.
Accumulated time	18.29 hrs.

Test 053. - May 19
Accelerated unit up to speed at 0.9 0/F ratio. Switched to 2.7 0/F ratio and ran for about 1 hour at 3 KW equivalent load. Scroll temperature reached 1250°F. Pulsing rate 6.5 secs. Switched back to 0.9 ratio and operated a short time. Oil pressure dropped and unit was shutdown. The oil pressure

hose feeding the alternator cooling jacket failed due to close proximity with the scroll. Replaced all rubber hoses, in the vicinity of the scroll with metal lines.

Running time	1 hr. 22 min.
Accumulated time	19.66 hrs.

Test 054. - May 20
Started unit and ran 2 hours of the following endurance load schedule:

	0/F Ratio	Equiv. Load KW	Actual Electrical Load KW	Running Time Min.
1	0.9	3.0	2.0	15
2	2.7	3.0	2.0	25
3	0.9	3.0	2.0	10
4	0.9	4.5	3.5	10

The unit was then shutdown to check the effectiveness of the water spray system. Found water spray inadequate to maintain proper altitude chamber temperature. Increased the water flow rate to 10 gallons per hour.

Running time	2 hrs. 31 min.
Accumulated time	22.18 hrs.

Test 055. - May 20
Started unit and ran 1 hour of the above endurance schedule. Performance was normal. Unit was shutdown to prepare for long endurance tests.

Running time	1 hr. 20 min.
Accumulated time	23.51 hrs.

0/F ratios for the above test were 0.89 and 2.60 by actual flow measurement.

Test 056. - May 24
Started unit and began endurance at the following schedule:

	O/F Ratio	Equiv. Power KW	Running Time
1	0.9	3.0	50 min.
2	0.9	4.5	10 min.
3	0.9	3.0	50 min.
4	0.9	4.5	10 min.
5	2.7	3.0	50 min.
6	0.9	4.5	10 min.
7	2.7	3.0	50 min.
8	0.9	4.5	50 min.

Repeat above every 4 hours.

After 1 hr. 28 min. of endurance running the unit suddently pulsed at the rate of 1 pulse/second for 5 pulses. Unit was manually shutdown to investigate. It was found that the laboratory scavenge pump had stopped, thus flooding bearing and alternator cavities with oil and causing high friction loss (33 HP). No damage to the unit was apparent. The scavenge pump was freed from binding and the unit was restarted. Scavenge pressures were fluctuating and unit was shutdown to tighten scavenge connections and to tighten relief valve fitting. Unit was restarted and endurance test was continued. After 54 minutes of operation at the endurance schedule it was noted that the Moog valve flange temperatures were below 30°F.

The unit was shutdown manually and a failed oxidizer tube was found in the 2.7 injector.

Running time	3.22 hrs.
Accumulated time	26.73 hrs.

Endurance running time during May included 3 hours in Tests 054 and 055 and 2 hrs. 22 min. during Test 056 for a total of 5.37 hours.

An analysis of valve flange temperatures indicated that all tubes were intact during Test 054, and Test 055. The tube failed during the last portion of Test 056 between 3:51 and 3:59 p.m. Actual manual shutdown occurred at 4:54 p.m.

Discussions with NASA-Houston were held on June 2, 1966. It was thought that fuel dribble volume was mixing with oxidizer in the oxidizer tubes. Altitude pressure variation was undoubtedly aggravating this condition. Overheating of tubes was also

thought by NASA to be a contributing factor. Weakening of tubes during manufacturing processing was also a suspected cause.

After the oxidizer tube failure it was mutually agreed by NASA and TRW to rebuild Unit No. 1 with a dual injector with the following changes:

1. Operate at 2.7 0/F ratio only.
2. Point injector down.
3. Use no injector cooling water.
4. Reduce altitude pressure variation, if possible.
5. Support the tubes by potting with epoxy.

The unit was rebuilt with the above changes. A 22" dia. altitude chamber exhaust pipe was installed and the installation was readied for endurance test.

Test 057. - June 23
The unit was accelerated to speed at 2.7 0/F ratio. Century traces of fuel and oxidizer flow were taken. Unit was shutdown to trim the 0/F ratio. 0/F ratio was calculated to be 2.3. An .073" fuel trim orifice was installed and fuel and oxidizer pressures were increased from 190 psig to 195 psig.

Running time	4 min. 30 sec.
Accumulated time	26.81 hrs.

Test 058. - June 23
Accelerated unit up to speed at 2.7 0/F ratio. Operating speed was reached in 35 pulses (3.5 min). Ran at no load for 20 minutes and at 2.2 KW (equivalent load) for 45 minutes then reduced load and shutdown to check data.

Running time	1.26 hrs.
Accumulated time	28.07 hrs.

0/F ratio was 2.90. An .079" fuel trim orifice was installed.

Test 059. - June 24
Accelerated unit up to speed at 2.7 0/F ratio. Pulsing rate at no load was 17 secs. Applied load of 3 KW (equivalent) Pulsing rate - 6.5 secs. Ran 10 mins.

Reduced load as a precaution due to an excessive valve temperature reading (600°F). This reading proved to be erroneous. Applied endurance test load at 11:00 a.m. and ran at that condition until 6.05 p.m. Critical temperatures held as follows:

Scroll temperature	1300°F
Roller bearing	160°F
Ball bearing	210° and 270°F
Seal	310°F

Load was reduced at 6:05. Injector head heat soak back was evident for several minutes of running at no load and resulted in reduced 0/F ratio and more frequent pulsing than normal. No cooling water was used in the injector head for these tests. After running at no load for 6 minutes injector head temperatures began to drop and pulsing began to return toward normal. It is intended to install a circular copper cooling fin on the gas generator to eliminate the heat soak back problem. This will be incorporated in fugure designs.

Shutdown occurred at 6:11 p.m.

Running time	8.1 hrs.
Accumulated time	36.17 hrs.

Test 060. - June 27
Accelerated unit up to speed at 2.7 0/F ratio. Applied endurance test load. After running several hours the oil scavenge pump motor stopped and the alternator cavity overloaded with oil. Unit pulsed each second for 4 seconds and was manually shutdown.

Running time	4 hrs. 17 min.
Accumulated time	40.45 hrs.

Test 061. - June 28
Installed new scavenge pump motor.

Accelerated unit up to speed and scavenge pump pressure was erratic. Shutdown. Found air leak in scavenge pump valve.

Running time	5 min.
Accumulated time	40.53 hrs.

Test 062. - June 28
Accelerated unit up to speed and applied endurance test load (3 KW equivalent). After several hours of running a thunderstorm cut off the 110 volt AC power and the unit automatically shutdown. A short period of coasting occurred with no oil pressure available and then the power returned and the oil pressure was restored. The unit then slowly coasted to 0 rpm normally.

Running time	3 hrs. 50 min.
Accumulated time	44.20 hrs.

Test 063. - June 29
Accelerated unit up to speed in 38 pulses. Applied endurance load and ran for several hours. With no warning unit shutdown automatically. Could find nothing wrong with the control system.

Running time	4 hrs. 10 min.
Accumulated time	48.37 hrs.

During Test 063, 1 pint of oil was consumed. No evidence of oil consumption has been seen prior to this time. This seal will be carefully inspected at disassembly to determine the cause of leakage. It may be that an "O" ring seal will be required to seal the mating ring - shaft assembly. This will be added, if required. Also, an improved seal built by the Koppers Co. is available and will be installed at the next reassembly.

Test 064. - June 29
Accelerated unit up to speed and at the 32nd pulse, the pulses terminated and unit coasted down in speed. Could find nothing wrong with the control.

Running time	3.2 min.
Accumulated time	48.42 hrs.

Test 065. - June 29
Accelerated unit up to speed and ran for 20 minutes normally. Shutdown at 7:20 p.m.

Running time	20 min.
Accumulated time	48.75 hrs.

Test 066. June 30
Accelerated unit up to speed and applied endurance test load. After several hours unit shutdown automatically. Could find nothing wrong with the control.

Running time	3 hrs. 56 min.
Accumulated time	52.68 hrs.

Test 067. - June 30
Accelerated unit up to speed and applied endurance test load. After 55 minutes unit shutdown automatically. It was found that the automatic over temperature trip was actuating at a temperature 30° lower than the set point. The trip circuit was then disabled prior to the next run.

Running time	55 min.
Accumulated time	53.60 hrs.

Test 068. - June 30
Accelerated unit up to speed and applied endurance test load. Shutdown manually at 6:00 p.m.

Running time	2 hrs. 28 min.
Accumulated time	56.07 hrs.

Test 069. - July 1
Accelerated up to speed at 2.7 O/F ratio and applied endurance test load. After running for several hours the injector head temperature reached 290°F. Shutdown to check fuel cooling coil.

Running time	3 hrs. 15 min.
Accumulated time	59.32 hrs.

Test 070. - July 1
Accelerated unit up to speed at 2.7 O/F ratio. Applied endurance test load. Injector head temperature increasing. Turned on altitude chamber spray nozzle which reduced chamber temperature from 250°F to 210°F and injector head temperature dropped from 268°F to 259°F. Shutdown at the end of the day.

Running time	5 hrs.
Accumulated time	64.32 hrs.

Test 071. - July 5
Accelerated unit up to speed at 2.7 O/F ratio. Applied endurance test load and ran throughout the day.

Running time	7 hrs. 10 min.
Accumulated time	71.49 hrs.

During the above test oxidizer pressure was increased from 190 to 195 psi to trim the propellant flows to spec. values.

Test 072. - July 6
Accelerated unit up to speed at 2.7 O/F ratio. Applied endurance test load and ran throughout the day.

Running time	8 hrs. 45 min.
Accumulated time	80.24 hrs.

After the above test the unit was removed from the chamber, returned to Cleveland and disassembled for inspection. All parts were in excellent condition. A loose fitting "O" ring was observed on the seal cartridge where it mates with the alternator housing. Some oil by-passed the seal at this point during running. Future units will incorporate a slightly larger "O" ring.

The second prototype unit was assembled and installed in the altitude chamber for acceptance test.

Tests on 2nd Prototype Unit

During July Tests No. 1 through 9 were completed. A summary of these is given below:

Test No. 1 - July 13
The first start-up of the unit was made by applying 10 pulses at 0.9 O/F ratio. Flow recordings were made to determine O/F ratio. Shutdown to analyze data.

Running time	1 min.
Accumulated time	.02 hrs.

Test No. 2 - July 13
Unit was accelerated by applying 15 pulses at 2.7 O/F ratio. Shutdown to check and trim oxidizer and propellant flows. At shutdown found an oil leak around the roller bearing thermocouple hole. Removed the .075" 0.9 fuel trim orifice and installed the .086" trim orifice.

Running time	1.5 min.
Accumulated time	.04 hrs.

Test No. 3 - July 13
Accelerated unit by applying 25 pulses at 0.9 O/F ratio. Shutdown to examine propellant flows and to inspect unit.

Running time	3 min.
Accumulated time	.09 hrs.

Test No. 4 - July 13
Accelerated unit up to speed at 0.9 O/F ratio. Automatic control system transferred properly at the 40th pulse. After running for a few minutes at no load the oil scavenge pressure showed fluctuations. Shutdown to investigate. Found a loose Swagelok oil fitting.

Running time	20 min.
Accumulated time	.42 hrs.

Test No. 5 - July 13
Accelerated unit up to speed at 0.9 0/F ratio. Transferred to automatic speed control at the 39th pulse. At this point the magnetic pick-up overspeed circuit shut unit down.

Running time	4 min.
Accumulated time	.49 hrs.

The overspeed trip was reset from 36,000 to 37,500 rpm.

Test No. 6 - July 14
Accelerated unit up to speed at 0.9 0/F ratio. After speed control transferred to automatic, the 0/F ratio was switched to 2.7. After a few minutes load was applied at which point the magnetic pick-up overspeed trip shutdown. It was found that the filter in the magnetic pick-up output circuit was malfunctioning causing erratic shutdown signals. The low pass filter band was readjusted for the next test.

Running time	11 min.
Accumulated time	.67 hrs.

Test No. 7 - July 14
Unit was accelerated up to speed at 0.9 0/F ratio. After a few minutes the 0/F ratio was switched to 2.7 and electrical load was applied. The magnetic overspeed trip circuit again shut the unit down. This circuit was then disconnected for the remaining tests.

Running time	10 min.
Accumulated time	.83 hrs.

Test No. 8 - July 14
Accelerated unit up to speed at 0.9 0/F ratio. After a few minutes switched to 2.7 0/F ratio and began the following Acceptance Test:

25 minutes at 3 KW at 2.7 0/F

25 minutes at 3 KW at 0.9 0/F

10 minutes at 4.5 KW at 0.9 0/F

After completing the 2.7 0/F ratio running and 20 minutes of the 0.9 0/F ratio running at 3 KW injector head heat soak back caused 0/F ratio shift and more frequent pulsing. Load was removed and operation was continued for about 35 minutes and injector head temperatures were gradually dropping, however the pulsing rate remained slightly above normal. The unit was shutdown to attach the injector cooling coil.

Running time	1 hr. 26 min.
Accumulated time	2.26 hrs.

Test No. 9 - July 14

Accelerated unit up to speed and completed the Acceptance Test Schedule. Injector cooling water was used a few times to maintain injector head temperature at 200°F. Pulsing rate was normal. Actual loads were 2.1 KW and 3.6 KW. At 4.5 KW equivalent load pulses occurred every 4.5 secs. Scroll temperature reached 1480°F (at hottest point). At the completion of the Acceptance Schedule, the unit was shutdown. In general the unit operated similarly to Unit No. 1. Scroll temperatures were slightly higher probably caused by the turbine tip clearance of .045" minimum compared with .037"-.038" for Unit No. 1.

Running time	23 min. 40 sec.
Accumulated time	2.66 hrs.